Design of a groundwater-based Model Predictive Control algorithm for the operation of water table control systems

A proof of concept

MSc Thesis

Noortje Romeijn

Delft University of Technology

TU Delft

Witteveen + Bos

Hoogheemraadschap van Rijnland

Design of a groundwater-based Model Predictive Control algorithm for the operation of water table control systems

A proof of concept

by

Noortje Romeijn

to obtain the degree of Master of Science
at the Delft University of Technology,
to be defended publicly on Friday April 14, 2023 at 11.00 AM.

Student number:	4651464	
Project duration:	May 16, 2022 – April 14, 2023	
Thesis committee:	Dr. R.R.P. (Ronald) van Nooijen,	TU Delft, chair
	Prof.dr.ir. M. (Mark) Bakker,	TU Delft
	ir. B. (Bart) Dekens,	Witteveen+Bos

Cover: a sump for composite controlled drainage (photograph taken by Noortje Romeijn, during a field visit to Polder Het Langeveld).

TU Delft

Preface

During the past 11 months, I have been working on the MSc thesis before you. Witteveen+Bos proposed the idea of investigating the feasibility of groundwater-dependent surface water control, which drew my attention as it sounds interesting, challenging and practice-oriented. With the support of my supervisors, I was able to make the research my own, which has resulted in this thesis titled *Design of a groundwater-based Model Predictive Control algorithm for the operation of water table control systems*. The research has been conducted in collaboration with water board *Hoogheemraadschap van Rijnland*.

This thesis concludes my MSc Civil Engineering (Water Management track) at Delft University of Technology. After almost 6 years of study, I am proud to (soon) be a TU Delft graduate. It has been a long, but worthwhile journey, in which I overcame many challenges and experienced personal growth. I feel very privileged to have had the opportunity of educating and developing myself for such a long time, as I know education cannot be taken for granted in many other parts of the world.

I would like to express my gratitude to all of my committee members: Ronald van Nooijen, Mark Bakker and Bart Dekens. Special thanks to my daily university supervisor Ronald, who really guided my through the process and was always available for meetings (without paying much attention to the time). I would also like to thank my daily company supervisor Bart. Besides his supervision and our weekly meetings, he introduced me to Witteveen+Bos and familiarized me with the company.

Furthermore, I would like to thank Witteveen+Bos for giving me the opportunity of working together and getting to know the company. Although I was not involved in projects, I felt included and at ease, because people were interested in me and my research. I would like to thank my group members from ”Wateroverlast” for inviting me to their group meetings and coffee moments. I am really looking forward to join the group as an employee and collaborate in the future. Due to my research topic, I was in close contact with the ”Geohydrologie” group too. I would like to thank Stijn Klop for his guidance during the construction of the MODFLOW groundwater model. He was always available for questions and proposed interesting solutions to problems that I encountered. Sanne de Smet and Pierrick Spekreijse deserve special mention too, because they were always willing to look into my code and taught me helpful Python tricks.

Also, I was lucky to cooperate with *Hoogheemraadschap van Rijnland*, which enabled me to link my research to practice and perform a case study. I would like to thank my contact persons Arjen Oord, Joost van der Zwet and Jan Jelle Reitsma for providing me useful practical insights. Additionally, I would like to thank Robert van Wieringen and Martin Varkevisser for showing me around Polder Het Langeveld and explaining me about operational water management.

Last but not least, I would like to thank my dear family and friends, who have unconditionally supported me. Firstly, my parents, Jacomina and Eric Romeijn, and my brother, Luuk Romeijn. I learned that my mom has the best pep talks, and my dad was always willing to exchange knowledge on civil engineering during dinner (although this was not appreciated by other family members at all times). Special thanks to my close friends Chantal Muishout, María Fonseca, Naomi Dommerholt and Irene de Vries for their support and the fun we had. You made my university time an unforgettable experience.

Noortje Romeijn
Delft, March 2023

Summary

Rapid discharge of excess water has always been the core of Dutch water management. Due to climate change, a change in strategy is required. A future-proof drainage strategy consists of three steps: 1) retention, 2) storage, and 3) controlled removal. The water system is currently managed based on actual measurements of surface water level. Since actual soil moisture conditions and groundwater levels are not taken into account, control decisions are based on incomplete information of the available storage capacity and the available storage capacity is not fully utilized. For that reason water boards have been looking into methods to control surface water levels based on actual measurements of groundwater level, which is called groundwater-dependent surface water control. Furthermore, there is a shift from traditional drainage to controlled drainage, for which multiple water table control systems are available. Considering the slow response of the groundwater system, Model Predictive Control (MPC) is expected to be useful for groundwater-based control of these systems. MPC is a model-based controller that uses forecasts of disturbances to minimize deviations from setpoint during a specific time horizon. Since the forecast horizon for which accurate precipitation forecasts are available is restricted, the feasibility of groundwater-based MPC is dependent on the response time of the groundwater system.

This research, which is executed as a model study, comprises the design and evaluation of an algorithm for groundwater-based MPC of water table control systems in polder areas. The objective is to maximize retention of precipitation, thereby contributing to the first component of the new drainage strategy. As a first approach, this is attempted by maintaining groundwater levels at the maximum admissible level. The control algorithm is developed for water table control on a single plot surrounded by a ditch, and three variants of water table control systems are considered: 1) water table control without drains, 2) water table control with submerged drains, controlled by ditch water level, and 3) water table control with submerged drains, controlled by sump water level. The controller adjusts the crest level of a weir that manages the ditch or sump water level. Its performance is assessed through model simulations for two case study areas with distinct geohydrological response times within the management area of *Hoogheemraadschap van Rijnland*: 1) *Polder Het Langeveld*, a sandy polder located in the Flower Bulb Region, and 2) *Polder Vierambacht*, a clayey polder located in the Green Heart.

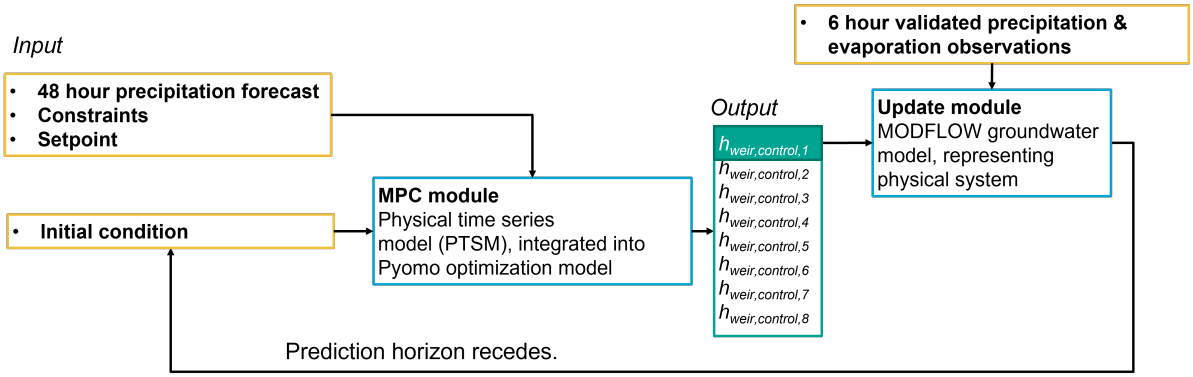

Figure 1: Summary MPC algorithm.

Figure 1 depicts a summary of the developed control algorithm. It consists of two main modules: 1) an MPC module (representing the controller), and 2) an update module (representing the physical system). The update module contains a MODFLOW 6 groundwater model and is used to update the system state, representing the physical system. MODFLOW simulations are performed to evaluate the geohydrological response of both case study areas in combination with each of the three water table

control systems. A physical time series model (PTSM) is derived to simulate the groundwater response in the centre of the plot with limited computational effort and sufficient accuracy. The PTSM is calibrated to MODFLOW groundwater level time series and applied as internal model in the MPC module. The MPC module is constructed according to MPC theory using Python Optimization Modeling Objects (Pyomo) software. It takes a 48 hour precipitation forecast, constraints, a groundwater level setpoint and an initial condition as its input. Optimized weir crest levels are determined for each control time step within the prediction horizon by minimizing the difference between the actual groundwater level in the centre of the plot and setpoint. Only the optimal weir crest level for control time step 1 is forwarded to the update module. The update module contains the MODFLOW groundwater model and updates the initial condition. It takes 6 hour validated precipitation and evaporation observations as input. As the prediction horizon recedes, the renewed initial conditions are again forwarded to the MPC module and a new precipitation forecast becomes available. The MPC algorithm is run using HARMONIE historical precipitation forecasts and validated precipitation and evaporation data from Meteobase to evaluate its performance. A relatively high, fixed setpoint is applied to maximize retention of precipitation. The present control is simulated for comparison. A constant weir crest level, equal to target water level, is assumed for the present control.

Some design steps were straightforward, while others required extensions to existing software or workarounds to circumvent software limitations. Firstly, a workaround was required that enables MODFLOW to correctly represent the two-way interaction between the groundwater and surface water system. Surface water levels are typically imposed as a boundary condition. An iterative loop was constructed in which surface water levels are continuously updated based on MODFLOW's volume budget. This workaround is suitable for variant 1 and 2. Secondly, a workaround was required to avoid the use of if- and max-statements for the construction of the Pyomo optimization model.

Long-term simulations show that advantages of groundwater-based MPC compared to the current control are:

- Groundwater-based MPC anticipates precipitation events, while the original control does not.
- Groundwater-based MPC regulates groundwater levels, while groundwater levels are presently not taken into account by the control.

The complexity of groundwater-based MPC is an important disadvantage. In contrast to the present control, groundwater-based MPC requires: 1) high-quality precipitation forecasts, 2) a groundwater model, 3) an extensive network of groundwater monitoring wells, and 4) automatic weirs. All of these involve costs.

A one-to-one relationship between groundwater level and groundwater storage is observed, which means that maximization of groundwater level results in maximization of groundwater storage, thereby (in potential) fulfilling the research objective. The groundwater response time is long in case of variant 1 Polder Het Langeveld ($\pm$ 40 days) and variant 2 Polder Vierambacht ($\pm$ 20 days). Although rain events are anticipated, only minor improvements are observed compared to the present control. The controller should be given more room for anticipation, which could be realized by applying longer precipitation forecasts or adaptation of the objective function such that temporary low or high groundwater tables are more acceptable. Proper control of the systems is hard, but the systems are applicable for water retention, considering the significant bulging of the groundwater table. Due to the presence of drains, the response time of variant 2 Polder Het Langeveld is considerably lower ($\pm$ 3 days) than the response time of variant 1 Polder Het Langeveld, which enables proper control. However, the bulging of the groundwater table is very limited, such that the system is not suitable for water retention. It is therefore recommended to increase the drain spacing or install smaller drains if a relatively high groundwater setpoint is desired, but this is at the expense of the system response time. A trade-off between controllability and water storage should be made. A sensitivity analysis shows that, for the applied weir settings and objective function, a system response time lower than 10 days is required for proper control. Furthermore, it is shown that the direct control of groundwater levels could induce a certain groundwater storage or water retention, depending on the applied setpoint. However, this should not be at the expense of setpoint exceedance, which is why a system should be able to anticipate and the

feasibility of groundwater-based MPC is limited to systems with a relatively fast groundwater response.

Recommendations for extension of the developed control algorithm and recommendations for further evaluation of the MPC algorithm are:

- Add water supply to the optimization problem. This also allows for longer simulations for evaluation, since excessive falling of water levels is prevented.
- Adapt the objective function and internal model to allow for maximization of fresh water volume rather than groundwater level.
- Study required/allowable groundwater levels for specific land uses and agricultural activities and perform a year-round simulation.
- Better simulate the present control.
- Apply longer precipitation forecasts.
- Study the effect of precipitation forecast quality on the observed performance of the MPC algorithm.
- Determine the sensitivity to precipitation forecast length and imperfections in the internal model.

Contents

Preface i

Summary ii

Nomenclature viii

1 Introduction 1
- 1.1 Relevance of the research . . . 1
- 1.2 State-of-the-art . . . 2
- 1.3 Research problem . . . 3
- 1.4 Reading guide . . . 3

2 Background information 4
- 2.1 Water table control systems . . . 4
- 2.2 Model Predictive Control (MPC) . . . 7

3 Methodology 11
- 3.1 Envisaged control . . . 11
- 3.2 Procedure . . . 12
- 3.3 Software description . . . 17
  - 3.3.1 MODFLOW 6 . . . 17
  - 3.3.2 Python Optimization Modeling Objects (Pyomo) software . . . 18
- 3.4 Description data . . . 18
  - 3.4.1 HARMONIE historical precipitation forecasts . . . 18
  - 3.4.2 Meteobase historical precipitation and evaporation data . . . 19

4 Description case study area and its water system 20
- 4.1 Description management area Hoogheemraadschap van Rijnland . . . 20
- 4.2 Description selection case study areas . . . 23
- 4.3 Description case study areas . . . 23
  - 4.3.1 Sandy polder - Polder Het Langeveld . . . 23
  - 4.3.2 Clayey polder - Polder Vierambacht . . . 26

5 Construction of groundwater models 29
- 5.1 MODFLOW groundwater models . . . 29
  - 5.1.1 Base model . . . 29
  - 5.1.2 Overview of selected case study area-specific parameters . . . 32
  - 5.1.3 Extension to include groundwater-surface water interaction . . . 35
  - 5.1.4 Adjustments to simulate present state . . . 36
  - 5.1.5 Schematization hydrological processes . . . 37
- 5.2 Physical time series models . . . 39
  - 5.2.1 Two alternatives . . . 39
  - 5.2.2 Extension to include groundwater-surface water interaction . . . 40

6 Setup MPC module 42
- 6.1 Model formulation . . . 42
- 6.2 Definition of setpoint and weir settings . . . 46

7 Evaluation of geohydrological response 47
- 7.1 Overview MODFLOW simulations . . . 47
- 7.2 Geohydrological response . . . 50
  - 7.2.1 Starting point (steady-state solution) . . . 50
  - 7.2.2 Excluding feedback . . . 51

7.2.3 Including feedback . . . 56

8 Physical time series model calibration and verification 62
8.1 Model calibration . . . 62
8.1.1 Excluding feedback . . . 62
8.1.2 Including feedback . . . 62
8.2 Model verification . . . 65
8.2.1 Excluding feedback . . . 65
8.2.2 Including feedback . . . 67

9 Evaluation performance MPC algorithm 70
9.1 Performance MPC module . . . 70
9.2 Performance MPC algorithm . . . 72
9.2.1 Simulation period 1 | Polder Het Langeveld . . . 73
9.2.2 Simulation period 2 | Polder Het Langeveld . . . 77
9.2.3 Simulation period 1 | Polder Vierambacht . . . 79
9.2.4 Simulation period 2 | Polder Vierambacht . . . 80
9.3 Performance for incorrect precipitation forecasts . . . 81

10 Sensitivity to response time groundwater system 85
10.1 Description of systems and corresponding MODFLOW models . . . 85
10.2 PTSM calibration . . . 87
10.3 Performance MPC algorithm . . . 89
10.3.1 System 1 . . . 90
10.3.2 System 2 . . . 91
10.3.3 System 3 . . . 92

11 Discussion 97
11.1 MPC algorithm design: reflection and further study . . . 97
11.2 Performance MPC algorithm vs. present control . . . 99

12 Conclusion & Recommendations 104

A Background information 1: examples of operational control 110

B Background information 2: motivation for Model Predictive Control (MPC) 115

C Overview FloPy packages 118

D Explanation case study area-specific parameters | Polder Het Langeveld 119
D.1 Plot size: plot length (L_{plot}) and plot width (W_{plot}) . . . 119
D.2 Surface level (h_{SL}) . . . 120
D.3 Soil profile and soil-related properties: top layer thickness (d), horizontal and vertical hydraulic conductivity (k and k_{33}), specific yield (S_y), specific storage (S_s) and resistance confining layer (c) . . . 120
D.4 Piezometric heads: initial groundwater head ($h_{GW,initial}$) and head in lower aquifer (h_{aq}) 124
D.5 Characteristics ditch: width (W_{ditch}), bottom elevation ($h_{bot,ditch}$) and bed hydraulic resistance (c_{ditch}) . . . 128
D.6 Characteristics drains: diameter (D_{drain}), drain resistance (c_{drain}) and bottom elevation ($h_{bot,drain}$) . . . 128

E Explanation case study area-specific parameters | Polder Vierambacht 131
E.1 Plot size: plot length (L_{plot}) and plot width (W_{plot}) . . . 131
E.2 Surface level (h_{SL}) . . . 132
E.3 Soil profile and soil-related properties: top layer thickness (d), horizontal and vertical hydraulic conductivity (k and k_{33}), specific yield (S_y), specific storage (S_s) and resistance confining layer (c) . . . 132
E.4 Piezometric heads: initial groundwater head ($h_{GW,initial}$) and head in lower aquifer (h_{aq}) 137
E.5 Characteristics ditch: width (W_{ditch}), bottom elevation ($h_{bot,ditch}$) and bed hydraulic resistance (c_{ditch}) . . . 140

E.6 Characteristics drains: diameter (D_{drain}), drain resistance (c_{drain}) and bottom elevation ($h_{bot,drain}$) . . . 140

F Overview MODFLOW simulations 143
F.1 Excluding feedback . . . 143
F.2 Including feedback . . . 144

G MODFLOW model verification 145
G.1 Spatial discretization . . . 145
G.2 Temporal discretization . . . 146
G.3 Model schematization . . . 148
G.4 Representation of the physical system . . . 150

Nomenclature

Below, an overview of the frequently recurring symbology is provided.

Symbol	Definition	Unit
A_{GW}	Surface area of the groundwater system	[m^2]
A_{sump}	Surface area of the sump	[m^2]
A_{SW}	Surface area of the ditch	[m^2]
c	Resistance confining layer	[d]
C	Conductance confining layer	[m^2/d]
c_{ditch}	Bed hydraulic resistance	[d]
C_{ditch}	Conductance ditch cells	[m^2/d]
c_{drain}	Drain resistance	[d]
C_{drain}	Conductance drain cells	[m^2/d]
d	Top layer thickness	[m]
D_{drain}	Drain diameter	[m]
e_{GW}	Difference between the groundwater head calculated by MODFLOW and the groundwater head calculated by the physical time series model at the end of a simulation	[mm]
$e_{GW,max}$	Maximum absolute error between MODFLOW and physical time series model simulation results	[mm]
E_o	Open water evaporation	[mm/hr or m/d]
E_{ref}	Reference evaporation	[mm/hr or m/d]
h_{aq}	Head in lower aquifer	[m NAP]
$h_{bot,ditch}$	Bottom elevation ditch	[m NAP]
$h_{bot,drain}$	Bottom elevation drains	[m NAP]
h_{drain}	Pressure head that is exerted on the drains	[m NAP]
h_{GW}	Groundwater level in the centre of the field	[m NAP]
$h_{GW,initial}$	Initial groundwater level in the centre of the field	[m NAP]
$h_{GW,setpoint}$	Desired groundwater level in the centre of the field (setpoint)	[m NAP]
h_{SL}	Surface level	[m NAP]
h_{spill}	Spill flow over the weir	[m/model time step]
h_{SW}	Surface water level (in the ditch)	[m NAP]
$h_{SW,initial}$	Initial surface water level (in the ditch)	[m NAP]
$h_{SW,target}$	Target surface water level (in the ditch)	[m NAP]
h_{weir}	Weir crest level	[m NAP]
$h_{weir,control}$	Vector containing optimized weir crest levels	[m NAP]
$h_{weir,control,i}$	Optimized weir crest level control time step i	[m NAP]
$\Delta h_{weir,control}$	Change in weir crest level between consecutive control time steps	[m]
$\Delta h_{weir,control,max}$	Maximum absolute change in weir crest level between consecutive control time steps	[m]
$h_{weir,initial}$	Initial weir crest level	[m NAP]
$h_{weir,max}$	Maximum weir crest level	[m NAP]
$h_{weir,min}$	Minimum weir crest level	[m NAP]
I_{max}	Maximum infiltration rate	[m/d]
k	Horizontal hydraulic conductivity top layer	[m/d]
k_{33}	Vertical hydraulic conductivity top layer	[m/d]
L_{plot}	Plot length	[m]

Symbol	Definition	Unit
N_{drain}	Number of drains	[-]
P	Precipitation	[mm/hr or m/d]
q	Net flux between the surface water and groundwater system	[m/d]
q_v	Seepage flux	[m/d]
Q_f	Overland flow or fast runoff component	[m/d]
$Q_{IN,sump}$	Sump inflow	[m^3/model time step]
$Q_{OUT,sump}$	Sump outflow	[m^3/model time step]
$Q_{IN,SW}$	Ditch inflow	[m^3/model time step]
$Q_{OUT,SW}$	Ditch outflow	[m^3/model time step]
R	Groundwater recharge	[mm/d or m/d]
S_{drain}	Drain spacing	[m]
S_s	Specific storage	[m^{-1}]
S_y	Specific yield	[-]
t	Time	[d]
Δt	Model time step	[d]
$\Delta t_{control}$	Control time step	[hr]
t_1	An array of length 48, representing discrete time indices 0 through 47	-
t_2	An array of length 49, representing discrete time indices 0 through 48	-
$t_{1,obj}$	An array of length 8, representing discrete time indices 0 through 7	-
$t_{2,obj}$	An array of length 7, representing discrete time indices 0 through 8	-
W_{ditch}	Ditch width	[m]
W_{plot}	Plot width	[m]
Δx	Spatial discretization	[m]
α	Model parameter physical time series model 1 and 2	[d^{-1}]
β	Model parameter physical time series model 2	[d^{-1}]
γ	Drainage resistance	[d]
δ	Deficit	[m]
λ	Model parameter extended physical time series models	[-]
μ	Weighting factor objective function	[-]

1 Introduction

1.1. Relevance of the research

Rapid discharge of excess water has always been the core of Dutch polder water management. Polders are lowland areas that are encircled by embankments known as dikes. A polder is dependent on artificial drainage; surface water levels are controlled by pumping excess water into a higher elevated network of primary canals (Miltenburg 2020). The Dutch polders are designed to facilitate drainage on regional as well as plot scale. Drainage enables regulation of the groundwater table depth (Skaggs et al. 1999; Natural Resources Conservation Service 2001). Subsurface drainage is accomplished by means of deep open drains and underground pipe drains (Brouwer et al. 1985), which both form an essential part of the Dutch polder landscape. Since the Second World War, subsurface drainage pipes have been installed on 34.5% of the agricultural land (equivalent to 654,652 ha) to facilitate drainage on the plot scale (Massop et al. 2016; Ritzema et al. 2015; de Wit et al. 2022). This traditional approach seems logical as approximately 25% of the Netherlands lies below mean sea level (Ritzema et al. 2015), making the country flood prone and dependent on artificial drainage for guaranteeing flood safety. Additionally, agricultural drainage enhances agricultural production (Skaggs et al. 1999), favouring the Dutch economy.

Although the system has proven to be successful in flood control, it is vulnerable to droughts. The Dutch climate is characterized by a precipitation excess in winter, while a precipitation deficit prevails in summer (van Bakel 1986). The current water management strategy results in little water storage, such that deficit soil water conditions may occur during summer, with consequences for nature and agriculture (STOWA s.d.[a]). According to climate scenarios of the Royal Netherlands Meteorological Institute (KNMI), the following changes are to be expected as a result of climate change: 1) an increase of winter and summer temperatures, 2) an increase of total winter precipitation, 3) an increase of extreme precipitation amounts in winter and summer, and 4) a decrease of the number of rainy days in summer (Klein Tank et al. 2009; Royal Netherlands Meteorological Institute (KNMI) 2014). These changes further challenge the proper functioning of the water system. Higher summer temperatures will lead to increased evapotranspiration and a higher rainfall deficit. On the other hand, extreme rainfall events will result in high discharges (Ritzema et al. 2018). If the conventional water management is continued, the drainage and pumping capacity will need to be expanded to process future extreme precipitation events. Furthermore, water shortages will occur more frequently and will be more severe, as a consequence of reduced fresh water supply in combination with higher water demands.

A future-proof water system should thus be able to deal with both extremes: wet and dry. The focus should shift from rapid to gradual drainage of excess water in order to realize this. Ideally, the system is designed and managed such that as much as possible rain water is retained, without conflicting flood safety and crop production. This new approach consists of three steps, which are illustrated by Figure 1.1: 1) retention, 2) storage, and 3) controlled removal. Peak discharges are reduced during periods of excess precipitation, which is beneficial for the water authority. At the same time, water is stored for periods of water shortage, which benefits farmers (Ritzema et al. 2015).

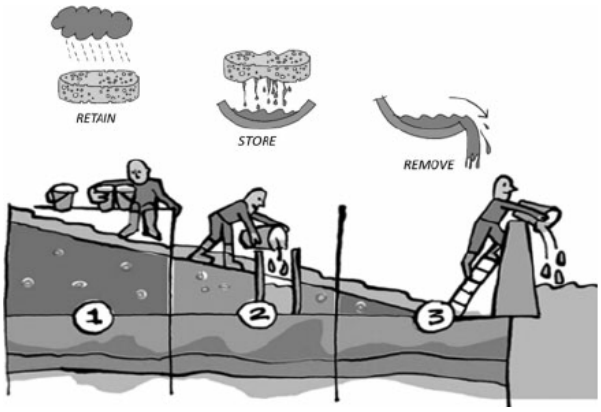

Figure 1.1: Visualization of the new drainage strategy (Ritzema et al. 2015).

1.2. State-of-the-art

A polder is typically divided into multiple ”peilgebieden”. A ”peilgebied” is defined by Bierkens et al. (1999) as ”a contiguous area consisting of multiple parcels for which the surface water levels in the ditches are controlled simultaneously at all times”. Water management is performed by the regional water management authority with the objective of groundwater table regulation. This objective is achieved by manipulation of the surface water level by means of pumps and adjustable weirs. A fixed target surface water level is assigned to each ”peilgebied”, depending on land use and associated drainage needs. A distinction is made between summer and winter target level to take into account the seasonal dynamics of the groundwater system. In winter, the average groundwater recharge is positive. A relatively low winter target level is maintained to prevent flooding. In summer, the average groundwater recharge is negative. A relatively high summer target water level is maintained to prevent excessive groundwater table falling. The pumps and weirs are operated based on actual measurements of surface water level. Since actual soil moisture conditions and groundwater levels are not observed and taken into account, control decisions are based on incomplete information of the available storage capacity in the water system. As a consequence, the available storage capacity is not fully utilized, while this is essential for implementing the new drainage strategy. For that reason water boards have been looking into methods to control surface water levels based on actual groundwater measurements, which is called groundwater-dependent surface water control (Bierkens et al. 1999).

Subsurface drains regulate drainage on the plot scale. From the 1990’s onward, there is a shift from conventional drainage to controlled drainage (de Wit et al. 2022), which is based on the idea that the maximum drainage intensity provided by a conventional drainage system is not required at all times (de Wit et al. 2022; Skaggs et al. 1999). The main objective of controlled drainage is to drain only the minimum amount of water, while still satisfying needs for crop production (Skaggs et al. 1999). Nowadays, controlled drainage is applied on 6.3% of the drained area in the Netherlands (Massop et al. 2016). Multiple water table control systems are available for controlled drainage. From 2018 onward, drainage systems are even adapted to facilitate subirrigation, which is active infiltration of water (de Wit et al. 2022).

Multiple control methods have been developed for groundwater-dependent control of water table control systems (Skaggs et al. 1999; van Bakel 1986; Wonink et al. 1997; STOWA s.d.[b]; Bartholomeus et al. 2015), but Model Predictive Control (MPC) has never been considered. MPC is a model-based controller that originates from the chemical industry and uses forecasts of disturbances to minimize deviations from setpoint during a specific time horizon. Constraints on control actions are also taken into account. Nowadays, MPC is found in many areas of control systems engineering, including operational water management (Arnold et al. 1999). Regarding the relatively slow response of the groundwater system, the anticipatory nature of MPC is expected to be very useful for water table control. However, since

the forecast horizon for which accurate precipitation forecasts are available is restricted, the feasibility of groundwater-based MPC is dependent on the response time of the groundwater system.

1.3. Research problem

This thesis comprises the design and evaluation of a groundwater-based MPC algorithm for the operation of water table control systems in polder areas. The objective is to maximize retention of precipitation, thereby contributing to the first component of the new drainage strategy. This is attempted by maintaining groundwater levels at the maximum admissible level. Geohydrological expertise and knowledge on operational control systems is integrated to resolve the research problem.

The research is executed as a model study and should be interpreted as a proof of concept. This implies that the focus is on demonstrating the feasibility of groundwater-based MPC rather than on delivering a control algorithm that could immediately be put into practice.

The control algorithm is developed for multiple water table control systems. Furthermore, its performance in combination with these systems is assessed for two different case study areas within the management area of water board *Hoogheemraadschap van Rijnland*. Two polders with distinct geohydrological behaviour are selected such that the feasibility of groundwater-based MPC can be determined for systems with varying groundwater response times. Model simulations are performed to compare the performance of the developed control to the performance of the current control. This allows for identification of advantages and disadvantages of groundwater-based MPC and determination of its application range regarding groundwater water response times.

The research problem is translated into the following research questions:

1. *What is encountered when designing a groundwater-based Model Predictive Control (MPC) algorithm and which topics require additional study in order to obtain a functioning control?*
2. *What are the advantages and disadvantages of groundwater-based Model Predictive Control (MPC) compared to the original control and how does this differ for geohydrologically distinct areas and various water table control systems?*

1.4. Reading guide

Chapter 2 provides background information on water table control systems and MPC. The applied methodology is covered in Chapter 3, whereafter Chapter 4 contains a description of the case study polders. Groundwater model construction is discussed in Chapter 5, while the setup of the MPC module is explained in Chapter 6. The results are covered in Chapter 7, 8, 9 and 10. Results concerning the geohydrological response of each system are provided in Chapter 7. Chapter 8 covers model calibration and verification. Results regarding the performance of the developed MPC algorithm are shown in Chapter 9. Chapter 10 covers the results of a sensitivity analysis. A discussion of the results is provided in Chapter 11. Finally, this thesis is concluded by answering the research questions and providing recommendations for future research.

2

Background information

This chapter provides background information on water table control systems and Model Predictive Control (MPC), which is required to resolve the research problem. Section 2.1 covers multiple water table control systems, whereas MPC theory is addressed in Section 2.2.

2.1. Water table control systems

Figure 2.1 schematizes four drainage systems for water table control (B to E) on an agricultural plot that is surrounded by a ditch. Additionally, the undrained situation is depicted (A). Figure 2.2 contains similar schematizations, but these are constructed from another viewpoint. It should be noted that the operational control of the depicted drainage systems is substantially different. The surface water level is maintained at a constant level (corresponding to summer or winter target level) in case of system A, B and E, while a variable surface water level is applied in case of system C and D. Figure 2.1 shows that weirs are used to regulate ditch and/or sump water level. Background information on the operational control of these weirs is provided in Appendix A.

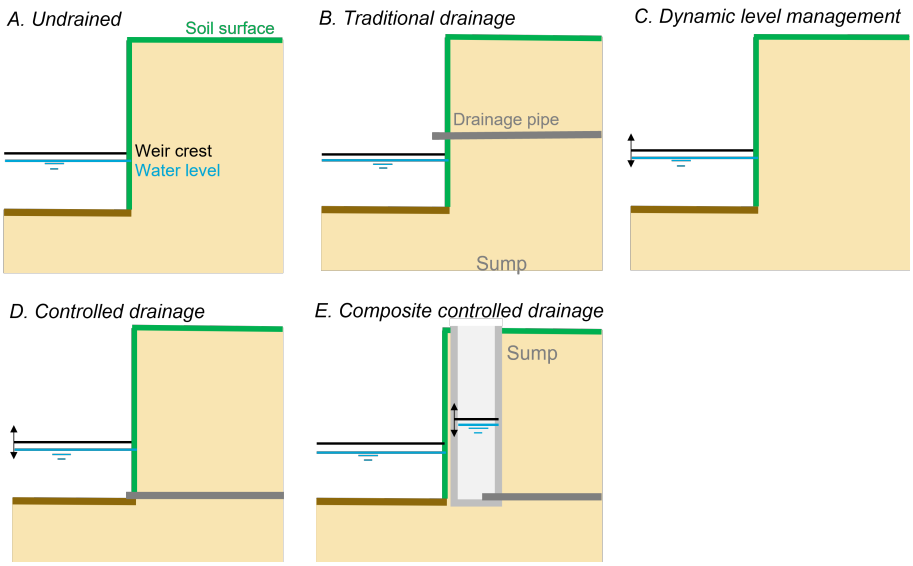

Figure 2.1: Schematic drawings water table control systems (B to E), viewpoint 1. Drawing A depicts the undrained situation.

Undrained

The undrained situation, which is depicted in Figure 2.1A, is considered to illustrate the need for drainage. Figure 2.2A shows significant bulging of the groundwater table, which typically occurs during

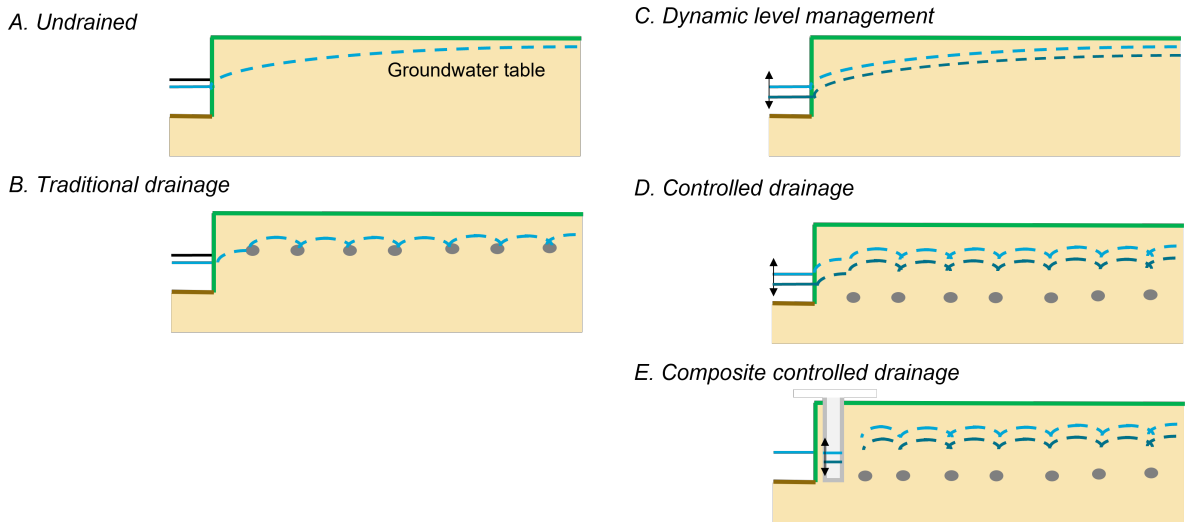

Figure 2.2: Schematic drawings water table control systems (B to E), viewpoint 2. Drawing A depicts the undrained situation.

periods of precipitation excess as a result of groundwater recharge (de Wit et al. 2022). The lower the hydraulic conductivity of the soil, the more convex the water table. The head gradient between the centre of the plot and the ditch induces a net flux from the groundwater system towards the surface water system. The bulging groundwater table leads to high soil moisture levels, especially in the centre of the field. The water table becomes concave during periods of precipitation deficit, such that a net flux from the surface water system towards the groundwater system develops. The falling ground water table leads to low soil moisture levels, especially in the centre of the field (Bierkens et al. 1999).

Traditional drainage

Traditionally, drainage pipes are installed at a certain depth below surface level and discharge into a ditch. The outflow point lies above ditch water level, like illustrated by Figure 2.1B. The drainage pipes actively discharge groundwater. Drainage ceases as soon as the groundwater level falls below the basis of the drainage system (de Wit et al. 2022). Figure 2.2B again depicts the groundwater table that occurs due to groundwater recharge. Compared to the undrained situation, traditional drainage leads to a significantly lower and more uniform groundwater table (van Bakel et al. 2013), which favours agricultural production (Ritzema et al. 2015; de Wit et al. 2022; Skaggs et al. 1999). Benefits of traditional drainage are: 1) improved workability (land cultivation is enabled early in the season, thereby lengthening the growing season), 2) improved aeration (favouring root activity), 3) improved sanitation (as stagnant water pools are prevented), and 4) a reduction in surface runoff (reducing erosion). Disadvantages of traditional drainage are: 1) disappearance of wetlands (valuable habitat of bird species), 2) summer drought stress (limited water storage), 3) high peak discharges during rain events, and 4) loss of nutrients (Skaggs et al. 1999).

Dynamic level management

Dynamic level management is a form of groundwater-dependent surface water control; measurements of the water table depth at a reference location determine the crest level of an adjustable weir, which in turn regulates the surface water level. This is illustrated by Figure 2.1C and Figure 2.2C. Note that subsurface drainage pipes are absent. Dynamic level management is founded on the fact that the groundwater table in the field directly depends on the surface water level in the encircling ditches, as the ditch water level acts as a boundary condition for the groundwater system (Bierkens et al. 1999; STOWA s.d.[b]). More storage capacity is created by raising the weir crest. As a consequence, the surface water level increases, groundwater discharge reduces and a higher groundwater table is obtained. On the other hand, groundwater discharge is enhanced by lowering the surface water level. In conclusion, the drainage intensity varies with surface water level, which implies that dynamic level management could be interpreted as a form of controlled drainage. If one is able to control the surface water level, the groundwater table can be controlled approximately (Bierkens et al. 1999). The delay

between weir crest level change and groundwater response is significant, which complicates control. Dynamic level control is more feasible in areas with permeable soils, due to the rapid interaction between the surface water and groundwater system (STOWA s.d.[b]).

Controlled drainage
Figure 2.1D depicts controlled drainage. The system components are comparable with traditional drainage, but the drainage pipes are submerged. The degree of drainage is again controlled by the ditch water level, because the water pressure in the drainage pipes is equal to the surface water level. This is illustrated by Figure 2.2D. Since surface water levels are maintained per ”peilgebied”, the same water pressure is exerted on all drainage pipes within one ”peilgebied” (de Wit et al. 2022). The delay between weir crest adjustment and groundwater response is much shorter compared to dynamic level management, due to the high density of drainage facilities. Nonetheless, the system response is still relatively slow, because large volumes of water must be moved to change the ditch water level due to the relatively large surface area of the ditch.

During periods of precipitation deficit, evaporation losses are not compensated. This leads to a gradual decrease in surface water and groundwater level. When the surface water level falls below the basis of the drainage system, the subsurface drains are no longer pressurized and a traditional drainage system is obtained. A falling surface water and groundwater level can be prevented by: 1) blocking the drainage outlet, and 2) guaranteeing continuous water supply to maintain a fixed surface water level. This triggers subirrigation (Skaggs et al. 1999), which is defined by Natural Resources Conservation Service (2001) as the ”application of irrigation water below the ground surface by raising the water table to within or near the root zone” (reverse drainage). Evaporation losses are thus compensated (Skaggs et al. 1999). This system is referred to as passive water infiltration system (PWIS) (Hoekstra et al. 2022). Through slight modifications, the water table control system depicted in Figure 2.1D can thus operate in three drainage modes: traditional drainage, controlled drainage and subirrigation (Skaggs et al. 1999).

Composite controlled drainage
Composite controlled drainage is a more advanced form of controlled drainage. Figure 2.1E shows that the drains are connected to a sump, instead of the ditch. Figure 2.3 contains a 3D image. The drain pipes are connected to a collector pipe at the end of the field. The collector pipe drains into a sump, which acts like a control pit as the sump water level determines the degree of drainage (Figure 2.2E). The water pressure in the drainage pipes is equal to the water level in the sump. Due to the sump, the system behaves independently from the ditch water level. As a consequence, the groundwater table can be regulated per agricultural plot instead of per ”peilgebied” (de Wit et al. 2022; Skaggs et al. 1999; STOWA s.d.[a]). Additionally, the system response time is very short, because of the small sump area.

Just like system D, system E can be modified to facilitate subirrigation. The obtained system is referred to as active water infiltration system (AWIS) (Hoekstra et al. 2022).

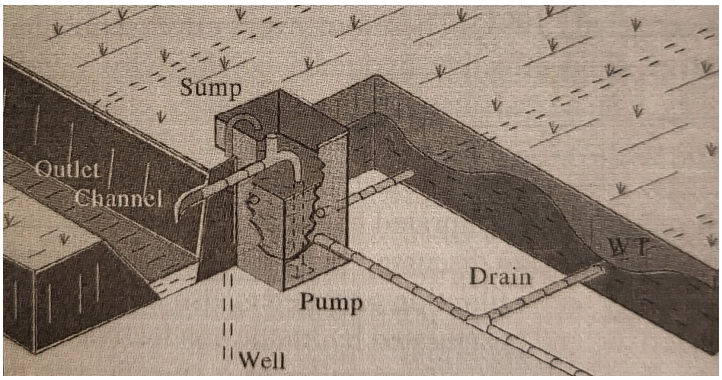

Figure 2.3: 3D drawing composite controlled drainage (Skaggs et al. 1999).

Advantages of groundwater-dependent surface water control and controlled drainage are:

- Reduced fluctuations of water table depth, leading to increased agricultural yield (Skaggs et al. 1999),
- Controlled durations of excessive and deficient soil moisture conditions, leading to increased agricultural yield (Fouss et al. 2007),
- Reduced irrigation water demands, leading to reduced energy requirements (Skaggs et al. 1999),
- Decrease in subsidence (relevant for peaty areas), resulting in lower costs for water management, and sewerage and road maintenance (STOWA s.d.[b]).

Specific advantages of (composite) controlled drainage are:

- Reduced agrochemical (e.g. fertilizers) losses from agricultural land, leading to improved water quality of drainage water (Fouss et al. 2007),
- Reduced surface runoff, leading to reduced erosion (Skaggs et al. 1999).

Disadvantages of groundwater-dependent surface water control and controlled drainage are:

- Costs; a composite controlled drainage system is approximately twice as expensive as a traditional drainage system (STOWA s.d.[a]) and groundwater monitoring wells have to be installed (STOWA s.d.[b]),
- Since average groundwater levels are higher, reduced storage capacity is available to accommodate extreme precipitation events (STOWA s.d.[b]),
- Risk of weak embankments, if large water level variations are applied (STOWA s.d.[b]).

Regarding feasibility, it should be noted that the systems only succeed in water retention if an impermeable layer or layer of low hydraulic conductivity (e.g. clay or peat layer) is found at some depth. The impermeable layer prevents downward seepage (Fouss et al. 2007; Skaggs et al. 1999).

Many pilots have been performed to test the potential of controlled drainage. Controlled drainage systems have been applied on peaty, sandy and clayey soils throughout the Netherlands (Stuyt 2016).

2.2. Model Predictive Control (MPC)

The control method Model Predictive Control (MPC) is a model-based controller that originates from the chemical industry. It is advanced and computationally expensive, which means that it is an appropriate method when quality standards are stringent. In 2006, van Overloop presented MPC for the control of hydraulic structures in open water systems. The information in this section is retrieved from van Overloop (2006), unless otherwise stated.

Figure 2.4 schematically summarizes water system management. Water system management aims at maintaining the system state close to the desired state, which is often defined in terms of water levels. A constant desired system state is called a *setpoint* (van Nooijen et al. 2021). Disturbances, like precipitation and evaporation, influence the water system and result in deviations from the desired system state. By measuring disturbances, required control actions to keep the system close to setpoint can be calculated and executed. This is called feedforward control. Disturbances are also known as uncontrolled inputs. Control actions are performed by *actuators* (van Nooijen et al. 2021). Weirs and pumps are common actuators for open water systems, such that examples of control actions are adjustments to weir crest height or pumping rate. By monitoring the actual state of the system, it can be checked whether the control actions were successful in keeping the system close to the desired state or whether additional control actions are required. This is called feedback control. Monitoring of the actual system state is performed by a *sensor*. The *process output* is typically a small part of the system state (van Nooijen et al. 2021). The frequency with which control actions are executed is determined by the *control time step*. The range of possible control actions is often constrained by the properties of the actuator (van Nooijen et al. 2021). Examples of physical constraints are maximum weir crest height and pumping capacity.

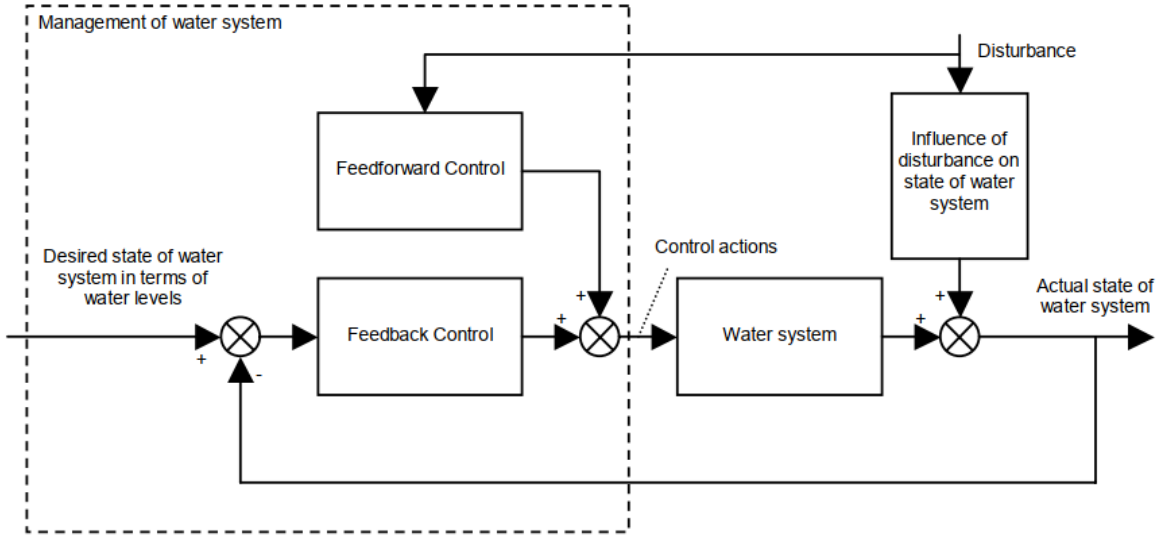

Figure 2.4: Schematic summary water system management (van Overloop 2006).

The required control actions are determined by the *controller*. The control actions may be directly forwarded to and implemented by the actuator. Sometimes human intervention is desired and the controller has an advisory role. The control actions are send to the responsible operator, who subsequently decides whether they should be implemented or not. This is the case for a Decision Support System (DSS). Disturbances are part of the controller input in case of feedforward control, while the process output is part of the controller input in case of feedback control. The usefulness of MPC is demonstrated in Appendix B.

Regarding water level control, MPC typically uses forecasts of disturbances to minimize deviations from setpoint during a specific prediction horizon. An internal model that represents the physical system is applied to determine the effect of control actions. In this respect, it can be seen as a repetitive optimization procedure in which feedback control on the measured water levels and feedforward control on the predicted disturbances are constantly alternated in order to determine the optimal control actions. Constraints on structures are also taken into account. The prediction horizon is subdivided into control time steps. The optimal control actions are determined for all control time steps within the prediction horizon, while the control action for the first step is actually implemented. The prediction horizon recedes such that control decisions are always based on the most recent forecasts of disturbances.

Figure 2.5 contains a structure diagram of MPC. The main characteristics of MPC are highlighted: 1) internal model, 2) objective function, 3) constraints, 4) optimization, and 5) receding horizon. Below, each component is discussed separately.

Internal model

The internal model is an approximation of the actual system and is used to predict future states of the controlled system. The internal model takes forecasts of future disturbances as input, as well as present and future control actions. Simulated process output (e.g. future water levels) forms the output of the internal model. The internal model should be sufficiently accurate to ensure a proper representation of the physical system. At the same time, the model run time should be limited to ensure that the optimization is completed within one control time step. Due to the receding prediction horizon, the model is continuously rerun and model predictions are restricted to the near future. This allows for the application of a relatively simple model, without compromising on accuracy. For example, the physical water system is non-linear and a linearization is often performed to convert the non-linear system into a linear system. The linear model is written in the state-space form:

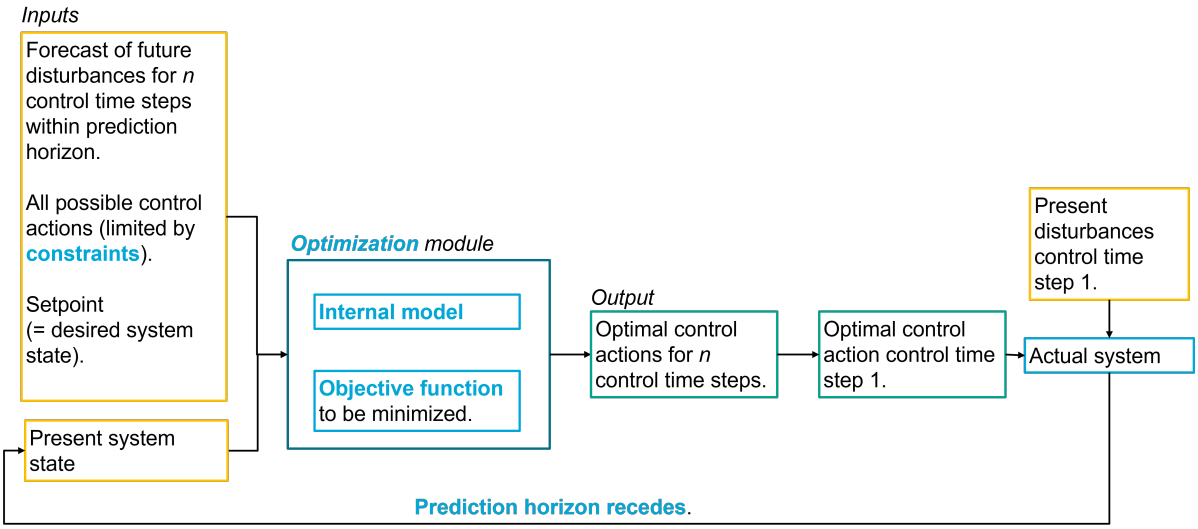

Figure 2.5: Structure diagram MPC.

$$x(k+1) = A(k) \cdot x(k) + B_u(k) \cdot u(k) + B_d(k) \cdot d(k) \tag{2.1}$$

$$y(k) = C \cdot x(k) \tag{2.2}$$

where x is a vector containing the states of the water system, A is the system matrix, B_u is the control input matrix, B_d is the disturbance input matrix, u is a vector containing the controlled inputs, d is a vector containing the disturbances, C is the output matrix, y is a vector containing the process outputs and k is the time step index.

Equation 2.1 determines the states in time step $k+1$ based on the states in time step k and the controlled and uncontrolled inputs. The matrices A, B_u and B_d represent the physical processes and determine the evolution of the system state. The state-space model can be extended over the prediction horizon. It is referred to van Overloop (2006) for a detailed explanation.

Objective function
The control objectives are translated into an objective function. The optimal control actions are found by minimizing the objective function. A distinction is made between the main objective and secondary objectives. The main objective is to maintain the system state close to setpoint. This implies that the deviation from setpoint should be minimized over the prediction horizon. Vector x, which contains the system states for the entire prediction horizon, should thus be part of the objective function. Possible secondary objectives are related to the frequency with which structure settings may be adjusted or minimization of energy consumption. Since these sub-objectives are related to the controlled input, the vector u is also included in the objective function. A quadratic objective function is commonly applied, such that both positive and negative deviations are penalized and higher absolute deviations are penalized more than proportional.

Weight matrices may be applied to indicate the relative importance of the sub-objectives. Sub-objectives may namely conflict with the primary objective and mutual conflicts may occur. Relative penalties are given to these sub-objectives via the weight matrix in order to obtain a sensible solution.

Constraints
Physical limitations and operational specifications may impose constraints on the possible solutions of the optimization problem, thereby narrowing the solution area. Physical limitations are often related to limited capacities of structures, like maximum pump capacity or maximum weir crest height. An

example of an operational specification is the specification of a range of acceptable water levels. Constraints may be hard or soft. Hard constraint may never be violated. Soft constraints may be violated, although this is prevented by assigning extra weights. The application of hard constraints is preferably avoided, because the application of numerous conflicting, hard constraints may disable solution finding.

Optimization
In order to determine the optimal control actions, the objective function is minimized. Several numerical optimization algorithms are available. The internal model is an integral part of the optimization algorithm. Attention should be paid to:

1. Computational speed,
2. Stability,
3. Robustness,
4. Performance.

Receding horizon
The optimization procedure determines the optimal control actions over the entire prediction horizon. However, only the first set of control actions is actually implemented. After one control time step, the entire optimization process is repeated. In this way, the horizon recedes into the future, always using the most recent measurements and predictions.

3

Methodology

3.1. Envisaged control

Based on the literature study, three variants of water table control systems are selected to be researched:

1. Water table control without drains (following the principles of dynamic level management, Figure 2.1C).
2. Water table control with submerged drains, controlled by ditch water level (following the principles of controlled drainage, Figure 2.1D).
3. Water table control with submerged drains, controlled by sump water level (following the principles of composite controlled drainage, Figure Figure 2.1E).

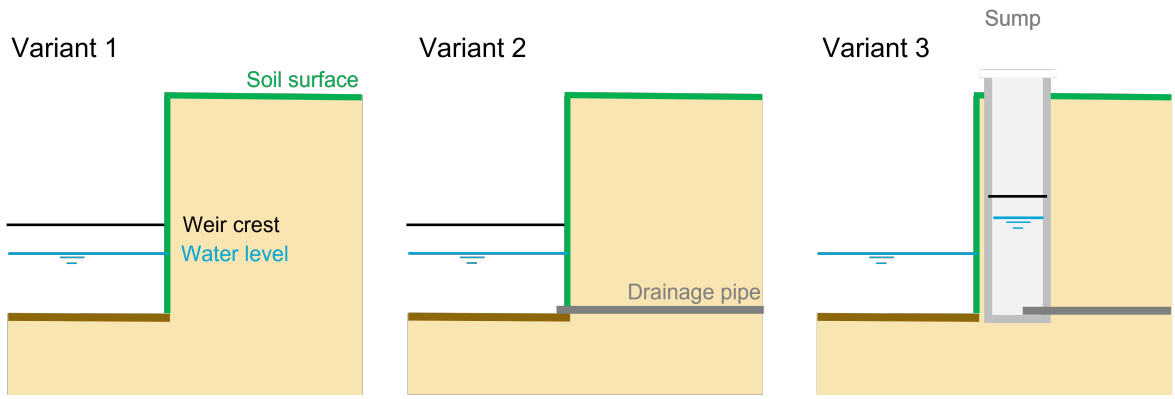

Figure 3.1: Three variants of water table control systems.

These will be referred to as variant 1 to 3. The variants are schematically illustrated by Figure 3.1. Like explained in Chapter 2, these systems may operate in various modes (traditional drainage, controlled drainage and subirrigation mode). The control algorithm that is developed in this thesis is limited to the controlled drainage mode, since retention, storage and controlled removal of rain water is of our interest. Firstly, the drains are positioned such that the elevation of the bottom of the drains coincides with the elevation of the bottom of the ditch, such that the drains are permanently pressurized. This avoids making design choices regarding the depth of the drainage pipes and the associated transition between traditional and controlled drainage. Secondly, external water supply by water inlets or pumping stations is not considered, which means that water levels fall during periods of precipitation deficit. The control problem is restricted to retention of precipitation and the control of water discharge during extreme precipitation events by means of a weir, which simplifies the control problem significantly.

A groundwater-based MPC algorithm is developed for the operation of each of these three water table control systems on a plot surrounded by a ditch. A top view of the plot is provided in Figure 3.2. The objective is to maximize retention of precipitation. As a first approach, this is attempted by maintaining the groundwater level in the centre of the field at the maximum admissible level (setpoint). This approach is in accordance with the nature of the research; a proof of concept. Concrete implications are:

- Dry periods must be anticipated for by storage of pre-drought precipitation and a temporary, high groundwater table must be accepted.
- Wet periods must be anticipated for by pre-storm groundwater discharge and a temporary, low groundwater table must be accepted.
- The groundwater storage must be effectively utilized.

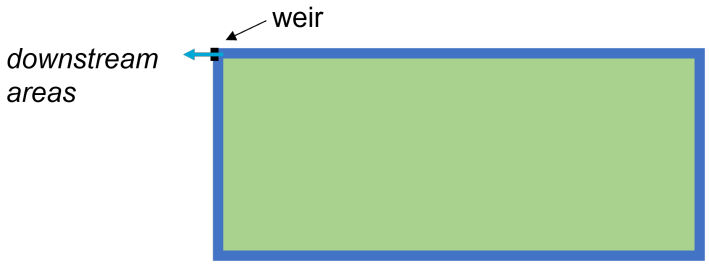

Figure 3.2: Top view plot.

The controller is designed to regulate the crest level of a weir (actuator). In variant 1 and 2, the weir controls the ditch water level and discharge to downstream areas. In variant 3, the weir determines the sump water level and discharge from the sump to the ditch. It should be noted that downstream areas are not considered, so downstream problems (e.g. floods, droughts) that occur due to the operation of the water system in the area under consideration are not taken into account. By affecting the ditch or sump water level, the weir indirectly determines the groundwater discharge and groundwater level. The controller inputs are precipitation forecasts and initial states of the system. In practice, the system state would be measured by a sensor that is installed in a groundwater monitoring well. Since this research is performed as a model study, the actual system state is simulated by a groundwater model. The controller output is the optimal weir crest height, that minimizes the deviation from setpoint up to the end of the time horizon.

3.2. Procedure

The applied procedure is summarized by Figure 3.3. The procedure is executed for two polders that are located in the management area of water board *Hoogheemraadschap van Rijnland*: *Polder Het Langeveld* and *Polder Vierambacht*. The soil profile in these areas are different so systems with different geohydrological response times are considered. A description of the case study areas is found in Chapter 4.

The research activities are subdivided into four main parts:

- I. Qualitative analysis water system,
- II. Modelling,
- III. Developing control,
- IV. Evaluation.

Part III forms the core of the research, as it comprises the development of the groundwater- and MPC-based control algorithm, whereas Part I and II serve as preparatory steps. A qualitative analysis of the existing water system is performed in Part 1. The groundwater models that are applied in the MPC algorithm are developed in Part II. Together, Part I to III address research question 1. Research question 2

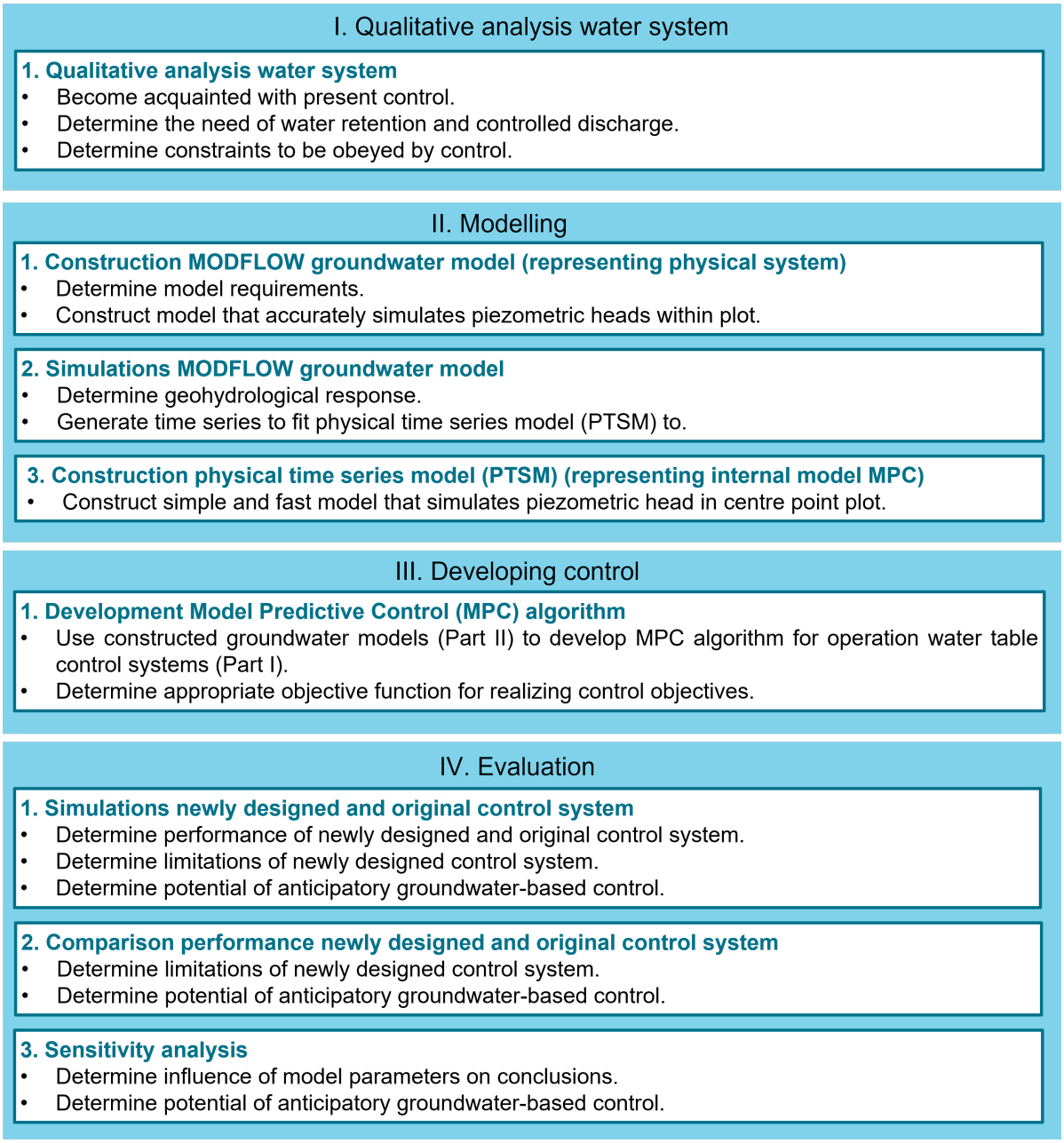

Figure 3.3: Overview applied procedure.

is addressed by Part IV, in which the performance of the developed groundwater-based MPC algorithm is evaluated and compared to the performance of the present control. An elaborate description of each research phase is provided below.

I. Qualitative analyse water system
The water systems of the two case study areas are qualitatively analyzed using drainage schemes and the ”legger” (valid on 25/07/2022) to become acquainted with the current control. The ”legger” is a register that is managed by the water board and contains the dimensions and locations of all ditches, canals, weirs, pumps and culverts within the management area. Furthermore, one of the two case study areas (*Polder Het Langeveld*) is visited with the responsible level manager (in Dutch: ”peilbeheerder”, who controls the pumping stations and automated weirs) and water system manager (in Dutch: “watersysteembeheerder”, who manages the manual weirs and keeps in contact with the population).

II. Modelling
A numerical groundwater model is developed for each case study area by means of MODFLOW 6 software, developed by the United States Geological Survey (USGS). FloPy, a Python package that was developed by Bakker et al. (2016), is used to set up the groundwater model. Subsection 3.3.1 provides background information on MODFLOW 6 and FloPy. The extent of the model is limited to one field that is surrounded by a ditch. The (geohydrological) characteristics of the plot are chosen such that the plot represents the ”average” plot within the polder. The MODFLOW model represents the physical system and is used to update the system state. Figure 3.4 shows the position of the MODFLOW model in the MPC algorithm. All variants of water table control systems can be simulated by the MODFLOW model. Additionally, the present situation can be modelled, which is required for research phase 4. Chapter 5 contains a detailed explanation of the MODFLOW model construction.

MODFLOW simulations are performed to evaluate the geohydrological response of both case study areas in combination with each of the three water table control systems. The simulations are performed for numerous purposes:

1. Verification of the model schematization,
2. Evaluation of the geohydrological response of plots that are located in different case study areas to all possible control actions,
3. Provision of groundwater level time series for physical time series model (PTSM) calibration.

Since the groundwater level in the centre of the field is of interest, specific attention is paid to the geohydrological response at this point.

The MPC internal model is usually written in the form of Equation 2.1, such that the optimization problem can be formulated in terms of matrix calculations and the internal model is integrated into the optimization problem. The MODFLOW groundwater model is run in separate software, which means that it cannot be integrated into the optimization problem. Therefore, the MODFLOW groundwater model should be run for all combinations of possible control actions to find the combination of control actions that minimizes the objective function. Many combinations exist due to the eight-dimensional solution space (eight control time steps within prediction horizon, which is explained below). For example, if four weir crest heights are possible per control time step, this would result into 4^8 possible combinations. Although advanced solution finding techniques could significantly reduce the amount of required calculations, 1000 required calculations are not unthinkable. For the smallest MODFLOW model (Polder Het Langeveld), the calculation time for a 48 hour simulation (length prediction horizon is 48 hours, which is explained below) is approximately 1 minute and 20 seconds. This would result in a calculation time of approximately 1 day per MPC step, which is not feasible. A physical time series model (PTSM) is derived from a differential equation, based on models described by van der Gaast et al. (2009). Unlike the MODFLOW model, the PTSM is restricted to the centre point of the plot and is written in the form of Equation 2.1. The PTSM is fitted to MODFLOW groundwater level time series, such that a fast groundwater model is obtained that reproduces the geohydrological behaviour with limited computational effort and sufficient accuracy. A discretized form of the PTSM is applied as internal model in the MPC module, which is illustrated by Figure 3.4. Section 5.2 contains a detailed description of the PTSM.

III. Developing control
Like explained, the constructed groundwater models are integrated into the MPC algorithm that is depicted in Figure 3.4 and constructed using the programming language Python. The algorithm consists of two main modules:

1. MPC module (representing the controller),
2. Update module (representing the physical system).

The optimal weir crest level is determined by the MPC module, which is developed using the Python-based software package *Python Optimization Modeling Objects* (Pyomo). Background information on this software is provided in subsection 3.3.2. The MPC module is constructed according to MPC theory, which means that it contains the standard MPC components. Chapter 6 covers the formulation of the Pyomo optimization model. Pyomo itself does not solve the optimization problem, but passes

the problem to an external solver (Bynum et al. 2021). The Interior Point Optimizer (IPOPT), which is an open-source solver for large-scale nonlinear programming, is applied as external solver (GAMS Development Corp. GAMS Software GmbH s.d.). The calculation time per MPC step is approximately 0.24 seconds, which is hardly anything compared to the time that would be needed if the MODFLOW model was applied as internal model.

The PTSM is applied as *internal model*. The *prediction horizon* and *control time step* are tuned to available precipitation forecast data, which are described in Section 3.4, resulting in a prediction horizon of 48 hours and a control time step of 6 hours. Continuous adjustments of weir crest level are avoided by limiting the adjustment frequency to 6 hours, such that the weir crest level is constant during one control time step. The controller output consists of 8 optimized weir crest levels ($h_{weir,control}$ [m NAP [1]]), since the prediction horizon consists of 8 control time steps.

The controller inputs are:

- A 48 hour weather forecast, providing forecasts on hourly precipitation (P [mm/hr]) and evaporation (reference evaporation (E_{ref} [mm/hr]) and open water evaporation (E_o [mm/hr]).
- Physical and operational *constraints* on weir settings ($h_{weir,control}$ [m NAP]). A minimum weir crest level ($h_{weir,min}$ [m NAP]) and a maximum weir crest level ($h_{weir,max}$ [m NAP]) are defined. The absolute change in weir crest level ($|\Delta h_{weir,control}|$ [m]) between consecutive control time steps is restricted by $\Delta h_{weir,control,max}$.
- A groundwater level *setpoint* ($h_{GW,setpoint}$ [m NAP]), representing the desired groundwater level in the centre of the field. To maximize retention of precipitation, the maximum admissible groundwater level is selected.
- Initial conditions, representing the present system states. $h_{GW,initial}$ [m NAP] represents the present groundwater level in the centre of the field, $h_{SW,initial}$ [m NAP] represents the present ditch/sump water level, and $h_{weir,initial}$ [m NAP] represents the present weir crest level.

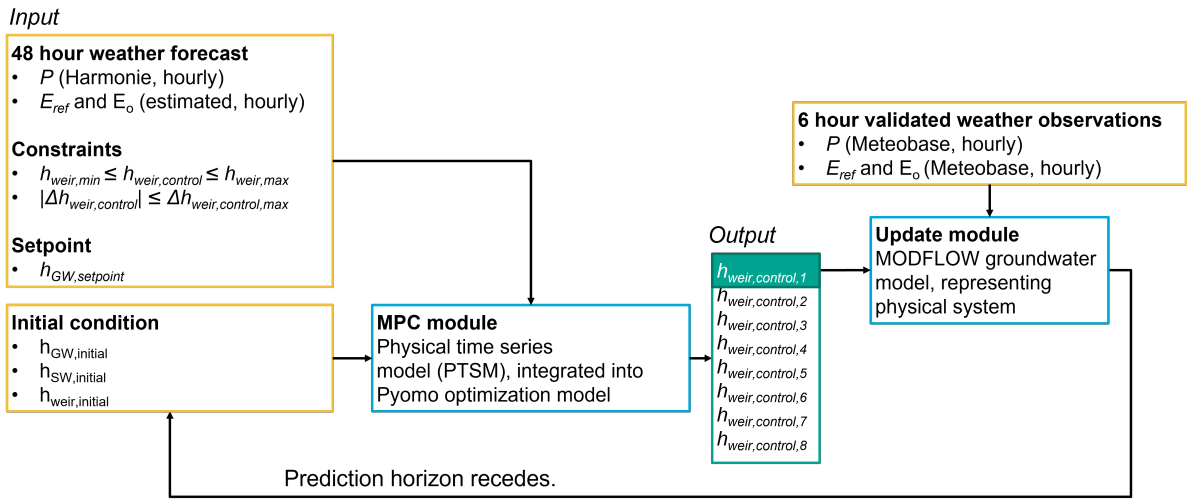

Figure 3.4: MPC algorithm.

The optimized weir crest levels are determined by minimizing an *objective function*, which takes the difference between the actual groundwater level and setpoint at the end of each control time step as input. Only $h_{weir,control,1}$, which is the optimal weir crest level for control time step 1, is forwarded to the update module. The update module contains the MODFLOW groundwater model and updates the initial condition. It takes 6 hour validated precipitation and evaporation observations as input. The observed precipitation may differ from the forecasted precipitation, which means that the actual system state may differ from the predicted system state. As the prediction horizon recedes, the renewed initial

[1] NAP stands for "Normaal Amsterdams Peil" and is a vertical datum to which height measurements in the Netherlands are related.

conditions are again forwarded to the MPC module and a new precipitation forecast becomes available. As such, control actions are always based on the most recent forecast. Delays due to forecast retrieval, MPC calculations and actuator response are neglected.

IV. Evaluation
The final step includes a performance evaluation of the developed MPC algorithm and a sensitivity analysis.

Performance evaluation
The MPC algorithm is run using historical precipitation forecasts and historical validated precipitation and evaporation data. The historical precipitation forecasts originate from the HARMONIE (HIRLAM ALADIN Research on Mesoscale Operational NWP in Euromed) weather model, which is owned by KNMI (Royal Netherlands Meteorological Institute (KNMI) s.d.[b]). The applied data set, which is supplied by Hoogheemraadschap De Stichtse Rijnlanden (HDSR), runs from 01/06/2018 to 31/12/2018. Although HARMONIE delivers forecasts of evaporation related parameters, these are unfortunately not at our disposal. Therefore, a constant monthly evaporation is assumed, based on Figure 4.5. Subsection 3.4.1 contains a brief description of the HARMONIE data. Historical precipitation and evaporation data are downloaded for the same time period via Meteobase, an online archive for the Netherlands (Versteeg et al. 2013). Some background information is provided in subsection 3.4.2. HARMONIE as well as Meteobase data are delivered in a country-wide raster format such that distinct data sets are obtained for both polders.

Three types of simulations are performed:

1. Simulations to evaluate the performance of the MPC module (i.e Pyomo model),
2. Simulations to evaluate the performance of the MPC algorithm,
3. Simulations to assess the performance of the MPC algorithm for incorrect precipitation forecasts.

Since water supply is not considered, the MPC algorithm is not suitable for periods of long-term drought. This would result in extremely low ditch water levels, which is not realistic as external water inlet from canals and rivers is typically possible in a polder system. For that reason, short periods of time with substantial precipitation amounts are selected from the available data. To assess the performance of the MPC algorithm, the present control is simulated for the same time periods. It is difficult to describe the present control by a model, because weirs are often manually adjusted according to system insight, meaning that weir operations may even be operator dependent. The water board strives to maintain the ditch water level close to a specific target level by means of weirs and pumps. Since water inlet is not controlled by the MPC algorithm, water levels drop during periods of drought. Because the present control includes external water supply, it is an inappropriate reference for performance evaluation of the MPC algorithm. It is therefore decided to neglect water supply in the present situation and assume a constant weir crest level, equal to target water level. The surface water level may fall below target water level during periods of drought. The transition from summer to winter target level takes place instantaneously at 23/09/2018, which is exactly halfway the regular transition period (Waterschap Brabantse Delta s.d.) [2]. This is believed to be the best possible approximation of the present control. An elaborate description of the performed simulations is provided in Chapter 9.

Sensitivity analysis
A sensitivity analysis is performed to determine the influence of the selected model parameters on the obtained results and to further evaluate the potential of groundwater-based MPC for systems with different groundwater response times. The analysis is limited to variant 2, Polder Het Langeveld, for which a reason is provided later. The geohydrological characteristics of the plot and drain spacing are adjusted multiple times, such that systems with different geohydrological response times are obtained. Once the required models are constructed, the MPC algorithm is run to evaluate its performance for each system. This allows for determination of its application range regarding groundwater response times. A complete description is provided in Chapter 10.

[2] The transition period is the same for every water board.

3.3. Software description

3.3.1. MODFLOW 6

MODFLOW is a widely used model to simulate groundwater flow. It has been under development by the United States Geological Survey (USGS) since 1981.

Three-dimensional groundwater flow is described analytically by Darcy's law:

$$\mathbf{q} = -\mathbf{K}\nabla h \tag{3.1}$$

where **q** is the specific discharge vector [m/d], **K** is the hydraulic conductivity tensor that contains the values of hydraulic conductivity along the x, y and z coordinate axes [m/d], h is the piezometric head [m], and ∇h is the head-gradient vector [-]. If the x, y and z directions are the principle directions of the hydraulic conductivity tensor, Equation 3.1 can be written as:

$$\begin{pmatrix} q_x \\ q_y \\ q_z \end{pmatrix} = - \begin{pmatrix} K_{xx} & 0 & 0 \\ 0 & K_{yy} & 0 \\ 0 & 0 & K_{zz} \end{pmatrix} \begin{pmatrix} \frac{\partial h}{\partial x} \\ \frac{\partial h}{\partial y} \\ \frac{\partial h}{\partial z} \end{pmatrix} \tag{3.2}$$

When Equation 3.2 is combined with a water balance on a small control volume, the following partial differential equation is obtained:

$$\frac{\partial}{\partial x}\left(K_{xx}\frac{\partial h}{\partial x}\right) + \frac{\partial}{\partial y}\left(K_{yy}\frac{\partial h}{\partial y}\right) + \frac{\partial}{\partial z}\left(K_{zz}\frac{\partial h}{\partial z}\right) + Q'_s = S\frac{\partial h}{\partial t} \tag{3.3}$$

where Q'_s is the volumetric flux per unit volume [d^{-1}], representing sources and sinks of water, S is the storage coefficient [m^{-1}], and t represents time [d].

Equation 3.3 can be solved analytically for simple groundwater flow situations, whereas numerical methods are required for complex cases. Various 2D and 3D finite-difference models were developed in the past. MODFLOW was developed in the 1980's to merge all developed models into one code, using the FORTRAN programming language. Initially, the focus was on solving the groundwater flow equation (Equation 3.3), but the capabilities of MODFLOW were gradually expanded by adding other related equations. The groundwater flow equation is tackled by the Groundwater Flow (GWF) Process (Langevin et al. 2017).

The latest version of MODFLOW is MODFLOW 6, which implements the principles of objected-oriented programming (OOP) (Langevin et al. 2017). Similar program functions, computational options and hydrological features are grouped into classes. A class represents a blueprint, which contains information on the characteristics that are shared by all instances of the class. The class blueprints are used to construct concrete objects. For example, the well class may be used as a blueprint to define all wells. The functions that are contained by a class are called methods. These may describe operations or relationships with other classes (Bakker et al. 2009) (Doherty 2020). The result is a modular structure in which each option is independent of other options (Langevin et al. 2017).

The GWF Model is divided into packages. There are three types of packages:

1. Hydrologic/Internal packages, which define the spatial and temporal discretization, initial conditions etc.
2. Hydrologic/Stress packages, which include the description of boundary conditions, recharge etc.
3. Hydrologic/Advanced Stress packages, which contain similar functionalities as the Hydrological/Stress packages, but are of higher complexity (Langevin et al. 2017).

The control-volume finite-difference (CVFD) method is the standard method applied by MODFLOW to solve Equation 3.3 numerically. The continuous system is discretized in space and time. The spatial domain is divided into cells, whose centres are called nodes. The head values are evaluated at these nodes for discrete points in time. Thereafter, the partial derivatives between adjacent cells are calculated from the differences in head values. Subsequently, the groundwater flow between cells is expressed as a function of the partial derivatives and the conductance (the ease with which water

flows) between cells. The temporal discretization is performed according to the backward-difference scheme. The CVFD equations are obtained by applying the continuity equation for each cell. This results in a system of linear equations. The solution, which contains head values at each node at the end of a given time step, is found using iterative methods. The calculation is started by assigning trial values for the head at each node. The trial values are updated through a number of iterations until the heads converge towards the solution and improvements resulting from succeeding iterations become negligible. This calculation procedure is repeated for every time step. For a complete description of all associated equations, it is referred to Langevin et al. (2017).

When the CFVD method fails to converge, the Newton-Raphson method can be applied instead. This method is more advanced. A description can be found in Langevin et al. (2017).

FloPy is used to set up the groundwater model. FloPy is a Python package that was developed by Bakker et al. (2016) to build and run MODFLOW models and analyze model results. The user defines the model grid, temporal discretization, aquifer characteristics, initial conditions, boundary conditions and solver parameters by setting Python variables. MODFLOW input files are then automatically generated by FloPy. Finally, the script can be used to run the model and process results.

3.3.2. Python Optimization Modeling Objects (Pyomo) software

Python Optimization Modeling Objects (Pyomo) software aids the formulation of complex optimization problems. Pyomo is an algebraic modelling language (AML), which allows modelers to formulate optimization problems on a conceptual level and automates the translation into a mathematical problem (Fourer 2013). Pyomo models can be constructed using Python. A model object is constructed, after which model attributes can be defined.

Since multiple optimization problems of the same kind are often involved, abstract models are preferred. An abstract model represents a general optimization model, which can be initialized by providing specific data. The following modelling components can be assigned to a Pyomo model:

1. Decision variables,
2. Objective expressions,
3. Constraint expressions,
4. Set data that is used to define a model instance (set data typically specifies the indices for indexed components),
5. Parameter data that is used to define a model instance.

Together, these components define the optimization problem. The model requires an objective function, which is either minimized or maximized. Once all model components are defined, data can be passed to the model to create a model instance. Pyomo itself does not solve the optimization problem, but passes the problem to an external solver. The solver reports the results to Pyomo, such that the data can be analyzed. The values of the decision variables that result in the best possible value of the objective function are considered as the optimal values and form the solution to the optimization problem (Bynum et al. 2021).

3.4. Description data

3.4.1. HARMONIE historical precipitation forecasts

HARMONIE (HIRLAM ALADIN Research on Mesoscale Operational NWP in Euromed) is a weather model that is owned by KNMI. It came into operation in 2012 and is specifically developed for short-term weather predictions. The model area consists of 2.5 km by 2.5 km cells that cover the Netherlands and its surroundings (Royal Netherlands Meteorological Institute (KNMI) s.d.[b]). HARMONIE delivers 48 hour forecasts for many weather related parameters, like temperature, relative humidity, total precipitation, wind speed and latent heat flux. The forecasts are updated every 6 hours; at +00h = 00, 06, 12 and 18 UTC (Royal Netherlands Meteorological Institute (KNMI) s.d.[a]). HARMONIE historical weather forecasts are stored in the Weer Informatie Waterbeheer (WIWB) database, which was developed by HKV lijn in water, Hydroconsult Siebe Bosch and HydroLogic on behalf of all water boards, KNMI, Het

Waterschapshuis, Rijkswaterstaat and STOWA. Data requests are processed via the WIWB Application Programming Interface (API) and are solely intended for water boards (Het Waterschapshuis s.d. Het Waterschapshuis 2022). For each case study area, the raster data (netCDF) are converted to time series. A code developed by Witteveen+Bos (W+B) is used to extract precipitation time series based on a shapefile of the case study area and the relative share of raster cells that lie within this polygon.

3.4.2. Meteobase historical precipitation and evaporation data

Raster data (1 km by 1 km) of validated historical precipitation and Makkink reference evaporation data are downloaded via Meteobase. Meteobase is originally developed by STOWA, but it became part of the WIWB project in 2018. The precipitation raster is obtained through post-processing of radar images. Again, a code developed by W+B is applied to convert the raster data to time series. Precipitation observations are available on an hourly basis, while evaporation data are gathered at a daily frequency. The daily evaporation data are reprocessed to hourly data by assuming a uniform distribution of evaporation throughout the day. In contrast to the HARMONIE data set, Meteobase data are publicly available (Versteeg et al. 2013).

4

Description case study area and its water system

This chapter contains a description of the case study area and its water system. The management area of Hoogheemraadschap van Rijnland is described in Section 4.1. The water system is analyzed on a regional level in this paragraph. As explained before, the procedure that was described in Section 3.2 is applied to two polders within the management area: Polder Het Langeveld and Polder Vierambacht. The selection of these two polders is explained in Section 4.2. A description of the two polders and an analysis of their water system are provided in Section 4.3. In case references are absent, the information was retrieved during the field visit or during conversations with the water board.

4.1. Description management area Hoogheemraadschap van Rijnland

Hoogheemraadschap van Rijnland is responsible for the regional water management, regulation of groundwater abstractions, most flood defences and urban waste water treatment (Mostert 2019) in management area 14, which is indicated by Figure 4.1 (Unie van Waterschappen 2018). The area is located in the west of the Netherlands, along the North Sea. It stretches from the Noordzeekanaal in the north to Wassenaar in the south. The eastern boundary runs from the east of Amsterdam, via Schiphol, to Gouda. It covers an area of approximately 1100 km^2 (Hoogheemraadschap van Rijnland s.d.), which is inhabited by approximately 1.3 million people (Wikipedia s.d.). The area is part of the Rhine River Delta, which explains its name (Hoogheemraadschap van Rijnland s.d.).

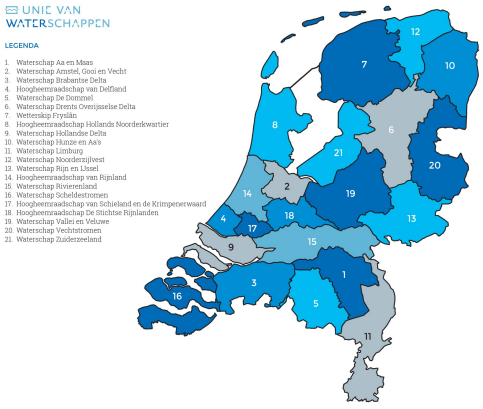

Figure 4.1: Location management area Rijnland (14) (Unie van Waterschappen 2018).

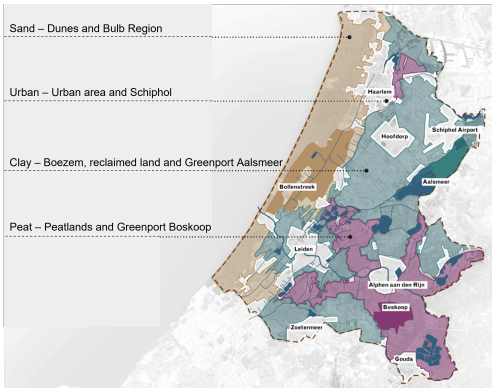

Figure 4.2: Four distinct regions within Rijnland. Adjusted from Wijnakker et al. (2021).

Figure 4.2 shows that four regions can be distinguished: 1) a sandy region, known for its dunes and flower bulb cultivation, 2) an urban region, including Amsterdam Airport Schiphol, 3) a clayey region, characterized by deep polders, and 4) a peaty region. The water-related challenges differ per area. For example, the deep polders are affected by salinization, while the peaty region suffers from land subsidence due to peat oxidation (Wijnakker et al. 2021).

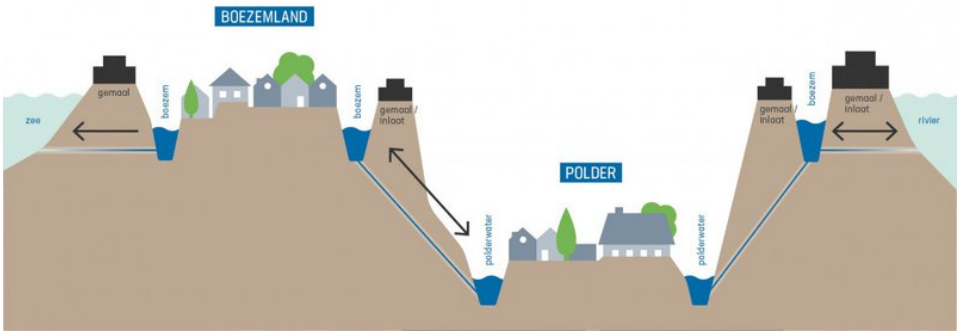

Figure 4.3: Water system Rijnland (Hoogheemraadschap van Rijnland s.d.).

Figure 4.3 illustrates Rijnland's characteristic water system (Hoogheemraadschap van Rijnland s.d.). Rijnland can be viewed as a bathtub, as the majority of the region lies below sea level. 200 low-lying polders are surrounded by rivers and canals, like the Hollandse IJssel, the Amsterdam Rijnkanaal and the Noordzeekanaal (Wijnakker et al. 2021; Hoogheemraadschap van Rijnland s.d.). A canal system, called the "boezem", runs through the entire management area, connecting the different landscapes. All surface waters that are contained in the hatched area of Figure 4.4 are part of the "boezem" system. This can be lakes and waterways. The surface water level is maintained at a single, fixed level throughout the entire boezem. The summer target level is -0.61 m NAP, while the winter target level is -0.64 m NAP (Hoogheemraadschap van Rijnland s.d.). Most polders are located below "boezem" and river level, meaning that artificial drainage is required to drain excess precipitation and seepage. Water can also be let into the polder, which is a gravity-driven process.

Figure 4.4: Canal system ("boezem") Rijnland and major pumping stations ("boezemgemalen").

Pumps are employed to maintain the surface water level in the polders at target water level. The water is discharged to the “boezem” by 375 small pumping stations. Subsequently, the “boezem” water is discharged to the North Sea. Water is discharged using four major pumping stations (in Dutch: “boezemgemalen”). Their locations are indicated in Figure 4.4. The water is discharged to the North Sea, mainly via the Noordzeekanaal (Hoogheemraadschap van Rijnland s.d.). Water discharge mostly takes place at Spaarndam and Halfweg. The pumping station at Katwijk is not often used. Freshwater is pumped into the area at Gouda. Freshwater is also supplied by the climate-resilient water supply (in Dutch: “Klimaatbestendige Wateraanvoer” (KWA)) at Bodegraven, via the river Oude Rijn. The freshwater originates from the management area of HDSR (management area 18, Figure 4.1) (Duijkers 2021). Rijnland is thus flushed from south to north. Since Rijnland is affected by salty seepage (especially in the deep Haarlemmermeerpolder), regular flushing is important for fresh water availability and water quality. Rijnland delivers water to Hoogheemraadschap van Delfland and Hoogheemraadschap van Schieland.

Water level management is performed by 6 surface water level managers, each responsible for a part of the management area. They are supported by a DSS, which was designed by the engineering company Nelen & Schuurmans and makes use of the Deltares software Delft-FEWS and RTC-Tools (Nelen & Schuurmans s.d.). The most important pumping stations are included, like the four major pumping stations and the most important polder pumping stations. The optimal control actions are determined based on 4 control variables (in order of priority): 1) surface water level, 2) salt concentration, 3) energy consumption, and 4) discharge at low tide, which is most relevant for the pumping station at Katwijk. The optimal control actions determined by the DSS are not implemented directly. Human intervention is required, because erroneous control actions could have huge consequences. The pumps are remotely controlled via a computer system called Central Automation Water Management (in Dutch: “Centrale Automatisering Waterbeheer” (CAW)).

Most polder pumping stations and weirs are not part of the DSS. They are managed according to an area regulation (in Dutch: “gebiedsregeling”). Water level sensors are positioned. If the water level exceeds a certain level, the polder pumping station switches on. Adjustment of weir crest heights is avoided as much as possible. The majority of the weirs are operated manually. Preferably, they are only adjusted during the transition from summer to winter level and vice versa. They are managed by the water system managers and operated based on system knowledge and experience.

Climate

The Netherlands has a temperate maritime climate with relatively mild winters, mild summers and all-year-round precipitation. The yearly precipitation equals around 800 mm (Klimaatinfo s.d.). The yearly evaporation amounts approximately 500 mm. This implies that the average groundwater recharge equals 0.7 mm/d, which can be applied for steady-state groundwater calculations (Bot 2016). The Netherlands experiences a precipitation excess in winter, while a precipitation deficit prevails in summer. Figure 4.5 shows the average monthly precipitation and evaporation, and confirms this pattern.

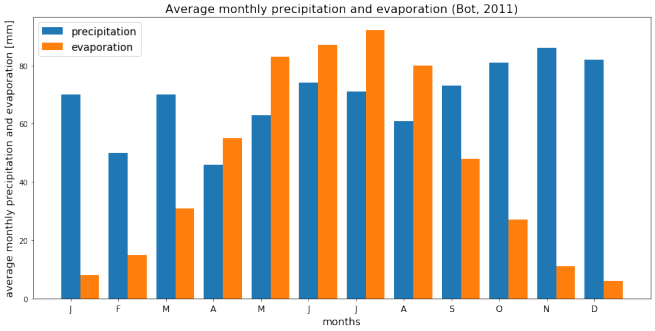

Figure 4.5: Average precipitation and evaporation in the Netherlands, based on Bot (2016).

4.2. Description selection case study areas

The objective is to select two polders with distinct geohydrological responses. The selection is based on a soil map (Figure 4.6) and seepage map (Figure 4.7). Figure 4.6 shows that the main soil types within Rijnland are sandy soils, peaty soils and clayey soils. Since relatively much research has already been done on the application of controlled drainage systems in areas with peaty soils, it is chosen to select a sandy and clayey polder. Sandy soils are typically located at a higher elevation than clayey soils. Therefore, sandy polders often experience downward seepage, while the majority of the clayey polders are affected by upward seepage. To ensure that the majority of the polders within Rijnland are covered by this research, a sandy polder with downward seepage and a clayey polder with upward seepage are selected.

A sandy polder that experiences downward seepage is Polder Het Langeveld, which can be derived from Figure 4.6 and Figure 4.7. According to these figures, Polder Vierambacht is characterized by a clayey soil and upward seepage.

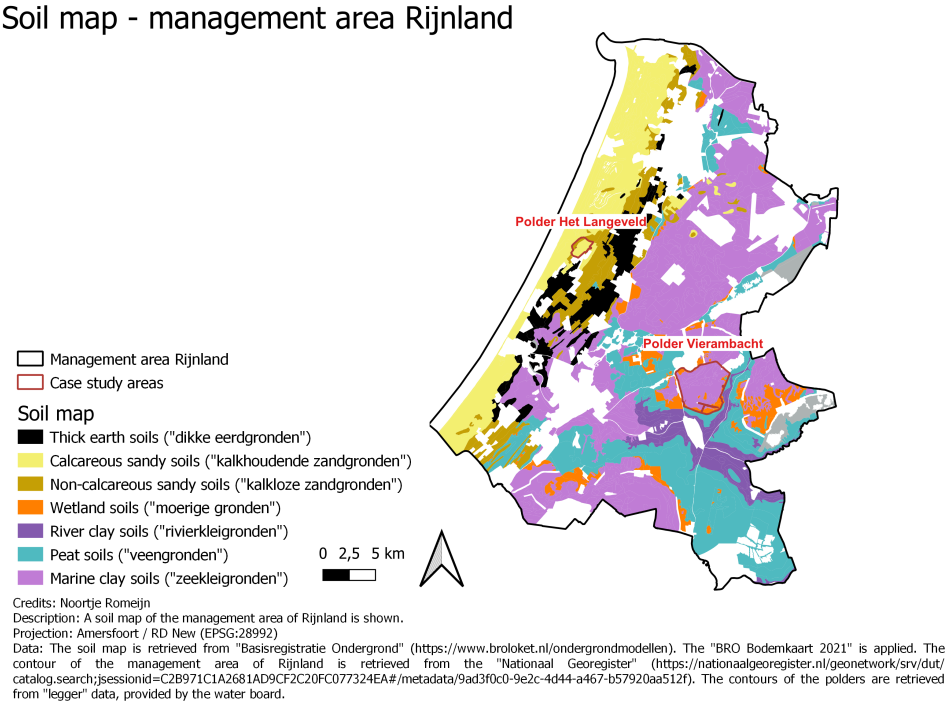

Figure 4.6: Soil map of management area Rijnland.

4.3. Description case study areas

4.3.1. Sandy polder - Polder Het Langeveld

Polder Het Langeveld is located north west of Noordwijkerhout and is part of the Flower Bulb Region. The polder is approximately 1.5 km wide and 2 km long. Dunes mark the western boundary, like shown by Figure 4.8. A large part of the polder is used for high-quality agriculture and horticulture, with a focus on bulbs and perennial plants. Considering the high economic value of these agricultural goods, proper water management is extremely important to prevent damages and economic loss. The western part is a nature reserve, which requires another water management strategy.

Polder Het Langeveld is located above NAP, like shown by Figure 4.9. Except in the nature reserve, the target water levels vary seasonally. This implies that a summer and winter target level can be distinguished. Figure 4.10 shows the summer target levels for the various ”peilgebieden”. The target

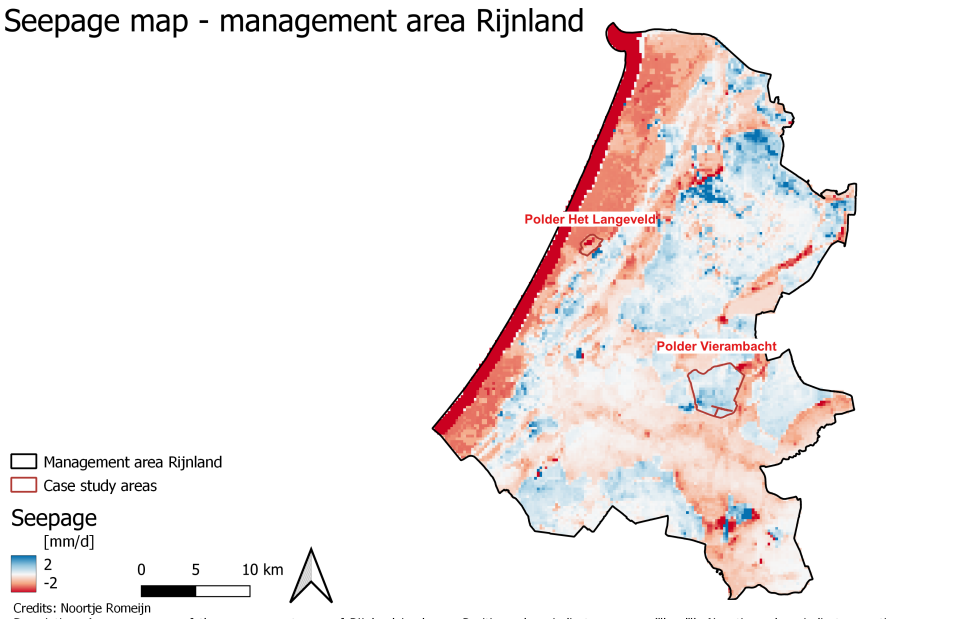

Credits: Noortje Romeijn
Description: A seepage map of the management area of Rijnland is shown. Positive values indicate seepage ("kwel"). Negative values indicate negative seepage ("wegzijging").
Projection: Amersfoort / RD New (EPSG:28992)
Data: The seepage map is retrieved from the Dutch Hydrological Instrumentation (NHI) Data Portal (https://data.nhi.nu/). The layer "LHM4.1 Gemiddelde kwel-inzijging 2011-2018 (mm/dag)" is applied. The contour of the management area of Rijnland is retrieved from the "Nationaal Georegister" (https://nationaalgeoregister.nl/geonetwork/srv/dut/catalog.search;jsessionid=C2B971C1A2681AD9CF2C20FC077324EA#/metadata/9ad3f0c0-9e2c-4d44-a467-b57920aa512f). The contours of the polders are retrieved from "legger" data, provided by the water board.

Figure 4.7: Seepage map of management area Rijnland.

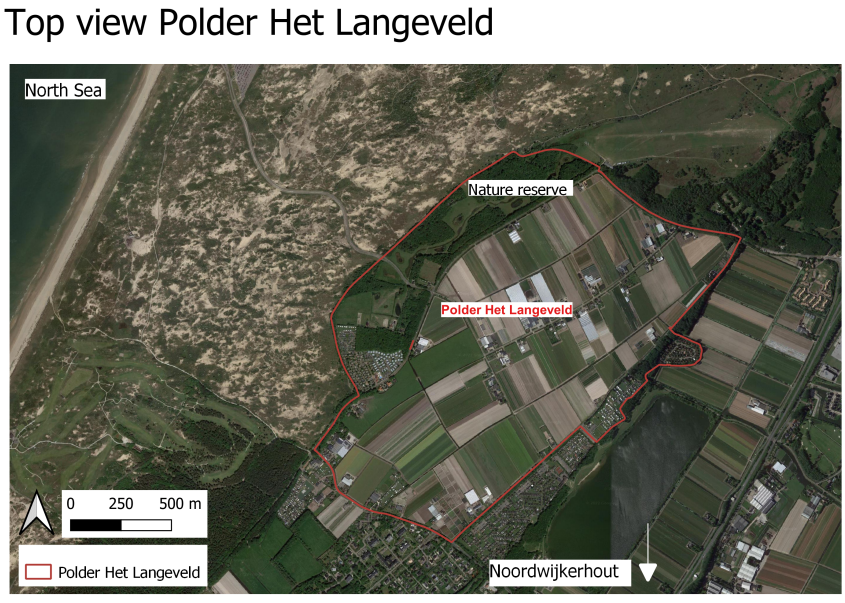

Credits: Noortje Romeijn
Description: Top view Polder Het Langeveld.
Projection: Amersfoort / RD New (EPSG:28992)
Data: The satellite map is retrieved from Google Satellite. The contour of Polder Het Langeveld is retrieved from the "legger", which is provided by the water board.

Figure 4.8: Top view Polder Het Langeveld.

water levels are higher than the water level in the “boezem”, meaning that pumping is required for water supply and water can be discharged by gravity.

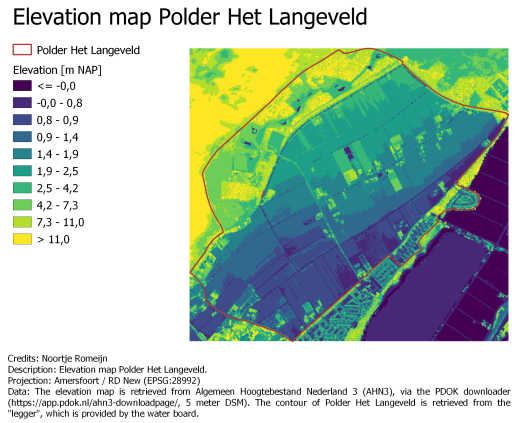

Figure 4.9: Elevation map Polder Het Langeveld.

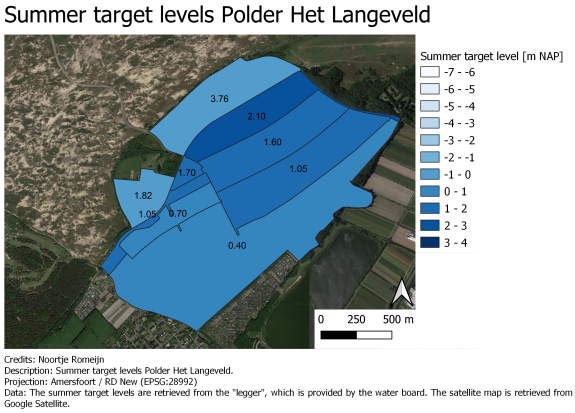

Figure 4.10: Summer target levels Polder Het Langeveld.

Figure 4.11 shows the position of the most important weirs, culvert and pumping station. The flow direction is also indicated. First, water is pumped into a reservoir. Next, the water is divided among three ditches by means of manual weirs. Water may leave the polder via a culvert or manual weir in the south or via an automated, remotely controlled weir in the east. The crest level heights of all weirs are preferably only adjusted during the transition from summer to winter level. The pumping station is controlled based on the water level in front of the automatic weir. Since there is a delay between water level change in the reservoir and water level change in front of the weir, undershoot and overshoot of the minimum and maximum levels may occur. Due to negative seepage to the deep groundwater and seepage to low-lying, adjacent polders, frequent pumping is required.

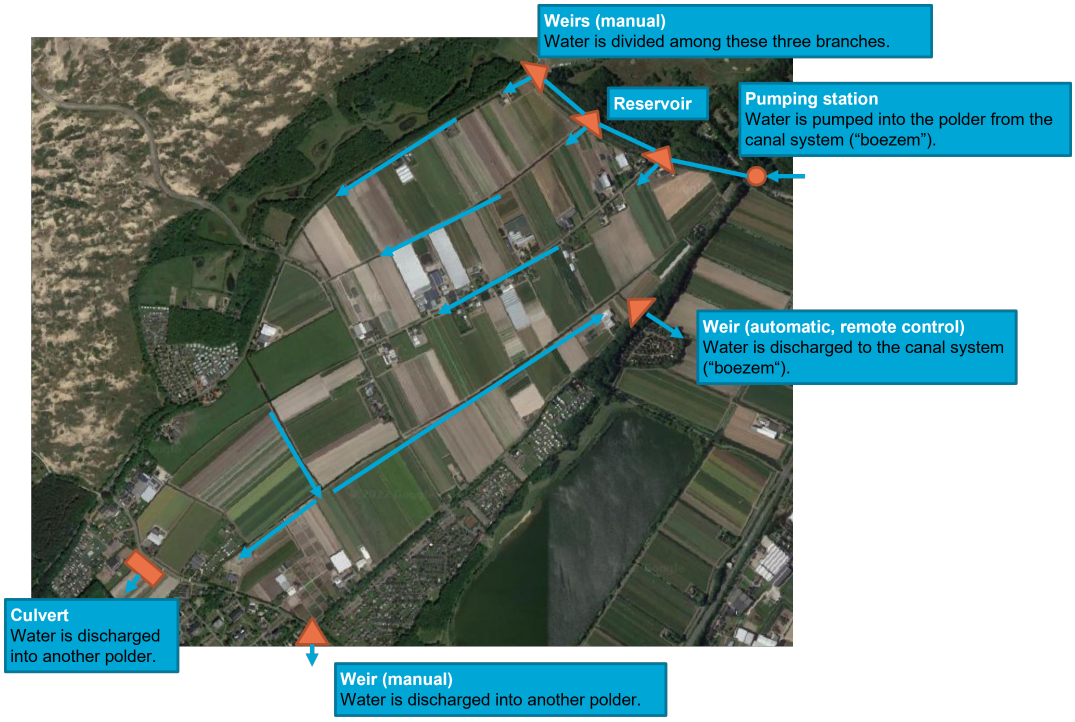

Figure 4.11: Location of the most important weirs and pumping stations in Polder Het Langeveld. Water flow directions are also indicated.

Added value of water retention through groundwater-based MPC

Under the current climate conditions, water supply is still larger than water demand. However, due to water quality related issues (that worsen due to climate change), water retention could be beneficial for Polder Het Langeveld. Water quality is under pressure due to salinization. A lock at Spaarndam,

between the “boezem” and the Noordzeekanaal, causes salt water to enter the boezem system. By means of water inlet at another location, Rijnland is flushed. However, in summers with limited water supply, flushing is limited and salt water could potentially reach the Flower Bulb Region. If more water is retained, the required water inlet decreases. The smaller the water demand, the lower the risk of salinization. Additionally, seen from a water quality perspective, it is beneficial to limit foreign water intake.

Points of attention
The following points of attention for the implementation of water table control systems were mentioned by the water system manager and water level manager of Polder Het Langeveld during a field visit (02-09-2022). These points are not always restricted to Polder Het Langeveld.

- Changes in ditch water level should be gradual to prevent instability of embankments.
- Bulbs and dahlias are more resilient to low moisture contents than to high moisture contents. At the moment, composite controlled drainage is applied by farmers to keep the groundwater level artificially low. This was also observed. The sump water level was lower than the ditch water level.
- The space for extra water storage is very limited in Polder Het Langeveld. Bulbs require a minimum drainage depth of 0.60 to 0.80 m, which is already almost violated at a considerable number of locations.
- Precipitation or irrigation is required to guarantee the efficiency of fertilizers. After the application of fertilizers, the land is typically irrigated once or twice. Farmers cannot completely rely on subirrigation.
- Nematodes threaten crops. Nematodes are located at the groundwater table. The higher the groundwater table, the closer the nematodes are to the crops.

4.3.2. Clayey polder - Polder Vierambacht

Polder Vierambacht lies to the north of Alphen a/d Rijn and is part of the Green Heart, a rural area surrounded by the major Dutch cities. The polder also belongs to the Dutch Lake District, which has a typical Dutch landscape, with lakes, mills, old villages and nature areas. In the 16th century, peat extraction became popular in the area. Due to peat extraction, several areas flooded and became lakes. The flooded areas were reclaimed by pumping. Polder Vierambacht was reclaimed in 1744. The land is used for agriculture and dairy farming (Provincie Zuid-Holland 2012). Figure 4.12 contains a satellite image. The polder is approximately 5 km wide and 4.5 km long.

Figure 4.13 shows that Polder Vierambacht is a rather deep polder. The surface level lies around -5 m NAP. Approximately 70% of the surface waters have a seasonal target water level. The remaining 30% has a fixed target level. Figure 4.14 shows the summer target levels for the various ”peilgebieden”. The target water levels are much lower than the water level in the “boezem”, meaning that artificial drainage is required to get rid of excess water. Figure 4.15 shows the position of the most important weirs and pumping stations. Water is discharged to the “boezem” using two pumping stations. Water inlet takes place via three weirs. Additionally, multiple water inlets are present throughout the polder.

Added value of water retention through groundwater-based MPC
Since Polder Vierambacht is a relatively deep polder, salinization of groundwater through salty seepage threatens fresh water availability (Provincie Zuid-Holland 2012). Salty seepage can be prevented by offering counter-pressure. Counter-pressure can be realized through a relatively high groundwater table. Since the aim of the groundwater-based MPC algorithm is to increase the groundwater level or, at least, limit groundwater table falling, water retention through groundwater-based MPC has a large potential in this area.

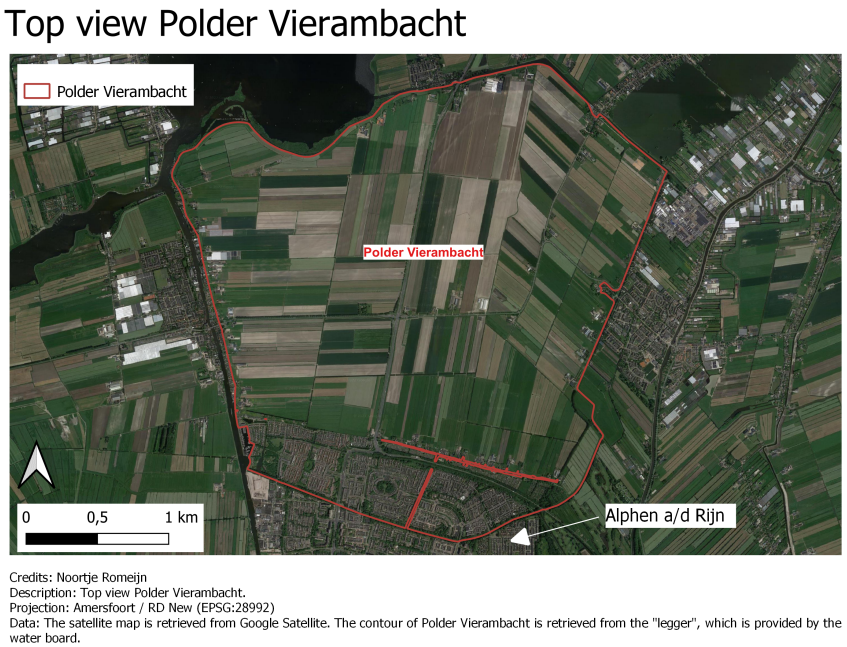

Figure 4.12: Top view Polder Vierambacht.

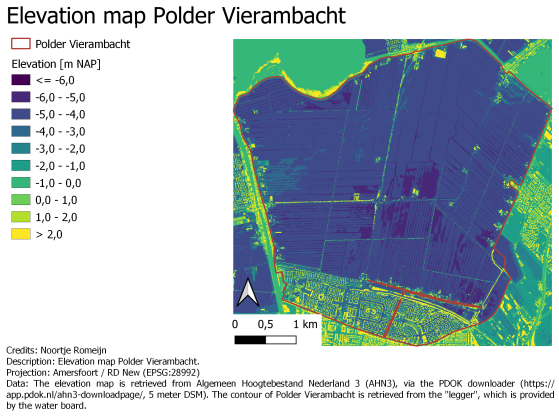

Figure 4.13: Elevation map Polder Vierambacht.

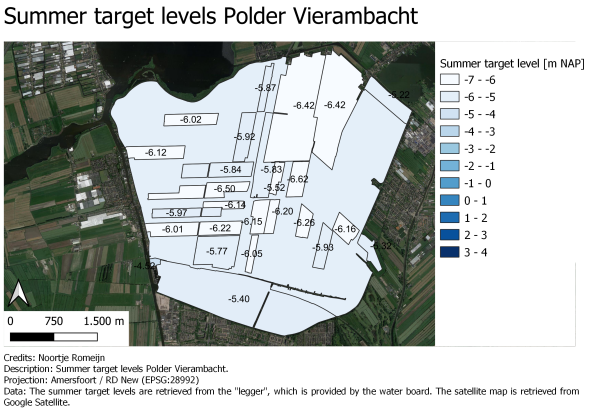

Figure 4.14: Summer target levels Vierambacht.

Figure 4.15: Location of the most important weirs and pumping stations in Polder Vierambacht. Water flow directions are also indicated.

5

Construction of groundwater models

Groundwater models of different complexity are constructed for both case study areas, as explained in Chapter 3. Section 5.1 discusses the setup of the MODFLOW groundwater models. Section 5.2 describes the formulation of a simple and fast model that simulates the groundwater response at the centre of the plot.

5.1. MODFLOW groundwater models

The construction of the MODFLOW groundwater models is described in this section. Sub-section 5.1.1 provides a description of the base model, which forms the blueprint for all MODFLOW models. Its model schematization is applicable for all case study areas and variants. A specific MODFLOW model is constructed by specifying the model parameters, which differ per case study area and variant. An overview of the selected model parameters is provided in subsection 5.1.2. Subsection 5.1.3 exposes a limitation of MODFLOW that hampers a realistic representation of the surface water-groundwater system. Subsequently, a solution is proposed and implemented. A slightly adjusted version of the base model is constructed to simulate the present situation, in which traditional drains are applied instead of submerged drains. The adjustments are covered in Section 5.1.4. A simplified hydrological model is applied to calculate the groundwater recharge and other important fluxes, which is discussed in Section 5.1.5.

5.1.1. Base model

The base model represents an agricultural plot of length L_{plot} [m] and width W_{plot} [m] that is surrounded by a ditch of width W_{ditch} [m], like illustrated by Figure 5.1. Below, the model schematization is discussed, including the applied FloPy packages. A Python class named `basic MODFLOW model` is built, following the principles of object-oriented programming. The class is able to construct and run MODFLOW groundwater models according to the described model schematization. Case study area- and variant-specific MODFLOW models are created as instances of the class. The class is subdivided into multiple functions, which each define a specific FloPy package. Appendix C contains an overview of the applied FloPy packages.

Figure 5.1 shows that the edge of the model area coincides with the centre of the ditch, such that only half of the ditch is part of the model. By applying this model boundary, a symmetric situation is created. This implies that, while only one plot is actually modelled, the presence of the surrounding plots is assumed and implicitly taken into account. The model boundary is indicated by the red, dashed line. It should be noted that the geohydrological characteristics of the neighbouring plots are assumed to be exactly the same as the characteristics of the target plot. The (geohydrological) characteristics of the plot are selected such that the plot represents the average plot within the polder.

L_{plot}, W_{plot} and W_{ditch} are based on the average plot length, plot width and ditch width respectively. Additionally, L_{plot}, W_{plot} and spatial discretization Δx [m] are tuned in such a way that the transverse

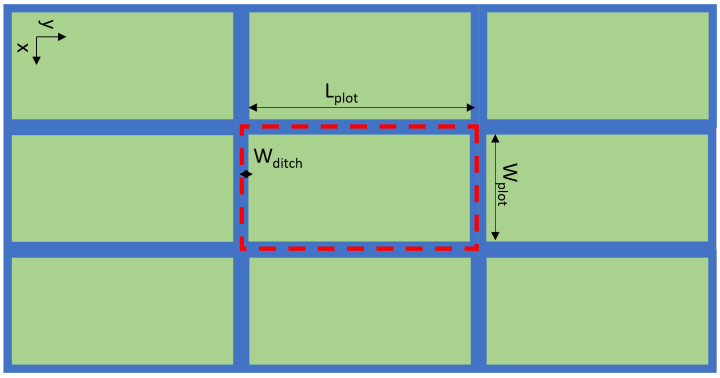

Figure 5.1: Model schematization plot.

(x) and longitudinal (y) model direction are covered by an odd number of cells. MODFLOW evaluates the heads in the model cells' centres, which means that an odd number of cells is required to determine the groundwater head exactly in the middle of the plot. It is essential to be able to simulate the piezometric head at the plot's centre, since the groundwater table will be controlled based on this point. It is also ensured that the midpoint of the plot is located in between two drains (relevant for variant 2 and variant 3), which requires an even number of drains (N_{drain} [-]). This affects L_{plot}, since the drains are placed along the transverse direction. The drain spacing S_{drain} [m] differs per polder, because to meet similar discharge requirements soils with low hydraulic conductivity require a denser drainage system than soils with high hydraulic conductivity. Normally, an optimization procedure is applied to determine S_{drain} and D_{drain} (drain diameter [m]) (Skaggs et al. 1999), but they are selected based on common values provided by Bot (2016) here.

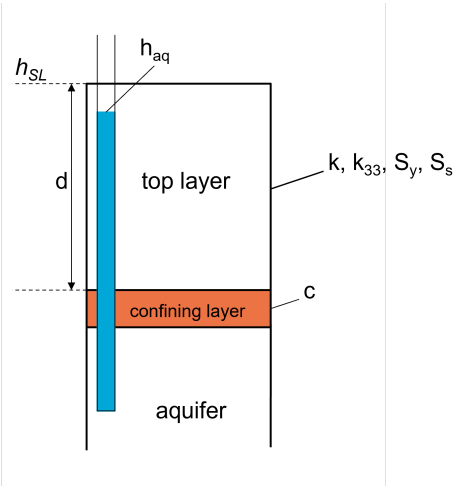

Figure 5.2: Model schematization cross-section.

A representative soil profile is derived for both polders based on geological research data obtained from DINOloket (TNO s.d.[a]). Because the relevant groundwater flow processes occur in the top few metres of the soil column, the depth of the groundwater models is restricted. Both case study areas are characterized by a relatively thick top layer that is separated from a lower-lying sandy aquifer by a thin layer with low hydraulic conductivity. Figure 5.2 illustrates the situation. The surface level is represented by h_{SL} [m NAP]. Only the thick top layer is modelled explicitly. The lower layers are included through a boundary condition by means of the FloPy General Head Boundary (GHB) package. The GHB package simulates the flow between a cell and external source in proportion to the head difference. The groundwater flow (direction) across the confining layer is thus determined by the difference between the groundwater head in the top layer (h_{GW} [m NAP]) and the groundwater head in the bottom aquifer (h_{aq} [m NAP]). h_{aq} is assumed to be constant in time. The flow is calculated by multiplying the

head difference by the conductance of the confining layer (C [m^2/d]), which represents the ease with which water flows through the confining layer (Langevin et al. 2017). The conductance is defined as:

$$C = \frac{\Delta x * \Delta x}{c} \tag{5.1}$$

where c represents the confining layer resistance [d]. Since the top layer is not spatially discretized in the vertical (z) direction, a two dimensional groundwater model is obtained. The top layer has thickness d [m] and is assigned a horizontal and vertical hydraulic conductivity, k [m/d] and k_{33} [m/d] respectively. Furthermore, the specific yield (S_y [-]) and specific storage (S_s [m^{-1}]) are defined.

Figure 5.3 and 5.4 illustrate the model schematization concerning the ditch and drains. Obviously, drains are absent in variant 1. In variant 2, the pressure head that is exerted on the drains (h_{drain} [m NAP]) coincides with the surface water level in the ditch (h_{SW} [m NAP]). In variant 3, h_{drain} is independent from h_{SW}. The control pit is not explicitly modelled, i.e. only the imposed pressure heads h_{drain} and h_{SW} may differ from each other.

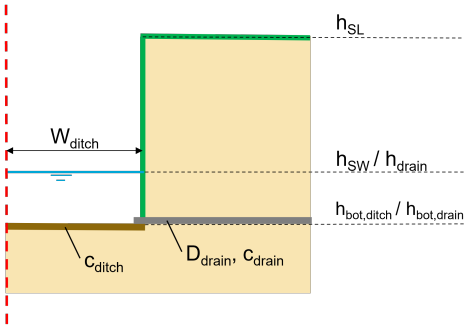

Figure 5.3: Model schematization ditch and drains - variant 1 and 2.

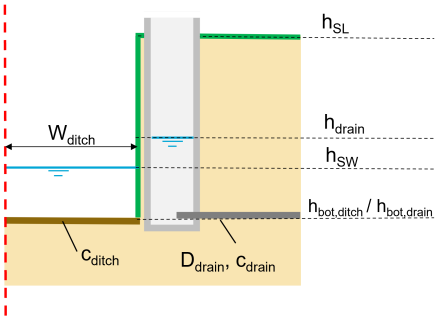

Figure 5.4: Model schematization ditch and drains - variant 3.

The ditch and drains are simulated using the FloPy River (RIV) package. In contrast to the Drain (DRN) package, the RIV package enables modelling of pressurized drains and facilitates both drainage and subirrigation. Similarly to the GHB package, the groundwater exchange is proportional to the head difference between the ditch or drain cell and the underlying aquifer cell. Again, a conductance functions as proportionality coefficient. The conductance that is passed to each ditch cell (C_{ditch} [m^2/d]) is calculated as follows:

$$C_{ditch} = \frac{\Delta x * W_{ditch}}{c_{ditch}} \tag{5.2}$$

where c_{ditch} represents the hydraulic resistance of the ditch bottom [d]. The numerator contains the area of the ditch in each cell. W_{ditch} is smaller than Δx. The length of the ditch in a cell equals Δx. The conductance of each drain cell (C_{drain} [m^2/d]) is calculated according to:

$$C_{drain} = \frac{\Delta x * D_{drain} * \pi}{c_{drain}} \tag{5.3}$$

where c_{drain} represents the drain entrance resistance [d]. The numerator contains the area of the drain in each cell. The length of the drain in a cell equals Δx. The circumference of the drain is multiplied by Δx, which implies that permanent submergence is assumed. In practice, the drain may not be submerged entirely such that only part of the drain area contributes to drainage. The drains are positioned such that the elevation of the bottom of the drains ($h_{bot,drain}$ [m NAP]) coincides with the elevation of the bottom of the ditch ($h_{bot,ditch}$ [m NAP]). This means that the drains are always pressurized during normal conditions. Only during extremely dry periods, the surface water level may fall below the basis of the drainage system. It should be noted that the RIV package resembles a boundary condition, which means that h_{SW} and h_{drain} are constant during one stress period. Stress

periods are time intervals during which the model inputs remain constant. The surface water level is thus not affected by groundwater in- or outflow, which implies that a sufficient water supply and discharge capacity are implicitly assumed.

5.1.2. Overview of selected case study area-specific parameters

By specifying the parameters that were mentioned in the previous section, a MODFLOW model is constructed for a specific case study area and variant. Table 5.1 specifies all case study area-specific parameters. Also the FloPy packages to which the parameters are passed are indicated. For each polder, the obtained MODFLOW model is briefly described. A complete explanation and justification of the selected parameter values for Polder Het Langeveld and Polder Vierambacht are provided in Appendix D and E respectively.

It should be stressed that the models are not thoroughly calibrated to groundwater measurements. The parameter values are selected based on literature and observations. However, it is confirmed whether realistic results are obtained (Chapter 7/Appendix G). Model parameters like k and c are tuned until realistic results are obtained. Table 5.1 contains final parameter values.

Table 5.1: Overview of selected case study area-specific parameters

Symbol	Description	Package	Polder Het Langeveld	Polder Vierambacht	Appendix
L_{plot}	Plot length [m]	DIS	296	628	D.1/E.1
W_{plot}	Plot width [m]	DIS	152	160	D.1/E.1
Δx	Spatial discretization [m]	DIS	2	2	-
h_{SL}	Surface level [m NAP]	DIS	1.0	-5.0	D.2/E.2
d	Top layer thickness [m]	DIS	10	6	D.3/E.3
k	Horizontal hydraulic conductivity top layer [m/d]	NPF	7.0	0.1	D.3/E.3
k_{33}	Vertical hydraulic conductivity top layer [m/d]	NPF	1.4	0.02	D.3/E.3
S_y	Specific yield [-]	STO	0.2	0.08	D.3/E.3
S_s	Specific storage [m^{-1}]	STO	$4*10^{-5}$	$4*10^{-5}$	D.3/E.3
c	Resistance confining layer [d]	GHB	1000	500	D.3/E.3
h_{aq}	Head in lower aquifer [m NAP]	GHB	0.10	-4.50	D.4/E.4
W_{ditch}	Ditch width [m]	RIV (ditch)	1.0	1.0	D.5/E.5
c_{ditch}	Bed hydraulic resistance [d]	RIV (ditch)	2.0	5.0	D.5/E.5
$h_{bot,ditch}$	Bottom elevation ditch [m NAP]	RIV (ditch)	0.05	-6.18	D.5/E.5
D_{drain}	Drain diameter [m]	RIV (drains)	0.10	0.10	D.6/E.6
c_{drain}	Drain resistance [d]	RIV (drains)	0.14	7.0	D.6/E.6
$h_{bot,drain}$	Bottom elevation drains [m NAP]	RIV (drains)	0.05	-6.18	D.6/E.6
S_{drain}	Drain spacing [m]	RIV (drains)	8	4	-
N_{drain}	Number of drains [-]	RIV (drains)	36	156	-
$h_{GW,initial}$	Initial groundwater head [m NAP], equal to summer target level ($h_{SW,target}$) [m NAP]	IC	0.40	-5.83	D.4/E.4

Polder Het Langeveld

Figure 5.5 shows the top view of the MODFLOW groundwater model for the average plot in Polder Het Langeveld. The model area is 298 m long and 154 m wide and contains a plot of 296 m by 152 m, surrounded by a 1 m wide ditch. Δx equals 2 m, which is substantiated in Appendix G. The blue coloured cells indicate the location of the ditch, whereas the drains are indicated by the brownish colour. The drain spacing equals 8 m, which is in accordance with the spacing applied on an agricultural plot in Polder Het Langeveld that was visited during the field visit. Figure 5.6 depicts the side view of the MODFLOW model.

Figure 5.7 illustrates the representative soil profile of Polder Het Langeveld. The top layer is 10 m thick and consists of sand. A 2 m thick clay layer functions as confining layer.

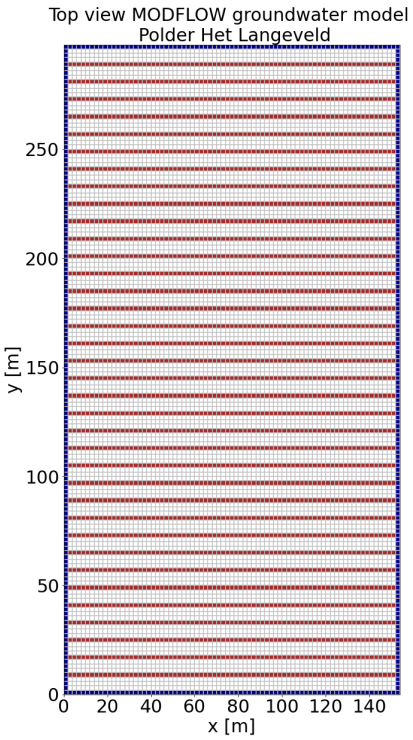

Figure 5.5: Top view MODFLOW groundwater model - Polder Het Langeveld.

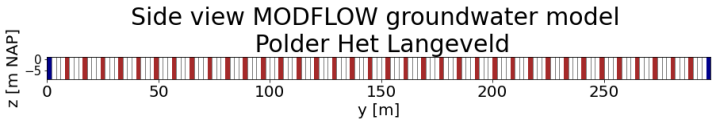

Figure 5.6: Side view MODFLOW groundwater model - Polder Het Langeveld.

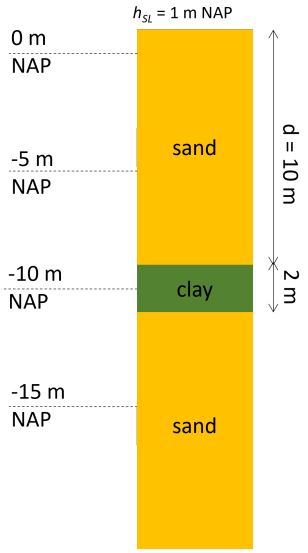

Figure 5.7: Soil profile Polder Het Langeveld.

Polder Vierambacht
The average plot in Polder Vierambacht is larger than the average plot in Polder Het Langeveld, resulting in a significantly larger model area. The model area contains a plot of 628 m by 160 m, surrounded by a 1 m wide ditch. Again, Δx equals 2 m (Appendix G). Figure 5.8 depicts part of the top view of the MODFLOW groundwater model for Polder Vierambacht. The cells in which the ditch is located are indicated by the blue colour. The cells in which the drains are located are highlighted by the brownish colour. The drain spacing equals 4 m, which is in correspondence with typical values for drains applied on a clay soil (Bot 2016). Figure 5.9 depicts the side view of the MODFLOW model.

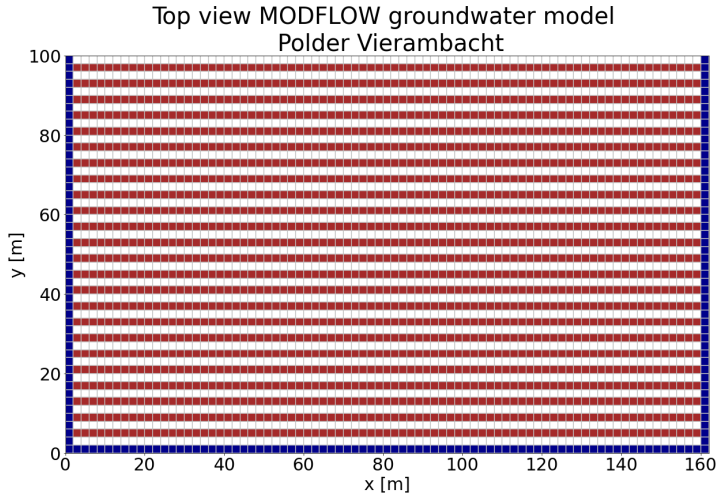

Figure 5.8: Top view MODFLOW groundwater model - Polder Vierambacht (only southern 100 m is shown).

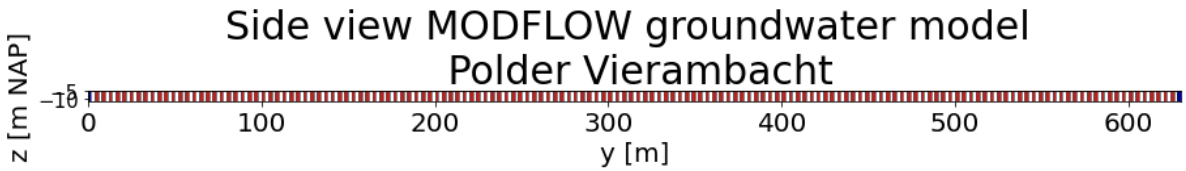

Figure 5.9: Side view MODFLOW groundwater model - Polder Vierambacht.

The representative soil profile of Polder Vierambacht is depicted in Figure 5.10. The top layer has a thickness of 6 m and consists of sandy clay and loam. The confining layer is represented by a thin peat layer.

Considering the low altitude of Polder Vierambacht and the risk of salty seepage, the occurring chloride concentrations are checked using measurements from DINOloket (groundwater well B31A0106) (TNO s.d.[a]). Just below the confining layer, the chloride concentration is approximately 40 mg/l. Only at greater depth (25 m below surface level), the chloride concentration is about 800 mg/l. According to the World Health Organization, the chloride concentration of freshwater is below 250 mg/l (World Health Organization 2022). This means that the groundwater just below the confining layer can be considered fresh and no adjustments to the MODFLOW model are required.

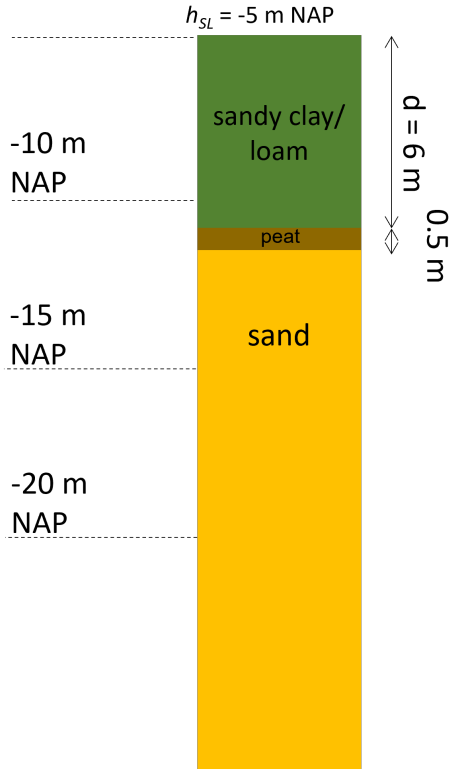

Figure 5.10: Soil profile Polder Vierambacht.

5.1.3. Extension to include groundwater-surface water interaction

In Section 5.1.1, it was mentioned that h_{SW} and h_{drain} are imposed as a boundary condition. Therefore, h_{SW} and h_{drain} are constant during one stress period and need to be specified by the modeller. The groundwater-surface water interaction is thus only one-way; the groundwater level is affected by the surface water level, while the surface water level is not affected by the groundwater level. Infinite water supply and discharge capacity are thus implicitly assumed. The groundwater-surface water interaction is thus not well described by the `basic MODFLOW model`, which is problematic as water table control systems rely on this interaction.

A workaround is invented, which enables MODFLOW to approximately simulate the groundwater-surface water feedback. Figure 5.11 shows the iterative loop that is developed to update h_{SW}. This workaround is suitable for variant 1 and 2.

Instead of a single model, $N+1$ models are required to simulate the groundwater level during $N\Delta t$ days. These models differ only in boundary condition. Model 0 determines the initial groundwater situation ($h_{GW,0}$) and is constructed using the `basic MODFLOW model` class. $h_{GW,0}$ corresponds to the steady-state solution for the average daily groundwater recharge (R [mm/d]). h_{SW} and/or h_{drain} are initially equal to the summer target water level ($h_{SW,target}$ [m NAP]). $h_{GW,0}$, $h_{SW,0}$ and $h_{drain,0}$ are passed on to model 1. Model 1 to N are constructed using the `update MODFLOW model` class. This class loads, updates and runs existing MODFLOW groundwater models and can be applied for all variants and both case study areas. The temporal discretization, initial groundwater situation, h_{SW}, h_{drain} and R of an existing MODFLOW model can be adjusted. As such, model 1 is based on model 0, model 2 is based on model 1, etc.

Model 1 calculates the transient groundwater response between t = 0 and t = Δt days. The outputs of model 1 are h_{GW} at t = Δt days ($h_{GW,1}$), the ditch inflow between t = 0 and t = Δt days ($Q_{IN,SW,0}$) and the ditch outflow between t = 0 and t = Δt days ($Q_{OUT,SW,0}$). The latter two are obtained from the volume budget calculated by MODFLOW and are used to update h_{SW} according to the displayed equa-

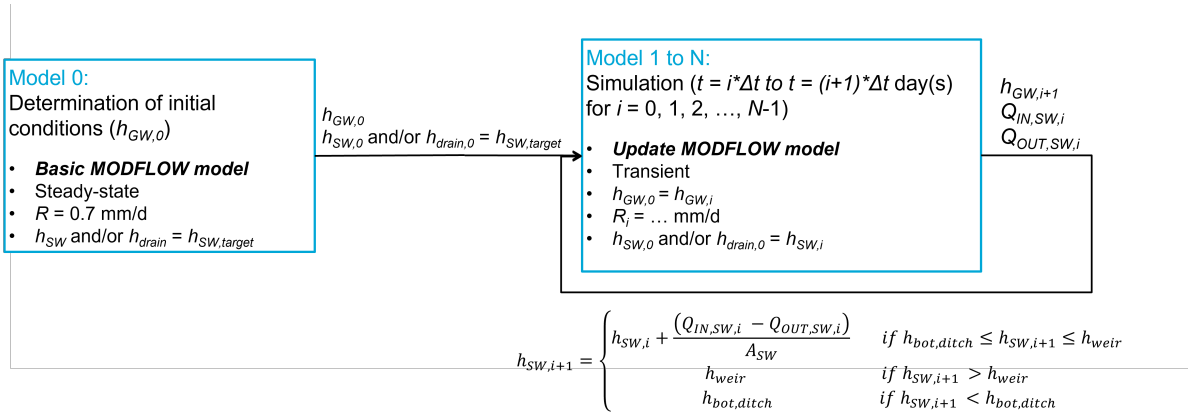

Figure 5.11: Iterative loop that is developed to update h_{SW}. $N + 1$ MODFLOW models, that differ only in boundary condition, are required to simulate the groundwater level during $N\Delta t$ days.

tion. $Q_{IN,SW,0}$ represents groundwater discharge, which occurs either directly or via the submerged drains (in case of variant 2). $Q_{OUT,SW,0}$ represents ditch water infiltration, which may also occur directly or via the submerged drains (variant 2). A_{SW} represents the surface area of the ditch [m^2]. h_{SW} is restricted to the weir crest level (h_{weir} [m NAP]). This is a simplification, because the discharge rate depends on the difference between h_{SW} and h_{weir} according to the weir formula. The lower limit of h_{SW} is restricted to $h_{bot,ditch}$. The updated h_{SW} ($h_{SW,1}$) and h_{GW} ($h_{GW,1}$) are forwarded to model 2. This iterative procedure is repeated N times.

The MODFLOW feedback loop can be interpreted as a combined model for groundwater and surface water levels. In principle, a similar feedback loop could be established for variant 3 to update the sump water level:

$$h_{drain,i+1} = \begin{cases} h_{drain,i} + \frac{Q_{IN,sump,i} - Q_{OUT,sump,i}}{A_{sump}}, & \text{if} h_{bot,drain} \leq h_{drain,i+1} \leq h_{weir} \\ h_{weir}, & \text{if } h_{drain,i+1} > h_{weir} \\ h_{bot,drain}, & \text{if } h_{drain,i+1} < h_{bot,drain} \end{cases} \tag{5.4}$$

where h_{drain} represents the sump water level (i.e. the pressure on the drains) [m], $Q_{IN,sump}$ represents groundwater discharge via the submerged drains [m^3], $Q_{OUT,sump}$ represents sump water infiltration via the submerged drains [m^3] and A_{sump} is the surface area of the sump [m^2]. However, it becomes clear in Chapter 7 that this leads to problems due to the small surface area of the sump. A_{sump} is equated to 1 m^2, which corresponds to the area of a sump in Polder Het Langeveld, that was visited during the field visit (and is depicted on the front page).

5.1.4. Adjustments to simulate present state

Presently, submerged drainage is not (commonly) applied in Polder Het Langeveld and Polder Vierambacht. A slightly adjusted version of the base model, in which the submerged drains are replaced by traditional drains, is constructed to be able to correctly represent the present state. Furthermore, the option to not include drains remains.

In practice this means that the RIV package (drains) is replaced by the DRN package. The model schematization is depicted in Figure 5.12. Except for $h_{bot,drain}$, all model parameter values remain unchanged. Again, fully submerged drains are assumed. This means that c_{drain} remains the same too. The new Python class is called `current situation MODFLOW model`.

The Python class `update current situation MODFLOW model` is constructed, which loads, updates and runs existing MODFLOW groundwater models. The newly obtained models are also included in a feedback loop, such that the groundwater-surface water interaction is correctly modelled.

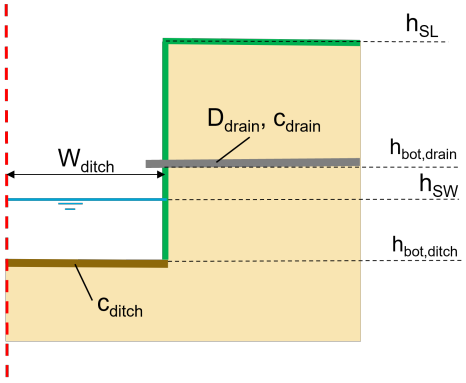

Figure 5.12: Model schematization ditch and drains - present state.

As explained in Chapter 4, composite controlled drainage systems are currently applied on some plots in Polder Het Langeveld. The systems are managed by farmers, based on system insight and experience. This implies that a (mathematical) description of the present control lacks, such that it cannot be modelled. Therefore, drains are presently assumed to be absent in Polder Het Langeveld. The sandy soil is highly permeable, so artificial drainage is not absolutely necessary. Traditional drains are present in Polder Vierambacht. According to Bot (2016), a drain depth of 75 cm below surface level is common for grassland. $h_{bot,drain}$ is therefore equal to -5.75 m NAP.

5.1.5. Schematization hydrological processes

Figure 5.13 shows how the hydrological processes are schematized.

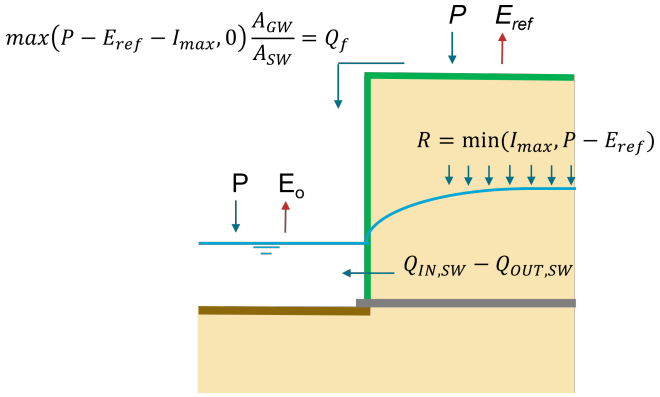

Figure 5.13: Schematization hydrological processes.

The groundwater recharge rate (R [m/d]) is approximated by the net precipitation rate (precipitation rate (P [m/d]) minus reference evaporation rate (E_{ref} [m/d])), and is restricted by the maximum infiltration rate (I_{max} [m/d]):

$$R = \min(I_{max}, P - E_{ref}) \tag{5.5}$$

E_{ref} is the Makkink reference evaporation [m/d], which applies to the reference crop (grassland). It should be noted that the term ”recharge” is used in the remaining of this thesis, while this actually refers to the net precipitation.

Precipitation excess results in overland flow and fast runoff towards the ditch, represented by Q_f [m/d]. Q_f is calculated as follows:

$$Q_f = \max(P - E_{ref} - I_{max}, 0)\frac{A_{GW}}{A_{SW}} \tag{5.6}$$

in which A_{GW} represents the surface area of the groundwater system [m^2].

There is also a slow runoff component towards the ditch, which is related to groundwater discharge and calculated by MODFLOW, like explained in Section 5.1.3. Furthermore, the ditch is affected by direct precipitation and open water evaporation (E_o [m/d]) (Penman-Monteith evaporation). The following relation is assumed between E_o and E_{ref}:

$$E_o = 1.25E_{ref} \tag{5.7}$$

which is based on the fact that the reference evaporation according to Makkink amounts approximately 80% of the potential evaporation according to Penman (Grondwaterformules.nl s.d.[b]).

Figure 5.13 indicates that also the fast runoff component and direct precipitation and evaporation affect h_{SW}. The MODFLOW feedback loop is therefore slightly adjusted:

$$h_{SW,i+1} = \begin{cases} h_{SW,i} + \frac{Q_{IN,SW,i} - Q_{OUT,SW,i}}{A_{SW}} + \Delta t(P - E_o) + \\ \Delta t \frac{A_{GW}}{A_{SW}} \max(P - E_{ref} - I_{max}, 0), & \text{if } h_{bot,ditch} \leq h_{SW,i+1} \leq h_{weir} \\ h_{weir}, & \text{if } h_{SW,i+1} > h_{weir} \\ h_{bot,ditch}, & \text{if } h_{SW,i+1} < h_{bot,ditch} \end{cases} \tag{5.8}$$

where Δt is the model time step [d]. The unsaturated zone is ignored, as well as delays.

I_{max} is equal to 20 mm/hr in Polder Het Langeveld, while I_{max} is equal to 5 mm/hr in Polder Vierambacht, which are typical infiltration rates for sand and clay (Brouwer et al. 1988). These values are converted to the correct unit ([m/d]).

5.2. Physical time series models

Two alternative physical time series models (PTSMs) are constructed to simulate the groundwater response in the centre of the plot. The objective is to construct a fast model that simulates the groundwater response in the centre of the plot with sufficient accuracy. The PTSMs are derived from a differential equation, based on models described by van der Gaast et al. (2009). Section 5.2.1 presents two PTSMs. An extension to the PTSMs is proposed in Section 5.2.2, which allows for a proper description of the groundwater-surface water interaction.

5.2.1. Two alternatives

Both alternatives are suitable for all three variants of water table control systems. However, the displayed equations hold for variant 1 and 2. By replacing h_{SW} by the sump water level, the equations are adjusted for variant 3.

PTSM 1

PTSM 1 simulates the groundwater response in the centre of the plot by considering two processes:

1. Groundwater recharge,
2. Flux between surface water and groundwater system.

These processes are represented by the following differential equation:

$$\begin{aligned} \frac{dh_{GW}}{dt} &= \frac{R}{S_y} + \alpha(h_{SW} - h_{GW}(t)) \\ h_{GW}(0) &= h_{GW,0} \end{aligned} \tag{5.9}$$

where h_{GW} is the groundwater head in the centre point of the plot [m NAP], R is the groundwater recharge [m/d], S_y represents the specific yield [-], α is a model parameter [d^{-1}], h_{SW} is the surface water level [m NAP] and t represents time [d]. An initial condition is also specified.

The differential equation is solved, which yields the following solution:

$$h_{GW}(t) = h_{GW,0}e^{-\alpha t} + \frac{R}{\alpha S_y}(1 - e^{-\alpha t}) + h_{SW}(1 - e^{-\alpha t}) \tag{5.10}$$

The obtained solution is identical to the physical time series model described by van der Gaast et al. (2009). α is case study area- and variant-specific and is determined through calibration against MODFLOW simulation results (Chapter 8). According to van der Gaast et al. (2009), α is related to the drainage resistance γ [d] and S_y:

$$\gamma = \frac{1}{\alpha S_y} \tag{5.11}$$

γ is a measure for the total resistance that is experienced by the groundwater as it flows towards the drainage system (Jousma et al. 1996).

The discretized form of Equation 5.9 is applied as internal model in the MPC algorithm:

$$h_{GW}(t + \Delta t) = h_{GW}(t) + \frac{\Delta t R}{S_y} + \alpha \Delta t(h_{SW} - h_{GW}(t)) \tag{5.12}$$

where Δt represents the model time step [d].

PTSM 2

PTSM 2 considers three processes to simulate the groundwater response in the centre of plot:

1. Groundwater recharge,
2. Flux between surface water and groundwater system,
3. Seepage flux between top layer and bottom aquifer.

Depending on the relevant groundwater flow processes, PTSM 1 may outperform PTSM 2 and vice versa. Since the seepage flux is taken into account by PTSM 2, it is expected that model 2 performs well in case study areas that experience significant seepage. PTSM 2 is expressed by the following differential equation:

$$\frac{dh_{GW}}{dt} = \frac{R}{S_y} + \alpha(h_{SW} - h_{GW}(t)) + \beta(h_{aq} - h_{GW}(t)) \qquad h_{GW}(0) = h_{GW,0} \tag{5.13}$$

The seepage flux is represented by the third term, in which β is a model parameter [d^{-1}] and h_{aq} represents the head in the lower aquifer [m NAP].

Equation 5.14 presents the solution to the differential equation:

$$h_{GW}(t) = h_{GW,0}e^{-(\alpha+\beta)t} + \frac{R}{(\alpha+\beta)S_y}(1 - e^{-(\alpha+\beta)t}) + \frac{\alpha}{(\alpha+\beta)}h_{SW}(1 - e^{-(\alpha+\beta)t}) + \frac{\beta}{(\alpha+\beta)}h_{SW}(1 - e^{-(\alpha+\beta)t}) \tag{5.14}$$

The model parameters, α and β, are determined through calibration against MODFLOW simulation results (Chapter 8). Since PTSM 2 differs slightly from the PTSM described by van der Gaast et al. (2009), it is probable that α cannot be directly linked to the drainage resistance. The seepage flux (q_v [m/d]) can be calculated according to the following equation:

$$q_v = \frac{h_{aq} - h_{SW}}{c} \tag{5.15}$$

where c is the resistance of the confining layer [d] (van der Gaast et al. 2009). This means that β is likely related to the reciprocal of c.

The discretized form of Equation 5.13 is applied as internal model in the MPC algorithm:

$$h_{GW}(t + \Delta t) = h_{GW}(t) + \frac{\Delta t R}{S_y} + \alpha\Delta t(h_{SW} - h_{GW}(t)) + \beta\Delta t(h_{aq} - h_{GW}(t)) \tag{5.16}$$

5.2.2. Extension to include groundwater-surface water interaction

The PTSMs that are proposed in 5.2.1 assume a constant surface water level. Like explained in Section 5.1.3, the assumption of a constant surface water level hampers a correct representation of the groundwater-surface water interaction. Therefore, h_{SW} is made time dependent. The flux between the surface water and groundwater system, P, E_o and Q_f are used to update h_{SW}. According to van der Gaast et al. (2009), the flux between the surface water and groundwater system (q [m/d]) can be described by the following equation:

$$q = \frac{h_{GW} - h_{SW}}{\gamma} \tag{5.17}$$

The extended PTSMs are valid for variant 1 and 2.

Extended PTSM 1

Equation 5.12 is extended as follows:

$$h_{GW}(t + \Delta t) = h_{GW}(t) + \frac{\Delta t R}{S_y} + \alpha\Delta t(h_{SW}(t) - h_{GW}(t)) \tag{5.18}$$

$$h_{SW}(t + \Delta t) = \begin{cases} h_{SW}(t) + \lambda\Delta t\frac{A_{GW}}{A_{SW}}\alpha S_y(h_{GW}(t) - h_{SW}(t)) + \Delta t(P - E_o) + \\ \Delta t\frac{A_{GW}}{A_{SW}}\ \mathsf{max}(P - E_{ref} - I_{max}, 0), & \text{if } h_{SW}(t + \Delta t) \leq h_{weir} \\ h_{weir}, & \text{if } h_{SW}(t + \Delta t) > h_{weir} \end{cases}$$

where $\frac{A_{GW}}{A_{SW}}$ is the ratio between the area of the groundwater system and the area of the surface water system [-], P represents direct precipitation [m/d], E_o represents open water evaporation [m/d], E_{ref} is the reference evaporation [m/d] and I_{max} represents the maximum infiltration rate [m/d]. A factor λ is added to make up for possible deviations. λ is determined through calibration against MODFLOW simulation results (Chapter 8). Note that $\frac{1}{\alpha S_y}$ is substituted for γ.

Extended PTSM 2

Although PTSM 2 does not completely correspond to the theory described by van der Gaast et al. (2009), Equation 5.17 is applied to determine the groundwater-surface water flux too. Equation 5.16 is extended as follows:

$$h_{GW}(t+\Delta t) = h_{GW}(t) + \frac{\Delta t R}{S_y} + \alpha \Delta t (h_{SW}(t) - h_{GW}(t)) + \beta \Delta t (h_{aq} - h_{GW}(t)) \tag{5.19}$$

$$h_{SW}(t+\Delta t) = \begin{cases} h_{SW}(t) + \lambda \Delta t \frac{A_{GW}}{A_{SW}} \alpha S_y (h_{GW}(t) - h_{SW}(t)) + \Delta t (P - E_o) + \\ \Delta t \frac{A_{GW}}{A_{SW}} \max(P - E_{ref} - I_{max}, 0), & \text{if } h_{SW}(t+\Delta t) \leq h_{weir} \\ h_{weir}, & \text{if } h_{SW}(t+\Delta t) > h_{weir} \end{cases}$$

6

Setup MPC module

This chapter discusses the setup of the MPC module, which is constructed using Pyomo software. The main characteristics of the module were already mentioned in Section 3.2. The formulation of an abstract Pyomo model is covered in this chapter. The model is defined within a Python function, called `optimization module including feedback`, such that a model instance is initialized by calling this function and specifying the required input data. The following Pyomo modelling components are defined:

1. Sets,
2. Decision variables,
3. Parameters,
4. Objective expression,
5. Constraint expressions.

In Section 6.1, the model formulation is discussed by covering these modelling components. As explained in Section 5.1.3, the groundwater-surface water interaction cannot be correctly modelled in case of variant 3. The MPC module is therefore constructed for variant 1 and 2. In Section 6.2, setpoint and weir settings are defined for each case study area.

6.1. Model formulation

Sets

Table 6.1 contains an overview of all sets. The sets represent arrays of discrete time indices and are used to define the domain of decision variables and parameters.

1. The length of t_1 corresponds to the length of the prediction horizon (48 hours). It is used to define the domain of model inputs, like P, E_{ref} etc.
2. t_2 contains one time index more than t_1. It is therefore used to define the domain of control variables that require an initial condition.
3. The length of $t_{1,obj}$ corresponds to the number of control actions within one prediction horizon. It is therefore used to define the domain of control variable $h_{weir,control}$.
4. $t_{2,obj}$ contains one time index less than $t_{1,obj}$. It is used to ensure that $|\Delta h_{weir,control}| \leq \Delta h_{weir,control,max}$, which involves seven inequalities.

Table 6.1: Overview Pyomo sets.

Symbol	Type	Interpretation
t_1	An array of length 48	Discrete time indices 0 through 47
t_2	An array of length 49	Discrete time indices 0 through 48
$t_{1,obj}$	An array of length 8	Discrete time indices 0 through 7
$t_{2,obj}$	An array of length 7	Discrete time indices 0 through 6

Decision variables
Table 6.2 defines all decision variables that are added to the model.

Because the internal model is imposed in terms of constraints, h_{GW} and h_{SW} are also included in the list of decision variables. h_{GW} and h_{SW} are calculated on an hourly basis for the entire prediction horizon. Furthermore, an initial condition is specified. Therefore, their domain is defined by t_2.

The decision variable that corresponds to the control action is h_{weir}. For simplicity, h_{weir} is determined on an hourly basis, which means that its domain is defined by t_1. A constraint is added to ensure that h_{weir} is constant within one control time step (of 6 hours), which is explained later. This requires the formulation of another control variable, $h_{weir,control}$, whose domain is described by $t_{1,obj}$.

The final two decision variables are defined to regulate the flow over the weir, which is elaborated on later. h_{spill} represents the spill flow over the weir. It is expressed in terms of m water column and relates to A_{SW}. δ [m] represents a "deficit", which is defined as h_{weir} minus h_{SW}. The domain of both variables is described by t_1.

Table 6.2: Overview Pyomo decision variables.

Symbol	Description	Domain
h_{GW}	Midpoint groundwater head [m NAP]	t_2
h_{SW}	Ditch water level [m NAP]	t_2
h_{weir}	Weir crest height [m NAP]	t_1
$h_{weir,control}$	Weir crest height [m NAP]	$t_{1,obj}$
h_{spill}	Spill [m]	t_1
δ	Deficit [m]	t_1

Parameters
Table 6.3 contains an overview of all parameters.

Table 6.3: Overview Pyomo parameters.

Symbol	Description	Domain	Notes
P	Precipitation [m/d] (dictionary)	t_1	
E_{ref}	Reference evaporation [m/d] (dictionary)	t_1	
E_o	Open water evaporation [m/d] (dictionary)	t_1	
I_{max}	Maximum infiltration rate [m/d]		
Δt	Model time step [d]		
$\Delta t_{control}$	Control time step [hr]		
S_y	Specific yield [-]		
α	PTSM parameter [d^{-1}]		
β	PTSM parameter [d^{-1}]		PTSM 2 only
h_{aq}	Head in lower aquifer [m NAP]		PTSM 2 only
$h_{weir,initial}$	Initial weir crest height [m NAP]		
$h_{weir,max}$	Maximum weir crest height [m NAP]		
$h_{weir,min}$	Minimum weir crest height [m NAP]		
$h_{GW,setpoint}$	Setpoint midpoint groundwater level [m NAP]		
$h_{SW,initial}$	Initial ditch water level [m NAP]		
$h_{GW,initial}$	Initial groundwater level [m NAP]		
A_{GW}	Area groundwater system [m^2]		
A_{SW}	Area surface water system [m^2]		
$\Delta h_{weir,control,max}$	Maximum change in weir crest height between control time steps [m]		

Objective expression
Equation 6.1 describes the objective function.

$$\underset{h_{weir,control}}{\textit{minimize}}\ J = \mu \sum_{k=1}^{len(t_{1,obj})} (h_{GW}(\Delta t_{control}(t_{1,obj,k}+1)) - h_{GW,setpoint})^2 + \sum_{i=1}^{len(t_1)} (h_{spill}(t_{1,i}) + \delta(t_{1,i})) \tag{6.1}$$

The first term sums the difference between the actual groundwater level and setpoint at the end of each control time step, i.e. at t = 6, 12, 18, ..., 48 hours. The second term is not related to MPC, but is required to correctly describe the system dynamics. An explanation is provided in the next section. The objective function is minimized by the optimal control actions $h_{weir,control}$. Weighting factor μ is introduced to ensure that both terms have the same order of magnitude. The optimal weighting factor is determined through trial and error.

Constraints
Various constraints are defined.

Equations 6.2 to 6.4 describe the constraints that add the internal model. Equation 6.2 corresponds to PTSM 1, while equation 6.3 corresponds to PTSM 2. Equation 6.4 is valid in both cases.

PTSM 1:
For $i = 2, 3, ..., len(t_2)$:

$$\begin{aligned} h_{GW}(t_{2,1}) &= h_{GW,initial} \\ h_{GW}(t_{2,i}) &= h_{GW}(t_{2,(i-1)}) + \frac{\Delta t R(t_{2,(i-1)})}{S_y} + \alpha \Delta t (h_{SW}(t_{2,(i-1)}) - h_{GW}(t_{2,(i-1)})) \end{aligned} \tag{6.2}$$

PTSM 2:
For $i = 2, 3, ..., len(t_2)$:

$$\begin{aligned} h_{GW}(t_{2,1}) &= h_{GW,initial} \\ h_{GW}(t_{2,i}) &= h_{GW}(t_{2,(i-1)}) + \frac{\Delta t R(t_{2,(i-1)})}{S_y} + \alpha \Delta t (h_{SW}(t_{2,(i-1)}) - h_{GW}(t_{2,(i-1)})) + \\ &\quad \beta \Delta t (h_{aq} - h_{GW}(t_{2,(i-1)})) \end{aligned} \tag{6.3}$$

PTSM 1 and PTSM 2:
For $i = 2, 3, ..., len(t_2)$:

$$\begin{aligned} h_{SW}(t_{2,1}) &= h_{SW,initial} \\ h_{SW}(t_{2,i}) &= h_{SW}(t_{2,(i-1)}) + \lambda \Delta t \frac{A_{GW}}{A_{SW}} \alpha S_y (h_{GW}(t_{2,(i-1)}) - h_{SW}(t_{2,(i-1)})) + \\ &\quad \Delta t (P(t_{2,(i-1)}) - E_o(t_{2,(i-1)})) + \Delta t \frac{A_{GW}}{A_{SW}} \max(P(t_{2,(i-1)}) - E_{ref}(t_{2,(i-1)}) - I_{max}, 0) - h_{spill}(t_{2,(i-1)}) \end{aligned} \tag{6.4}$$

Equation 6.4 deviates from Equation 5.19. The inequality cannot be implemented in Pyomo, because h_{weir} is a control variable. Pyomo cannot deal with if- and max-statements that involve control variables (whose values are not known a priori). In principle, the flow over the weir could be calculated by using the weir formula. However, the weir formula includes a max-statement too since spill must only take place when h_{SW} exceeds h_{weir}, so it cannot be inserted in Pyomo as well. The spill flow should thus be defined differently.

To ensure that h_{SW} does not exceed h_{weir}, control variables h_{spill} and δ are introduced, which were defined before. This method is invented by Celeste et al. (2010) to explicitly incorporate spills into

reservoir optimization models. Celeste et al. (2010) propose and test a method that prevents spill to take place when the storage is below total capacity. Since spill can only take place if h_{SW} exceeds h_{weir}, the method of Celeste et al. (2010) can be used to enforce the desired behaviour and limit h_{SW}. This requires the following constraint, which can be interpreted as a water balance:

For $i = 1, 2, ..., len(t_1)$:

$$h_{SW}(t_{1,i}) + \lambda \Delta t \frac{A_{GW}}{A_{SW}} \alpha S_y (h_{GW}(t_{1,i}) - h_{SW}(t_{1,i})) + \Delta t (P(t_{1,i}) - E_o(t_{1,i})) + \Delta t \frac{A_{GW}}{A_{SW}} \max(P(t_{1,i}) - E_{ref}(t_{1,i}) - I_{max}, 0) - h_{spill}(t_{1,i}) + \delta(t_{1,i}) = h_{weir}(t_{1,i}) \tag{6.5}$$

Furthermore, δ is by definition greater than zero, which is also added as constraint:

For $i = 1, 2, ..., len(t_1)$:

$$\delta(t_{1,i}) \geq 0 \tag{6.6}$$

The desired behaviour is enforced by minimizing the sum of h_{spill} and δ over the entire prediction horizon, leading to the second term in the objective function.

Figure 6.1 schematically illustrates the meaning of h_{spill} and δ and shows why minimizing the sum of h_{spill} and δ guarantees the desired behaviour. Images 1a and 1b show a situation in which the weir crest level (black line) exceeds the surface water level (blue line), which means that a deficit prevails (δ > 0). It is shown that the sum of h_{spill} and δ is minimized when h_{spill} equals 0, which is desired in case of a deficit. The surface water level (blue line) exceeds the weir crest level (black line) in case of image 2a and 2b, which leads to spill. It is demonstrated that the sum of h_{spill} and δ is minimized when δ equals 0, which is desired if there is spill. The surface water level that is obtained after water is spilled is indicated by the dashed blue line.

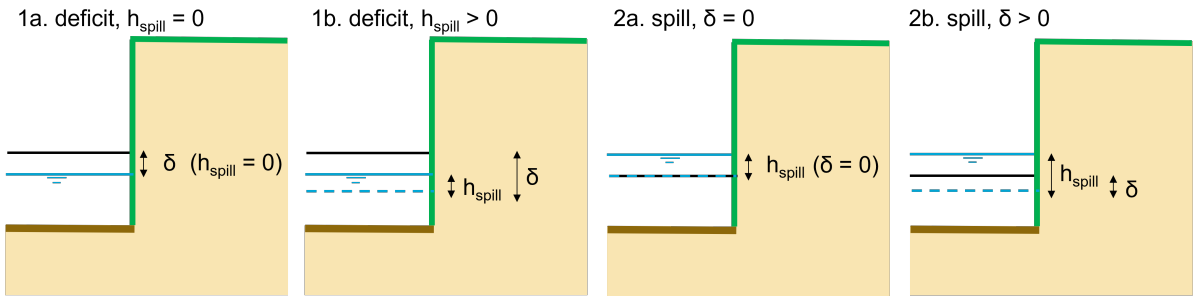

Figure 6.1: Schematic illustration of h_{spill} and δ. The figures show why minimizing the sum of h_{spill} and δ guarantees the desired behaviour: 1) zero spill in case of a deficit, and 2) zero deficit in case of spill (Celeste et al. 2010). The black lines represent the weir crest level, the blue lines represent the surface water level and the dashed blue lines represent the obtained surface water level after water is spilled.

The final constraints are more straightforward:

For $i = 1, 2, ..., len(t_1)$:

$$\begin{aligned} h_{weir}(t_{1,i}) &\geq h_{weir,min} \\ h_{weir}(t_{1,i}) &\leq h_{weir,max} \end{aligned} \tag{6.7}$$

For $i = 1, 2, ..., len(t_{2,obj})$:

$$\begin{aligned} h_{weir,control}(t_{2,obj,i+1}) - h_{weir,control}(t_{2,obj,i}) &\leq \Delta h_{weir,control} \\ h_{weir,control}(t_{2,obj,i+1}) - h_{weir,control}(t_{2,obj,i}) &\geq -\Delta h_{weir,control} \end{aligned} \tag{6.8}$$

$$\begin{aligned} h_{weir,control}(0) - h_{weir,initial} &\leq \Delta h_{weir,control} \\ h_{weir,control}(0) - h_{weir,initial} &\geq -\Delta h_{weir,control} \end{aligned} \tag{6.9}$$

For $i = 1, 2, ..., len(t_{1,obj})$:

For $j = 1 + 6(i-1), ..., 6i$:

$$h_{weir}(t_{1,obj,j}) = h_{weir,control}(i) \tag{6.10}$$

6.2. Definition of setpoint and weir settings

In this section, setpoint and weir settings are defined for each case study area. Table 6.4 contains a summary.

Like described in Section 3.2, the maximum admissible groundwater level is selected as setpoint to maximize retention of precipitation. Since a large part of Polder Het Langeveld is devoted to flower bulb cultivation, the minimum dewatering depth (in Dutch: ”ontwateringsdiepte”) for flower bulb growth in a sandy area is selected as setpoint, which is 40 cm according to Bot (2016). This corresponds to values mentioned by Reijers et al. (2001). The main agricultural activities in Polder Vierambacht are food crop production and dairy farming. The minimum dewatering depth for grassland is therefore selected as groundwater level setpoint, which is 35 cm according to Bot (2016).

$h_{weir,max}$ and $h_{weir,min}$ are based on the current winter and summer target levels. $h_{weir,max}$ is 5 cm above winter target level, whereas $h_{weir,min}$ is 5 cm below summer target level. This means that the possible range of weir positions is 20 cm in Polder Het Langeveld and 25 cm in Polder Vierambacht. $\Delta h_{weir,control}$ is equated to 0.05 m.

Table 6.4: Definition of setpoint and weir settings.

Parameter	Polder Het Langeveld	Polder Vierambacht
$h_{GW,setpoint}$	0.60 m NAP	-5.35 m NAP
$h_{weir,max}$	0.45 m NAP	-5.78 m NAP
$h_{weir,min}$	0.25 m NAP	-6.03 m NAP
$\Delta h_{weir,control}$	0.05 m	0.05 m

7

Evaluation of geohydrological response

The geohydrological response of both case study areas is evaluated for each water table control system by performing MODFLOW simulations. Section 7.1 contains an overview of the simulations and explains the rationale behind them. The simulation results are displayed and analyzed in Section 7.2.

As indicated in Chapter 3, simulations are also executed to verify the model schematization of the MODFLOW models. These simulations and results are covered in Appendix G.

7.1. Overview MODFLOW simulations

The objective is to fully describe the geohydrological response of a plot that is affected by a water table control system. To obtain a complete description of the groundwater response, all possible control actions are simulated. Figure 7.1 summarizes all possible short-term control actions. The figure is established by reasoning that the optimal short-term control action is dependent on the current groundwater situation, the forecasted short-term meteorological situation and the expected meteorological situation in the long-term.

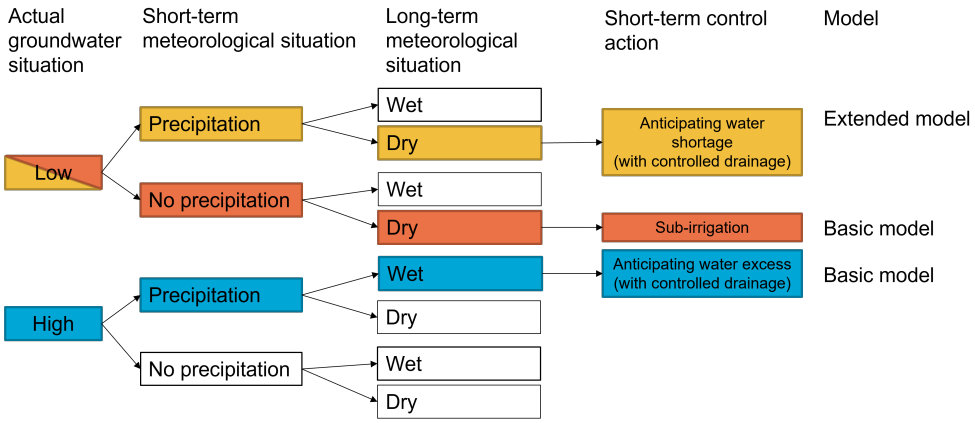

Figure 7.1: Overview of possible short-term control actions.

The coloured boxes indicate combinations of actual groundwater situation, short-term meteorological situation and long-term meteorological situation for which the required short-term control actions are straightforward:

1. Anticipation of water shortage is desirable in case of a low initial groundwater table, forecasted precipitation in the short-term and dry conditions in the long-term (yellow ”track”). Water shortage

can be anticipated by retention of rain water through controlled drainage. By raising the weir crest, the water storage capacity increases.

2. Subirrigation is required to maintain groundwater levels close to setpoint in absence of precipitation (orange ”track”). This entails the continuous supply of water to the ditch or sump such that a constant ditch water level is realized. Please note that subirrigation is not considered in this thesis.
3. Water excess can be prevented by anticipative discharge of ditch water through controlled drainage, which is desirable in case of a high initial groundwater table and forecasted precipitation in the near and distant future (blue ”track”). Water is discharged by lowering the weir crest.

The optimal control actions for the remaining combinations are not directly clear, but always come down to either 1) anticipating water shortage, 2) subirrigation, or 3) anticipating water excess. For instance, it depends on the extremity of the forecasted precipitation event. As such, three possible control actions are identified, of which two should be represented by the MODFLOW simulations.

Figure 7.1 also shows whether the basic or extended MODFLOW model is required to correctly describe the groundwater-surface water interaction. The extended MODFLOW model is necessary to simulate anticipation to water shortage, because the water level gradually increases when the weir is raised. Because a constant ditch/sump water level is maintained in case of subirrigation, the basic MODFLOW model is sufficient. The basic MODFLOW model also suffices in case of anticipation to water excess, since the ditch/sump water level does not fall below weir crest level and is thus constant in time as well.

Appendix F contains an overview of the performed simulations. The simulations are organized according to short-term control action. Although the extended MODFLOW model (including feedback) is required to correctly describe the groundwater response to anticipating water shortage, simulations are performed with the basic MODFLOW model too (excluding feedback). Firstly, this enables demonstration of the usefulness of the extended MODFLOW model. Secondly, these simulations are required for calibration of the PTSMs.

Figure 7.2 and Figure 7.3 illustrate the underlying idea of the simulations that are performed with the basic MODFLOW model. The figures correspond to Appendix F. The starting point of a simulation is the steady-state solution for R = 0.7 mm/d, which is the average groundwater recharge in the Netherlands. Furthermore, the surface water level and sump water level are equal to $h_{SW,target}$, which represents the summer target level. In case of variant 1 and 2, h_{SW} is instantaneously raised at t = 0 days by Δh_{SW}. In case of variant 2, this also affects h_{drain}. In case of variant 3, the sump water level is instantaneously raised at t = 0 days by Δh_{drain}. This only affects h_{drain}. In all cases, a specific R is imposed from t = 0 on. The transient groundwater response in the centre point of the plot is of interest. Appendix F contains information on the simulation length and model time step, which differ per polder and variant. The simulation length is tuned to the response time of the system, such that unnecessarily long simulations are prevented. The required model time steps are determined through a convergence analysis, which is described in Appendix G. It should be noted that the modelled situations do not occur in reality, but are solely intended to research the groundwater response to specific control actions.

Figure 7.4 and Figure 7.5 illustrate the underlying idea of the simulations that are performed with the extended MODFLOW model. The figures correspond to Appendix F. The starting positions are the same as for the simulations excluding feedback. However, instead of instantaneously raising the ditch or sump water level, the weir crest level is raised by Δh_{weir}. In case of variant 1 and 2, h_{SW} gradually increases to h_{weir}. In case of variant 3, the sump water level increases to h_{weir}. Again, a specific R is also imposed from t = 0 on. Only groundwater discharge contributes to the rise in h_{SW} or sump water level (direct precipitation, evaporation and fast runoff are ignored for these simulations). Appendix F again contains information on the simulation length and model time step. The required model time step is determined by means of a convergence analysis, which results are shown in Appendix G.

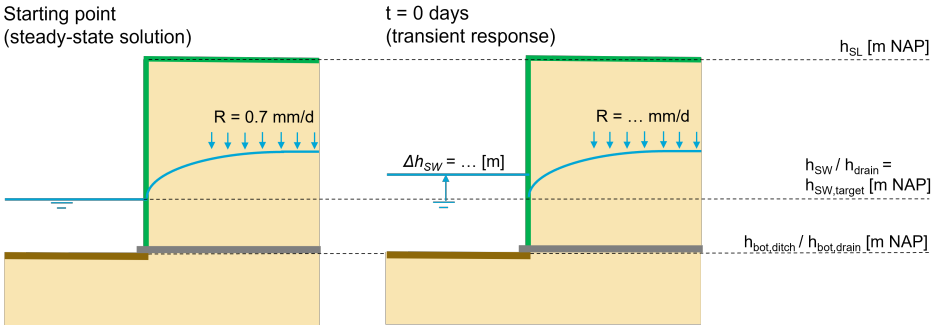

Figure 7.2: Schematization of underlying idea simulations excluding feedback - variant 1 & 2.

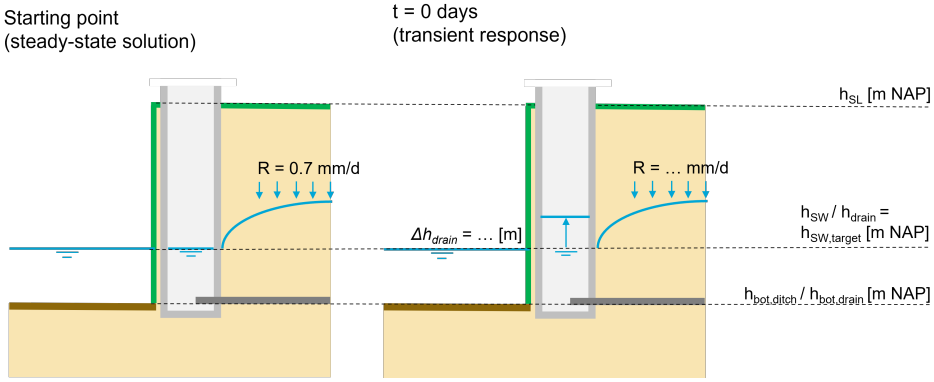

Figure 7.3: Schematization of underlying idea simulations excluding feedback - variant 3.

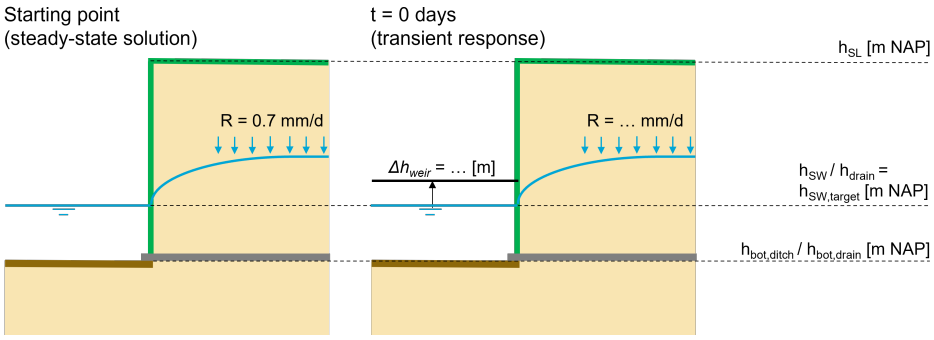

Figure 7.4: Schematization of underlying idea simulations including feedback - variant 1 & 2.

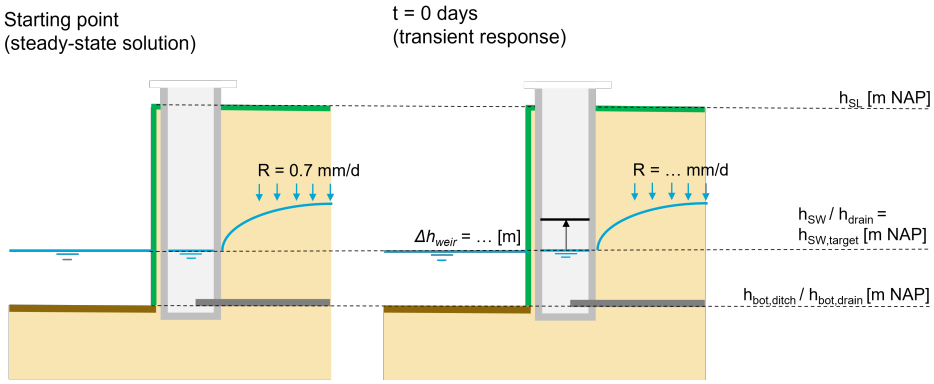

Figure 7.5: Schematization of underlying idea simulations including feedback - variant 3.

7.2. Geohydrological response

7.2.1. Starting point (steady-state solution)

Figure 7.6 depicts the groundwater situation at the starting point of the simulations. The groundwater heads along a cross-section that is perpendicular to the drains and includes the centre point of the plot are plotted for both case study areas and all variants. The groundwater table is indicated by the blue dotted line, while the green dashed line represents the surface level.

It can be observed that a bulging groundwater table occurs in case of variant 1 Polder Het Langeveld. The bulging is very limited compared to variant 1 Polder Vierambacht. It can be observed that the groundwater level exceeds the surface level in case of variant 1 Polder Vierambacht. Because the hydraulic conductivity of the clayey top layer is relatively low, the groundwater table bulges significantly and groundwater discharge is a slow process. Furthermore, groundwater is only discharged via the ditch. In the beginning of the steady-state calculation, the ”container” fills by upward seepage and recharge. Once h_{GW} exceeds h_{aq}, the direction of seepage reverses such that the seepage flux balances the recharge. Apparently, subsurface drains are necessary to avoid water problems. The presence of drainage pipes in Polder Vierambacht is confirmed by the ”Buisdrainagekaart” (Massop et al. 2016) and the water board. Variant 1 is thus not viable in Polder Vierambacht and is therefore omitted.

In case of variant 2 and 3, the groundwater table bulges in-between drainage pipes. This results in an oscillating pattern. However, this pattern is barely visible in Figure 7.6 (due to the scale of the figure). The bulging is very limited in case of Polder Het Langeveld, caused by the high hydraulic conductivity of sand.

The modelled groundwater heads correspond quite well to actual groundwater observations, like shown in Appendix G.4. Model parameters k and c are (to some extent) calibrated against these measurements. Consequently, it is believed that the constructed MODFLOW models realistically describe the groundwater behaviour of these systems.

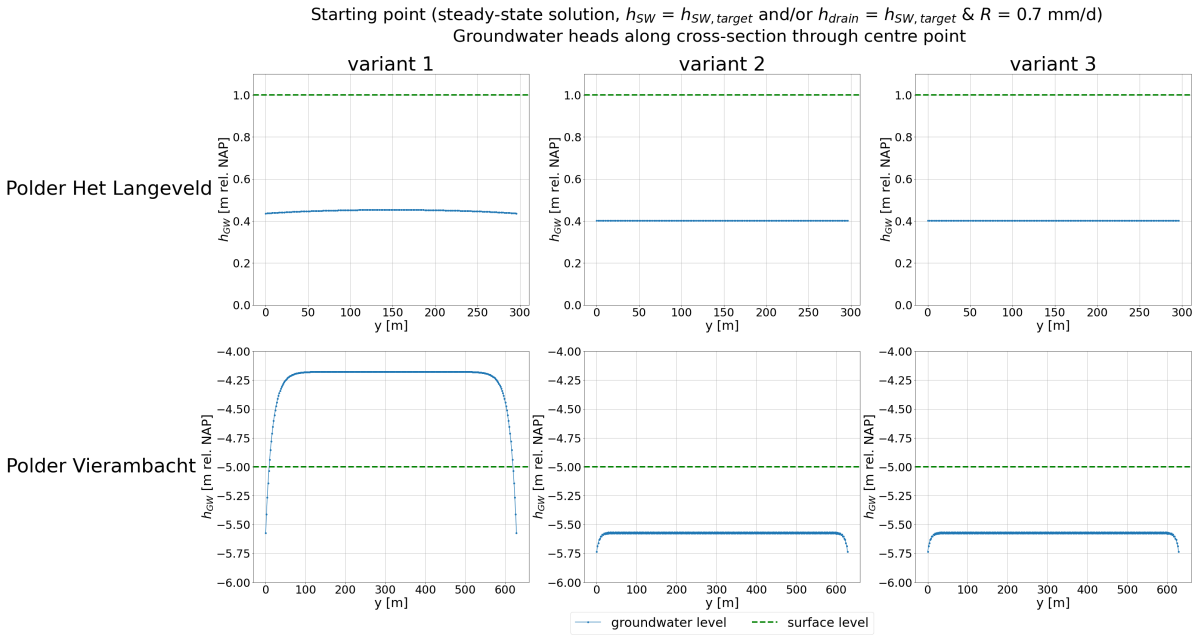

Figure 7.6: Starting point of all simulations; steady-state groundwater situation for R = 0.7 mm/d and h_{SW} = $h_{SW,target}$ and/or h_{drain} = $h_{SW,target}$.

7.2.2. Excluding feedback

Figures 7.7 and 7.8 contain the results of the simulations with the basic MODFLOW model (excluding the groundwater-surface water feedback). Each line shows the development of the groundwater head in time, in the centre of the plot, and belongs to a specific simulation.

Figure 7.7 is dedicated to Polder Het Langeveld. The following observations are made:

1. It takes approximately 40 days before a new equilibrium is obtained in case of variant 1.
2. Given variant 2, the system returns to a new equilibrium state in approximately 3 days. The interaction between the surface water and groundwater system is clearly enhanced by the submerged drains.
3. In case of variant 3, a new steady-state is reached in 3 days as well. The midpoint groundwater response is similar to the midpoint groundwater response in case of variant 2.
4. Compared to variant 1, the difference between h_{GW} at t = 0 d and h_{GW} at t = 5 d is very small for variant 2 and 3, which means that much water is discharged and water retention is limited. Furthermore, the difference in groundwater head is only weakly dependent on R.

The simulation results for Polder Vierambacht are depicted in Figure 7.8, which contains similar graphs. Variant 1 is not considered, like explained above. Based on Figure 7.8, the following points are raised:

1. In case of both variants, it takes approximately 20 days before the new steady-state is reached. The midpoint groundwater response is similar for both variants.
2. The difference between h_{GW} at t = 0 d and h_{GW} at t = 5 d is quite significant, especially compared to Polder Het Langeveld variant 2 and 3, which means that much water is retained.

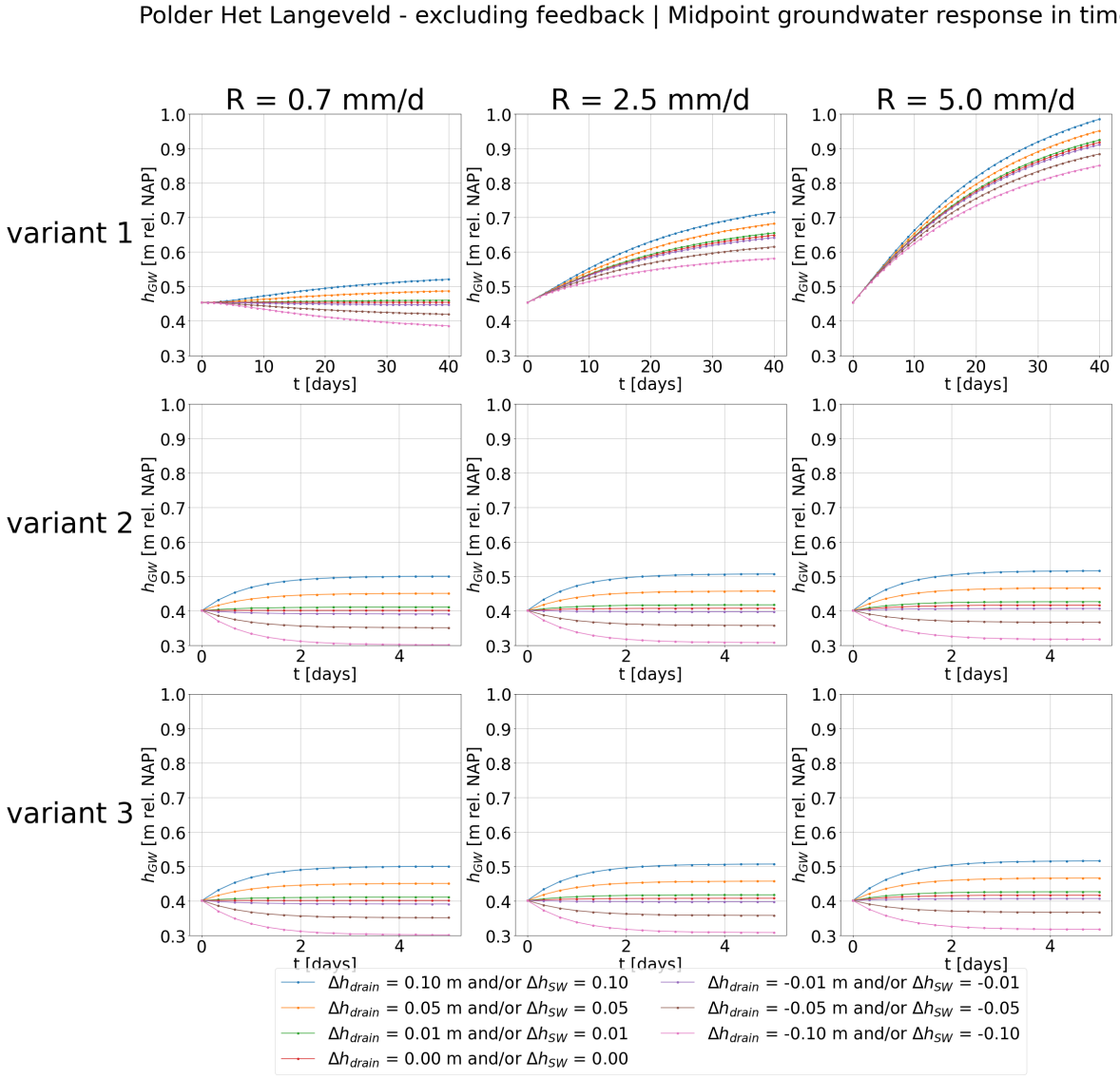

Figure 7.7: Midpoint groundwater response in time Polder Het Langeveld - excluding feedback.

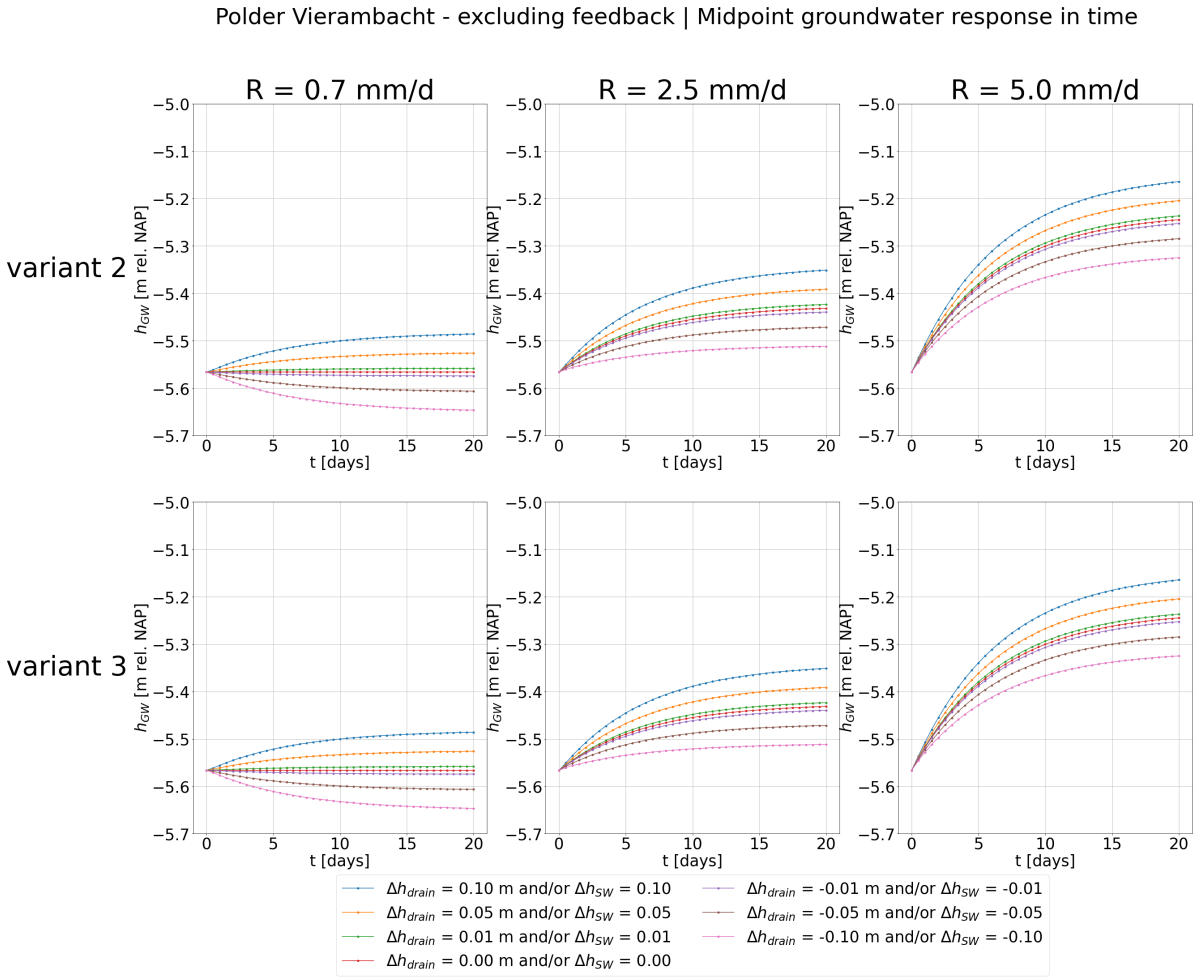

Figure 7.8: Midpoint groundwater response in time Polder Vierambacht - excluding feedback.

The groundwater behaviour and the contribution of various groundwater flow processes is further analyzed by means of the volume budget that is calculated by MODFLOW. Figures 7.9 and 7.10 contain water balances for Polder Het Langeveld and Polder Vierambacht respectively. They belong to the simulations with R equal to 2.5 mm/d and Δh_{SW} and/or Δh_{drain} equal to 0.01, 0.05 and 0.10 m. The x-axes represent time in d, while the y-axes represent the cumulative volume change in m^3. The following water balance components are plotted:

1. Groundwater storage (specific yield, increase in groundwater storage is positive) (blue lines),
2. Upward seepage (upward seepage is positive) (orange lines),
3. Recharge (downward recharge flux is positive) (green lines),
4. Infiltration ditch (flow from ditch to groundwater is positive, which is in accordance with MODFLOW's definition of positive flow direction) (red lines),
5. Infiltration drains (flow from drains to groundwater is positive) (purple lines).

The contribution of specific storage is not reviewed, since it is negligible compared to the other components.

Hereafter, the figures are discussed per case study area and variant. Most attention is paid to the flux between the ditch and the groundwater system, and the flux between the drains and the groundwater system.

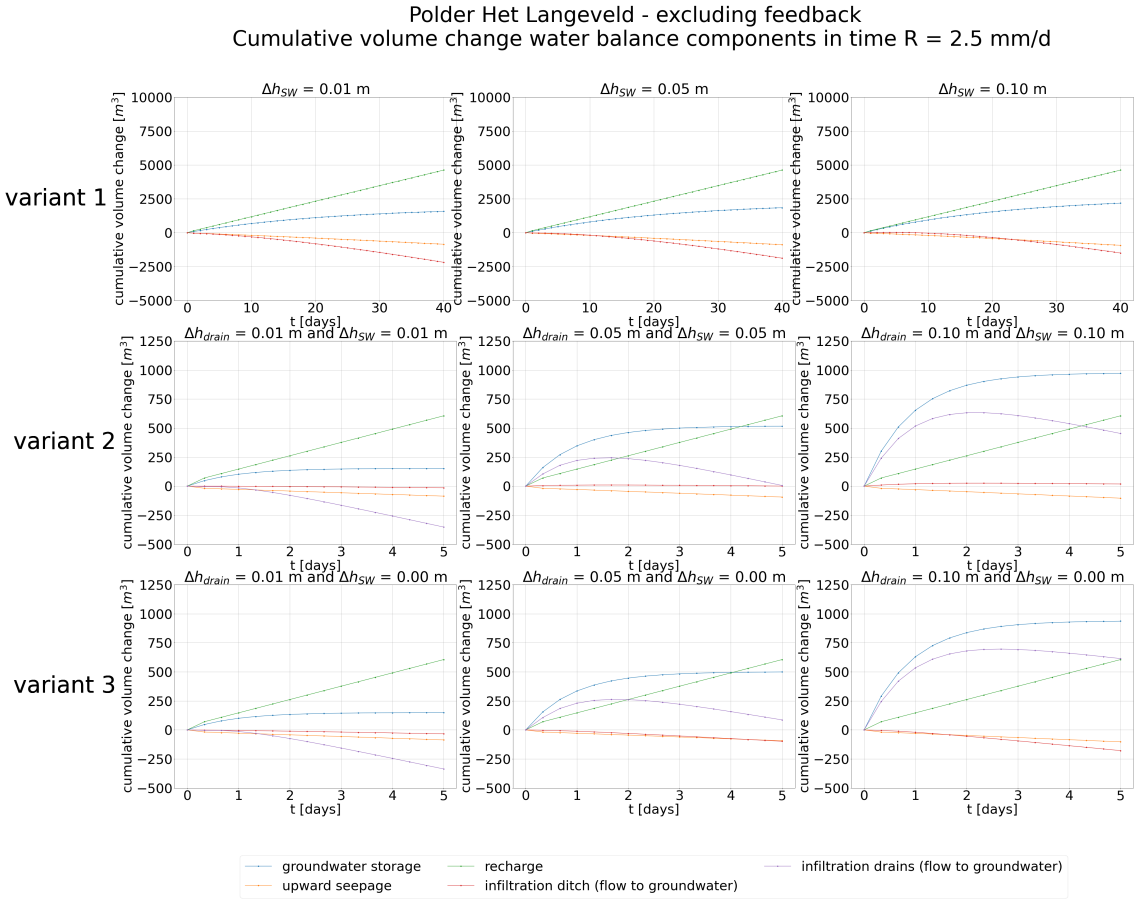

Figure 7.9: Cumulative volume change water balance components in time - Polder Het Langeveld, excluding feedback.

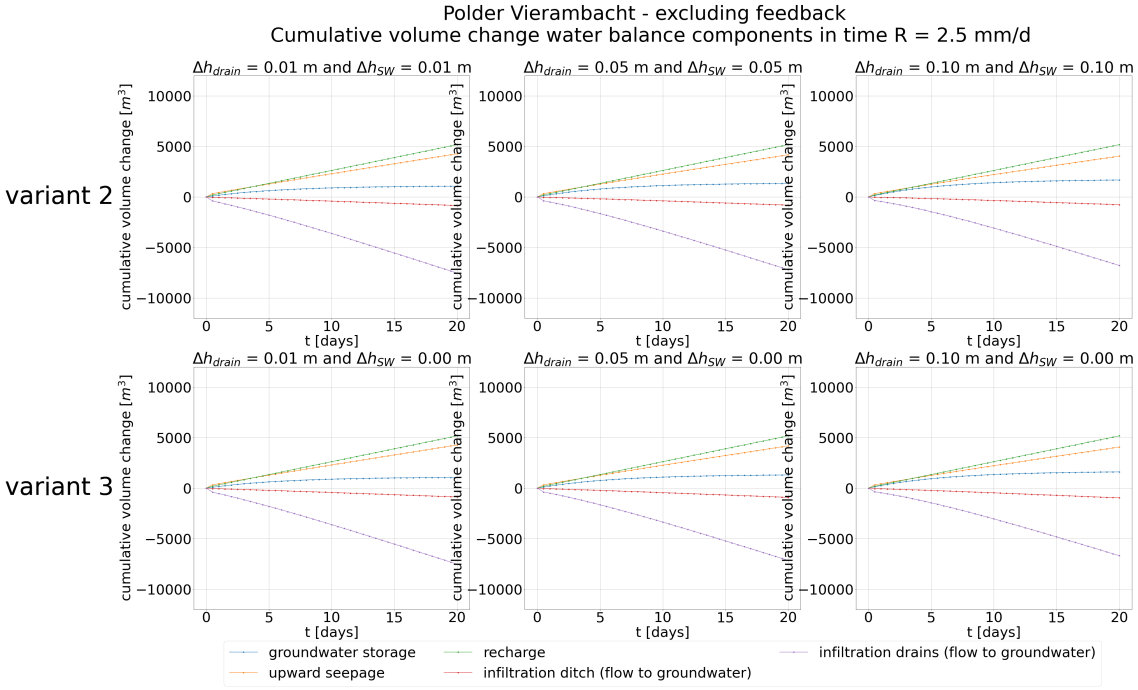

Figure 7.10: Cumulative volume change water balance components in time - Polder Vierambacht, excluding feedback.

Polder Het Langeveld

Variant 1

The orange lines demonstrate the occurrence of downward seepage. The seepage rate equals approximately -0.5 mm/d, which is in accordance with Figure 4.7 (a similar seepage rate is observed for the other variants).

A small amount of ditch water infiltrates to the groundwater system in case of Δh_{SW} = 10 cm, since the red line is slightly above zero during the first few days of the simulation. This can be explained by the fact that the ditch water level is raised instantaneously. Furthermore, the ditch water level is imposed as a constant boundary condition, assuming continuous and unlimited water supply. As a result, the water flow towards the groundwater system dominates the water flow towards the ditch, resulting in subirrigation. Gradually groundwater discharge dominates again, such that the ”infiltration ditch”-component becomes negative. In reality, the assumption of unrestricted water supply does not (always) hold, which means that the ditch water level cannot be assumed constant. Although the amount of subirrigation is very small, the graph shows why the extended MODFLOW model is required to correctly simulate the groundwater-surface water interaction.

Variant 2

The (undesired) effect of the assumption of a constant ditch water level becomes more pronounced here. The purple lines, which represent the ”infiltration drains”-component, are above the x-axis in case of Δh_{drain} = 5 cm and Δh_{SW} = 5 cm, and in case of Δh_{drain} = 10 cm and Δh_{SW} = 10 cm. This implies that subirrigation takes place via the drains. While the ditch water level is raised to create extra storage capacity for rain water, the space created is occupied by ditch water that infiltrates via the drainage pipes. This is not desirable, because the main objective of the designed controller is to retain and store precipitation as much as possible. This explains why the extended MODFLOW model is required. After a certain amount of time a tipping point occurs, at which the cumulative volume change of the ”infiltration drains”- component reaches a maximum, which marks the transition between subirrigation and groundwater discharge. The ”infiltration ditch”-component, represented by the red line, is above the x-axis for most of the time too, meaning that ditch water is also directly infiltrated.

Variant 3

The water balance of variant 3 is very similar to the water balance of variant 2. Subirrigation occurs. However, since h_{SW} is not raised, the increase in groundwater level is accompanied by increased groundwater discharge towards the ditch. The infiltrated water or rain water is discharged, which is not very efficient.

Polder Vierambacht

Variant 2

The orange lines (”upward seepage”-component) demonstrate the occurrence of upward seepage. The seepage rate equals approximately 2 mm/d, which seems reasonable based on Figure 4.7. A similar seepage rate occurs in case of variant 3.

In contrast to Polder Het Langeveld, subirrigation does not occur here. The red and purple lines are below the x-axis. Due to the bulging groundwater table, the groundwater table is higher than the surface water level. Subirrigation would occur if a different starting point would have been selected. For example, if the initial groundwater level would be lower than the water level to which h_{SW} is raised. Application of the basic MODFLOW model would be less problematic for the simulations performed here, but the extended MODFLOW model is required to properly simulate all possible situations.

Variant 3

Again, the water balance of variant 3 is very similar to the water balance of variant 2. Because the groundwater level increases while h_{SW} is not raised, groundwater discharge towards the ditch increases slightly. Infiltrated water or rain water is thus lost.

Based on the above observations, it can be concluded that the application of the extended MODFLOW model becomes less relevant for situations with less permeable soils and less drainage capacity (re-

lated to the presence of drainage pipes). The greater the groundwater-surface water interaction, the more important the use of the extended model.

7.2.3. Including feedback

Like suggested in Section 5.1.3, it is questionable whether the extended MODFLOW model is appropriate for variant 3. Figures 7.11 and 7.12 contain the results of a specific simulation with the extended MODFLOW model (including feedback). The midpoint groundwater response and development of sump water level in time for Δh_{weir} = 0.05 m and R = 2.5 mm/d is depicted for both polders. The applied model time step is one hour. The ditch water level, which is indicated by the dark blue line, is constant. The weir crest level is indicated by the dashed black line.

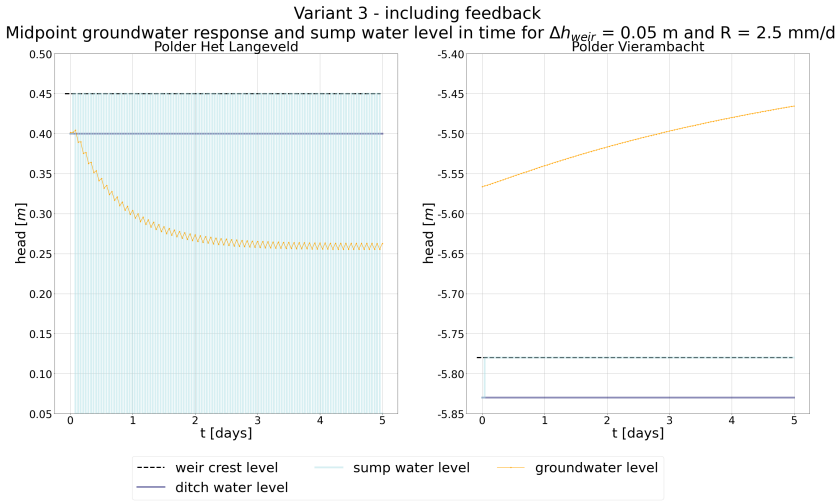

Figure 7.11: Midpoint groundwater response variant 3 - including feedback.

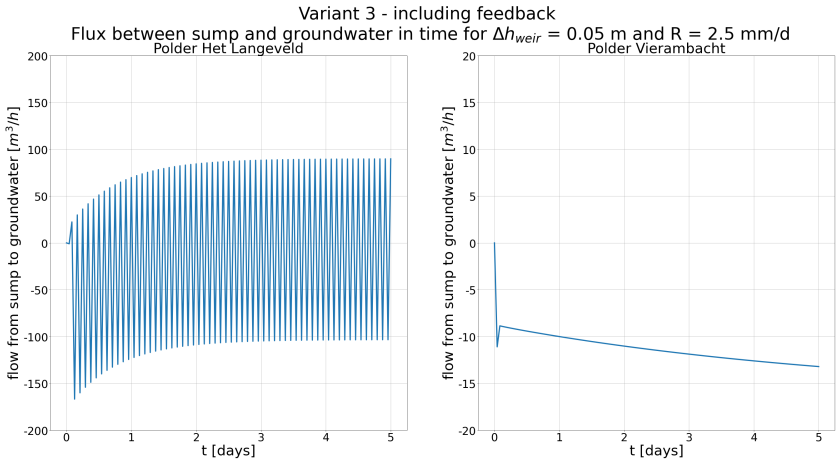

Figure 7.12: Flux between sump and groundwater variant 3 - including feedback.

It can be observed in Figure 7.11 that the sump water level in Polder Het Langeveld fluctuates between the maximum and minimum level. The maximum level is defined by the weir crest height, which is 0.45 m NAP, while the minimum level is regulated by $h_{bot,drain}$, which is 0.05 m NAP. Figure 7.12 shows the flux between the sump and the groundwater system for each model time step [m^3/h]. The sump water level is updated according to Equation 5.4. Because the area of the sump is relatively small and the flux per model time step is considerable, the changes in sump water level are enormous, resulting in an oscillating pattern. The model time step is thus too large for the size of the sump and the occurring flow

rates. In reality, these fluctuations do not occur. Figure 7.11 shows that the sump water level initially equals 0.40 m NAP. When the weir is raised, the sump gets filled up to weir crest level by groundwater discharge within one time step. Because the sump water level exceeds the groundwater level, subirrigation takes place during the next time step and the sump is completely emptied. This leads to an enormous deviation between sump and groundwater level, leading to a huge amount of groundwater discharge during the subsequent time step, such that the sump is full again. This process repeats itself during the consecutive time steps. It is expected that the groundwater-surface water dynamics can only be correctly simulated if the time step is very, very small. The oscillating pattern is even obtained when Δt equals 1 minute. Reducing Δt to seconds would lead to extremely large calculation times, which is not desirable. It is therefore decided to omit variant 3 for Polder Het Langeveld.

The graph on the right hand side in Figure 7.11 shows the results for Polder Vierambacht. Initially, the sump water level equals -5.83 m NAP. When the weir is raised, the sump gets filled up to weir crest level by groundwater discharge within one time step. Because the sump water level remains lower than the groundwater level, groundwater is continuously discharged during the consecutive time steps and the oscillating pattern is not obtained. Figure 7.12 shows that approximately 12 m^3/h needs to be discharged from the sump to the ditch. Based on this simulation, one could think that the basic MODFLOW model could be applied to represent variant 3 in Polder Vierambacht. However, it is expected that the oscillating pattern would occur for a different starting point, namely if the initial groundwater level would be lower than the level to which h_{weir} is raised. This is checked by an extra simulation. Its result is depicted in Figure 7.13. It is therefore also decided to omit variant 3 for Polder Vierambacht.

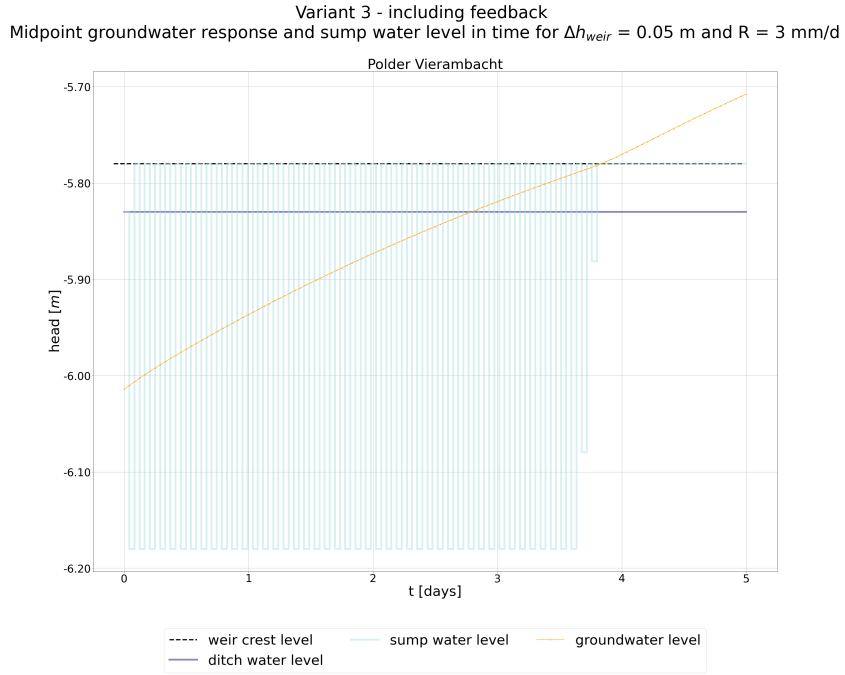

Figure 7.13: Midpoint groundwater response Polder Vierambacht variant 3 - including feedback.

For the other variants, various simulations including feedback are performed (Table F.3). The results are depicted in Figure 7.14, 7.15 and 7.16 for Polder Het Langeveld variant 1, Polder Het Langeveld variant 2 and Polder Vierambacht variant 3 respectively. The evolution of the midpoint groundwater head and ditch water level are shown. The ditch water level is represented by the dark blue line, whereas the groundwater level is represented by the light blue line. The weir crest level is indicated by the black dashed line. It can be observed that the ditch water level gradually increases up to h_{weir}. The groundwater level adapts accordingly. The filling time depends on R and Δh_{weir}. While the groundwater flow processes are relatively slow in Polder Vierambacht, the filling time is very short. This can be explained by the large seepage rate.

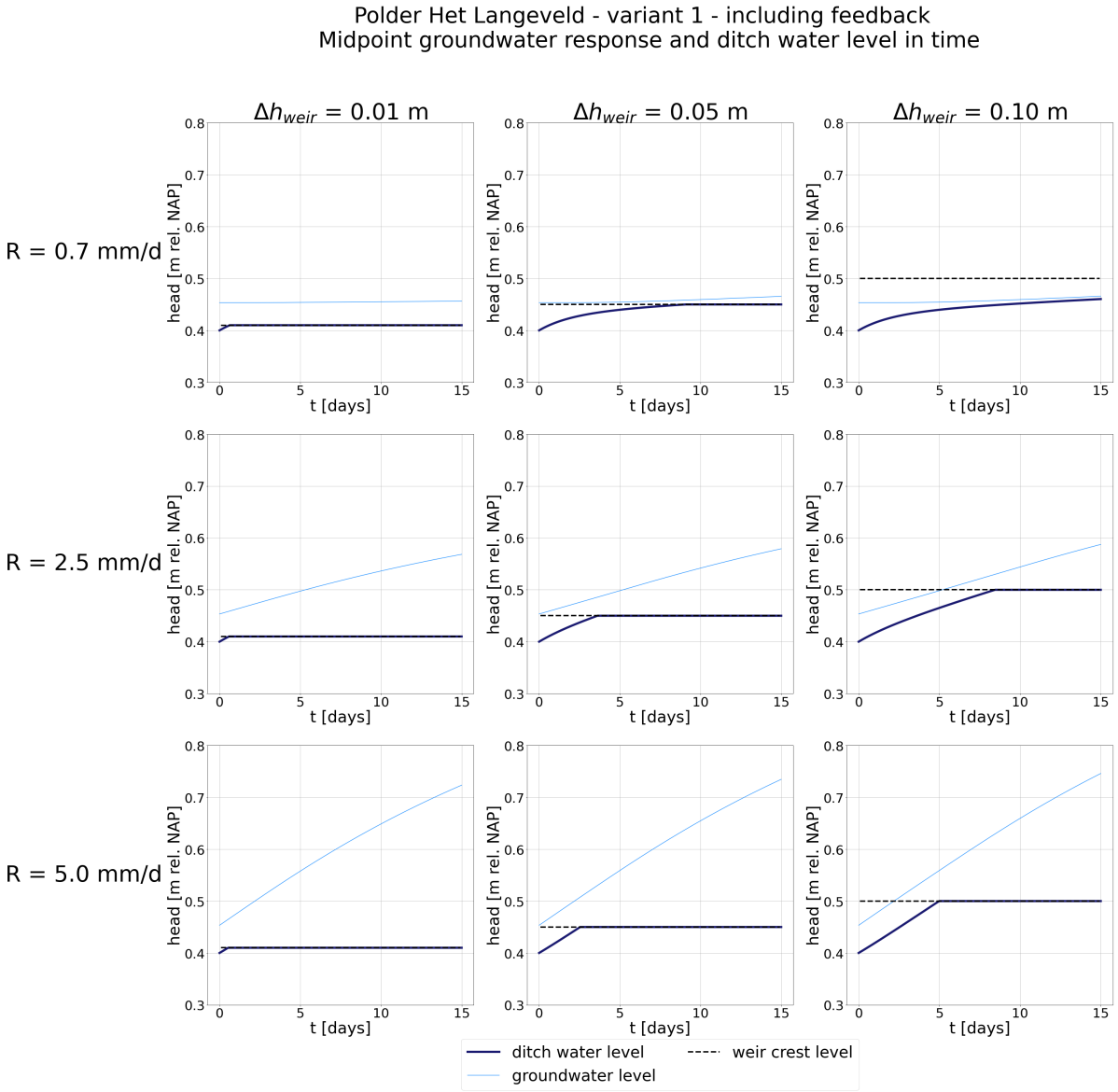

Figure 7.14: Midpoint groundwater response Polder Het Langeveld variant 1 - including feedback.

Figure 7.17 depicts the water balances for the remaining variants of Polder Het Langeveld (variant 1 and 2). It can be observed that subirrigation no longer occurs as the red and purple lines remain below the x-axis. Considering variant 2, recharge leads to an increase in groundwater storage during the first 10 days of the simulation. Only a small part is discharged by the drains. The storage capacity is reached after approximately 10 days. At this point, the drains start discharging the excess water.

Figure 7.18 depicts the water balances for the remaining variant of Polder Vierambacht (variant 2).

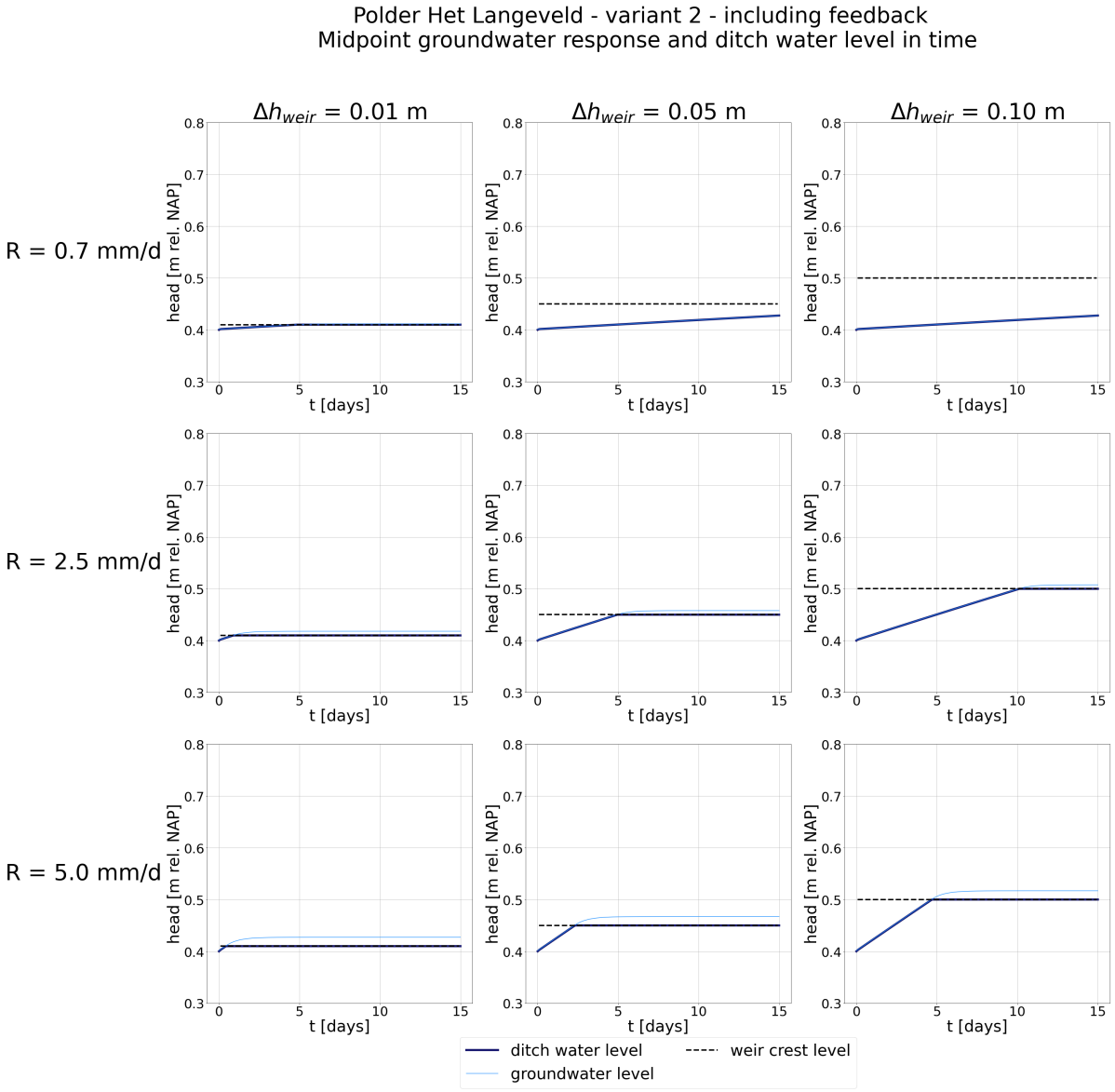

Figure 7.15: Midpoint groundwater response Polder Het Langeveld variant 2 - including feedback.

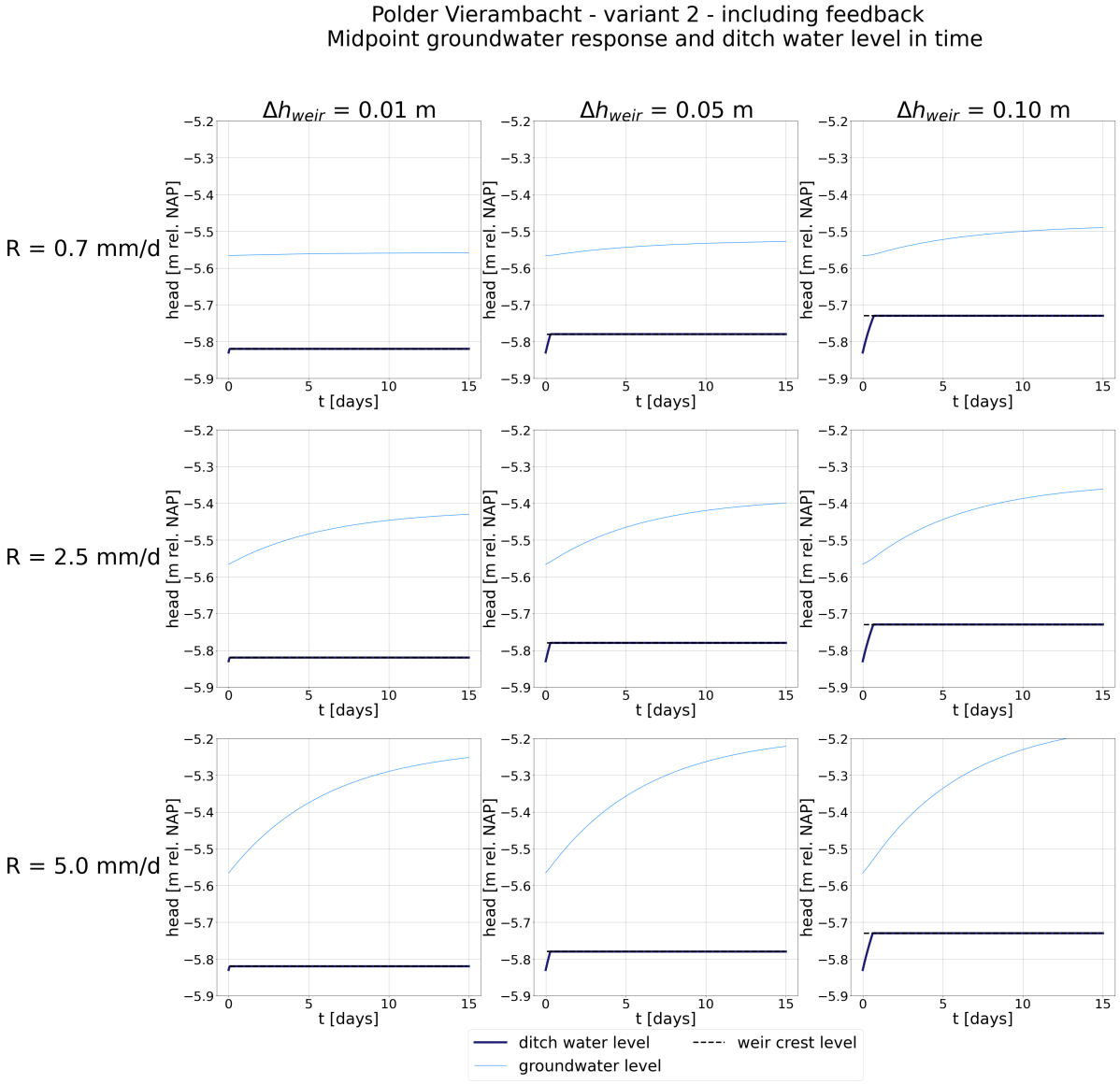

Figure 7.16: Midpoint groundwater response Polder Vierambacht variant 2 - including feedback.

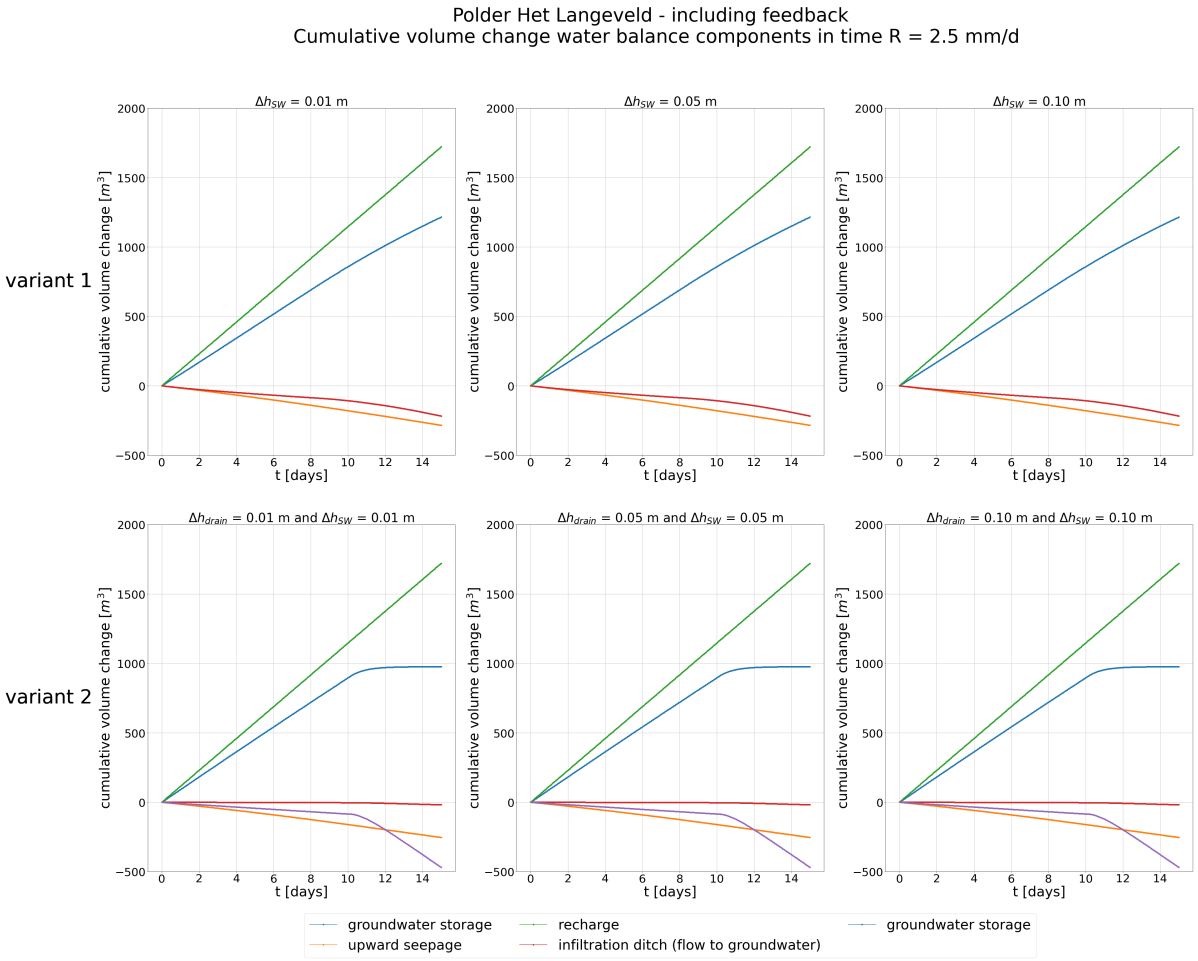

Figure 7.17: Cumulative volume change water balance components in time - Polder Het Langeveld, including feedback.

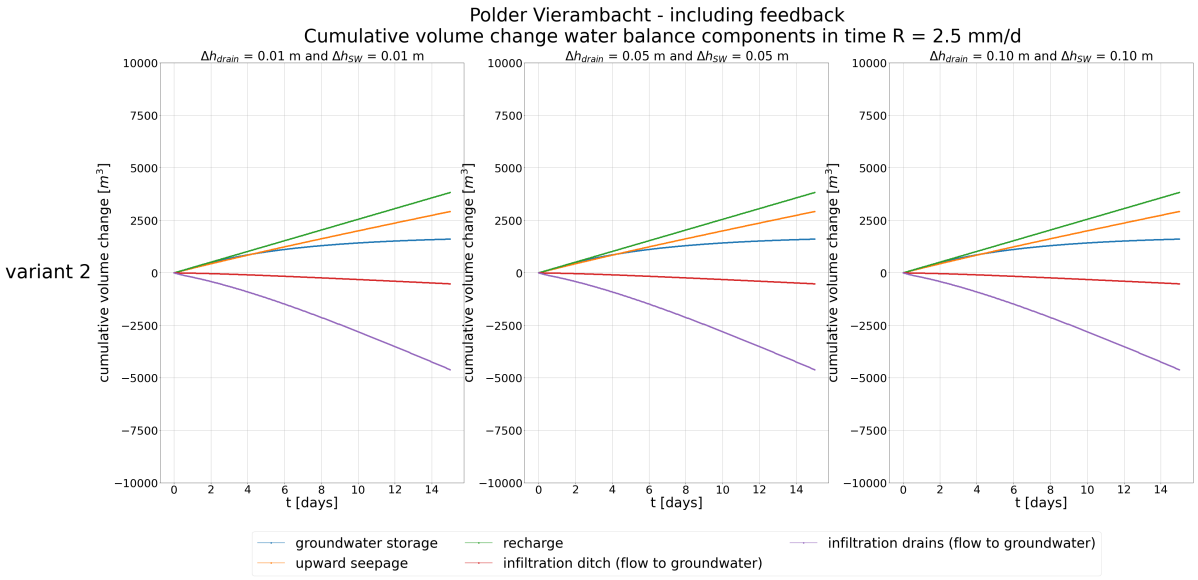

Figure 7.18: Cumulative volume change water balance components in time - Polder Vierambacht, including feedback.

8

Physical time series model calibration and verification

This chapter discusses calibration and verification of the PTSMs. Section 8.1 contains graphs that illustrate the calibration results. The PTSMs are calibrated against the result of one specific MODFLOW simulation. In Section 8.2, the obtained model parameters are verified by comparing the PTSM results to MODFLOW results for other simulations.

8.1. Model calibration

The model parameters (α and β) are found by calibrating the PTSMs to groundwater level time series. The groundwater level time series result from simulations with the basic MODFLOW model (excluding feedback, R = 2.5 mm/d, Δh_{drain} = 0.05 m and/or Δh_{SW} = 0.05 m). This is covered in subsection 8.1.1. The obtained model parameters are then used to fit the extended PTSM to MODFLOW simulations including feedback, which is discussed in subsection 8.1.2.

8.1.1. Excluding feedback

Figure 8.1 shows the calibration results for the combinations of polders and variants that are successfully modelled. The midpoint groundwater response in time is plotted and represented by the green dots. The blue line represents the model fit of PTSM 1, while the orange line represents the model fit of PTSM 2. The obtained model parameters are shown by the title of the graphs.

Information on the goodness of the fit is also provided in the title of the individual graphs. e_{GW} represents the difference between the groundwater head calculated by MODFLOW and the groundwater head calculated by the PTSM at the end of the simulation [mm]. At this point, the groundwater level is in (approximate) equilibrium. PTSM 2 outperforms PTSM 1 for all variants and case study areas, since e_{GW} is lower for model 2 than for model 1. This can also be concluded by looking at the figures. It is therefore decided to select model 2.

8.1.2. Including feedback

Subsequently, the extended version of PTSM 2 is used to simulate the groundwater level and ditch water level for R = 2.5 mm/d and Δh_{weir} = 0.05 m. The model parameter values that were determined in subsection 8.1.1 are applied and λ equals 1. The midpoint groundwater level as well as the ditch water level are plotted against time in Figure 8.2. The MODFLOW simulation results are also plotted, such that a comparison can be made and the performance of the PTSM can be determined. The ditch water level and groundwater level as determined by MODFLOW are depicted in dark and light blue respectively. The ditch water level and groundwater level as determined by PTSM 2 are represented by the red and orange line respectively. The weir crest level is indicated by the black dashed line. For variant 1 Polder Het Langeveld and variant 2 Polder Vierambacht, the PTSM results correspond

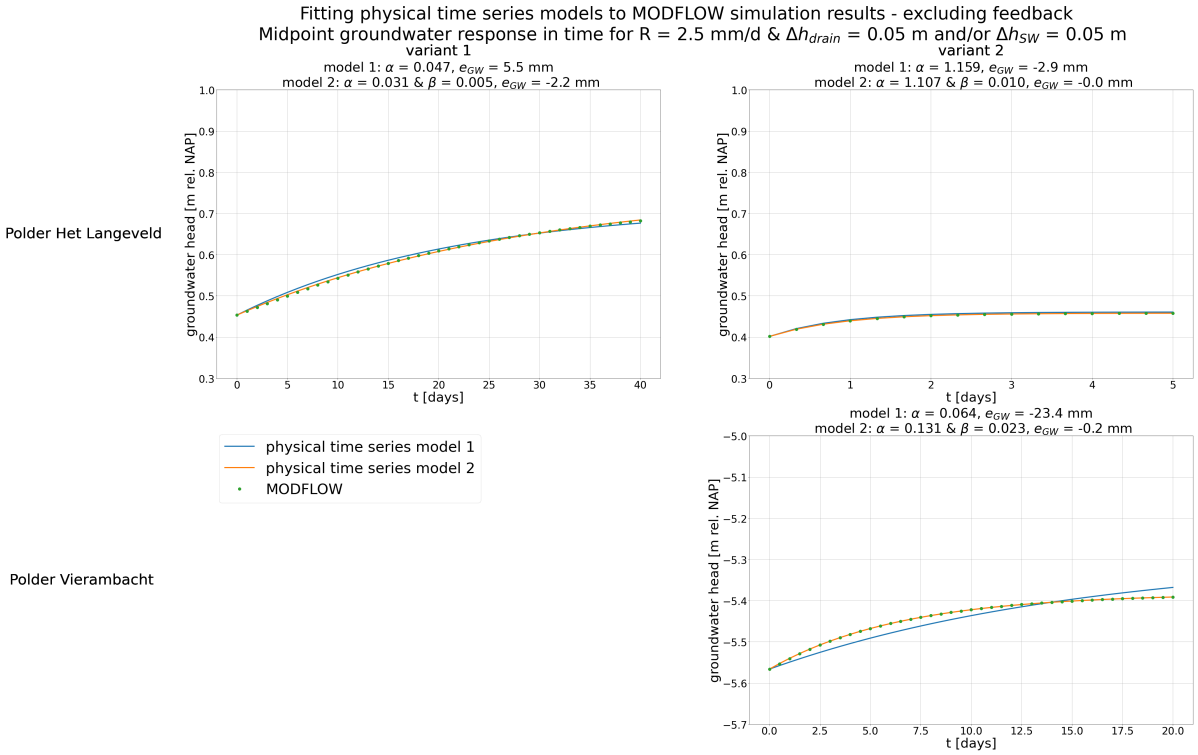

Figure 8.1: Fitting physical time series models to MODFLOW simulation results - excluding feedback.

(almost) exactly to the MODFLOW results. The deviation is a few millimeters at most. This is considered acceptable. The difference between the model results is bigger for variant 2 Polder Het Langeveld, even if λ is calibrated. It is therefore decided to apply PTSM 1 for variant 2 Polder Het Langeveld. According to Figure 8.1, PTSM 1 works quite well in this case.

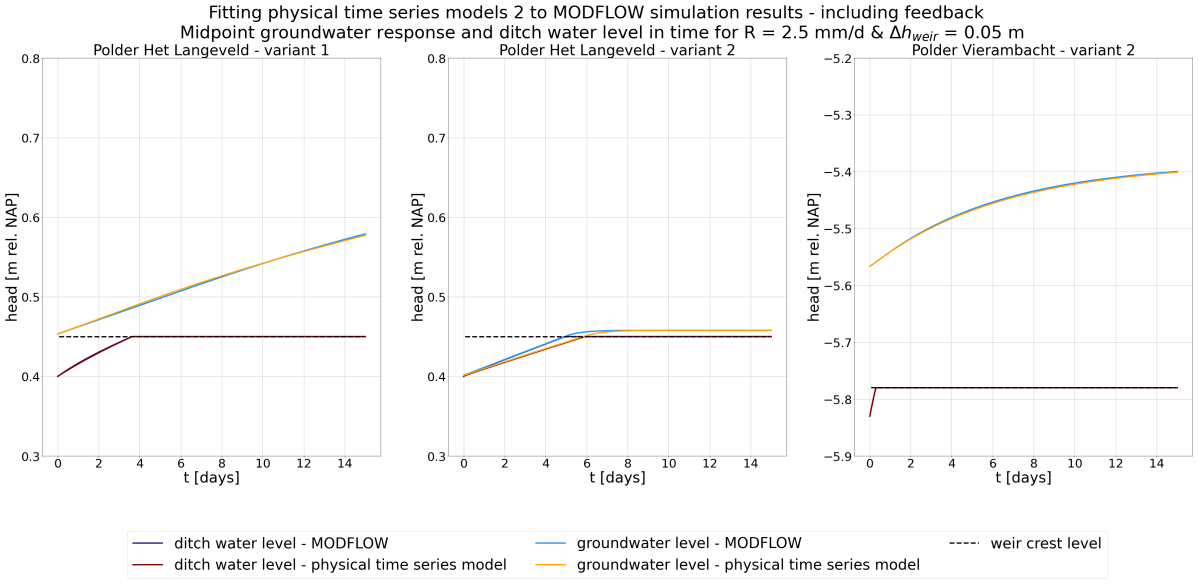

Figure 8.2: Fitting physical time series models 2 to MODFLOW simulation results - including feedback.

It is checked whether the extended version of PTSM 1 simulates the groundwater level and ditch water level well for variant 2 Polder Het Langeveld. The results are shown in Figure 8.3. The depicted results correspond to a transient calculation for R = 5 mm/d and Δh_{weir} = 0.10 m. Again, the midpoint groundwater response and ditch water level are plotted in time. The same colours are used. The left

hand graph shows the model fit for λ = 1. A deviation between PTSM 1 results and MODFLOW results is observed. However, when λ is calibrated, this deviation decreases and a fairly good fit is obtained, like shown by the right hand graph. λ equals approximately 0.6. It should be noted that λ is quite dependent on the simulation to which PTSM 1 is fit, i.e. a considerably different λ is obtained if PTSM 1 is fitted to a different MODFLOW simulation.

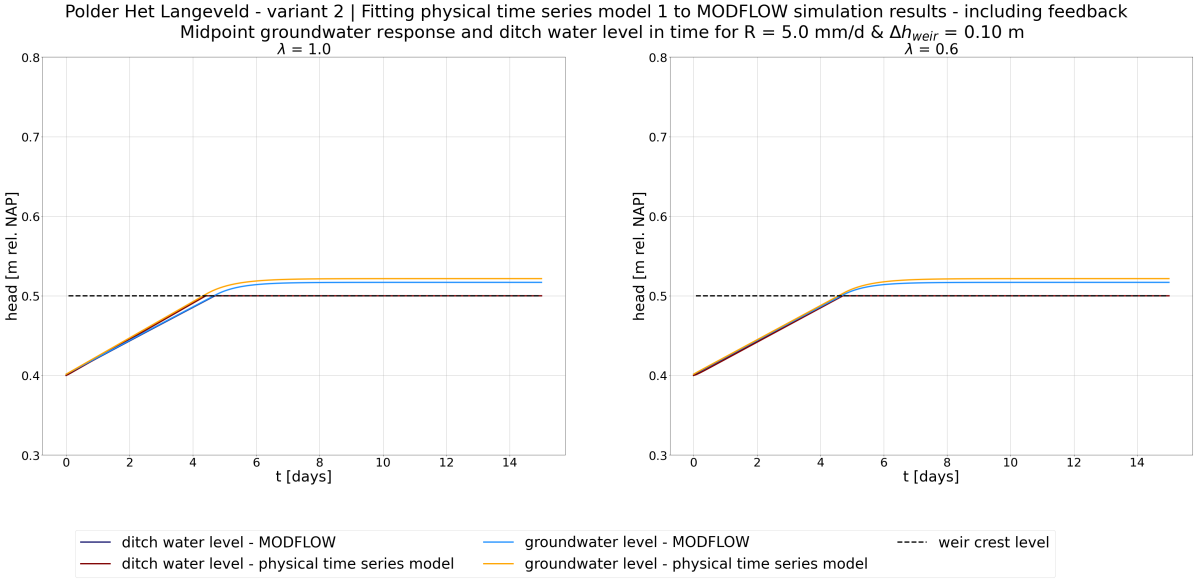

Figure 8.3: Fitting physical time series models 1 to MODFLOW simulation results variant 2 Polder Het Langeveld - including feedback.

A possible explanation for the obtained λ is found. The groundwater table between two canals is parabolic for a plot of infinite length and in the absence of drains. This implies that the groundwater table drop is not uniform, i.e. if the groundwater table drops by $h_1 - h_2$ m in the centre of the field, a smaller drop is observed elsewhere. Figure 8.4 shows two parabolas. It can be shown that the area between the parabolas equals 2/3 of the area of a rectangle that fits between the tops of the parabolas. Because the extent of the field is restricted and drains are present, it is logical that λ slightly differs from 2/3. This explains why λ = 0.6 is obtained.

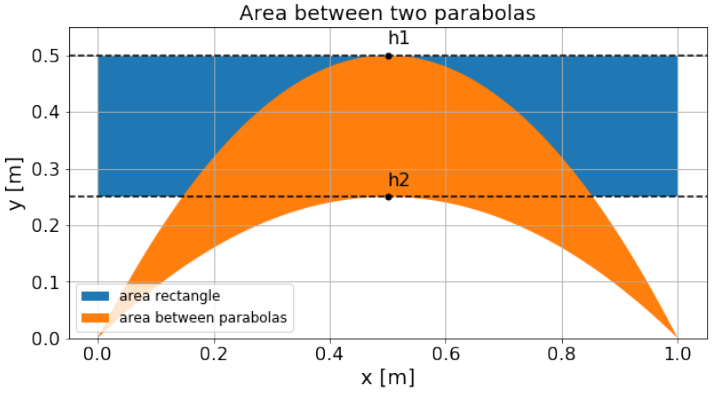

Figure 8.4: Figure showing the area between two parabolas and the area of a rectangle that fits between the tops of the parabolas. The orange area is 2/3 of blue area, which explains why λ = 0.6 is obtained.

The selected PTSMs and obtained model parameters for each variant and polder are summarized by Table 8.1. The obtained values for β do not exactly match with the reciprocal of c, which was expected based on Equation 5.15.

Table 8.1: Overview selected PTSMs and obtained model parameters.

Polder & variant	PTSM	α	β	λ
Polder Het Langeveld, variant 1	2	0.031	0.005	1
Polder Het Langeveld, variant 2	1	1.159	-	0.6
Polder Vierambacht, variant 2	2	0.131	0.023	1

8.2. Model verification

In this section, the obtained model parameters are verified by comparing the physical time series model results to MODFLOW results for other simulations.

8.2.1. Excluding feedback

All MODFLOW simulations excluding feedback (Table F.1) are repeated with the fitted PTSMs. Figure 8.5 shows the results. The MODFLOW results are represented by the coloured dots. The PTSM results are represented by the coloured lines. Each colour represents a specific simulation. The groundwater response in the centre of the plot is plotted against time. The dots and lines coincide, which means that the PTSM reproduces the groundwater behaviour well. Table 8.2 shows that e_{GW} is in the order of millimetres. Table 8.3 gives the maximum absolute error between t = 0 and time of equilibrium ($e_{GW,max}$ [mm]). The largest errors are obtained for Polder Het Langeveld, variant 1. The largest deviation is 14.36 mm. The errors are considered acceptable.

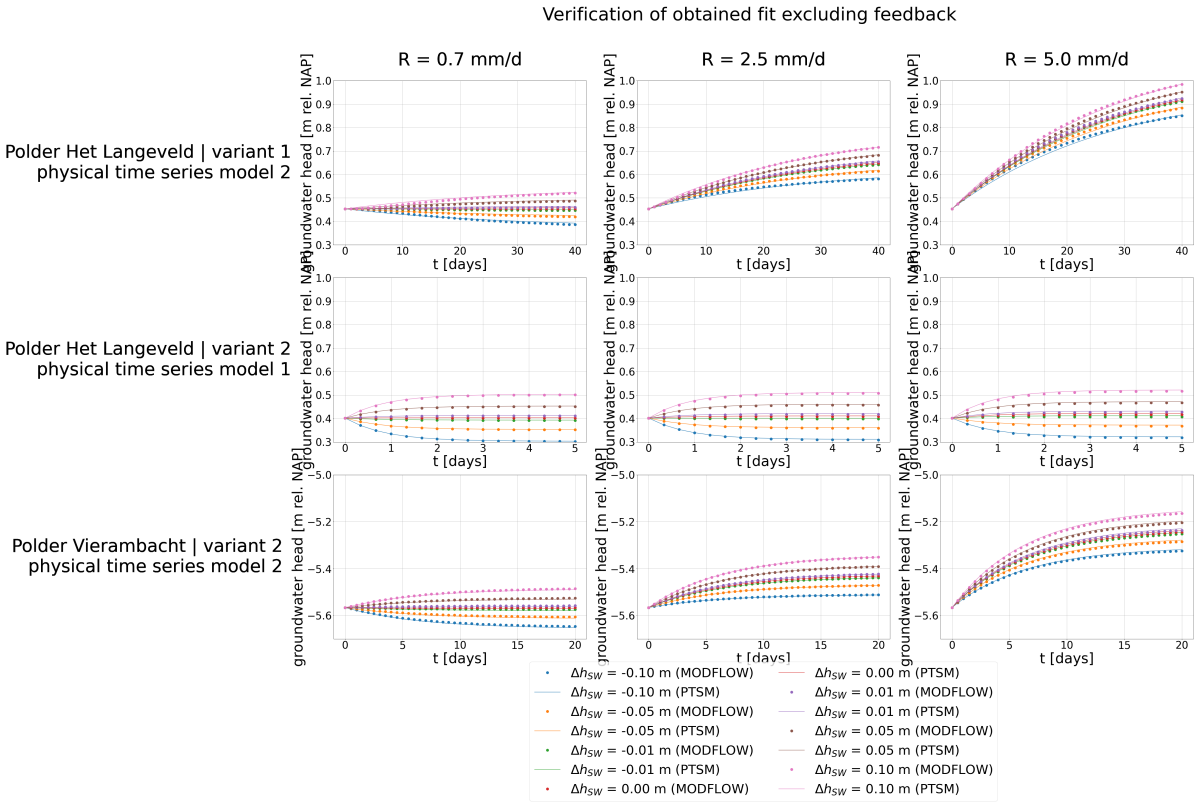

Figure 8.5: Verification of the obtained model parameters - excluding feedback. All MODFLOW simulations excluding feedback are repeated with the fitted PTSMs. The groundwater head in the centre of the field calculated by the PTSM (lines) and MODFLOW (dots) are plotted against time.

Table 8.2: The difference between the groundwater head calculated by MODFLOW and the groundwater head calculated by the PTSM at the end of each simulation (e_{GW} [mm]).

Forcing	Polder Het Langeveld v1	Polder Het Langeveld v2	Polder Vierambacht v2
R = 0.7 mm/d			
Δh_{SW} = -0.10 m	-6.58	-1.13	5.29
Δh_{SW} = -0.05 m	-5.74	-1.34	4.99
Δh_{SW} = -0.01 m	-5.04	-1.50	4.75
Δh_{SW} = 0 m	-4.86	-1.55	4.69
Δh_{SW} = 0.01 m	-4.68	-1.59	4.63
Δh_{SW} = 0.05 m	-3.94	-1.75	4.40
Δh_{SW} = 0.10 m	-3.00	-1.96	4.12
R = 2.5 mm/d			
Δh_{SW} = -0.10 m	-4.65	-2.28	0.79
Δh_{SW} = -0.05 m	-3.86	-2.49	0.47
Δh_{SW} = -0.01 m	-3.20	-2.66	0.21
Δh_{SW} = 0 m	-3.03	-2.70	0.15
Δh_{SW} = 0.01 m	-2.86	-2.74	0.09
Δh_{SW} = 0.05 m	-2.16	-2.91	-0.16
Δh_{SW} = 0.10 m	-1.26	-3.12	-0.46
R = 5.0 mm/d			
Δh_{SW} = -0.10 m	-3.97	-3.88	-5.78
Δh_{SW} = -0.05 m	-3.23	-4.09	-6.13
Δh_{SW} = -0.01 m	-2.62	-4.26	-6.40
Δh_{SW} = 0 m	-2.46	-4.30	-6.47
Δh_{SW} = 0.01 m	-2.30	-4.35	-6.54
Δh_{SW} = 0.05 m	-1.66	-4.52	-6.81
Δh_{SW} = 0.10 m	-0.82	-4.73	-7.13

Table 8.3: The maximum absolute error between t = 0 and time of equilibrium ($e_{GW,max}$ [mm]).

Forcing	Polder Het Langeveld v1	Polder Het Langeveld v2	Polder Vierambacht v2
R = 0.7 mm/d			
Δh_{SW} = -0.10 m	6.58	1.13	5.29
Δh_{SW} = -0.05 m	5.74	1.34	4.99
Δh_{SW} = -0.01 m	5.04	1.50	4.75
Δh_{SW} = 0 m	4.86	1.55	4.69
Δh_{SW} = 0.01 m	4.68	1.59	4.63
Δh_{SW} = 0.05 m	5.24	1.90	4.40
Δh_{SW} = 0.10 m	8.82	2.55	4.12
R = 2.5 mm/d			
Δh_{SW} = -0.10 m	8.68	2.28	1.77
Δh_{SW} = -0.05 m	5.30	2.49	1.03
Δh_{SW} = -0.01 m	3.20	2.66	0.61
Δh_{SW} = 0 m	3.03	2.70	0.53
Δh_{SW} = 0.01 m	2.86	2.74	0.45
Δh_{SW} = 0.05 m	3.15	2.98	0.64
Δh_{SW} = 0.10 m	6.71	3.51	1.43
R = 5.0 mm/d			
Δh_{SW} = -0.10 m	14.36	3.88	5.78
Δh_{SW} = -0.05 m	12.01	4.09	6.13
Δh_{SW} = -0.01 m	10.55	4.26	6.40
Δh_{SW} = 0 m	10.24	4.30	6.47
Δh_{SW} = 0.01 m	9.94	4.35	6.54
Δh_{SW} = 0.05 m	8.96	4.55	6.81
Δh_{SW} = 0.10 m	8.12	4.97	7.13

8.2.2. Including feedback

The MODFLOW simulations including feedback (Table F.3) are also repeated with the fitted PTSMs. Figure 8.6, 8.7 and 8.8 show the results. The midpoint groundwater response and ditch water level are plotted in time. The ditch water level and groundwater level as determined by MODFLOW are represented by the dark blue and light blue lines respectively. The ditch water level and groundwater level as determined by the PTSM are represented by the red and orange lines respectively. The light blue and orange lines overlap, just like the dark blue and red lines. This means that the PTSM reproduces the groundwater behaviour well. The root mean square error (RMSE) is provided in the title of the graphs.

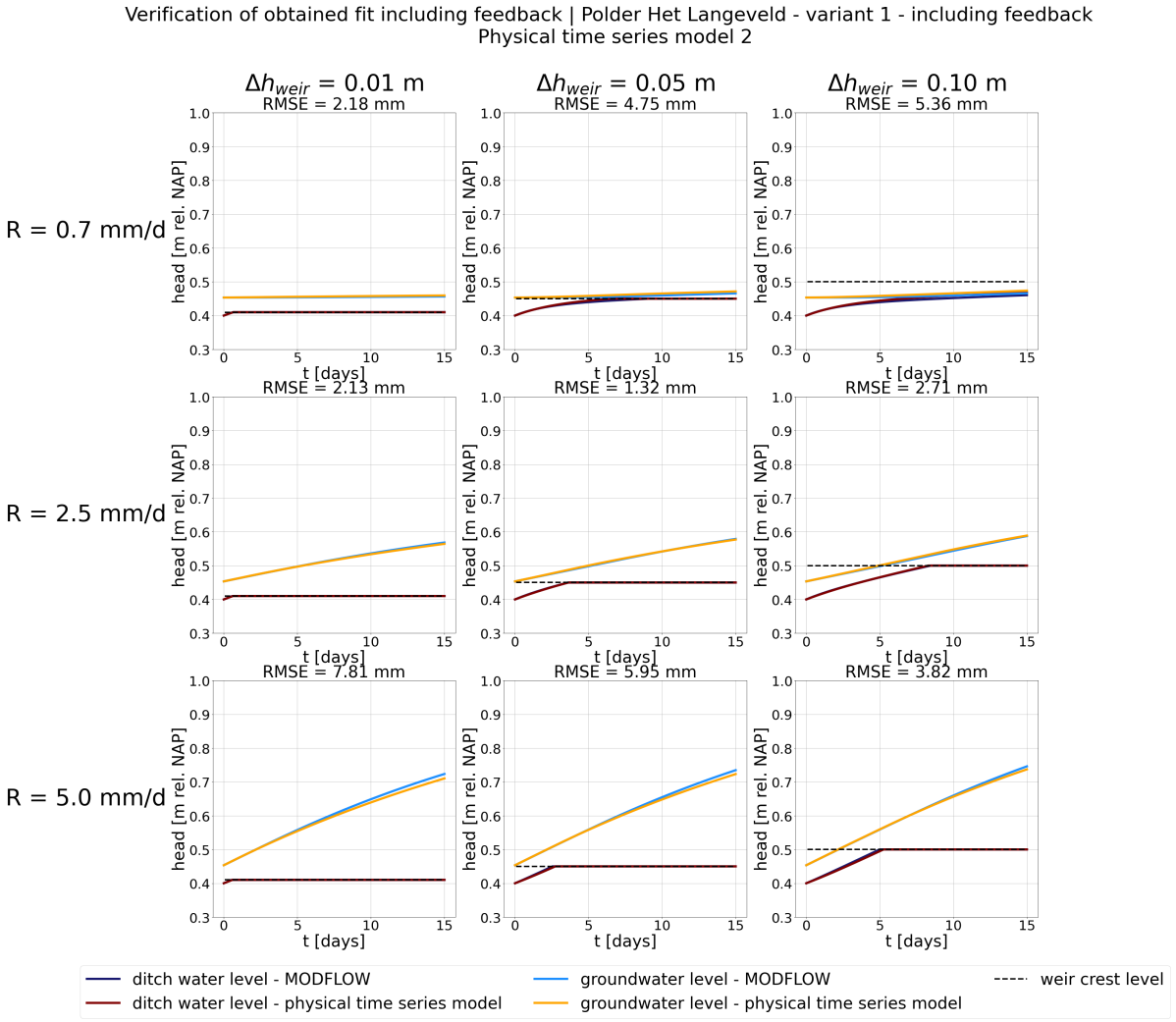

Figure 8.6: Verification of the obtained model parameters, variant 1 Polder Het Langeveld - including feedback. All MODFLOW simulations including feedback are repeated with the fitted PTSM 2. The simulated groundwater heads in the centre of the field and ditch water level are plotted against time.

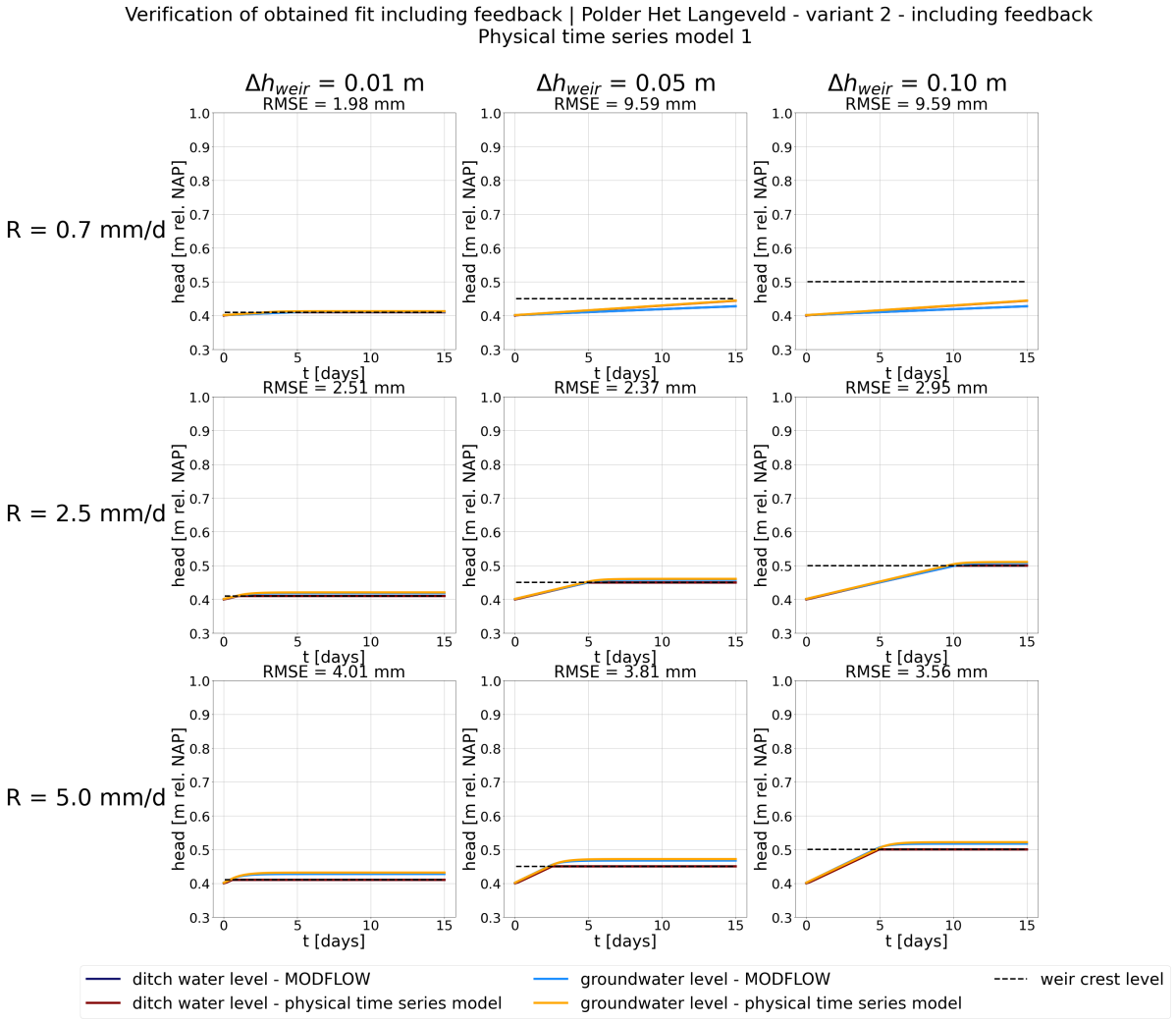

Figure 8.7: Verification of the obtained model parameters, variant 2 Polder Het Langeveld - including feedback. All MODFLOW simulations including feedback are repeated with the fitted PTSM 1. The simulated groundwater heads in the centre of the field and ditch water level are plotted against time.

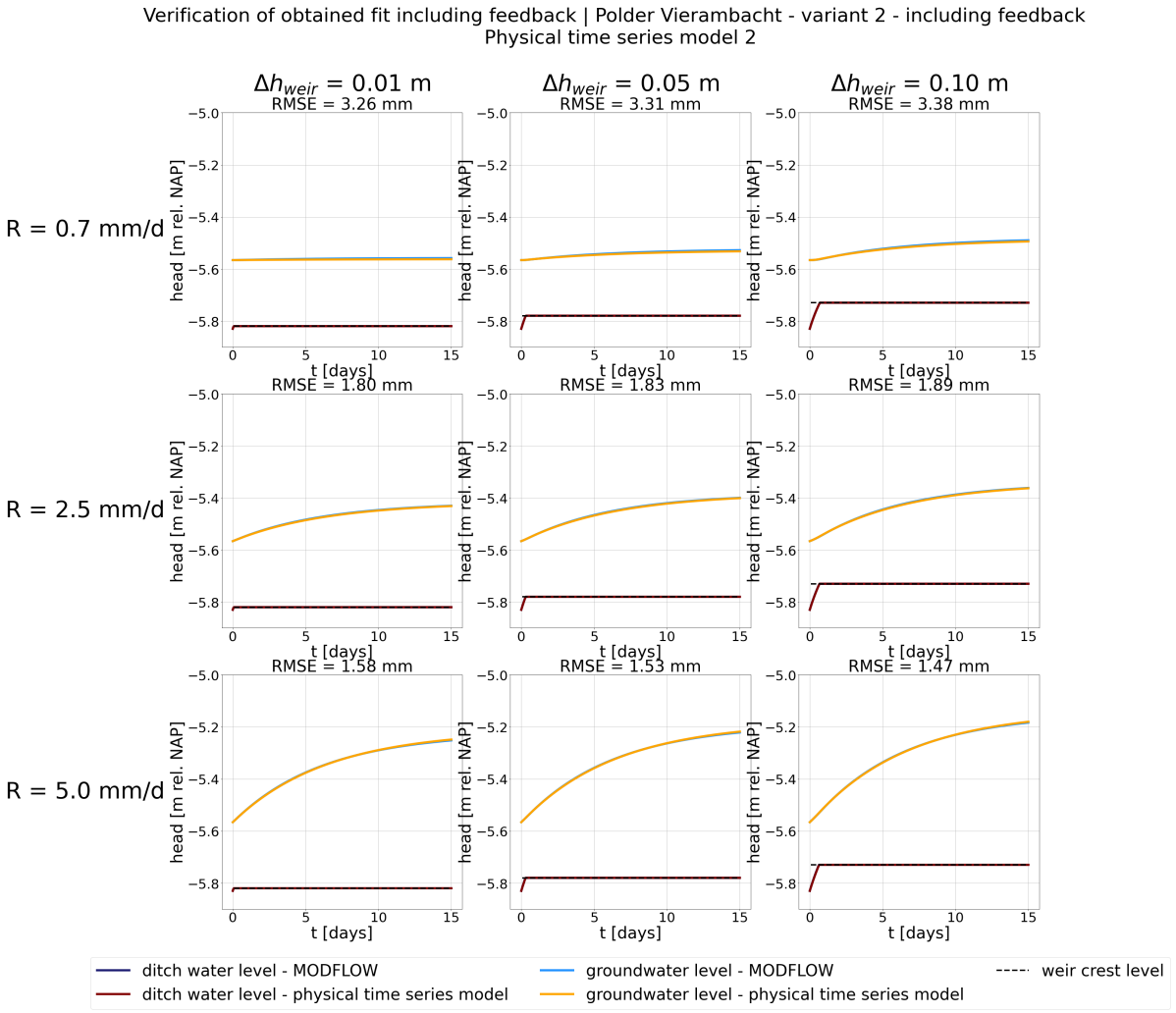

Figure 8.8: Verification of the obtained model parameters, variant 2 Polder Vierambacht - including feedback. All MODFLOW simulations including feedback are repeated with the fitted PTSM 2. The simulated groundwater heads in the centre of the field and ditch water level are plotted against time.

9

Evaluation performance MPC algorithm

This chapter discusses the results of the final research phase (IV. Evaluation). The constructed groundwater models are integrated into the MPC algorithm and it is run using historical precipitation forecasts and historical validated precipitation and evaporation data, like briefly explained in Section 3.2. The chapter is subdivided into three sections, according to the three simulation types:

1. Simulations to evaluate the performance of the MPC module (Section 9.1),
2. Simulations to evaluate the performance of the MPC algorithm (Section 9.2),
3. Simulations to assess the performance of the MPC algorithm for incorrect precipitation forecasts (Section 9.3).

The MPC algorithm is run for the water table control systems for which the model formulation was successful. An explanation of the simulations is also provided.

9.1. Performance MPC module

Performance assessment of the MPC module is complicated due to the receding horizon. Therefore, the performance of the MPC module (i.e. Pyomo model) is assessed by considering a single forecast. The HARMONIE precipitation and evaporation forecast of 01/06/2018 12:00:00 are forwarded to the MPC module, which calculates the optimal control actions for the considered prediction horizon ($h_{weir,control,1}$ up until $h_{weir,control,8}$). Instead of passing only $h_{weir,control,1}$ to the update module, all control actions are forwarded. Furthermore, the 48 hour precipitation forecast is inputted rather than the 6 hour validated precipitation observations. The forecasted precipitation thus forms the input of the MPC module as well as of the update model, implying a perfect precipitation forecast. This allows for verification of the MPC module, since a malfunctioning control can now only be assigned to a malfunctioning MPC module. The described simulation is performed for different weighting factors μ (1, 10, 100 and 1000) and different starting positions $h_{GW,initial}$. Table 9.1 summarizes the starting positions. $h_{SW,initial}$ and $h_{weir,initial}$ are equal to $h_{SW,target}$.

Figures 9.1 to 9.4 depict the simulation results for Polder Vierambacht, variant 2, starting position 1. Each figure belongs to a different weighting factor and consists of 3 subplots. The upper subplot dis-

Table 9.1: Description of starting positions ($h_{GW,initial}$) for simulations to evaluate the performance of the MPC module.

Polder & variant	Starting position 1	Starting position 2
Polder Het Langeveld, variant 1	Steady-state solution for R = 0.7 mm/d and h_{SW} = $h_{SW,target}$	Steady-state solution for R = 2.5 mm/d and h_{SW} = $h_{SW,target}$
Polder Het Langeveld, variant 2	Steady-state solution for R = 0.7 mm/d and h_{SW} = $h_{SW,target}$	-
Polder Vierambacht, variant 2	Steady-state solution for R = 0.7 mm/d and h_{SW} = $h_{SW,target}$	Steady-state solution for R = 5 mm/d and h_{SW} = $h_{SW,target}$

plays the 48 hour forecast of R [mm/hr]. Positive recharge is indicated by the blue coloured bars, whereas negative recharge is indicated by the red coloured bars. The middle subplot shows the development of weir crest level (thick grey line), surface water level (dark blue dots) and groundwater level (light blue dots) in time. Additionally, the setpoint (green dashed line) and possible weir settings (grey highlighted area) are indicated. The deficit (orange line) and spill (purple line) are plotted against time in the lower subplot.

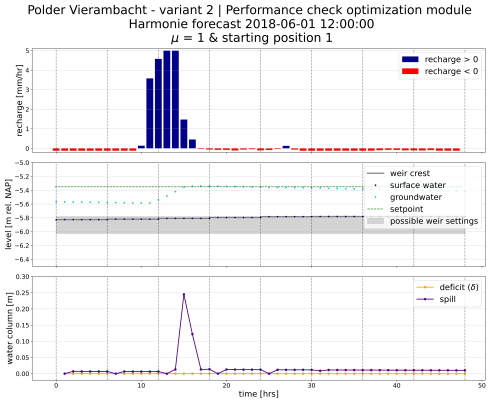

Figure 9.1: Performance check optimization module - Polder Vierambacht, variant 2, starting position 1, μ = 1.

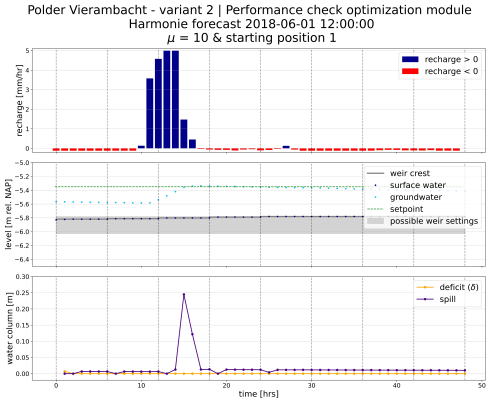

Figure 9.2: Performance check optimization module - Polder Vierambacht, variant 2, starting position 1, μ = 10.

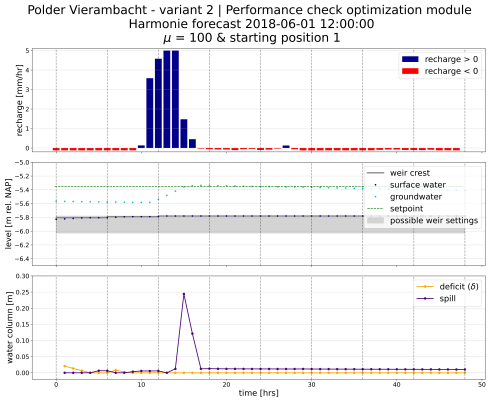

Figure 9.3: Performance check optimization module - Polder Vierambacht, variant 2, starting position 1, μ = 100.

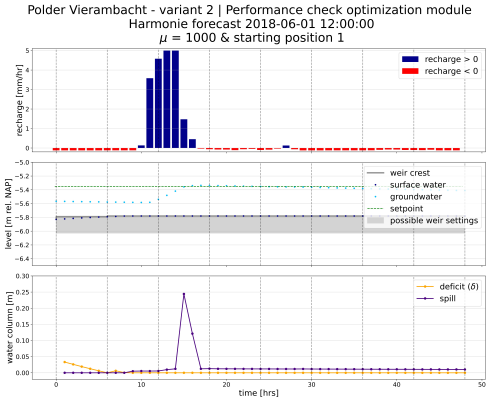

Figure 9.4: Performance check optimization module - Polder Vierambacht, variant 2, starting position 1, μ = 1000.

Figure 9.1 (μ = 1) shows that spill occurs during the first few hours of the simulation. This does not seem optimal, because the groundwater level is far below setpoint and the weir crest is not at its highest position. Water, which could have been stored in the system, is lost. Figure 9.2 shows that the weir crest level is raised to a slightly higher level for μ = 10. As as consequence, spill is reduced. The higher μ, the higher the "optimal" weir crest levels and the lower the spill, which pattern is also confirmed by the remaining figures (Figure 9.3 (μ = 100) and Figure 9.4 (μ = 1000)). Apparently, the second term of the objective function is of larger magnitude than the first term, that is responsible for minimizing the deviation from setpoint. The greater μ, the more weight is assigned to the first term and maintaining the groundwater level close to setpoint. However, this should not be at the expense of the second term, which means that μ cannot be increased infinitely. The desired spill behaviour is obtained for all μ.

The simulations are repeated for another starting position (starting position 2). In this case, $h_{GW,initial}$ is greater than $h_{GW,setpoint}$, which means that the weir crest level is expected to lower, anticipating

the rain event. Figures 9.5 to 9.8 show the simulation results. Figure 9.5 (μ = 1) clearly indicates that too little weight is assigned to the groundwater term in the objective function. The weir is raised, while $h_{GW,initial}$ is greater than $h_{GW,setpoint}$ and positive recharge is forecasted. Figure 9.2 shows that slightly better control actions are obtained for μ = 10. During the first 18 hours, the weir crest is lowered. However, the weir crest is raised again during the final 24 hours, while h_{GW} is still greater than $h_{GW,setpoint}$. Figure 9.7 and 9.8 illustrate that the "optimal" weir crest levels make more sense as μ increases. Though, the lower subplots indicate that this come at the expense of the desired spill behaviour, since deficit and spill should not coexist.

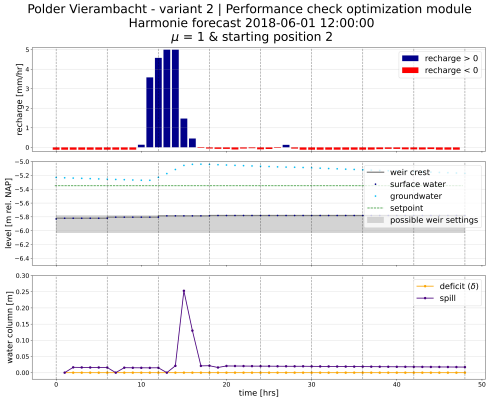

Figure 9.5: Performance check optimization module - Polder Vierambacht, variant 2, starting position 2, μ = 1.

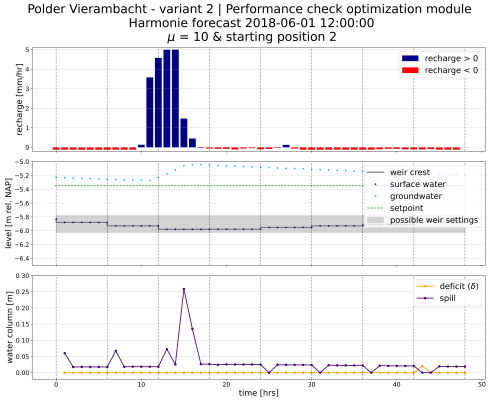

Figure 9.6: Performance check optimization module - Polder Vierambacht, variant 2, starting position 2, μ = 10.

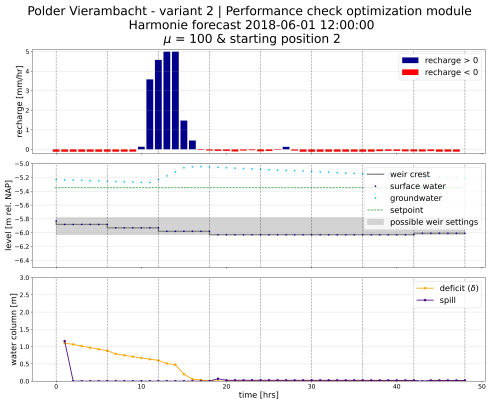

Figure 9.7: Performance check optimization module - Polder Vierambacht, variant 2, starting position 2, μ = 100.

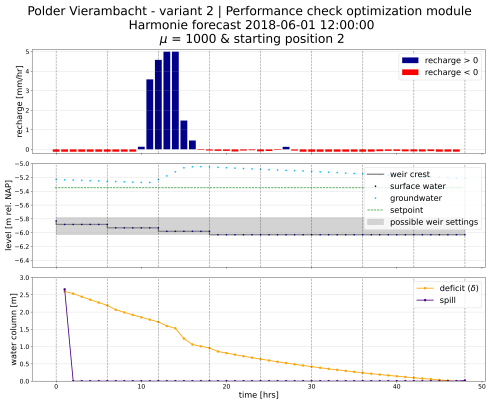

Figure 9.8: Performance check optimization module - Polder Vierambacht, variant 2, starting position 2, μ = 1000.

Similar simulation results are obtained for Polder Het Langeveld, variant 1 and 2.

μ = 1000 is selected and is used to evaluate the performance of the MPC algorithm (Section 9.2), since this demonstrably results in the most "optimal" control actions. Additionally, the update module is not affected by undesired spills and deficits determined by Pyomo, which means that this has limited consequences.

9.2. Performance MPC algorithm

The performance of the MPC algorithm is assessed by performing two long-term simulations. The full MPC algorithm is run for the following simulation periods:

1. 23/08/2018 00:00:00 to 08/09/2018 00:00:00,
2. 15/09/2018 00:00:00 to 15/10/2018 00:00:00.

The present control is simulated for the same time periods. Below, the results are organized per polder and simulation period. The initial groundwater situation of each simulation is the steady-state solution for R = 0.7 mm/d and h_{SW} = $h_{SW,target}$. $h_{weir,initial}$ is equal to $h_{SW,target}$. The present-day steady-state groundwater situation may differ from the steady-state groundwater situation for variant 1 and 2. This is the case for variant 2, Polder Het Langeveld and Polder Vierambacht. In case of Polder Het Langeveld (variant 2), the new steady-state groundwater level is approximately 5 cm lower compared to the present-day situation. However, considering the system's fast response, the influence of the initial condition is expected to be very minor. In case of Polder Vierambacht (variant 2), the new steady-state groundwater level is approximately 7 cm lower compared to the present-day situation. Due to the long system response time, the starting position has a considerable effect on the simulation results. Therefore, the present-day steady-state groundwater level is taken as starting position for the simulations to allow for proper comparison.

9.2.1. Simulation period 1 | Polder Het Langeveld

Figure 9.9 shows the simulation results for simulation period 1, Polder Het Langeveld, present control. The figure is subdivided into three subplots. The top plot depicts the validated recharge [mm/hr]. Positive recharge is again indicated by the blue coloured bars, whereas negative recharge is pointed out by the red coloured bars. The middle plot demonstrates the development of groundwater level (light blue line) and surface water level (dark blue line) in time. The constant weir crest level is plotted too (thick grey line), but is covered by the dark blue line. The envisaged setpoint is indicated by the green dashed line. The simulated groundwater and surface water levels make sense. Because h_{GW} is greater than h_{SW}, groundwater is continuously discharged towards the ditch and h_{SW} equals h_{weir}. Furthermore, the groundwater level increases during periods of positive recharge and decreases during periods of negative recharge. h_{GW} exceeds $h_{GW,setpoint}$ by a few mm at around 25/08/2018 06:00:00. $h_{GW,setpoint}$ is considerably exceeded during the rain events at the end of the simulation period. The bottom subplot visualizes the groundwater storage with respect to the initial groundwater situation [m^3], which is retrieved by cumulatively adding MODFLOW's volume budget. The groundwater storage follows the groundwater level. There is a net increase.

Figure 9.10 shows the simulation results for simulation period 1, Polder Het Langeveld, variant 1. The upper subplot depicts the forecasted and validated recharge [mm/hr]. The forecasted recharge is represented by the grey lines. Individual forecasts cannot be distinguished, but an indication of the forecast quality is provided. The middle plot demonstrates the development of groundwater level (light blue line), weir crest level (thick grey line) and surface water level (dark blue line). Setpoint (green dashed line) and possible weir settings (grey highlighted area) are plotted too. The bottom plot visualizes the groundwater storage with respect to the initial groundwater situation. By comparing Figure 9.10 to Figure 9.9, it can be observed that the obtained groundwater level does not differ much from the present situation. The effect of control actions is thus very limited, which can be explained by the slow response time of variant 1. Initially, h_{weir} is increased. At around 25/08/2018 04:00:00, the weir crest is lowered, anticipating to the forecasted precipitation. h_{GW} increases to $h_{GW,setpoint}$ and exceeds it by a few mm at around 25/08/2018 10:00:00. A slightly higher exceedance (order of mm) is obtained compared to the present situation, which can be explained by the increase in h_{weir} and h_{SW} before and during the first hours of the rain event. From 26/08/2018 18:00:00 on, h_{weir} and h_{SW} gradually increase to prevent rapid falling of the water table. At around 29/08/2018 00:00:00, h_{weir} is lowered, anticipating the forecasted precipitation, which magnitude turns out smaller than forecasted. By comparing Figure 9.9 to Figure 9.10, it can be concluded that this erroneous control action does not have a large effect on the groundwater level, which can be explained by the long system response time. The final precipitation events are anticipated by lowering h_{weir}. Exceedance of setpoint is not prevented, but the obtained groundwater table is approximately 5 mm lower compared to the present situation. At first sight it does not seem logical that the weir crest is not lowered well in advance of the precipitation event to prevent excessive exceedance of setpoint. There could be two reasons for this. Firstly, the prediction horizon is 48 hours, which means that precipitation events can be anticipated maximally 48 hours in advance.

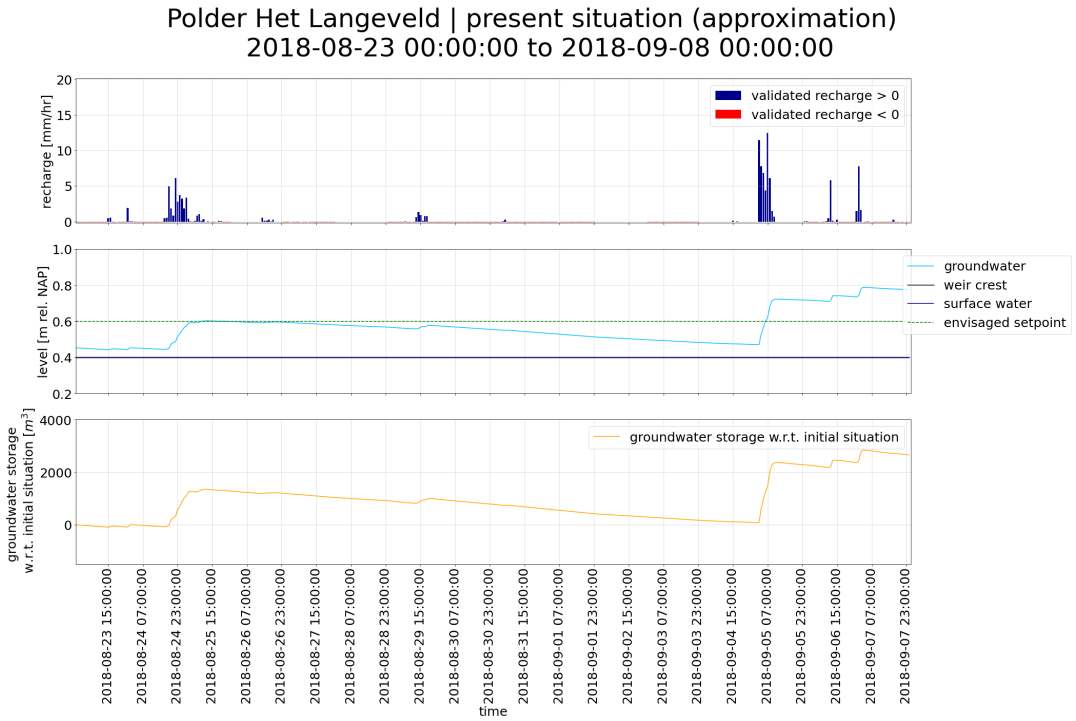

Figure 9.9: Simulation results long-term simulation present situation, Polder Het Langeveld - simulation period 1.

Secondly, earlier lowering of the weir crest would result in a larger undershoot before the precipitation event, which is also penalized by the MPC.

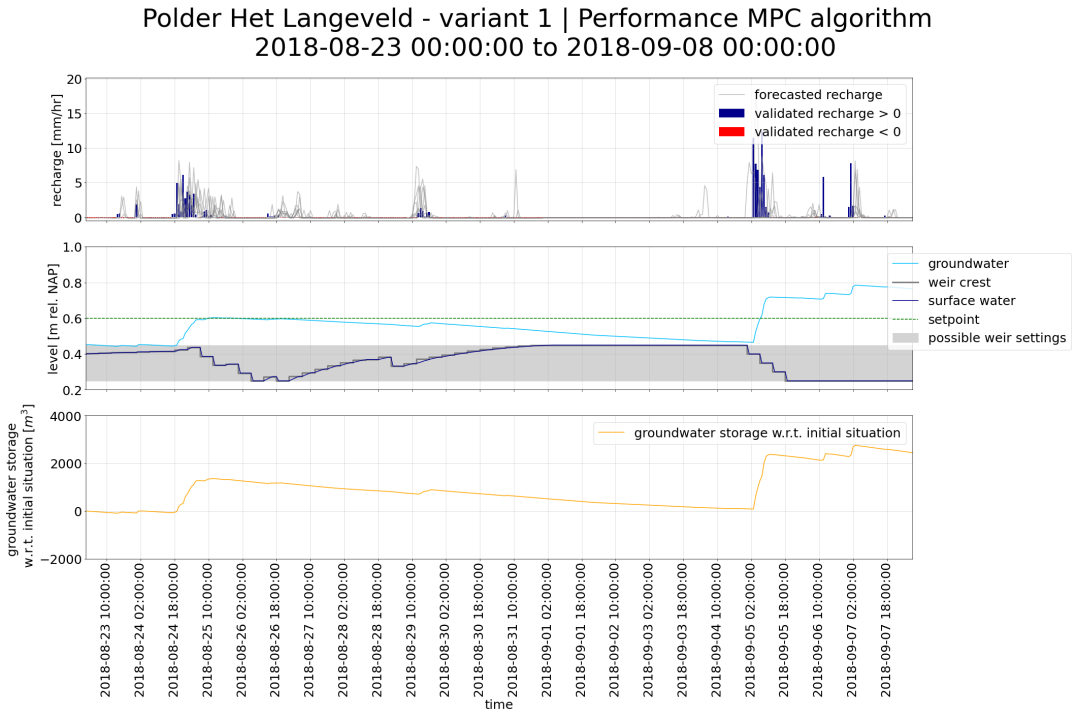

Figure 9.10: Simulation results long-term simulation MPC algorithm, variant 1, Polder Het Langeveld - simulation period 1

The simulation results for simulation period 1, Polder Het Langeveld, variant 2 are depicted in Figure 9.11, which has a similar layout as the previous figures. Like stated in Chapter 7, the bulging of the

groundwater table is very limited. As a consequence, h_{GW}, h_{weir} and h_{SW} coincide most of the time. Due to the limited bulging, groundwater discharge is also low. This explains the rapid decrease in h_{SW}. Additionally, the system has trouble to reach setpoint. Nevertheless, anticipation of precipitation events is evident. h_{weir} is increased to the highest possible level around 24/08/2018 18:00:00 to allow water retention during the first rain event. This leads to an increase in h_{GW}. Subsequently, the groundwater and surface water level recede. The final precipitation event is again anticipated by raising the weir crest, such that setpoint is exactly reached during the first precipitation peak.

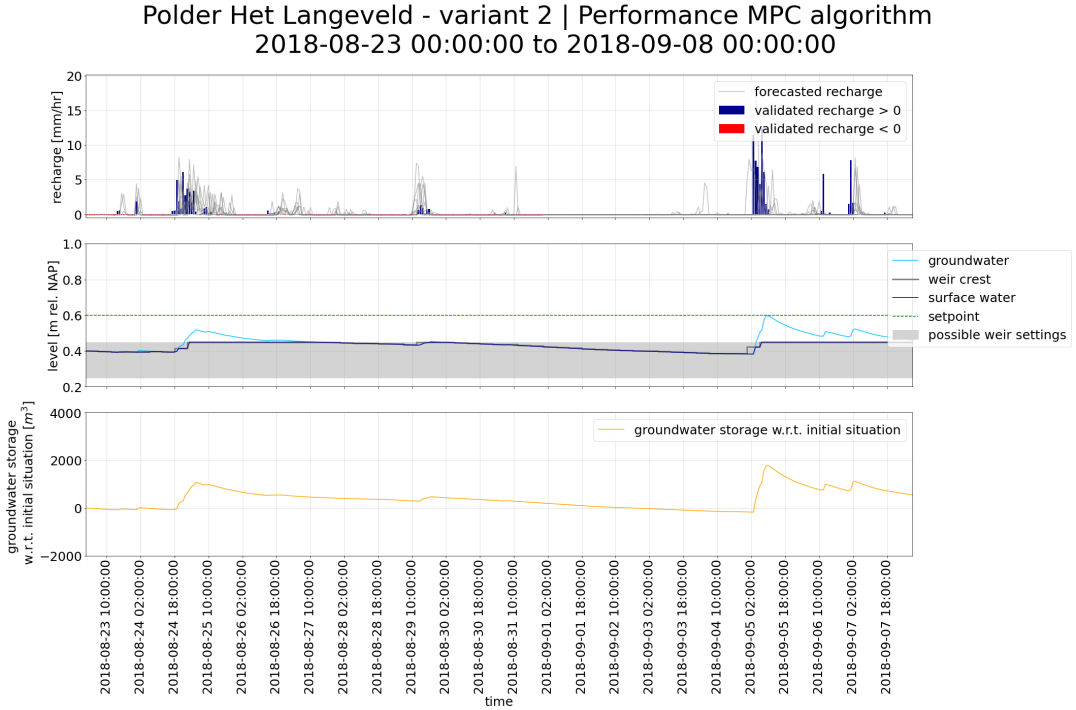

Figure 9.11: Simulation results long-term simulation MPC algorithm, variant 2, Polder Het Langeveld - simulation period 1

Two additional simulations are performed to verify the controllability of water table control system 2 in Polder Het Langeveld. The MPC algorithm is run for the same simulation period (period 1), but a lower, more feasible setpoint is applied. Figure 9.12 displays the simulation results for $h_{GW,setpoint}$ = 0.45 m NAP, while Figure 9.13 displays the simulation results for $h_{GW,setpoint}$ = 0.40 m NAP. Figure 9.12 shows that the weir crest is slightly lowered around 24/08/2018 18:00:00 to prevent excessive overshoot of setpoint during the recharge event. The groundwater level reaches setpoint. After the rain event, the groundwater table gradually falls below setpoint. From about 05/09/2018 02:00:00 on, the weir crest is raised such that precipitation is stored. The system gets filled by the precipitation and groundwater levels increase to setpoint. Compared to Figure 9.12, the weir crest is lowered more in Figure 9.13. This can be explained by the lower setpoint. It can be observed that the controller keeps the system quite close to setpoint in both cases.

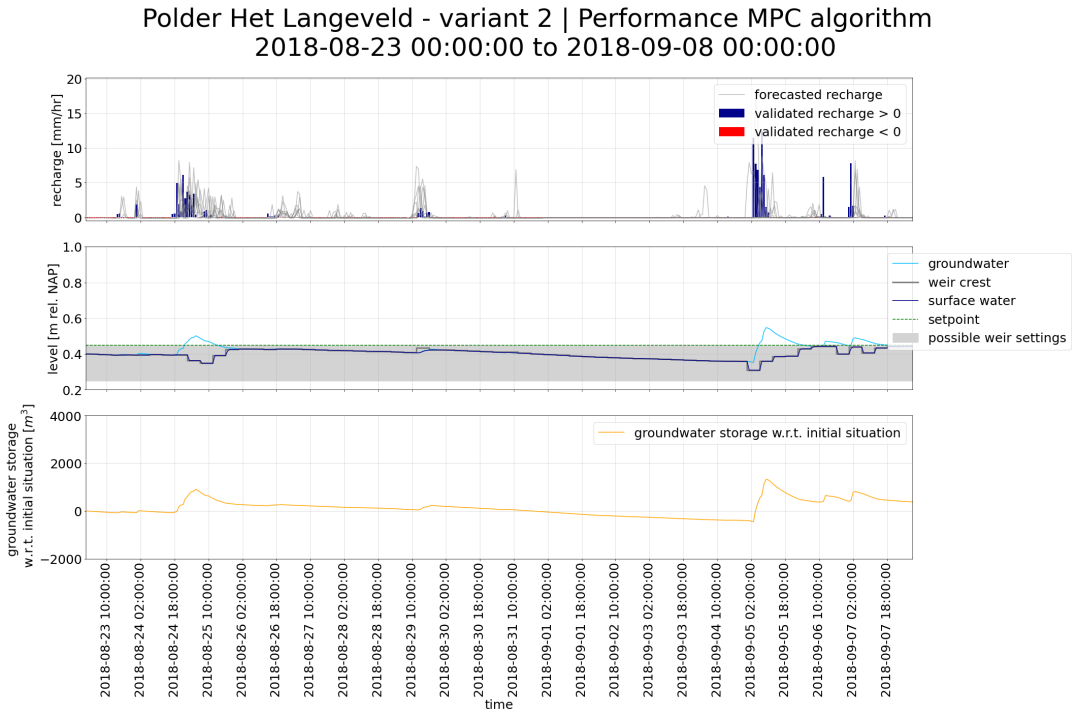

Figure 9.12: Simulation results long-term simulation MPC algorithm, variant 2, Polder Het Langeveld, $h_{GW,setpoint}$ = 0.45 m NAP - simulation period 1.

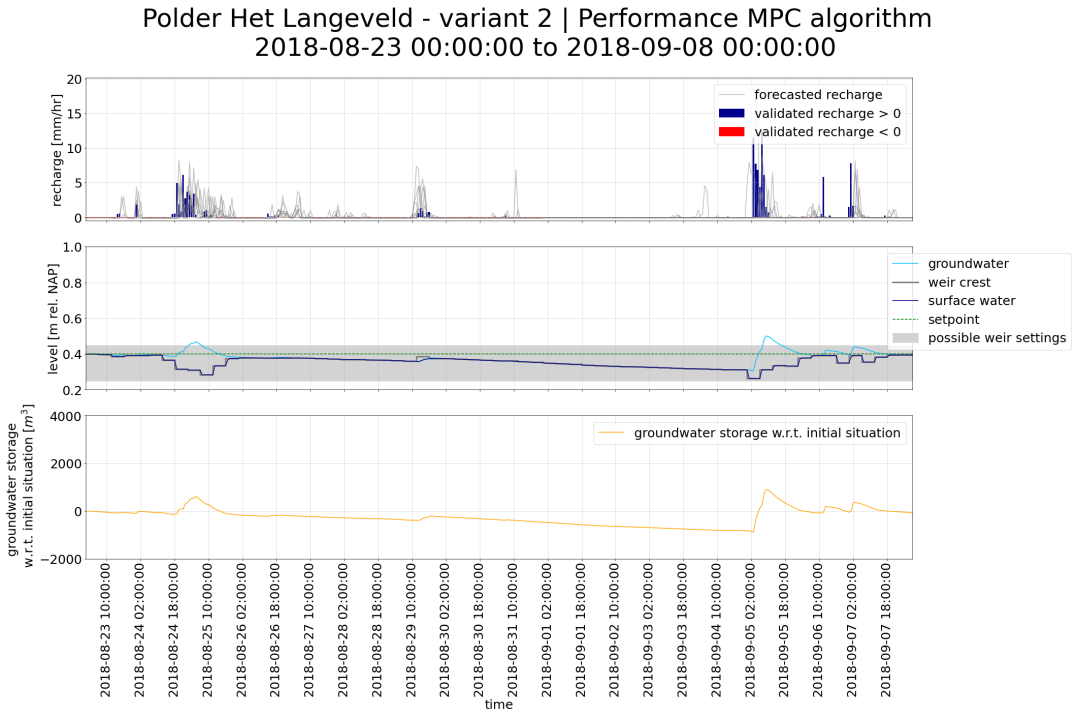

Figure 9.13: Simulation results long-term simulation MPC algorithm, variant 2, Polder Het Langeveld, $h_{GW,setpoint}$ = 0.40 m NAP - simulation period 1.

9.2.2. Simulation period 2 | Polder Het Langeveld

Figure 9.14 shows the simulation results for simulation period 2, Polder Het Langeveld, present control. Simulation period 2 contains the transition from summer to winter target level, which explains the sudden drop in h_{weir} and h_{SW} at 23/09/2018. There is a net decrease in groundwater storage of 1500 m^3.

The MPC algorithm is run for the same simulation period, which results in Figure 9.15 for variant 1 and Figure 9.16 for variant 2. For both systems, MPC succeeds in retaining more water than in the present situation; the net decrease in groundwater storage is approximately 1000 m^3. On the other hand, setpoint is not reached. There are two causes for this. Firstly, the precipitation amounts are insufficient to fill the system. Secondly, bulging of the groundwater table due to precipitation is very limited, especially for variant 2. Figure 9.15 shows that h_{weir} is raised during rain events, such that precipitation is retained. This is a rather slow process. Similarly, the recession of the groundwater table is slow. The groundwater flow processes take place on a smaller time scale in case of variant 2, which is clearly visible in Figure 9.15. The groundwater table and surface water level recede faster due to the presence of drains. Again, it can be observed that h_{weir} is raised to retain water during rain events.

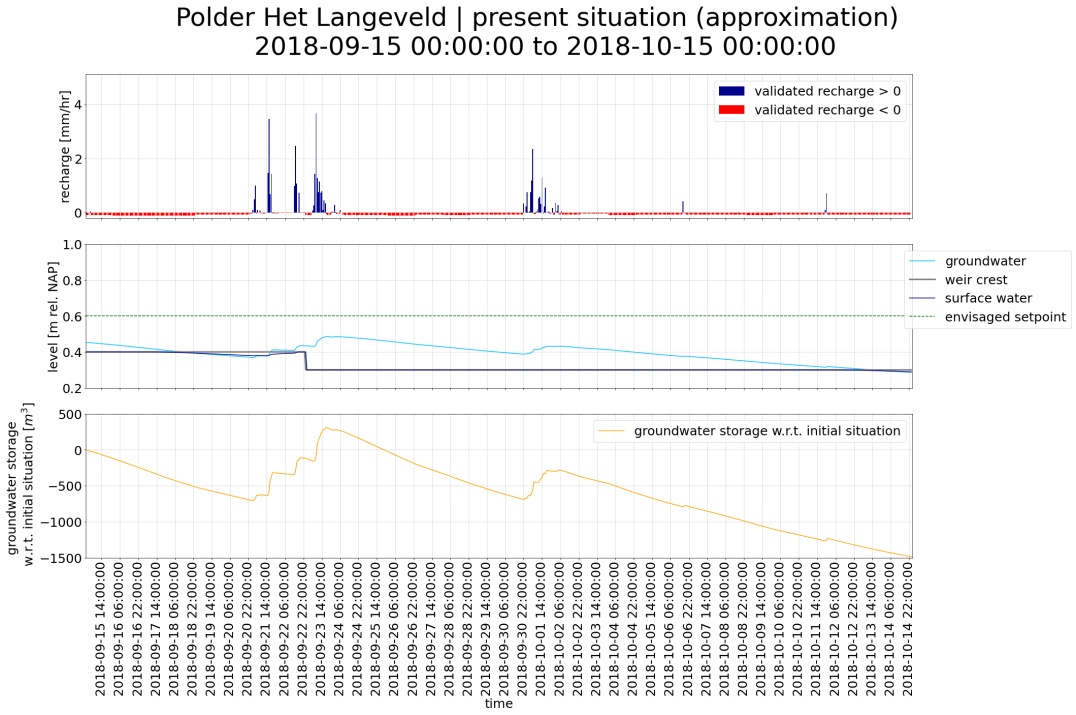

Figure 9.14: Simulation results long-term simulation present situation, Polder Het Langeveld - simulation period 2.

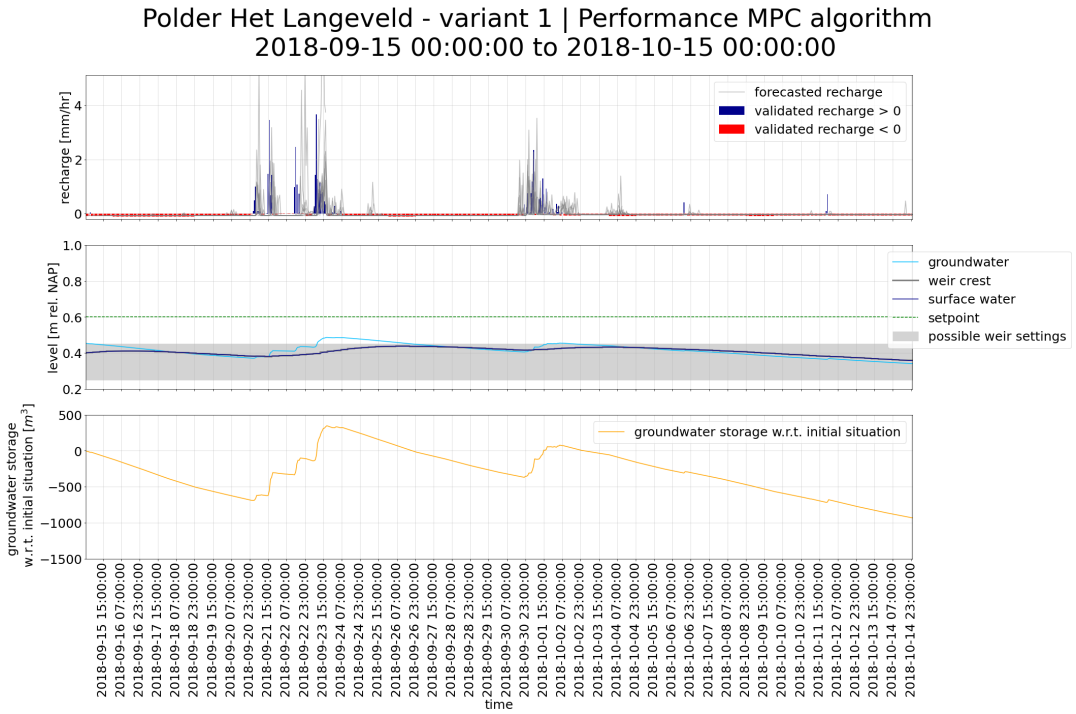

Figure 9.15: Simulation results long-term simulation MPC algorithm, variant 1, Polder Het Langeveld - simulation period 2

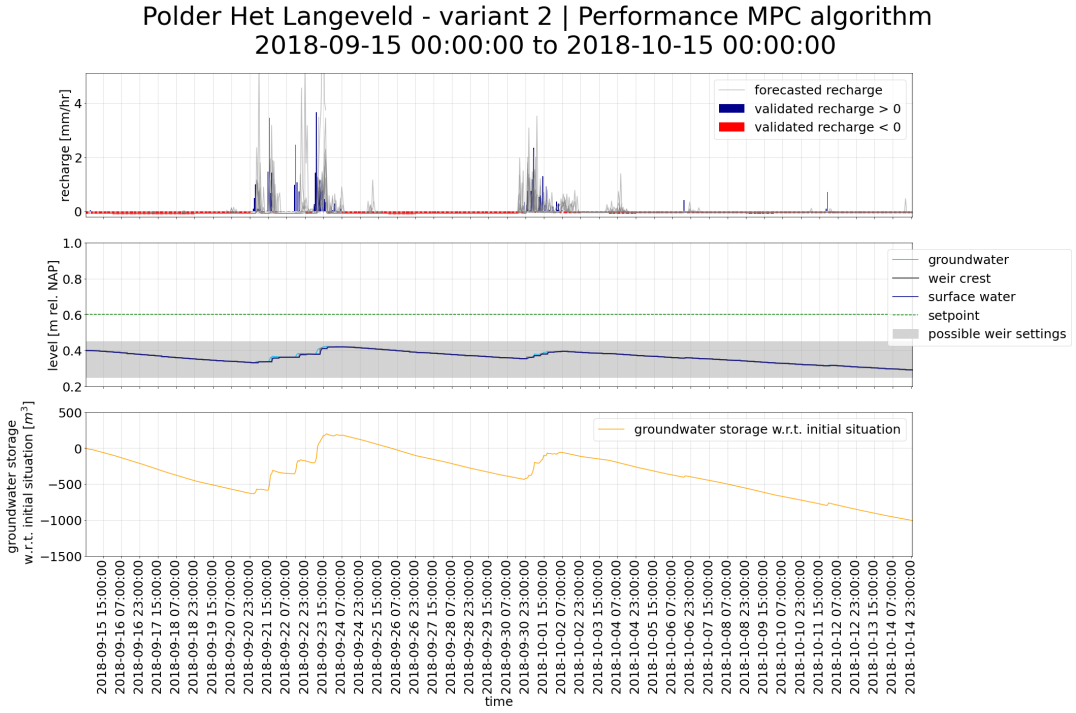

Figure 9.16: Simulation results long-term simulation MPC algorithm, variant 2, Polder Het Langeveld - simulation period 2

9.2.3. Simulation period 1 | Polder Vierambacht

Figure 9.17 shows the simulation results for simulation period 1, Polder Vierambacht, present control. The weir crest is at summer target level during the entire simulation. Because h_{GW} is greater than h_{SW}, groundwater is continuously discharged and h_{SW} is equal to h_{weir} during the entire simulation. Groundwater bulging is significant such that $h_{GW,initial}$ is approximately 30 cm above $h_{SW,initial}$. During the first rain event (24/08/2018 16:00:00 to 25/08/2018 08:00:00), the envisaged setpoint is exceeded by approximately 7 cm. Thereafter, h_{GW} recedes. A small precipitation event results in an increase of h_{GW} around 29/08/2018 15:00:00. During the final precipitation events (04/09/2018 22:00:00 to the end of the simulation), the envisaged setpoint is greatly exceeded and the groundwater table even reaches the surface level three times. The increase in groundwater storage is significant; approximately 4000 m^3.

Figure 9.18 depicts the simulation results for the same time period, Polder Vierambacht, variant 2. The MPC algorithm clearly anticipates the first rain event (24/08/2018 16:00:00 to 25/08/2018 08:00:00) by lowering the weir crest. Setpoint is reached and exceeded. Compared to the present situation, the exceedance is approximately 2 to 3 mm lower. This is a small improvement. The groundwater table falls below $h_{GW,setpoint}$ at around 26/08/2018 02:00:00, which is approximately 30 hours earlier compared to the present situation. Setpoint is unfortunately significantly exceeded during the final precipitation events (04/09/2018 22:00:00 to the end of the simulation), just like in the present situation. Although the weir crest is lowered, the considerable precipitation amount results in a sharp increase of h_{GW}. A slight improvement can be observed compared to the present situation, because the groundwater table does not reach the surface. Again, it can be questioned why the weir crest level is not lowered well in advance of the precipitation event to prevent excessive exceedance of setpoint. This can again be explained by the prediction horizon, which is restricted to 48 hours. Furthermore, earlier lowering of the weir crest would result in a larger undershoot before the precipitation event, which is also penalized by the MPC.

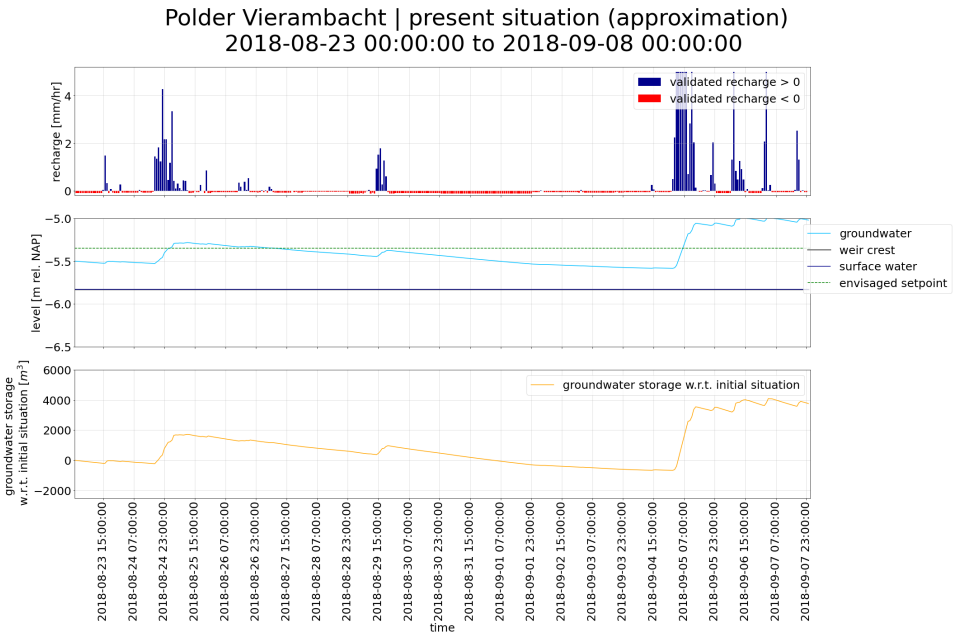

Figure 9.17: Simulation results long-term simulation present situation, Polder Vierambacht, simulation period 1.

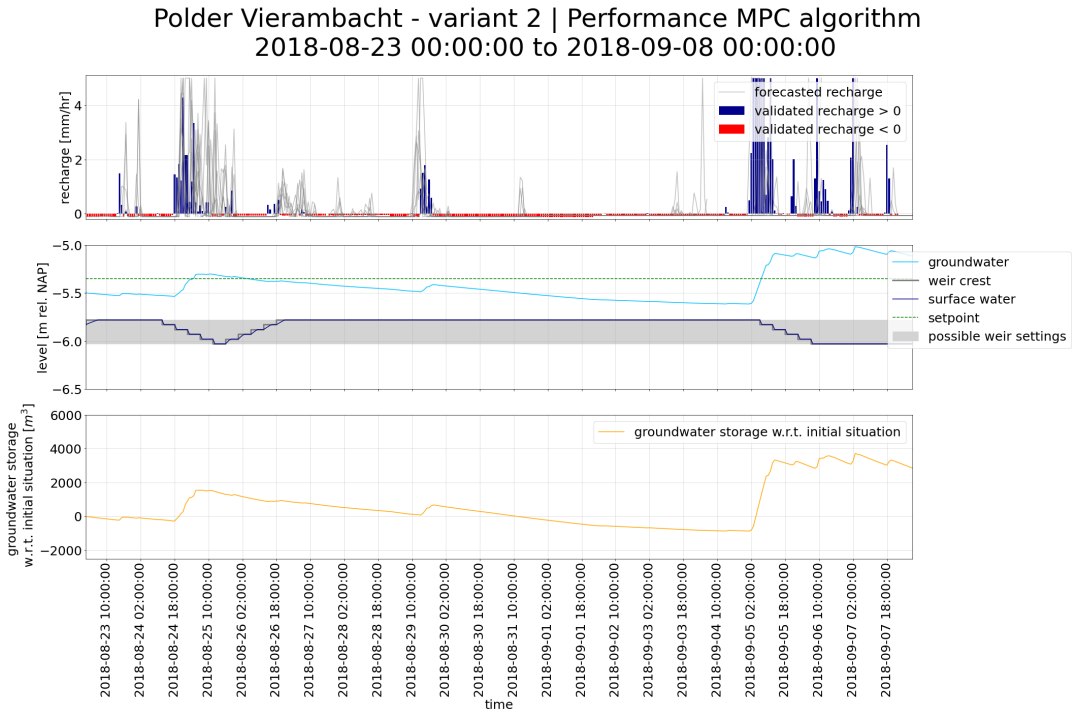

Figure 9.18: Simulation results long-term simulation MPC algorithm, variant 2, Polder Vierambacht - simulation period 1.

9.2.4. Simulation period 2 | Polder Vierambacht

Figure 9.19 shows the simulation results for simulation period 2, Polder Vierambacht, present control. Like stated before, the transition from summer to winter target level takes place at 23/09/2018, which explains the sudden change in h_{weir} and h_{SW}. The precipitation events between 21/09/2019 and 24/09/2018 result in exceedance of $h_{GW,setpoint}$, despite the transition from summer to winter target level just before the large peak. Afterwards, h_{GW} recedes, which is probably accelerated due to the transition from summer to winter target level.

The MPC algorithm is executed for the same simulation period for the new control (variant 2), which results in Figure 9.20. The weir crest is at its maximum level during the first days of the first precipitation event, such that precipitation is retained as much as possible. Eventually, the weir crest is lowered to prevent h_{GW} from exceeding $h_{GW,setpoint}$. The weir crest is not sufficiently lowered, because $h_{GW,setpoint}$ is still exceeded. Compared to the present situation, the exceedance is slightly reduced (order of mm).

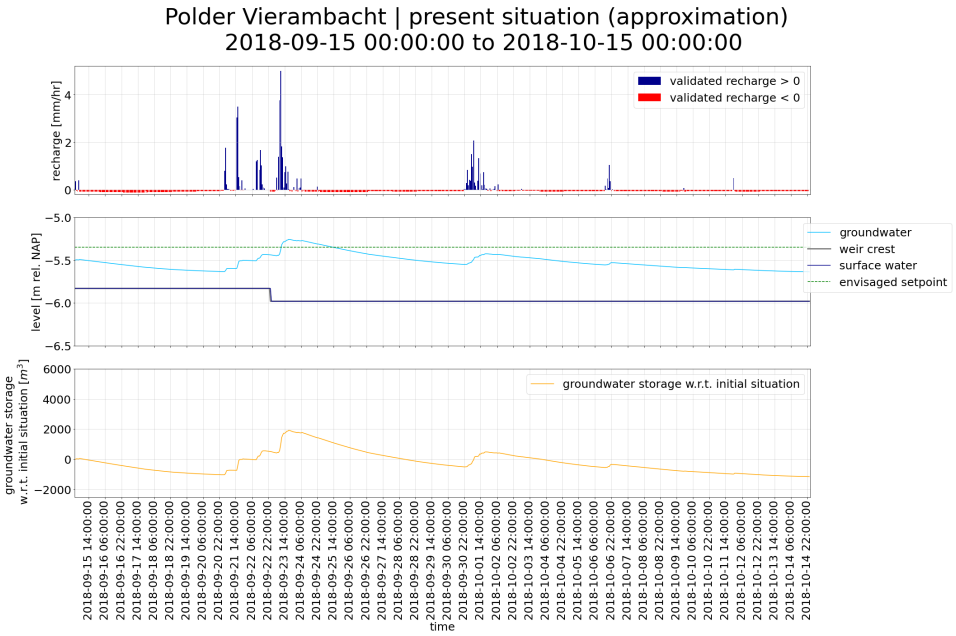

Figure 9.19: Simulation results long-term simulation present situation, Polder Vierambacht, simulation period 2.

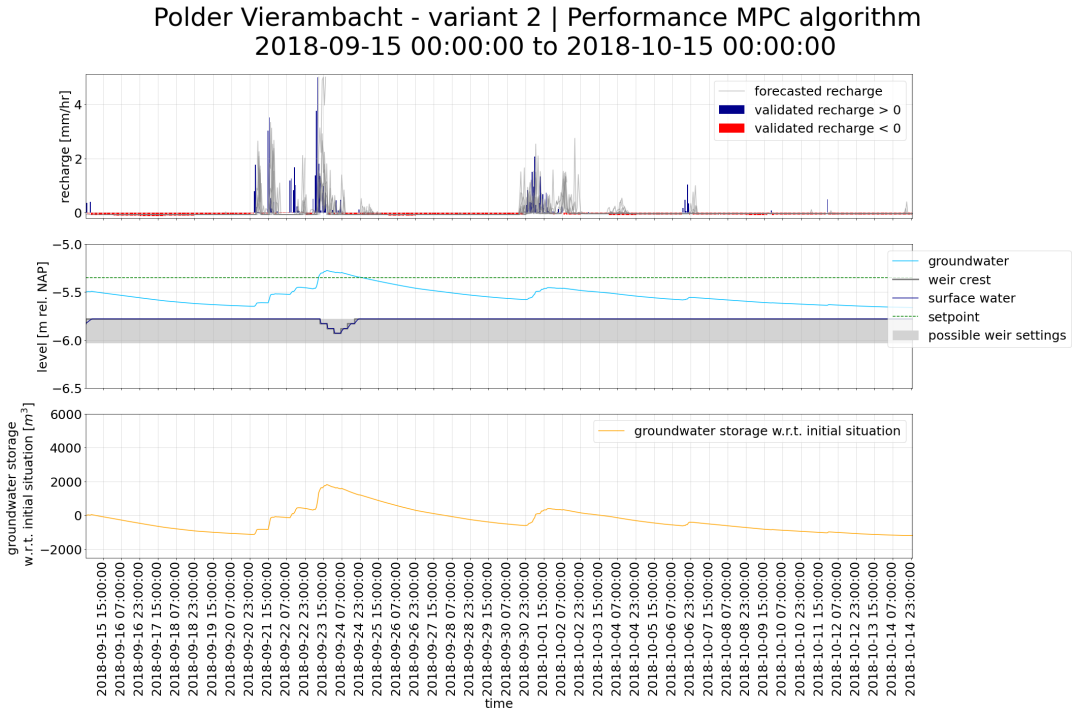

Figure 9.20: Simulation results long-term simulation MPC algorithm, variant 2, Polder Vierambacht - simulation period 2.

9.3. Performance for incorrect precipitation forecasts

Finally, the performance of the MPC algorithm for incorrect precipitation forecasts is assessed for each variant. A period with incorrect forecasts is selected by comparing the HARMONIE and Meteobase data sets: 01/06/2018 00:00:00 to 03/06/2018 12:00:00. This period consists of 10 control time steps of 6 hours. The MPC algorithm is run for this time period. Parallel to the MPC algorithm, additional MODFLOW simulations are performed. Instead of the validated precipitation and evaporation observations, the 6 hour forecast during the considered control time step is forwarded to the update module.

The results for Polder Het Langeveld, variant 1 are depicted in Figure 9.21. $h_{GW,initial}$ is based on the steady-state solution for R = 1 mm/d and h_{SW} = $h_{SW,initial}$. The validated recharge is again depicted in the top plot. Additionally, the forecasted recharge is depicted, which is updated every 6 hours. The vertical grey dashed lines represent the boundaries of the control time steps. The numbering of the control time steps matches the numbering of the forecasts. During control time step 1, forecast 1 is available to the MPC module. During control time step 2, forecast 2 is available to the MPC etc. The bottom figure depicts the results of the MPC algorithm and shows the development of weir crest level (thick grey line), surface water level (dark blue dots) and groundwater level (light blue and red dots) in time. The light blue dots represent the groundwater level based on the validated recharge, as calculated by the MPC algorithm. The red dots represent the groundwater level based on the forecasted recharge, which is calculated by the parallel simulations. It should be noted that the weir crest and surface water level result from the usual MPC algorithm, meaning that they are controlled based on the blue groundwater level. The setpoint (green dashed line) and possible weir settings (grey highlighted area) are indicated too.

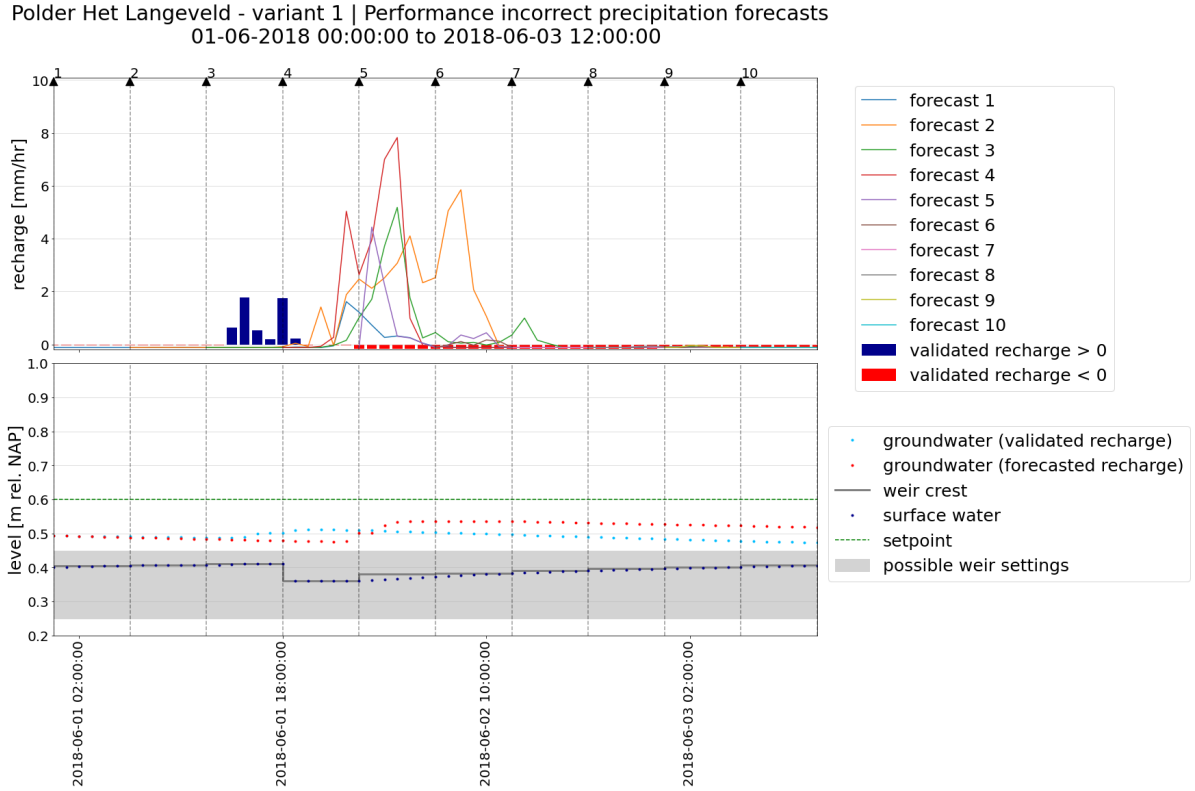

Figure 9.21: Simulation results to determine the performance of the MPC algorithm for incorrect precipitation forecasts - Polder Het Langeveld, variant 1.

It can be observed that the forecasted recharge deviates strongly from the validated recharge. Firstly, the validated recharge arrives much earlier than the forecasted recharge. Secondly, the magnitude of the recharge is overestimated by the forecast. During the first three control time steps the weir crest is gradually raised. h_{GW} based on the validated recharge is greater than h_{GW} based on the forecasted recharge during control time step 3, because recharge is not expected based on the forecasts. At the start of control time step 4, h_{weir} is decreased by approximately 5 cm. This decision is based on forecast 4, which predicts a considerable amount of precipitation. The predicted precipitation does not fall. At the start of time step 5, h_{weir} is increased slightly, because the updated forecast (forecast 5) expects less recharge compared to forecast 4. Only little recharge is expected from control time step 6 on, such that the weir is gradually raised. h_{SW} increases slowly, at the rate of groundwater discharge minus direct evaporation. The temporary lowering of the weir was unnecessary, which means that valuable water is unnecessarily discharged. The effect on the groundwater table is probably limited,

due to the slow response time of the groundwater-surface water system.

The results for Polder Het Langeveld, variant 2 are depicted in Figure 9.22. The forecasted and validated recharge are exactly the same as in Figure 9.21. Because the groundwater level is far below setpoint and bulging of the water table is very limited, the optimal weir settings for variant 2 differ much from the optimal weir settings for variant 1. All control actions within the simulation period are aimed at increasing the water table. The recharge during control time step 3 is not expected, such that the weir crest is not sufficiently raised. Further raising of the weir could have led to slightly more water retention. Significant precipitation is forecasted during control time step 4 and 5. The weir is therefore raised to retain water. h_{SW} stays much below h_{weir}, as the forecasted precipitation does not fall. The unnecessary raising of the weir does not have consequences. At the end of the simulation, the weir crest is lowered such that h_{weir} follows h_{SW}.

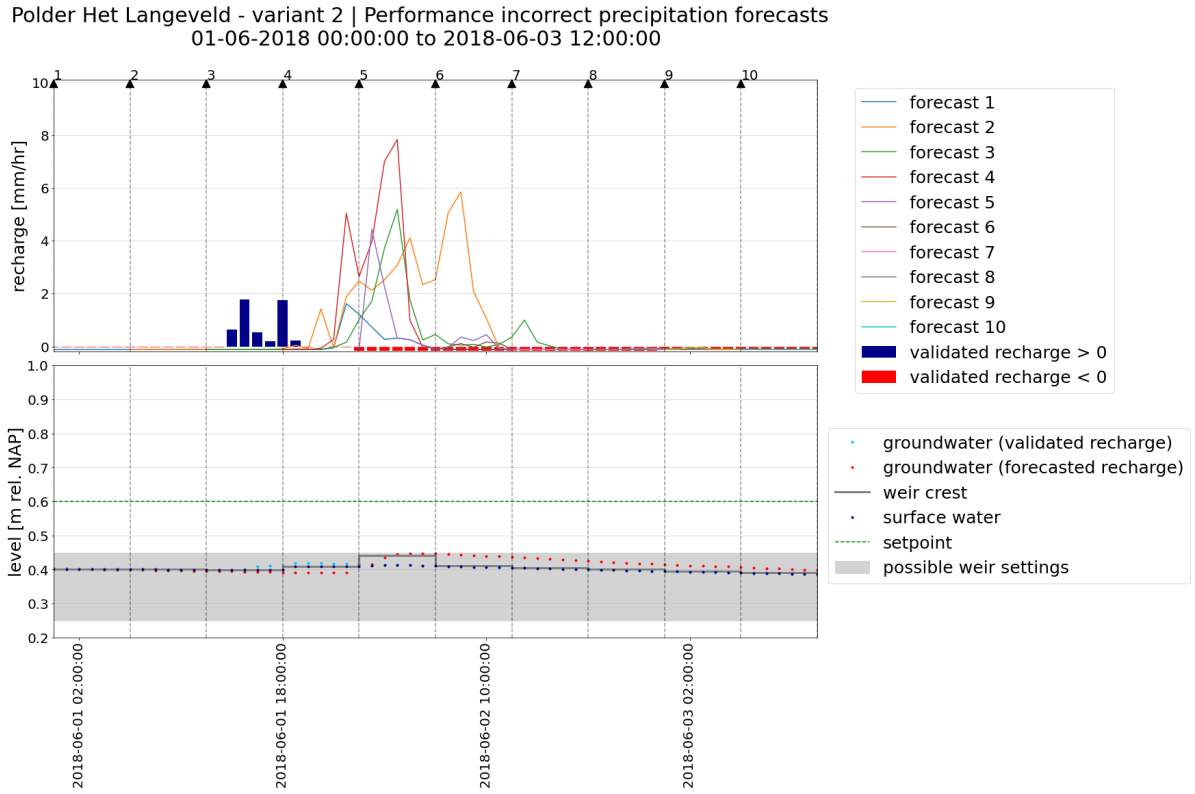

Figure 9.22: Simulation results to determine the performance of the MPC algorithm for incorrect precipitation forecasts - Polder Het Langeveld, variant 2.

Figure 9.23 depicts the results for Polder Vierambacht, variant 2. $h_{GW,initial}$ is based on the steady-state solution for R = 2.5 mm/d and h_{SW} = $h_{SW,initial}$. It can be observed that the forecasted recharge deviates strongly from the validated recharge. The forecasted recharge is slightly delayed and of much larger magnitude compared to the validated recharge. During control time step 1 and 2, the weir crest is raised to the maximum level. h_{SW} increases to h_{weir} due to groundwater discharge. Forecast 3 is received at the start of control time step 3 and predicts a considerable amount of recharge. Therefore, the weir crest is lowered by approximately 5 cm at the start of control time step 3 in anticipation of the rain event. At the start of the next time step, an updated forecast (forecast 4) is received that forecasts considerably less precipitation. As a consequence, the weir crest is raised again.

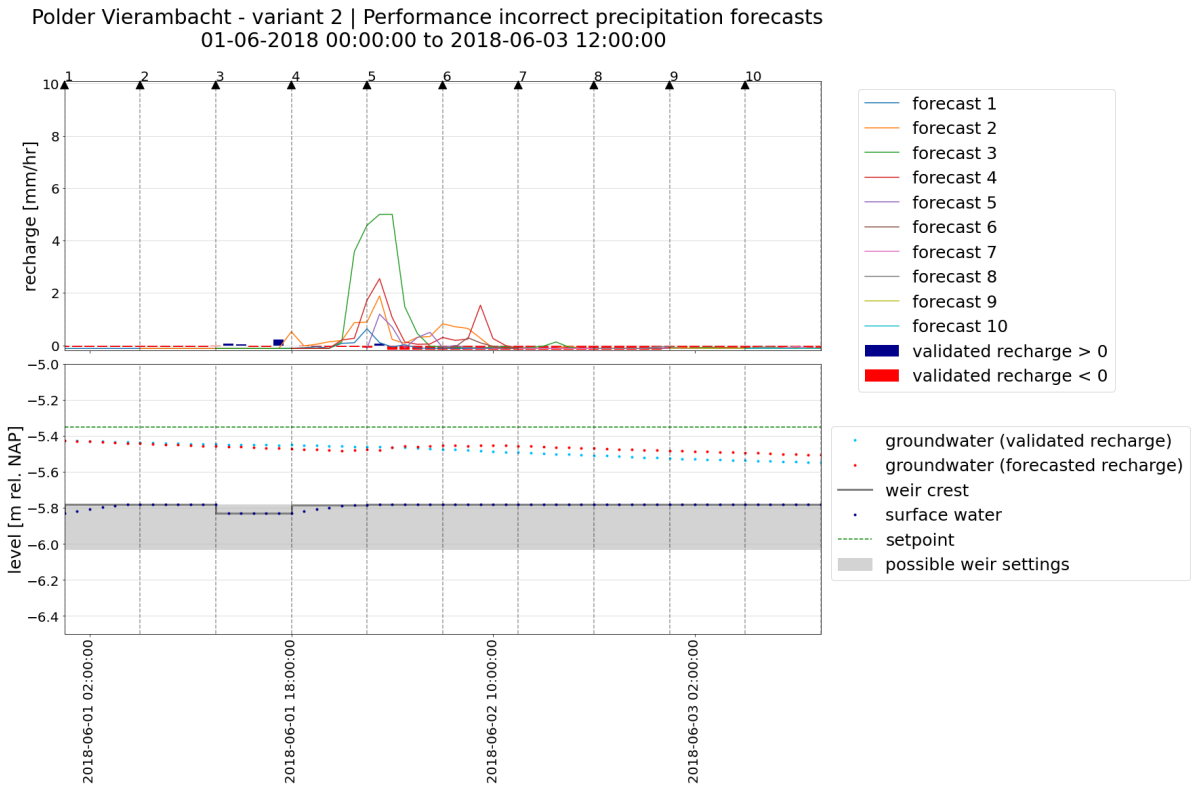

Figure 9.23: Simulation results to determine the performance of the MPC algorithm for incorrect precipitation forecasts - Polder Vierambacht, variant 2.

10

Sensitivity to response time groundwater system

Although the MPC algorithm has been run for three combinations of polders and variants with distinct geohydrological response times already, a sensitivity analysis is performed to determine the influence of the selected model parameters on the obtained results and to further examine its application range regarding groundwater response times. The following combinations have been considered:

- Variant 1 Polder Het Langeveld, for which a new steady-state is attained in approximately 40 days,
- Variant 2 Polder Vierambacht, with a time to equilibrium of approximately 20 days,
- Variant 2 Polder Het Langeveld, for which a new steady-state is reached in approximately 3 days.

Application of the MPC algorithm results in only minor differences compared to the present control in case of variant 1 Polder Het Langeveld and variant 2 Polder Vierambacht, like demonstrated in Chapter 9. This implies that further examination of systems with response times above 20 days is not useful. The sensitivity analysis is therefore restricted to variant 2 Polder Het Langeveld. Figures 9.11, 9.12 and 9.13 show that, for the selected model parameters, variant 2 can be properly controlled in Polder Het Langeveld, while it offers limited possibilities for water storage. For lower k and fewer drains, more groundwater table bulging is expected. However, this will be at the expense of the groundwater response time. k and N_{drain} are adjusted multiple times such that three systems with different geohydrological response times between 3 and 20 days are obtained.

Section 10.1 contains a description of the systems and the corresponding MODFLOW groundwater models. For each system, one MODFLOW simulation is executed to evaluate the geohydrological response. The simulation results also provide groundwater level time series for calibration of the PTSM, which is covered in Section 10.2. Once the required models are constructed, the MPC algorithm is run to evaluate its performance for each system. The simulation results are shown in Section 10.3.

10.1. Description of systems and corresponding MODFLOW models

Table 10.1 contains an overview of the considered systems, which are all based on variant 2 Polder Het Langeveld. System 0 corresponds to the original system, which was depicted in Figure 5.5. System 1 is obtained by halving the amount of drains. System 2 is obtained by reducing k. About 80% of the original number of drains is removed in case of system 3. Because c_{drain} is dependent on k and N_{drain}, four distinct values are obtained. These are determined through the calculation procedure described in Appendix D.6.

Table 10.1: Description of systems that are considered in the sensitivity analysis. All systems are based on variant 2 Polder Het Langeveld).

System	k [m/d]	N_{drain} [-]	c_{drain} [d]
0	7	36	0.14
1	7	18	0.20
2	2	36	0.53
3	7	8	0.23

The top views of the corresponding MODFLOW models are depicted in Figure 10.1 (system 1), Figure 10.2 (system 2) and Figure 10.3 (system 3).

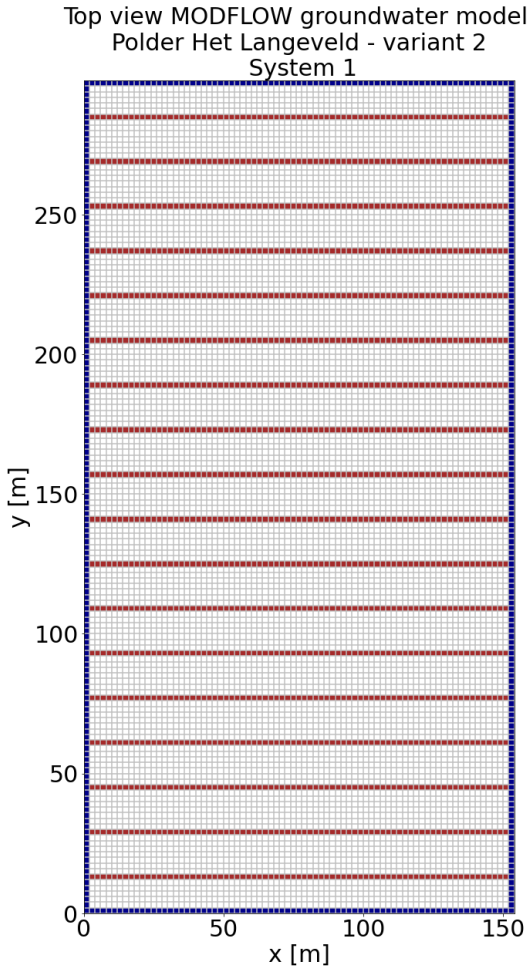

Figure 10.1: Top view MODFLOW groundwater model - system 1 (based on variant 2 Polder Het Langeveld).

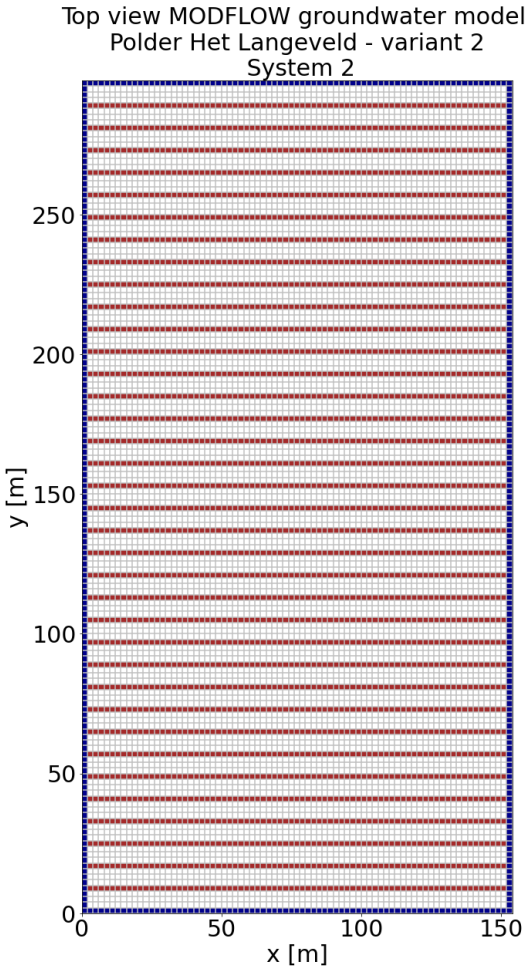

Figure 10.2: Top view MODFLOW groundwater model - system 2 (based on variant 2 Polder Het Langeveld).

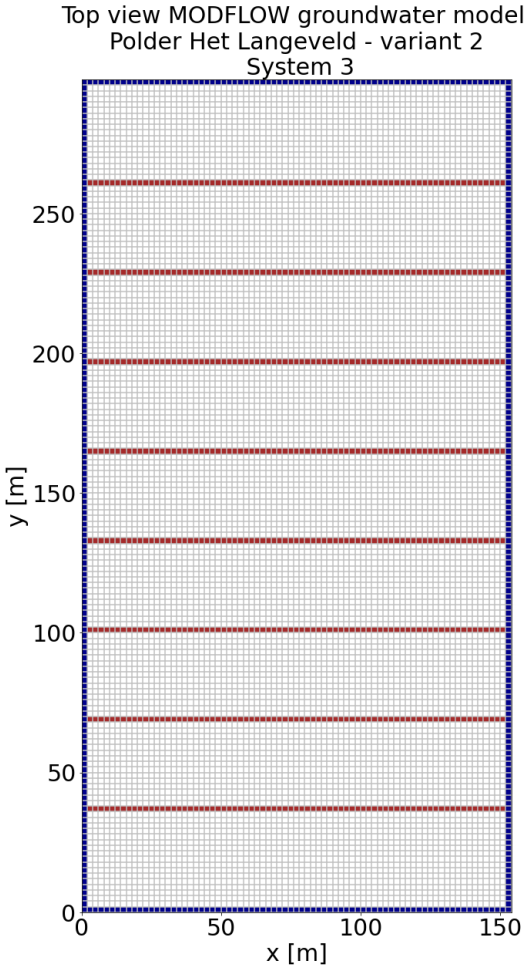

Figure 10.3: Top view MODFLOW groundwater model - system 3 (based on variant 2 Polder Het Langeveld).

10.2. PTSM calibration

For each system, one simulation is performed with the basic MODFLOW model (excluding feedback) and one simulation is performed with the extended MODFLOW model (including feedback).

The underlying idea of the simulation excluding feedback is demonstrated by Figure 7.2, with R = 2.5 mm/d, Δh_{drain} = 0.05 m and Δh_{SW} = 0.05 m. For each system, the simulation results are depicted in Figure 10.4. The midpoint groundwater response in time is plotted. Systems 1, 2 and 3 are represented by the blue, orange and green lines respectively. Three systems with distinct geohydrological response times between 3 and 20 days are clearly obtained. In case of system 1, a new steady-state groundwater situation is reached in approximately 7.5 days. The time to equilibrium equals 10 days for system 2, whereas system 3 requires approximately 17.5 days. Additionally, it can be observed that the slower the system response, the higher the steady-state groundwater table.

The underlying idea of the simulation including feedback is demonstrated by Figure 7.4, with R = 2.5 mm/d and Δh_{weir} = 0.05 m. The simulation results are depicted in Figure 10.5. For each system, the midpoint groundwater response as well as the ditch water level are plotted in time. The ditch water level and groundwater level as determined by MODFLOW are depicted in dark and light blue respectively.

The MODFLOW simulations excluding feedback are used to calibrate the PTSM. In Chapter 8, it was concluded that PTSM 1 is appropriate for variant 2, Polder Het Langeveld. Therefore, it is assumed that PTSM 1 is suitable for system 1 to 3 too. Figure 10.6 depicts the calibration results. The MODFLOW results are represented by the orange dots, whereas the PTSM results are represented by the

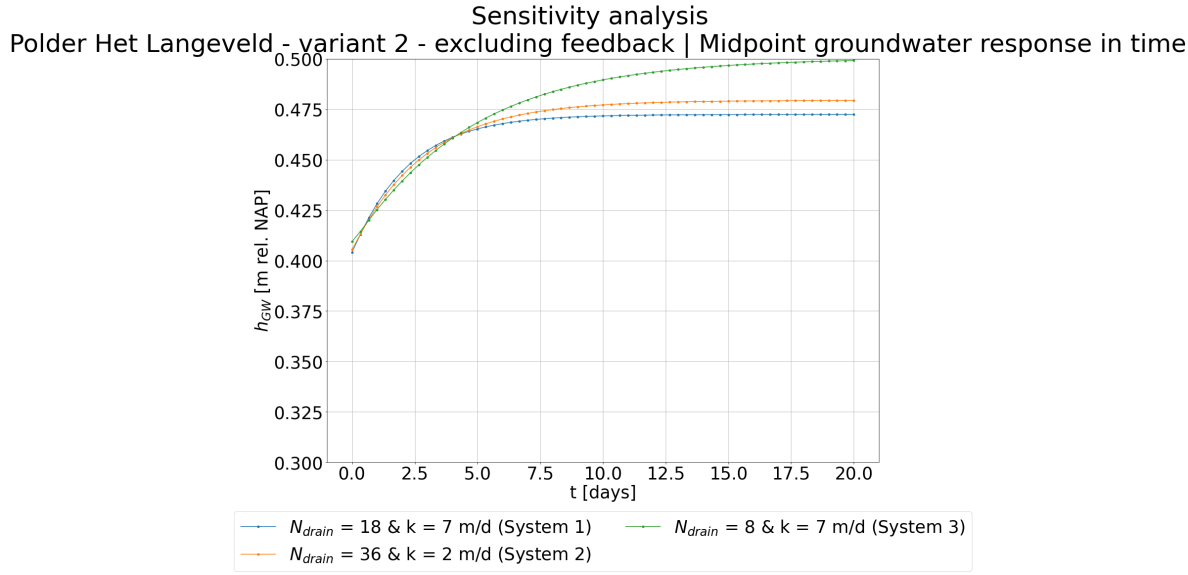

Figure 10.4: Midpoint groundwater response in time for system 1 to 3 - excluding feedback.

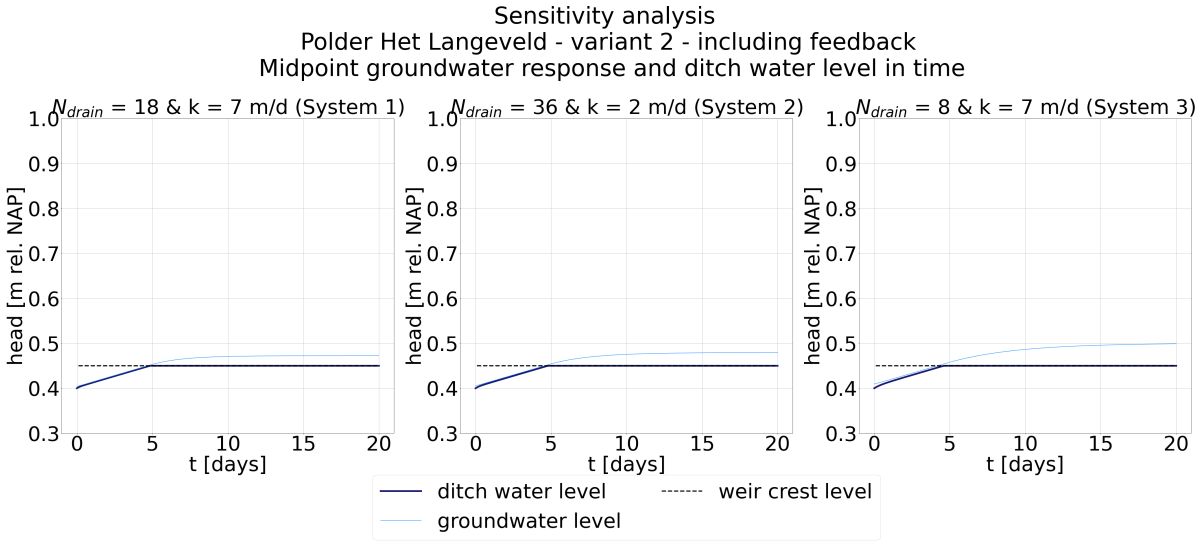

Figure 10.5: Midpoint groundwater response in time for system 1 to 3 - including feedback.

blue lines. The results of the calibrated PTSM correspond well to the MODFLOW results. The system response times and calibrated α values are summarized by Table 10.2.

Table 10.2: Overview system response time and model parameter α.

System	System response time [d]	α [d^{-1}] (PTSM 1)
0	3	1.159
1	7.5	0.559
2	10	0.433
3	17.5	0.260

Subsequently, the extended version of PTSM 1 is used to simulate the groundwater level and ditch water level for R = 2.5 mm/d and Δh_{weir} = 0.05 m. The calibrated α values are used and λ equals 0.6. For each system, the simulation results are depicted in Figure 10.7. The midpoint groundwater response and ditch water level are plotted in time. The ditch water level and groundwater level as

determined by MODFLOW are represented by the dark blue and light blue lines respectively. The ditch water level and groundwater level as determined by the PTSM are represented by the red and orange lines respectively. The light blue and orange lines overlap, just like the dark blue and red lines. This means that the PTSM reproduces the groundwater behaviour well in all cases.

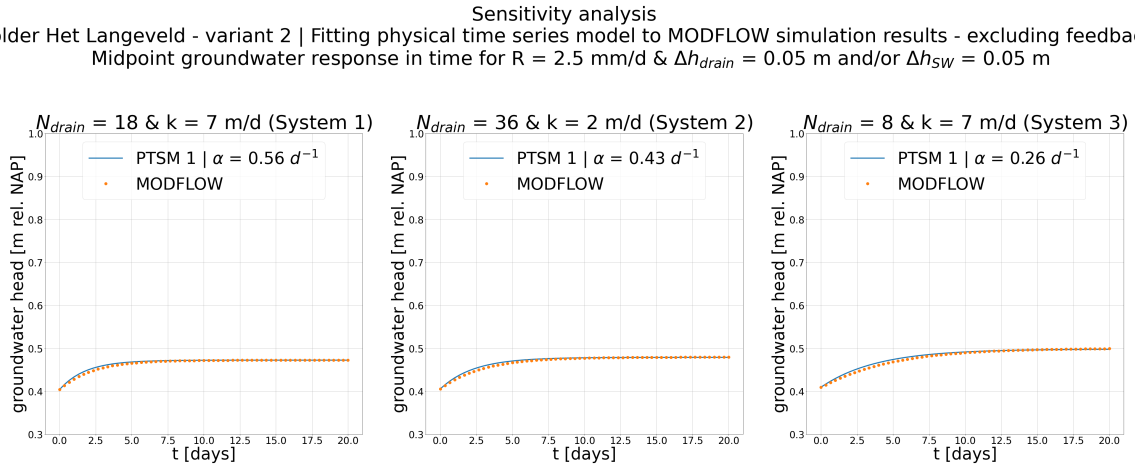

Figure 10.6: Fitting physical time series model 1 to MODFLOW simulation results system 1 to 3 - excluding feedback.

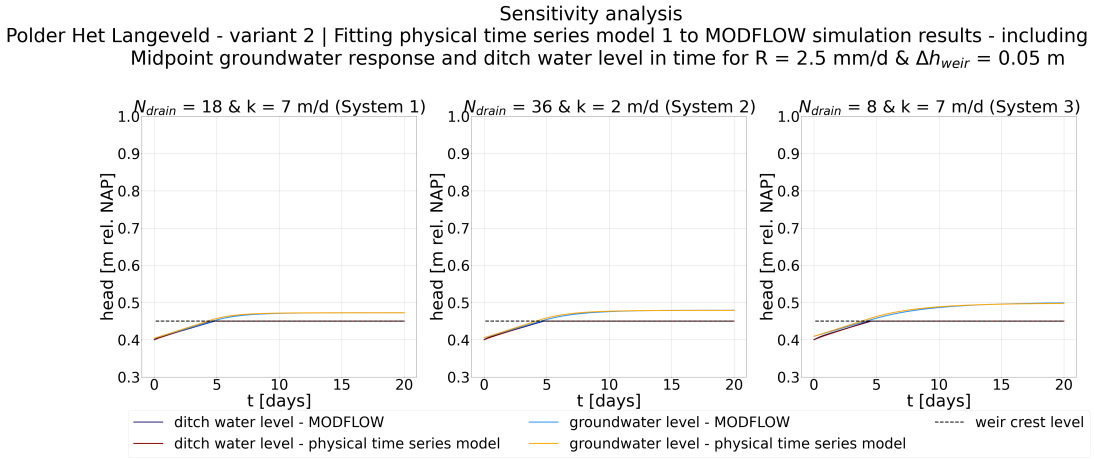

Figure 10.7: Fitting physical time series model 1 to MODFLOW simulation results system 1 to 3 - including feedback.

10.3. Performance MPC algorithm

For each system, the performance of the MPC algorithm is assessed by performing long-term simulations. The MPC algorithm is run for simulation period 1 (23/08/2018 00:00:00 to 08/09/2018 00:00:00) and two different setpoints:

1. $h_{GW,setpoint}$ = 0.45 m NAP, which is a relatively low setpoint,
2. $h_{GW,setpoint}$ = 0.60 m NAP, which is a relatively high setpoint.

The simulations for $h_{GW,setpoint}$ = 0.45 m NAP are intended to assess the system controllability, whereas the simulations for $h_{GW,setpoint}$ = 0.60 m NAP are intended to assess the system suitability for water storage. The assessment takes place by comparing the simulation results. The simulation results are compared with each other and with the simulation results of system 0 (original variant 2 Polder Het Langeveld).

The simulation results are displayed in the same way as in Section 9.2. The upper subplot depicts the forecasted and validated recharge [mm/hr]. The forecasted recharge is represented by the grey lines. Positive validated recharge is indicated by the blue coloured bars, whereas negative validated recharge is pointed out by the red coloured bars. The middle plot demonstrates the development of groundwater level (light blue line), weir crest level (thick grey line) and surface water level (dark blue line) in time. Setpoint (green dashed line) and possible weir settings (grey highlighted area) are plotted too. The bottom plot visualizes the groundwater storage with respect to the initial groundwater situation.

10.3.1. System 1

Figure 10.8 shows the simulation results for system 1 and $h_{GW,setpoint}$ = 0.45 m NAP. The system response time is approximately 7.5 days. Precipitation events are clearly anticipated by the MPC algorithm, because the weir crest level is adjusted downwards before and during precipitation events. Setpoint is slightly exceeded during the first precipitation event. At around 25/08/2018 04:00:00, h_{GW} reaches its maximum level. Comparing Figure 10.8 to Figure 9.12 shows that this maximum is approximately 2 cm higher compared to the maximum groundwater level that is obtained with system 0. Furthermore, compared to system 0, the control actions (i.e. changes in weir crest level) are more extreme in case of system 1. This can be explained by the relatively slow system response time of system 1; more extreme weir crest level adjustments are required to induce a significant system response within a limited amount of time. During the final precipitation events (05/09/2018 02:00:00 to the end of the simulation), setpoint is again exceeded. Compared to system 0 (Figure 9.12), the maximum groundwater level is approximately 4 cm higher. Despite of that, the MPC algorithm is able to maintain the groundwater level close to setpoint fairly well.

The simulation results for system 1 and $h_{GW,setpoint}$ = 0.60 m NAP are shown by Figure 10.9. The MPC algorithm anticipates precipitation events by raising the weir crest, such that water is retained. During the first precipitation event (24/08/2018 18:00:00 to 25/08/2018 10:00:00), the groundwater level does not reach setpoint. However, comparing Figure 10.9 to Figure 9.11 shows that a 3 cm higher groundwater level is obtained than in case of system 0. In contrast to system 0, system 1 is able to maintain the groundwater level close to setpoint during the final precipitation events (05/09/2018 02:00:00 to the end of the simulation). This is caused by slower recession of the groundwater table and higher groundwater table bulging.

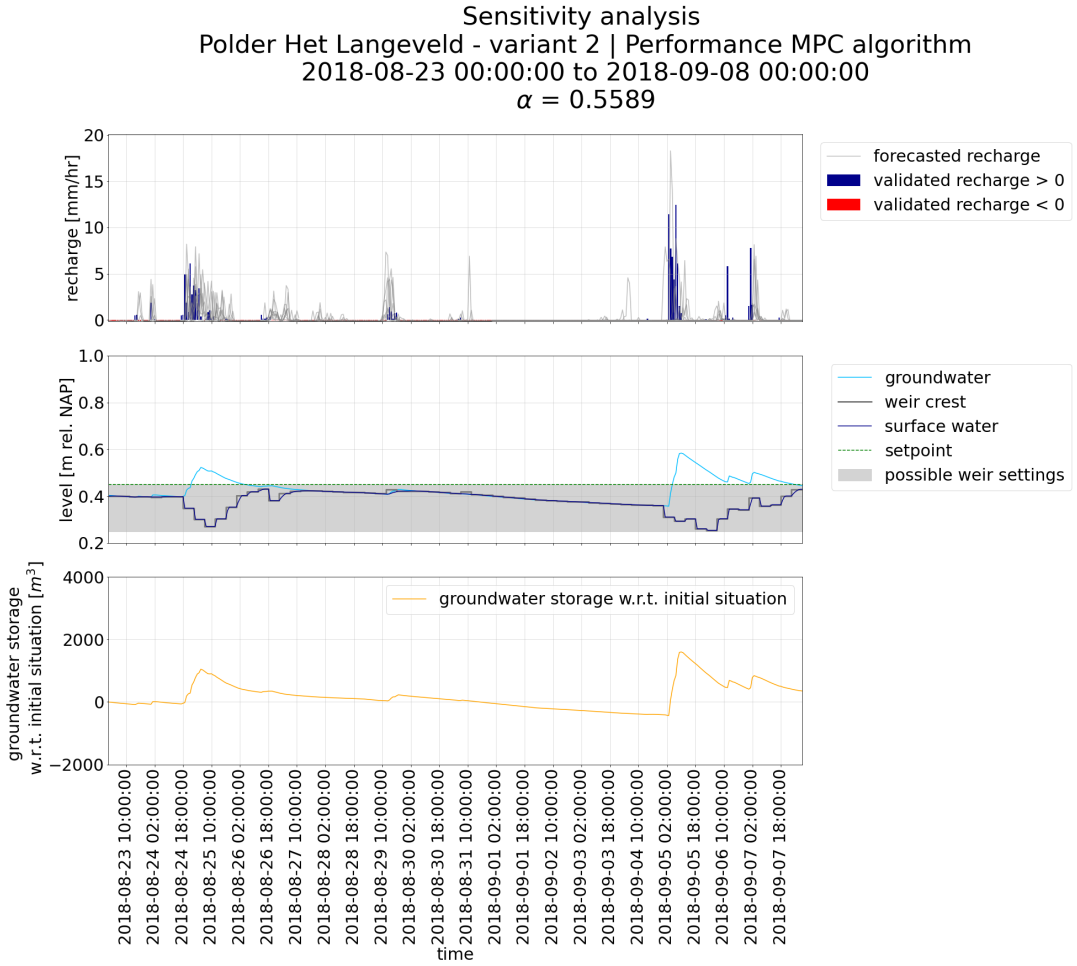

Figure 10.8: Simulation results long-term simulation MPC algorithm, system 1 (based on variant 2 Polder Het Langeveld) - simulation period 1, $h_{GW,setpoint}$ = 0.45 m NAP.

10.3.2. System 2

Figure 10.10 shows the simulation results for system 2 and $h_{GW,setpoint}$ = 0.45 m NAP. The system response time is approximately 10 days. Precipitation events are again clearly anticipated. Compared to system 1 (Figure 10.8), the weir crest level adjustments are more extreme. The response time of system 2 is longer than the response time of system 1, such that system 2 requires more extreme weir crest level adjustments to induce a similar system response within a limited amount of time. The exceedance of setpoint is generally greater in case of system 2 than in case of system 1 (order of cm). However, the MPC algorithm approximately takes the system back to setpoint after the final precipitation events (05/09/2018 02:00:00 to the end of the simulation).

The simulation results for system 2 and $h_{GW,setpoint}$ = 0.60 m NAP are displayed by Figure 10.11. The MPC algorithm raises the weir crest in anticipation of precipitation events. Again, the groundwater level does not reach setpoint during the first precipitation event. However, comparing Figure 10.11 to Figure 10.9 shows that a 5 mm higher groundwater level is obtained than in case of system 1. Compared to system 0 and 1, system 2 is able to maintain the groundwater level closer to setpoint during the final precipitation events.

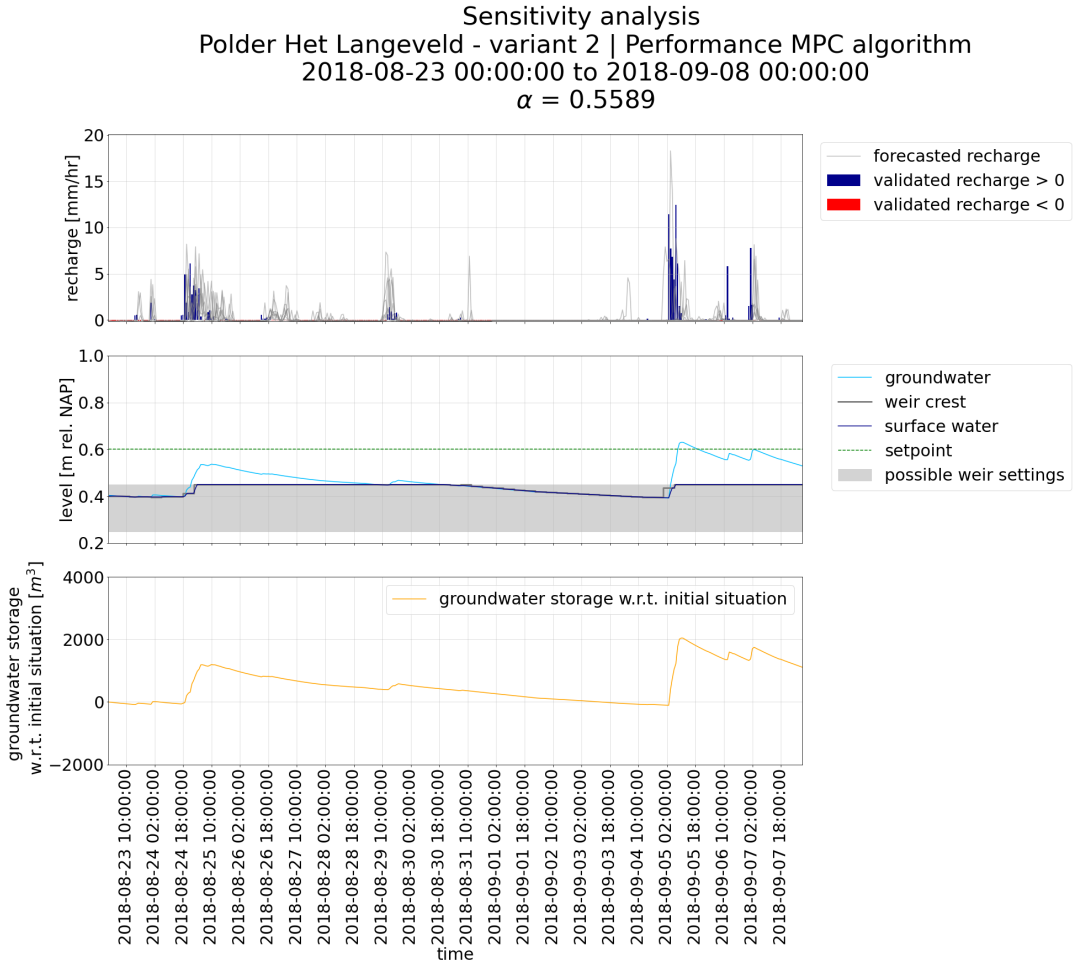

Figure 10.9: Simulation results long-term simulation MPC algorithm, system 1 (based on variant 2 Polder Het Langeveld) - simulation period 1, $h_{GW,setpoint}$ = 0.60 m NAP.

10.3.3. System 3

The simulation results for system 3 are shown by Figure 10.12 and Figure 10.13. Setpoint equals 0.45 m NAP in case of Figure 10.12, while setpoint equals 0.60 m NAP in case of Figure 10.13. The system response time is approximately 17.5 days. Precipitation events are anticipated by weir crest level adjustments. Compared to system 1 and 2, the weir crest level adjustments are more extreme, which can again be explained by the relatively long system response time.

Figure 10.12 shows that $h_{GW,setpoint}$ is greatly exceeded. The exceedance is greater than in case of system 1 and 2. Additionally, the MPC algorithm fails to take the system back to setpoint during the final precipitation events (05/09/2018 02:00:00). This shows that the system response is too slow for the applied prediction horizon and objective function.

Figure 10.13 shows that $h_{GW,setpoint}$ is again not reached during the first precipitation event. However, comparing Figure 10.13 to Figure 10.11 shows that a 1 to 2 cm higher groundwater level is obtained than in case of system 2. Just like system 2, system 3 is able to maintain the groundwater level close to setpoint during the final precipitation events. The groundwater level is slightly higher (order of cm) than in case of system 2.

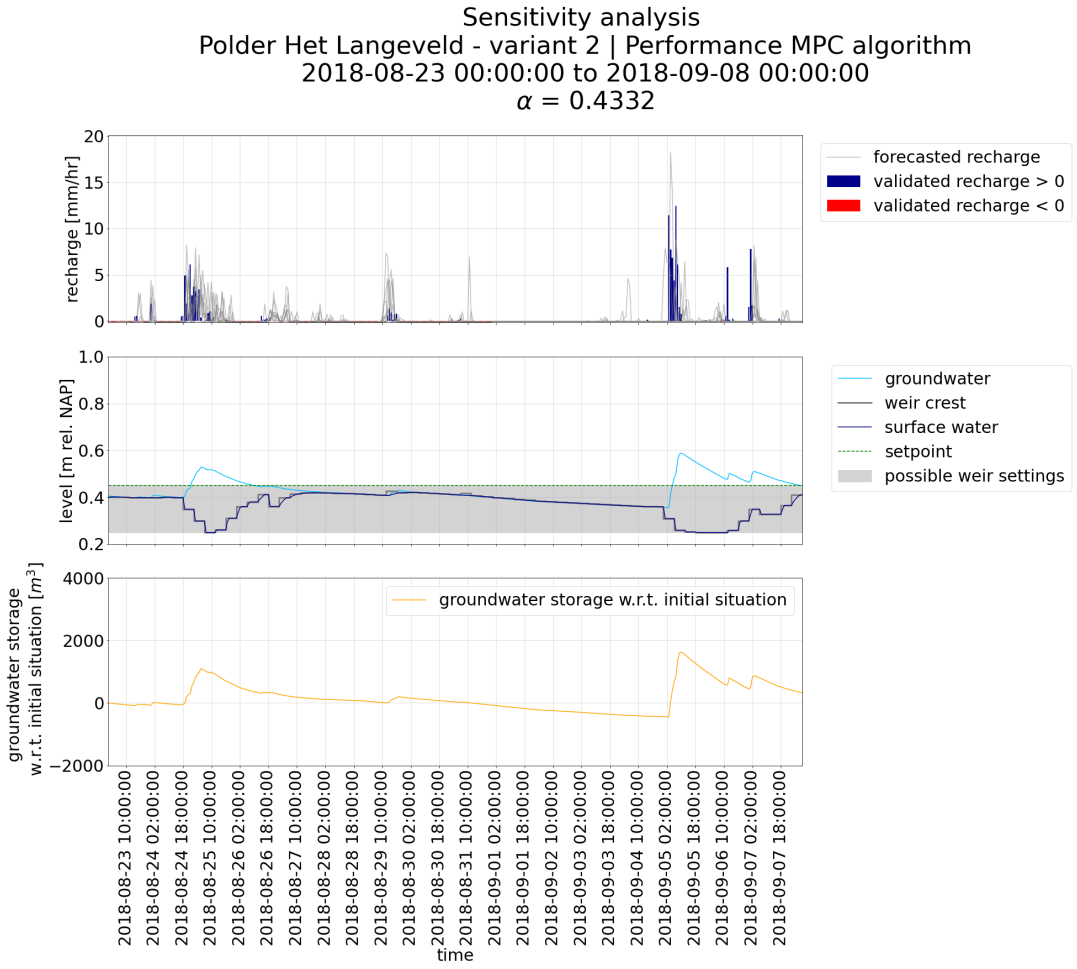

Figure 10.10: Simulation results long-term simulation MPC algorithm, system 2 (based on variant 2 Polder Het Langeveld) - simulation period 1, $h_{GW,setpoint}$ = 0.45 m NAP.

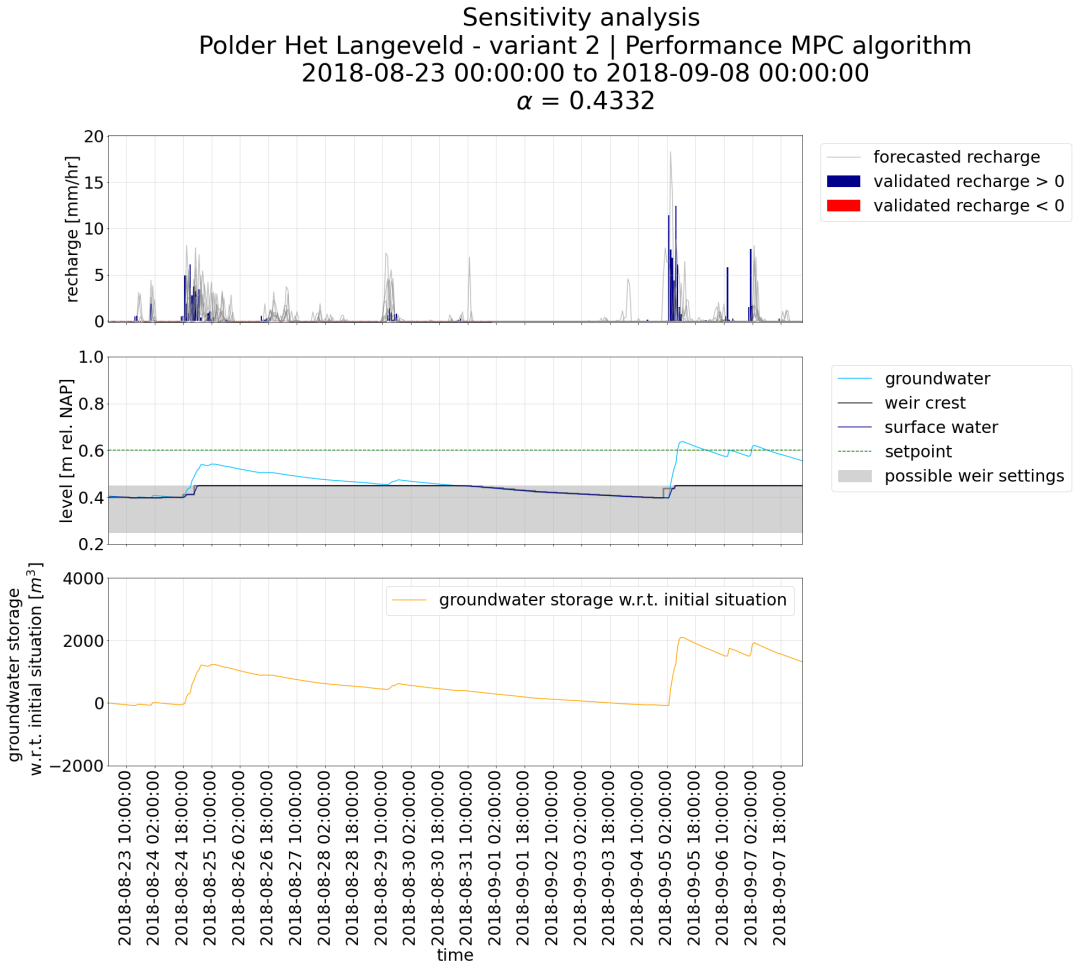

Figure 10.11: Simulation results long-term simulation MPC algorithm, system 2 (based on variant 2 Polder Het Langeveld) - simulation period 1, $h_{GW,setpoint}$ = 0.60 m NAP.

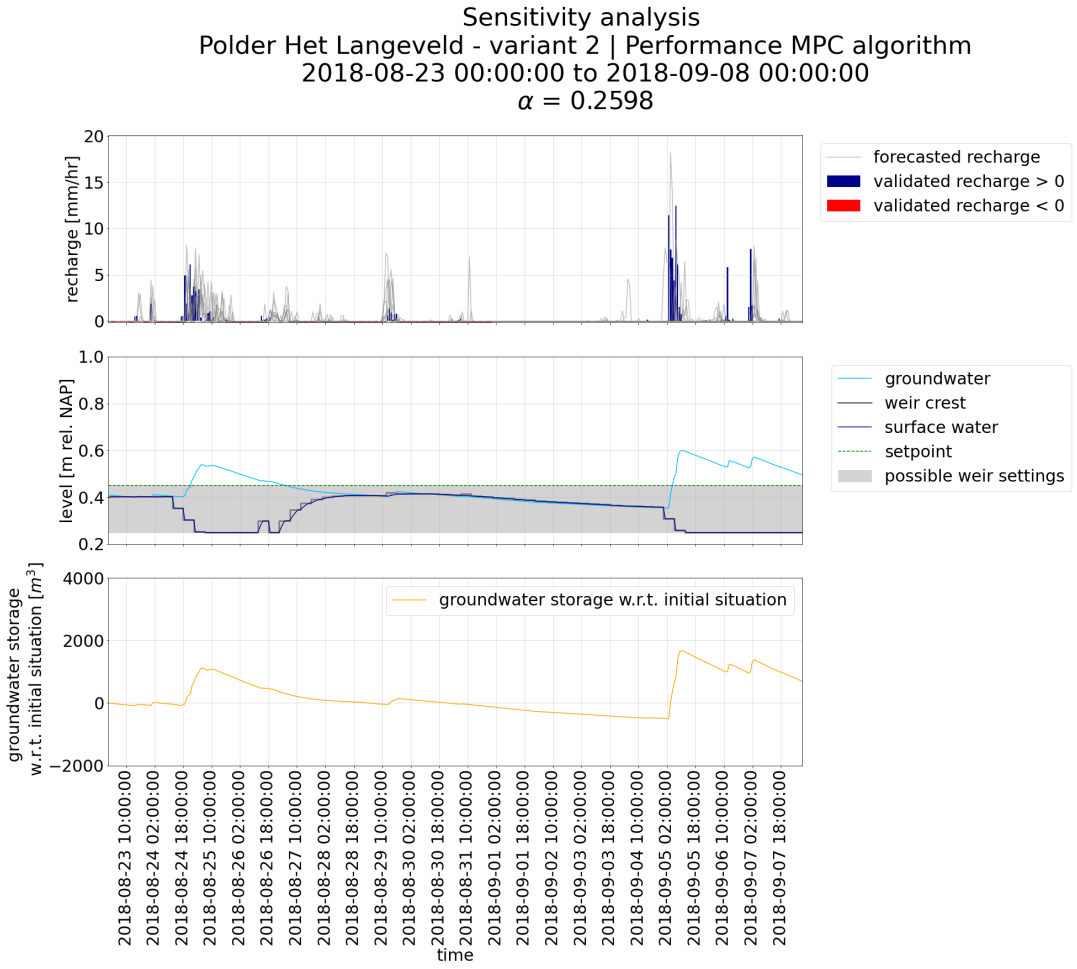

Figure 10.12: Simulation results long-term simulation MPC algorithm, system 3 (based on variant 2 Polder Het Langeveld) - simulation period 1, $h_{GW,setpoint}$ = 0.45 m NAP.

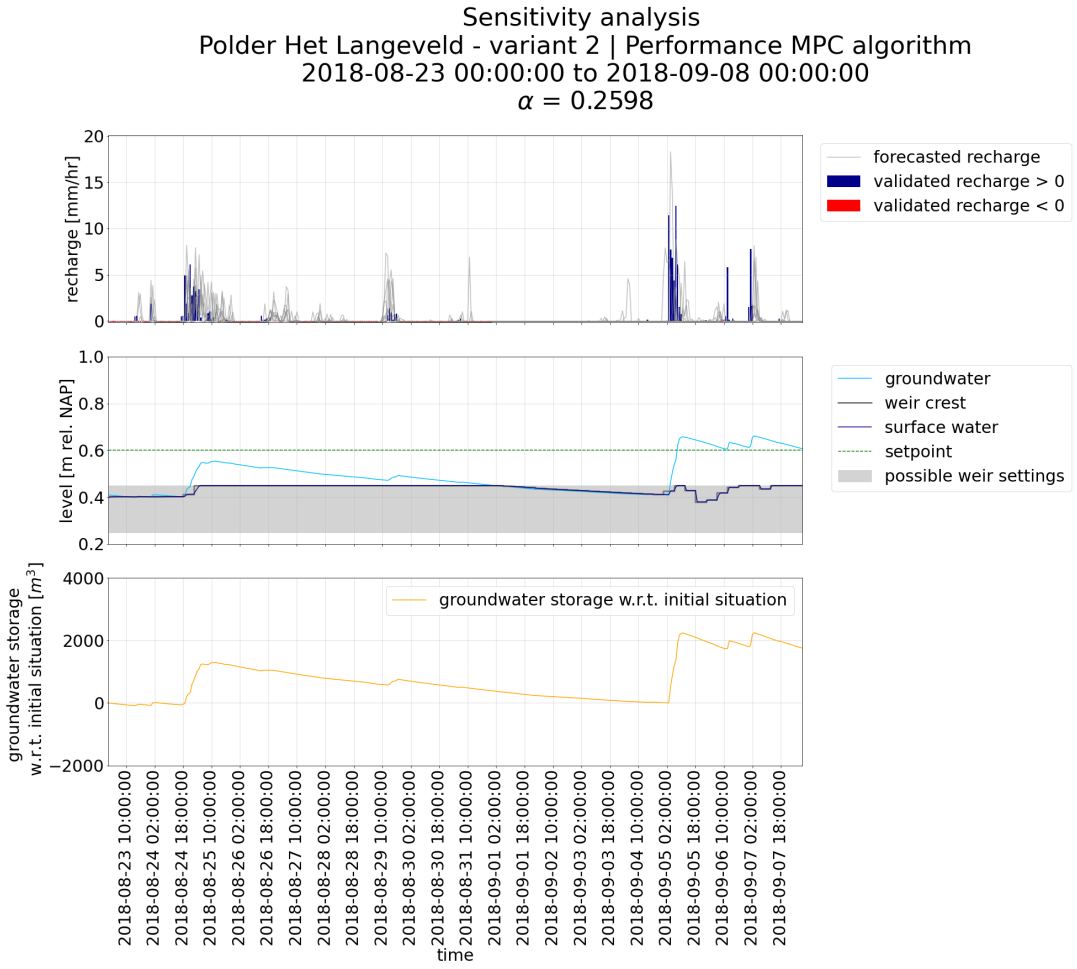

Figure 10.13: Simulation results long-term simulation MPC algorithm, system 3 (based on variant 2 Polder Het Langeveld) - simulation period 1, $h_{GW,setpoint}$ = 0.60 m NAP.

11

Discussion

The results that were shown in the previous chapters are discussed. The results are linked to the research questions to formulate answers. The discussion is subdivided into two sections, each covering a specific research question. Section 11.1 discusses what is encountered when designing a groundwater-based MPC algorithm and which topics require additional study, addressing the first research question. The second research question is addressed by Section 11.2, which discusses the performance of the MPC algorithm and reflects on the objective.

11.1. MPC algorithm design: reflection and further study

The discussion of the MPC algorithm is structured into three paragraphs: 1) reflection, 2) recommendations for further study, and 3) recommendations for extension control algorithm.

Reflection

The design of a groundwater-based MPC algorithm for the operation of multiple water table control systems was covered in Chapter 3, Chapter 5 and Chapter 6. Some design steps were straightforward, while others required extensions to existing software or workarounds to circumvent software limitations. These are discussed below.

Firstly, a workaround was invented that enables MODFLOW to correctly represent the two-way interaction between the groundwater and surface water system. Surface water level is typically imposed as a boundary condition, meaning that it is constant during one stress period, independent of groundwater discharge or ditch water infiltration. Controlled drainage relies on the groundwater-surface water interaction. Furthermore, a constant surface water level triggers subirrigation, like illustrated by Figure 7.9, which is not desired in a system that is designed for controlled drainage. Therefore, an iterative loop was constructed in which the surface water level is continuously updated based on the volume budget, which is calculated by MODFLOW. The workaround is applicable for variant 1 and 2. Figure 7.17 showed that subirrigation is avoided.

Secondly, considering the long computational time, the MODFLOW model could not be implemented in the MPC module. Therefore, a PTSM was developed to describe the evolution of groundwater head and surface water level. The PTSM was extended based on models described in van der Gaast et al. (2009) to correctly represent the two-way interaction between the groundwater and surface water system. Figures 8.5, 8.6, 8.7 and 8.8 demonstrate that the PTSM reproduces the groundwater behaviour simulated by MODFLOW with sufficient accuracy to be used as internal model.

Finally, also the available optimization software packages suffer from limitations. Initially the SciPy Python package, which provides algorithms for optimization, was used to construct the MPC module. However, SciPy experiences problems finding solutions for discontinuous functions. Consequently, it was decided to switch to Pyomo software. Since Pyomo cannot deal with if- and max-statements that

involve control variables (in this case h_{weir}), a workaround invented by Celeste et al. (2010) was applied to ensure that h_{SW} does not exceed h_{weir}. This approach requires the addition of an extra term to the objective function. Simulations were performed to assess the performance of the MPC module, whose results were shown in Section 9.1. Figure 9.1 to Figure 9.8 show that a weighting factor is required to correctly tune the objective function and that this weighting factor may be simulation dependent, which is not perfect.

Recommendations for further study
Various topics require additional study to improve the developed control algorithm.

Figures 7.11 to 7.13 illustrate that the extension to the MODFLOW model is inappropriate for variant 3. The area of the sump is too small, such that the sump water level oscillates between the minimum and maximum level. This means that variant 3 could not be further considered. Additional study is required to correctly represent variant 3.

Further study is also required to improve the Pyomo model. Figures 9.10, 9.11, 9.15, 9.16, 9.18 and 9.20 illustrate that the controller somehow minimizes the distance between h_{SW} and h_{weir}, which is not necessarily desirable. It can be explained by the second term of the objective function, which minimizes the sum of h_{spill} and δ. As such, δ itself is also indirectly minimized. The effect of this controller behaviour is expected to be minimal. However, in case of incorrect precipitation forecasts (underestimations) it could be that the weir is not sufficiently raised such that water is unnecessarily discharged. Additional study of the Pyomo model is therefore recommended.

A relatively simple objective function was established, which is in accordance with the nature of the research (proof of concept). Two extensions are proposed to improve the existing objective function:

1. Include a penalty for exceedance of certain groundwater levels,
2. Include a penalty for undershoot of certain groundwater levels.

Currently, the controller attaches the same value to exceedance and undershoot of $h_{GW,setpoint}$, which is clearly observed in Figure 9.10 and Figure 9.18. The final precipitation events (from 04/09/2018 22:00:00 to the end of the simulation) are anticipated, but not well in advance. Earlier lowering of the weir crest would result in an even larger undershoot just before the precipitation event, which is penalized by the MPC. However, by temporarily accepting low groundwater levels, water nuisance could possibly be prevented and more precipitation could be stored. This controller behaviour could be imposed by adding the proposed penalties and properly tuning weight factors, which is quite tricky. Another option would be to apply a flexible setpoint; a relatively low setpoint in between precipitation events and a higher setpoint during precipitation events.

Finally, it is recommended to improve the hydrological model, as the current hydrological model simplifies the hydrological processes significantly. Several processes are ignored as the unsaturated zone is neglected:

- The delay induced by infiltration through the unsaturated zone, known as unsaturated zone time lag, is neglected.
- The infiltration capacity is assumed constant, while it depends on the degree of saturation.

The effect of these simplifications must be studied.

Recommendations for extension control algorithm
Two recommendations are proposed for extension of the developed control algorithm.

Firstly, the MPC algorithm developed in this research is restricted to the regulation of water discharge. Like explained in Chapter 4, facilities for water supply exist and are used to prevent extreme lowering of water levels during periods of drought and for polder flushing. It is therefore recommended to add water supply to the optimization problem. Water supply facilitates subirrigation, which means that a second drainage mode is added to the problem. It is realized that this further complicates the objective function,

because filling the system with rain water (which is usually of good water quality) is preferred over filling the system with foreign water of unknown quality. Properly tuned weights should be assigned to the different types of water supply to induce the desired behaviour. Furthermore, it would be interesting to analyze the (possibly increased) external water demand due to the presence of submerged drains, because this is very useful information for water boards.

Secondly, it could be questioned whether a groundwater level setpoint achieves the control objective; maximum retention of precipitation. As a first approach, a very high groundwater level, corresponding to the minimum dewatering depth, was selected to enforce maximum water retention. Figure 9.9 to Figure 9.20 show a one-to-one relationship between groundwater level and groundwater storage, which implies that maximization of groundwater level results in maximization of groundwater storage and justifies the chosen approach. However, it should be noted that the relationship is not necessarily one-to-one for a larger, non-homogeneous area. For further research it is therefore advised to develop a control algorithm that is aimed at maximizing fresh water volume rather than groundwater level. This requires adaptation of the objective function and internal model. The internal model should be able to calculate the (ground)water storage for specific (ground)water levels. Alternatively, the MPC module could be adjusted to minimize water discharge (i.e. flow over the weir). This also requires specification of a maximum allowable groundwater level, which should not be exceeded.

11.2. Performance MPC algorithm vs. present control

The performance of the MPC algorithm is evaluated for the following combinations of case study areas and water table control systems:

- Polder Het Langeveld (sandy polder) and variant 1 (water table control without drains),
- Polder Het Langeveld (sandy polder) and variant 2 (water table control with submerged drains, controlled by ditch water level),
- Polder Vierambacht (clayey polder) and variant 2 (water table control with submerged drains, controlled by ditch water level).

The discussion is therefore restricted to these cases. The discussion is structured into three paragraphs: 1) advantages and disadvantages with respect to present control, 2) feasibility for different case study areas and water table control systems, and 3) recommendations for further study. The second paragraph also discusses the results of the sensitivity analysis and reflects on whether groundwater-based MPC really fulfils the objective of maximization of precipitation retention.

Advantages and disadvantages with respect to present control

Multiple advantages of groundwater-based MPC with respect to the present control are identified.

Figures 9.10, 9.11, 9.15, 9.16, 9.18 and 9.20 clearly show that groundwater-based MPC anticipates precipitation events. For example, Figure 9.10 shows that the weir crest is lowered to anticipate precipitation events and discharge water, while Figure 9.11 illustrates that the weir crest is raised to anticipate precipitation events and retain water. The corresponding present control, which is depicted in Figure 9.9, is unaware of precipitation predictions and does not anticipate; the weir crest is maintained at a constant level. Anticipation is an obvious advantage of groundwater-based MPC.

Another advantage of the developed control is direct regulation of groundwater levels. Groundwater levels are presently not taken into account by the control, which is peculiar since groundwater level is the determining factor for enabling specific agricultural activities. Furthermore, by taking into account actual measurements of groundwater level (feedback control), control actions are based on a complete picture of water storage. The present control only measures surface water storage.

The complexity of groundwater-based MPC is an important disadvantage. In contrast to the present control, groundwater-based MPC requires:

- High-quality precipitation forecasts,
- A groundwater model (internal model MPC),
- An extensive network of groundwater monitoring wells (providing updates on the system state),

- Automatic weirs.

All of these involve costs. Calibration and validation of the groundwater model is required, but can be difficult as geohydrological parameters, like hydraulic conductivity, are often unknown and groundwater time series are not always available. Nowadays most weirs are fixed, which means that replacement by automatic weirs is required. This is costly and time-consuming, meaning that a widespread application of groundwater-based MPC by water boards should be adopted as a long-term strategy. It is advised to perform a cost-benefit analysis and to consider the discussion points on feasibility that are raised in the next paragraph.

Feasibility for different case study areas and water table control systems
Long-term simulations were performed to assess the performance of the MPC algorithm. The results are discussed per case study area and variant.

Polder Het Langeveld, variant 1
Figure 9.10 shows that groundwater-based MPC anticipates recharge events, since the weir crest is adjusted to maintain h_{GW} close to setpoint. However, comparison of Figure 9.9 and Figure 9.10 reveals that the obtained groundwater levels do not differ much from the present situation, meaning that the impact of control actions is very little. Because the obtained groundwater levels (Figure 9.10) do not differ much from the present situation (Figure 9.9), the groundwater storage does not differ much from the present situation too. By looking closer into the simulation results, the following differences are found:

- Groundwater-based MPC results in a slightly higher exceedance (order of mm) of setpoint during the first precipitation event (25/08/2018 10:00:00),
- Groundwater-based MPC results in a slightly lower exceedance (approximately 5 mm) of setpoint during the final precipitation event (04/09/2018 22:00:00 to the end of the simulation).

The effect of control actions is very limited in the short-term due to the long system response time, such that groundwater-based MPC leads to minimal deviations from the present situation and setpoint is greatly exceeded. Figure 7.7 (top row) shows that a new steady-state is reached in approximately 40 days after an instantaneous rise of ditch water level, which illustrates the slow system response. Also, the development of the groundwater level is nearly independent of Δh_{SW} during the first few days, which proves that a minimal short-term effect of control actions is to be expected. The response time is even longer when the groundwater-surface water feedback is included, as h_{SW} increases gradually like shown by Figure 7.14. Although a slow response is disadvantageous on the one hand, it can also be beneficial. Namely, erroneous control actions due to incorrect precipitation forecasts do not have much effect initially, such that they do not do too much harm and can be improved during the next control time step.

The developed MPC algorithm in combination with water table control system 1 is thus not really feasible for application in Polder Het Langeveld. The controller should be given more room for anticipation to improve the feasibility. This could be realized by longer precipitation forecasts. Another option is to adjust the objective function such that temporary low or high groundwater tables are more accepted (like mentioned earlier).

Figure 9.15 shows that the precipitation amounts during simulation period 2 are too little to raise h_{GW} close to setpoint. However, variant 1 leads to more water retention than the present control (Figure 9.14). This can be explained by the fact that the MPC-based controller allows a much higher surface water level, thereby reducing groundwater discharge. As a result, an extra 500 m^3 is stored.

Polder Het Langeveld, variant 2
The application of a more advanced water table control system, like variant 2, is at first sight advantageous for the feasibility of groundwater-based MPC in Polder Het Langeveld. The installation of drains leads to a considerable decrease in response time, like shown by Figure 7.7 (middle row). The system returns to a new equilibrium state in approximately 3 days if boundary conditions are changed, which offers possibilities for MPC-based control. It should be noted that the response time increases slightly

due to inclusion of the groundwater-surface water feedback, depending on the recharge rate (Figure 7.15). However, Figure 7.7 also shows that bulging of the groundwater table is very limited (up to 1 cm above h_{SW} or h_{drain}) and nearly independent of R. This suggests that much water is discharged and the system is not suitable for water retention. The objective (maximum precipitation retention) can thus not be fulfilled. The desired setpoint of 0.60 m NAP is only reachable during extreme precipitation events or for extremely high ditch water levels, which is not desirable.

The mentioned discussion points are confirmed by the long-term runs of the MPC algorithm, which results are depicted in Figure 9.11 and Figure 9.16. The maximum weir crest height is usually insufficient to reach setpoint. Setpoint is only reached during an extreme precipitation event at 05/09/2018 (simulation 1, Figure 9.11). While the system can be properly controlled, it is not applicable for creating extra storage capacity. Figure 9.12 and 9.13 indicate that the system is applicable for water table control if lower setpoints are desired and high groundwater tables must be avoided as much as possible, favouring water discharge.

The limited bulging of the groundwater table is caused by the high density and large discharge capacity of the subsurface drains. To be able to use this system for water retention, it is recommended to reduce the amount of drains or select smaller drains. A fairly large drain diameter was selected for this research. It is a trade-off between system response time and groundwater table bulging. This trade-off was examined by means of a sensitivity analysis, which is discussed below.

Although a fast system response is advantageous for system control on the one hand, it can also be disadvantageous. Namely, erroneous control actions due to incorrect precipitation forecasts have a large effect. This is confirmed by Figure 7.7.

Polder Vierambacht, variant 2
Figure 7.8 shows that the response time of variant 2 in Polder Vierambacht lies in between the response times of the previous systems. It takes approximately 20 days to attain a new steady-state. Despite the relatively slow system response, the effect of different control actions is clearly visible, since the lines deviate quickly. Figure 7.16 shows that the response time is not much affected by inclusion of the groundwater-surface water feedback. Groundwater discharge is significant due to the considerable upward seepage flux. As a result, h_{SW} increases to h_{weir} within one day. The water table bulges significantly, like shown by Figure 7.8, which offers possibilities for water retention.

Figure 9.18 (simulation period 1) and Figure 9.20 (simulation period 2) contain the long-term simulation results. It can be observed that groundwater-based MPC anticipates recharge events, since the weir crest height is adjusted properly to maintain h_{GW} close to setpoint. The following improvements compared to the present situation are observed:

- During the first rain event of simulation period 1 (24/08/2018 16:00:00 to 25/08/2018 08:00:00), setpoint is less exceeded compared to the present situation (order of mm).
- The groundwater table exceeds setpoint, but does not reach the surface during the final precipitation events of simulation period 1 (04/09/2018 22:00:00 to the end of the simulation), like in the present situation.
- The exceedance of setpoint during the precipitation events between 21/09/2019 and 24/09/2018 (simulation period 2) is slightly less compared to the present situation (order of mm).

Because the obtained groundwater levels do not differ much from the present situation, the groundwater storage does not differ much from the present situation too. However, it is striking that although the exceedance of setpoint during the precipitation events between 21/09/2019 and 24/09/2018 (simulation period 2) is slightly less compared to the present situation, the final decrease in groundwater storage with respect to the initial situation is reduced by approximately 50 m^3 compared to the present situation.

The feasibility of the developed MPC algorithm in combination with water table control system 2 in Polder Vierambacht can be improved if the controller is given more room for anticipation. This could be realized by longer precipitation forecasts. Another option is to adjust the objective function such that temporary low or high groundwater tables are more accepted (like mentioned earlier). For example, this

could lead to earlier lowering of the weir crest before the final precipitation events of simulation period 1 (04/09/2018 22:00:00 to the end of the simulation, Figure 9.18), such that more water is discharged in advance, exceedance of setpoint is reduced or even avoided and more rain water can be retained.

Sensitivity analysis
The above discussion demonstrates that the developed control algorithm is not feasible for systems with response times greater than or equal to 20 days, since only minor improvements are observed compared to the present situation in case of variant 1 Polder Het Langeveld and variant 2 Polder Vierambacht. To further examine its feasibility for systems with response times lower than 20 days, a sensitivity analysis was performed. The sensitivity analysis was restricted to variant 2, Polder Het Langeveld. k and N_{drain} were adjusted multiple times such that three systems with different geohydrological response times were obtained:

1. System 1, which has a time to equilibrium of approximately 7.5 days,
2. System 2, which has a time to equilibrium of approximately 10 days,
3. System 3, which has a time to equilibrium of about 17.5 days.

Recall that the original system (variant 2, Polder Het Langeveld) is referred to as system 0 and has a response time of 3 days.

Figure 10.8 shows that the MPC algorithm is well capable of maintaining the groundwater level fairly close to a low setpoint in case of system 1, although some exceedance is observed. Figure 10.9 shows that the same system is better capable of water retention than system 0, due to slower recession of the groundwater table and higher groundwater table bulging. By comparing Figure 10.11 and Figure 10.9 it can be observed that system 2 is even better capable to maintain the groundwater level close to a high setpoint, which implies that it is applicable for water retention. Figure 10.10 shows that this is indeed at the expense of system controllability. However, the MPC algorithm approximately takes the system back to setpoint. In case of system 3, a high setpoint is easily reached, but the system is no longer controllable. This implies that, for the applied weir settings and objective function, a system response time lower than 10 days is required for proper control. The range of viable response times can probably be expanded by adjusting the objective function such that the controller is given more room for anticipation. Suggestions to realize this were already provided above. It should be noted that this conclusion is drawn based on a few simulations of limited length only.

Comparing Figure 10.8 to Figure 10.9, Figure 10.10 to Figure 10.11, and Figure 10.12 to Figure 10.13 shows that the direct control of groundwater levels could induce a certain groundwater storage or water retention, depending on the applied setpoint. However, this should not be at the expense of setpoint exceedance, which is why a system should be able to anticipate and the feasibility of groundwater-based MPC is limited to systems with a relatively fast groundwater response.

Recommendations for further study
Various recommendations are proposed for further evaluation of the MPC algorithm and its applicability for geohydrologically distinct areas and multiple water table control systems.

Firstly, it is recommended to include water supply. Water supply is typical during periods of drought and an important characteristic of polder water management. The inclusion of water supply allows for longer simulations, since dry periods should no longer be avoided, such that the performance of the MPC algorithm can be researched more in-depth and over larger time scales.

Secondly, it is recommended to further study the required/allowable groundwater levels for specific land uses and agricultural activities, which may also differ throughout the year. For example, the focus may be on maintaining a specific dewatering depth during the growing season, while maximizing water storage and prevention of water nuisance may be key objectives outside the growing season. A year-round simulation could show the potential of groundwater-based MPC for agriculture.

Thirdly, it is recommended to better simulate the present control. The MPC algorithm is run for short periods of time. To assess its performance, the present control is simulated for the same time periods.

A constant weir crest level, equal to target water level, is assumed for the present control, which is an approximation. If the description of the current control is improved, enhanced comparison and evaluation of the feasibility of groundwater-based MPC is enabled. However, this is challenging, because many weirs are presently human-controlled, based on system insight, and operational rules are lacking.

Fourthly, it is recommended to use longer precipitation forecasts. It is interesting to check whether this improves the performance of variant 1, Polder Het Langeveld and variant 2, Polder Vierambacht. It should be noted that the quality of long precipitation forecasts may be questionable.

Fifthly, practical experience of Witteveen+Bos on Decision Support Systems shows that the performance of control systems is largely dependent on the quality of precipitation forecasts. It is therefore recommended to study the effect of precipitation forecast quality on the observed performance of the MPC algorithm.

Finally, it is recommended to perform a more elaborate sensitivity analysis. The sensitivity to precipitation forecast length could be determined. Additionally, the sensitivity to an imperfect internal model could be researched.

12

Conclusion & Recommendations

Rapid discharge of excess water has always been the core of Dutch water management. Due to climate change, a change in strategy is required. A future-proof drainage strategy consists of three steps: 1) retention, 2) storage, and 3) controlled removal. The research objective was to develop and test a groundwater-based MPC algorithm, that supports the retention component of this strategy, for the operation of multiple water table control systems. The following water table control systems were considered:

1. Water table control without drains, following the principles of dynamic level management,
2. Water table control with submerged drains, controlled by ditch water level and following the principles of controlled drainage,
3. Water table control with submerged drains, controlled by sump water level and following the principles of composite controlled drainage.

By means of a modelling study, the MPC algorithm was tested for two geohydrologically distinct case study areas: 1. Polder Het Langeveld (sandy polder) and 2. Polder Vierambacht (clayey polder). The study was restricted to one field that is surrounded by a ditch. A MPC-based controller was constructed to regulate the crest level of a weir, which controls the ditch/sump water level and discharge to downstream areas. The control objective was to maximize retention of precipitation by maintaining the groundwater level in the centre of the field at the maximum admissible level. The research objective was translated into the following research questions:

1. *What is encountered when designing a groundwater-based Model Predictive Control (MPC) algorithm and which topics require additional study in order to obtain a functioning control?*
2. *What are the advantages and disadvantages of groundwater-based Model Predictive Control (MPC) compared to the original control and how does this differ for geohydrologically distinct areas and various water table control systems*?

Research question 1
Some design steps were straightforward, while others required extensions to existing software or workarounds to circumvent software limitations:

- A workaround was required that enables MODFLOW to correctly represent the two-way interaction between the groundwater and surface water system.
- Considering its long computational time, the developed MODFLOW model could not be implemented in the MPC module. A PTSM was required to efficiently, yet accurately describe the evolution of groundwater head and surface water level.
- A workaround was required to avoid the use of if- and max-statements for the construction of the Pyomo model.

Various topics require additional study to improve the developed control algorithm:

- Extension of the MODFLOW model for variant 3 to include the groundwater-surface water interaction.
- Pyomo model, related to the minimization of the distance between h_{SW} and h_{weir}.
- Extension of the objective function to improve anticipation. Temporary low groundwater levels must be accepted to prevent water nuisance and realize more water storage, whereas temporary high groundwater levels must be accepted to prevent water deficits during periods of drought.
- The effect of using a simplified hydrological model.

Research question 2
Advantages of groundwater-based MPC compared to the original control are:

- Groundwater-based MPC anticipates precipitation events, while the original control does not.
- Groundwater-based MPC regulates groundwater levels, while groundwater levels are presently not taken into account by the control.

The complexity of groundwater-based MPC is an important disadvantage.

The performance of the MPC algorithm was evaluated for 1) Polder Het Langeveld and variant 1, 2) Polder Het Langeveld and variant 2, and 3) Polder Vierambacht and variant 2. A one-to-one relationship between groundwater level and groundwater storage is observed, which means that maximization of groundwater level results in maximization of groundwater storage, thereby (in potential) fulfilling the research objective. The following conclusions are drawn regarding the feasibility of groundwater-based MPC:

- The groundwater response time is too long for Polder Het Langeveld variant 1 ($\pm$ 40 days). As a result, groundwater-based MPC leads to minimal deviations from the present situation and setpoint is exceeded during rain events. Although proper control of the system is hard, the system is applicable for water retention, considering the bulging groundwater table.
- Due to the installation of drains, the response time of Polder Het Langeveld variant 2 is considerably lower ($\pm$ 3 days). This enables proper control. However, the bulging of the groundwater table is very limited, such that the system cannot be applied for water retention.
- The groundwater response time of Polder Vierambacht variant 2 lies in between the response times of the previous systems ($\pm$ 20 days). Slight improvements are observed compared to the present situation. Although proper control of the system is hard, the system is applicable for water storage, considering the bulging groundwater table.

The MPC module could be improved to increase the feasibility of groundwater-based MPC for systems with long response times (variant 1 Polder Het Langeveld and variant 2 Polder Vierambacht). The improvements are aimed at providing more room for anticipation. A first improvement could be the application of a longer prediction horizon, which requires longer precipitation forecasts. A second improvement could be the adaptation of the objective function, such that temporary low or high groundwater tables are more acceptable. This results in stronger anticipation of precipitation or drought events.

It is recommended to increase the drain spacing or install smaller drains if the groundwater table bulging is insufficient to enable water retention (variant 2 Polder Het Langeveld). However, this will be at the expense of the system response time and its controllability. To further examine its feasibility for systems with response times lower than 20 days, a sensitivity analysis was performed. For the applied weir settings and objective function, a system response time lower than 10 days is required for proper control. Furthermore, it is shown that the direct control of groundwater levels could induce a certain groundwater storage or water retention, depending on the applied setpoint. However, this should not be at the expense of setpoint exceedance, which is why a system should be able to anticipate and the feasibility of groundwater-based MPC is limited to systems with a relatively fast groundwater response. The range of viable response times can probably be expanded by the above suggestions to provide more room for anticipation.

Recommendations
The recommendations are subdivided into two groups: 1) recommendations for extension developed

control algorithm, and 2) recommendations for further evaluation of the MPC algorithm.

Recommendations for extension developed control algorithm:

- Add water supply to the optimization problem. Properly tuned weights should be assigned to different types of water supply as filling the system with rain water is preferred over filling the system with foreign water.
- Adapt the objective function and internal model to allow for maximization of fresh water volume rather than groundwater level.

Recommendations for further evaluation of the MPC algorithm:

- Inclusion of water supply to the optimization problem, such that longer simulations can be run.
- Study required/allowable groundwater levels for specific land uses and agricultural activities and perform a year-round simulation.
- Improve representation present control.
- Apply longer precipitation forecasts.
- Study the effect of precipitation forecast quality on the observed performance of the MPC algorithm.
- Determine the sensitivity to precipitation forecast length and imperfectness internal model.

References

Actueel Hoogtebestand Nederland (s.d.). *AHN Viewer*. URL: https://www.ahn.nl/ahn-viewer (visited on 10/24/2022).

Arnold, E., H. Linke, and H. Puta (1999). "Nonlinear model predictive control for operational management of a canal system". In: *1999 European Control Conference (ECC)*. IEEE, pp. 4876–4880.

Åström, Karl Johan and Richard M. Murray (2008). *Feedback systems: an introduction for scientists and engineers*. eng. Princeton: Princeton University Press. ISBN: 9780691135.

Bakker, M. and V.A. Kelson (2009). "Writing Analytic Element Programs in Python". In: *Groundwater* 47.6, pp. 828–834. URL: https://ngwa.onlinelibrary.wiley.com/doi/abs/10.1111/j.1745-6584.2009.00583.x.

Bakker, M. et al. (2016). "Scripting MODFLOW Model Development Using Python and FloPy". In: *Groundwater* 54.5, pp. 733–739. URL: https://ngwa.onlinelibrary.wiley.com/doi/abs/10.1111/gwat.12413.

Bartholomeus, R., G. van den Eertwegh, and G. Simons (2015). "Naar online en optimale sturing van Klimaat Adaptieve Drainage [To online and optimale control of Climate Adaptive Drainage]". In: *Stromingen* 24.4, pp. 27–42.

Bierkens, M.F.P., P.J.T. van Bakel, and J.G. Wesseling (1999). "Comparison of two modes of surface water control using a soil water model and surface elevation data". In: *Geoderma* 89.1-2, pp. 149–175.

Bot, A.P. (2016). *Grondwaterzakboekje [Groundwater pocket book]*. Bot Raadgevend Ingenieur.

Brouwer, C., A. Goffeau, and M. Heibloem (1985). *Irrigation Water Management: Training manual no. 1 - Introduction into Irrigation. Food and Agriculture Organization of the United Nations*. FAO Land and Water Development Division.

Brouwer, C. et al. (1988). "Irrigation water management: irrigation methods". In: *Training manual FAO* 9.5, pp. 5–7.

Bynum, Michael L. et al. (2021). *Pyomo-optimization modeling in python*. Vol. 67. Springer.

Celeste, Alcigeimes B. and Max Billib (2010). "The role of spill and evaporation in reservoir optimization models". In: *Water resources management* 24.4, pp. 617–628.

de Wit, J.A. Janine et al. (2022). "Development of subsurface drainage systems: Discharge - retention - recharge". In: *Agricultural Water Management* 269, p. 107677.

Doherty, E. (2020). *What is object-oriented programming? OOP explained in depth*. URL: https://www.educative.io/blog/object-oriented-programming (visited on 10/17/2022).

Duijkers, Miriam (2021). "Extra zoetwater voor West-Nederland tijdens droogte [Extra freshwater for western Netherlands during droughts]". In: *Deltanieuws* 5.

Fourer, Robert (2013). "Algebraic Modeling Languages for Optimization". In: *Encyclopedia of Operations Research and Management Science*. Ed. by Saul I. Gass and Michael C. Fu. Boston, MA: Springer US, pp. 43–51. ISBN: 978-1-4419-1153-7. URL: https://doi.org/10.1007/978-1-4419-1153-7_25.

Fouss, James L. et al. (2007). "Water table control systems". In: *Design and Operation of Farm Irrigation Systems, 2nd Edition*. American Society of Agricultural and Biological Engineers, pp. 684–724.

GAMS Development Corp. GAMS Software GmbH (s.d.). *IPOPT and IPOPTH*. URL: https://www.gams.com/latest/docs/S_IPOPT.html (visited on 02/23/2023).

Grondwaterformules.nl (s.d.[a]). *Bergingscoëfficiënt van zand [Storage coefficient of sand]*. URL: http://grondwaterformules.nl/index.php/vuistregels/ondergrond/bergingscoefficient-van-zand (visited on 11/08/2022).

— (s.d.[b]). *Werkelijke verdamping [Actual evaporation]*. URL: http://grondwaterformules.nl/index.php/vuistregels/neerslag-en-verdamping/werkelijke-verdamping (visited on 02/24/2023).

Heath, R.C. (1983). *Basic ground-water hydrology*. U.S. Geological Survey Water-Supply Paper 2220.

Het Waterschapshuis (2022). *Technische Handleiding V16.0 Weer Informatie Waterbeheer (WIWB) API [Technical Manual V16.0 Weather Information Watermanagement (WIWB) API]*. Het Waterschapshuis.

Het Waterschapshuis (s.d.). *Neerslag - Weer Informatie Waterbeheer [Precipitation - Weather Information Watermanagement]*. URL: https://www.hetwaterschapshuis.nl/neerslag-weer-informatie-waterbeheer (visited on 02/08/2023).

Hoekstra, J. and A. van Schie (2022). *Sturen met grondwater - Bedrijvenproef Spengen 2017-2021 [Groundwater-based control - businesses test Spengen 2017-2021]*. Hoogheemraadschap De Stichtse Rijnlanden.

Hoogheemraadschap van Rijnland (s.d.). *Werkgebied Rijnland [Management area Rijnland]*. URL: https://www.rijnland.net/over-rijnland/organisatie/ons-werkgebied/ (visited on 01/20/2023).

Jousma, G. and H. Massop (1996). *Intreeweerstanden waterlopen, Inventarisatie en analyse [Entrance resistance watercourses, Inventarisation and analysis]*. TNO Grondwater en Geo-Energie.

Klein Tank, A.M.G. and G. Lenderink (2009). *Climate change in the Netherlands: Supplements to the KNMI'06 scenarios*. De Bilt, The Netherlands: Royal Netherlands Meteorological Institute (KNMI).

Klimaatinfo (s.d.). *Het Klimaat van Nederland [The climate of the Netherlands]*. URL: https://klimaatinfo.nl/klimaat/nederland/ (visited on 01/20/2023).

Langevin, C.D. et al. (2017). *Documentation for the MODFLOW 6 Groundwater Flow Model: U.S. Geological Survey Techniques and Methods*. Vol. 6, chap. A55, 197 p. Geological Survey Techniques and Methods. DOI: https://doi.org/10.3133/tm6A55.

Massop, H. and C. Schuiling (2016). *Buisdrainagekaart 2015: update landelijke buisdrainagekaart op basis van de landbouwmeitellingen van 2012 [Drainage map 2015: update national drainage map based on agricultural census of 2012]*. Alterra, Wageningen-UR.

Miltenburg, I. (2020). *Polder Management*. URL: https://oss.deltares.nl/nl/web/rtc-tools/-/2393381-4 (visited on 02/21/2023).

Morris, Donald Arthur and Arnold Ivan Johnson (1967). *Summary of hydrologic and physical properties of rock and soil materials, as analyzed by the hydrologic laboratory of the US Geological Survey, 1948-60*. Tech. rep. US Government Printing Office.

Mostert, Erik (2019). *Nederlands waterrecht voor niet-juristen [Dutch water law for non-lawyers]*. TU Delft Open.

Natural Resources Conservation Service (2001). *Part 624 Drainage National Engineering Handbook*. United States Department of Agriculture.

Nelen & Schuurmans (s.d.). *Operationele sturing Boezem en Polders – BOSBO 3.0 [Operational control boezem and polders - BOSBO 3.0]*. URL: https://nelen-schuurmans.nl/case/operationele-sturing-boezem-en-polders-bosbo-3-0/ (visited on 01/20/2023).

Provincie Zuid-Holland (2012). *Gebiedsprofiel Hollandse Plassen [Area profile Hollandse Plassen]*. Provincie Zuid-Holland.

Reijers, N., R. van der Laan, and A.M. van Dam (2001). *Grondwaterpeil in de Bollenstreek Studie naar (sub)optimale grondwaterstanden voor bloembollenteelt [Groundwater level in the Bulb Region Study for (sub)optimal groundwater levels for flower bulb cultivation]*. Tech. rep. Praktijkonderzoek Plant & Omgeving, sector Bloembollen.

Ritzema, H.P. and L.C.P.M. Stuyt (2015). "Land drainage strategies to cope with climate change in the Netherlands". In: *Acta Agriculturae Scandinavica, Section B — Soil & Plant Science* 65.sup1, pp. 80–92. URL: https://doi.org/10.1080/09064710.2014.994557.

Ritzema, H.P. and J.M. van Loon-Steensma (2018). "Coping with climate change in a densely populated delta: A paradigm shift in flood and water management in the Netherlands". In: *Irrigation and drainage* 67, pp. 52–65.

Royal Netherlands Meteorological Institute (KNMI) (2014). *KNMI'14 climate scenarios for the Netherlands; A guide for professionals in climate adaptation*. De Bilt, The Netherlands: Royal Netherlands Meteorological Institute (KNMI).

— (s.d.[a]). *dp1: KNMI HARMONIE40 datapakket nr. 1 [dp1: KNMI HARMONIE40 data package nr. 1]*. URL: https://www.knmidata.nl/data-services/knmi-producten-overzicht/atmosfeer-modeldata/data-product-1 (visited on 02/08/2023).

— (s.d.[b]). *Weermodellen [Weather models]*. URL: https://www.knmi.nl/kennis-en-datacentrum/uitleg/weermodellen (visited on 02/08/2023).

Skaggs, R. W. et al. (1999). *Agricultural drainage*. Number 38 in the series Agronomy. Madison, Wisconsin, USA: American Society of Agronomy, Inc.

Stafleu, Jan et al. (2019). *Totstandkomingsrapport GeoTOP [Origin report GeoTop]*. TNO.

STOWA (s.d.[a]). *Controlled drainage*. URL: https://www.stowa.nl/deltafacts/zoetwatervoorziening/delta-facts-english-versions/controlled-drainage (visited on 09/21/2022).
— (s.d.[b]). *Dynamic level management*. URL: https://www.stowa.nl/deltafacts/zoetwatervoorziening/delta-facts-english-versions/dynamic-level-management (visited on 09/21/2022).
Stuyt, L.C.P.M. (2016). *Regelbare drainage als schakel in toekomstig waterbeheer [Controlled drainage as a link to future water management]*. Alterra, Wageningen-UR.
Tian, X. (2015). "Model predictive control for operational water management: A case study of the Dutch water system". In.
TNO (s.d.[a]). *DINOloket Data and Information on the Dutch Subsurface*. URL: https://www.dinoloket.nl/en (visited on 10/24/2022).
— (s.d.[b]). *Grondwaterstanden in Beeld*. URL: https://www.grondwatertools.nl/gwsinbeeld/ (visited on 01/22/2023).
Unie van Waterschappen (2018). *Waterschapskaart [Map of water boards]*. URL: https://unievanwaterschappen.nl/publicaties/waterschapskaart/ (visited on 01/20/2023).
van Bakel, P.J.T. (1986). *Planning, design and operation of surface water management systems: A case study*. Instituut voor Cultuurtechniek en Waterhuishouding.
van Bakel, P.J.T. et al. (2013). *KlimaatAdaptieve Drainage - Landelijke geschiktheid van conventionele, samengestelde peilgestuurde en klimaatadaptieve drainage [Climate Adaptive Drainage - National suitability of traditional, composite controlled and climate adaptive drainage]*. FutureWater.
van de Craats, D., S.E.A.T.M. van der Zee, and A. Leijnse (2021). "Anticipatory Drainage Base Management for Groundwater Level Optimization". In: *Water Resources Research* 57.11, e2021WR029623.
van der Gaast, J.W.J., H. Massop, and H.R.J. Vroon (2009). *Effecten van klimaatverandering op de watervraag in de Nederlandse groene ruimte [Effects of climate change on the water demand in the Dutch green zones]*. Alterra Wageningen UR.
van Nooijen, R., D. Koutsoyiannis, and A. Kolechkina (2021). "Optimal and Real-Time Control of Water Infrastructures". In: *Oxford Research Encyclopedia of Environmental Science*. Oxford University Press. DOI: 10.1093/acrefore/9780199389414.013.627.
van Overloop, Peter-Jules (2006). *Model predictive control on open water systems*. IOS Press.
Versteeg, R. et al. (2013). *Meteobase Online archief voor neerslag- en verdampingsgegevens voor het waterbeheer [Meteobase Online archive for precipitation and evaporation data for water management]*. STOWA.
Waterschap Brabantse Delta (s.d.). *Peilbesluiten [Water level decrees]*. URL: https://www.brabantsedelta.nl/peilbesluiten (visited on 02/08/2023).
Watertechnolgie, TKI (s.d.). *Groundwater for crops*. URL: https://www.tkiwatertechnologie.nl/projecten/groundwater-for-crops/ (visited on 11/10/2022).
Wijnakker, R. and P. Plambeck (2021). *De Blauwe Lens Rijnland [The blue lens Rijnland]*. Amsterdam: Fabrications. + Buro Sant en Co landschapsarchitectuur.
Wikipedia (s.d.). *Hoogheemraadschap van Rijnland*. URL: https://nl.wikipedia.org/wiki/Hoogheemraadschap_van_Rijnland (visited on 01/20/2023).
Wonink, P. et al. (1997). *Verkennende studie naar de mogelijkheden van grondwaterstandsafhankelijk peilbeheer in de waterschappen Meppelerdiep en Wold en Wieden [A reconnaissance study of the possibility of groundwater-dependent surface water control for the water boards Meppelderdiep and Wold and Wieden]*. Tech. rep. Rapport 970940. Deventer: TauwMabeg Civiel en Bouw.
World Health Organization (2022). *Guidelines for drinking-water quality: fourth edition incorporating the first and second addenda*. World Health Organization.

A

Background information 1: examples of operational control

This appendix contains background information on the operational control of water table control systems C, D and E (Figure 2.1, Section 2.1). While Figure 2.1 shows that weirs are used to regulate ditch and/or sump water level, pumps may also be employed.

Operational control systems are designed to optimize some objective. Examples of operational objectives for water table control systems are:

1. Minimize the occurrence of excess soil moisture conditions in the root zone, caused by a precipitation excess.
2. Minimize the occurrence of soil moisture deficit in the root zone, caused by a precipitation deficit.
3. Minimize the need for subirrigation, i.e. prevent overdrainage of the soil and use infiltrated rainfall efficiently.
4. Provide proper soil conditions for land cultivation.
5. Minimize energy requirements (Skaggs et al. 1999; Fouss et al. 2007).

These objectives may be achieved by systems of different complexity. Below, various methods for operational control are discussed in order of increasing complexity.

Manual operation, based on insight in system response
Weirs and pumps may be controlled manually. The farmer or water authority should frequently visit the field to check the groundwater level. A groundwater observation well may be installed at the field's centre, while visual inspection of crops may also give an indication of the groundwater table. Depending on the observations, a farmer decides whether the surface or sump water level should be adjusted. This requires insight into the response of the (groundwater) system. For instance, due to the delay between weir adjustment and groundwater response, overdrainage may occur if raising of the weir is postponed until the midpoint groundwater level recedes to setpoint after a precipitation event (Skaggs et al. 1999).

Manual operation, based on decision rules
Manual operation may also be based on decision rules. Below, two examples of sets of operational rules for dynamic level management are given. Similar decision rules may be applied for controlled drainage and composite controlled drainage systems.

Figure A.1 contains a schematic overview of possible surface water target levels during the year intended for day-to-day surface water management. The scheme was developed by van Bakel (1986). Since remote control of weirs was not yet possible in 1986, his starting point was an adjustment frequency of 7 days. The difference between the lowest and highest target level is 70 cm, which is divided into steps of 10 cm. The operational rules can be summarized as follows:

- Phase 0, the lowest level, is the standard winter target level. When the groundwater level falls below a certain level, phase 2 is applied to prevent overdrainage.
- The transition period from winter to summer level should start no earlier than t_1.
- Figure A.2 contains a table that illustrates which target level corresponds to which groundwater level during the transition period. The lower the groundwater table, the higher the target level.
- A distinction can be made between a constant, dropping and rising groundwater table. If the groundwater table is rising, a lower target level is preferred to prevent waterlogging.
- The change in target level is restricted to 0.10 m per week, which should also be obeyed during the growing season.
- Phase 5 is the standard summer level.
- Phase 4, 5, 6 and 7 may only be applied when the water deficit in the root zone exceeds certain values, like shown by Figure A.3. This is to guarantee sufficient storage capacity in the root zone for extreme precipitation events.
- Phase 6 and 7 are only allowed after t_3.
- The start of the second transition period, t_4, depends on the water deficit in the root zone.

van Bakel (1986) determined the operational rules by trial and error.

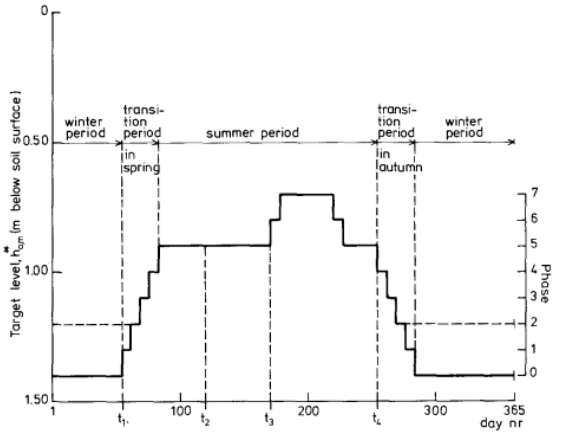

Figure A.1: Scheme intended for day-to-day surface water management, developed by van Bakel (1986).

Groundwater depth h^*_f (m below soil surface)	Phase	Target level h^*_m (m below soil surface)
>0.60	1	1.30
>0.70	2	1.20
>0.80	3	1.10
>0.90	4	1.00
>1.00	5	0.90
>1.10	6	0.80
>1.10	7	0.70

Figure A.2: Target water levels during transition periods shown in Figure A.1. The target water level is determined by groundwater depth (van Bakel 1986).

Figure A.4 contains another set of operational rules. These were determined by Wonink et al. (1997) for grassland on sandy soils through expert judgement and an optimization study. A relation between the actual groundwater level and target surface water level is provided, just like in Figure A.2. A distinction is made between the growing season and outside the growing season. A step function is used to prevent frequent adjustments of the weir crest. Measurements are taken once a day, so the adjustment frequency is at most once a day (Wonink et al. 1997; Bierkens et al. 1999).

Water deficit (mm)	Phase	Target level (m below soil surface)
$W_{r,d}$ > 10	4	$h^*_{o,m}$ = 1.00
> 20	5	= 0.90
> 30	6,7	= 0.80 and 0.70

Figure A.3: Target water levels during summer period shown in Figure A.1. The target water level is determined by the water deficit in the root zone (van Bakel 1986).

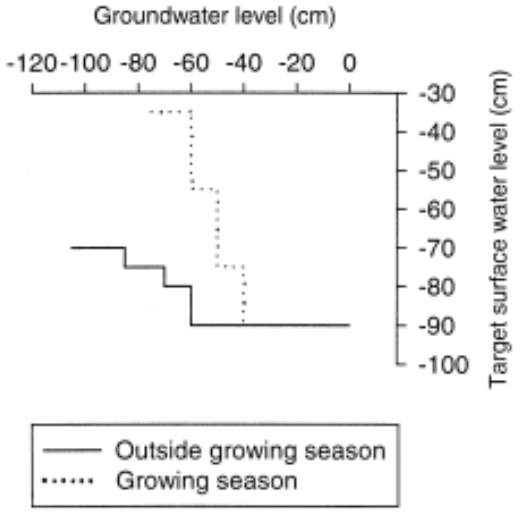

Figure A.4: Set of operational rules, determined by Wonink et al. (1997) for grassland on sandy soils. A relation between the actual groundwater level and target surface water level is provided.

Automated operation of a sump structure, with and without feedback

As indicated by van Bakel in 1986, surface water levels could in principle be managed automatically by sensors that observe soil moisture, groundwater table and surface water level. He stated in 1986 that “this method, however, is too sophisticated to apply in practice for the time being” (p. 61). Due to technological advancements, automated operation is possible nowadays.

Below, two control systems that could be applied to control the sump water level (SWL) are covered. It is assumed that the SWL is controlled through pumping. The system may operate in the controlled drainage mode (CD) as well as in the subirrigation mode (SI).

The first control system is called “float-switch activated control”. Four float-activated electrical switches are employed to operate the pump(s). In the CD-mode, the SWL is maintained between high-drainage (HD) and low-drainage (LD) level by means of a double-float switch. A double-float switch is also employed in the SI-mode. In this case, the SWL is maintained between low-irrigation (LI) and high-irrigation (HI) level. Single-float switches are applied at the maximum (MAX) and minimum (MIN) sump water level elevations. If the MAX level is exceeded, the system operation changes from SI to CD. If the SWL falls below MIN, the system operation changes from CD to SI. Observations of water table depth in the field are not used in the control. The switches may be repositioned manually to adjust the control elevations (Skaggs et al. 1999; Fouss et al. 2007).

The second control system, which is visualized in Figure A.5, is called “microprocessor-controlled system”. The operation of the microprocessor-controlled system is very similar to the operation of the float-activated control system; the control elevations (MIN, LD, HD, LI, HI and MAX) are alike. However, the water table depth at the field’s centre or any other location between drains is fed back to the control system. If the measured groundwater level is outside of the desired range for 24 hours, the

control elevations are adjusted upward or downward automatically. Once the groundwater level has returned to the desired range, the control elevations are reset to their standards. This type of control, including feedback, is advised to manage the system properly (Skaggs et al. 1999; Fouss et al. 2007).

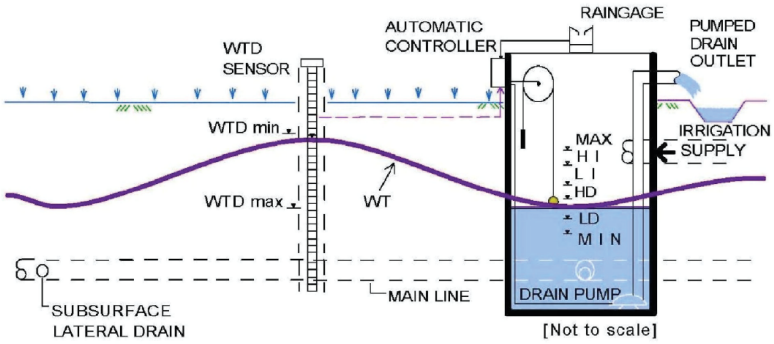

Figure A.5: Microprocessor-controlled system. Four float-activated electrical switches are employed to operate the pump(s) and maintain the sump water level between high-drainage (HD) and low-drainage (LD) level or low-irrigation (LI) and high-irrigation (HI) level. Based on field observations of the groundwater table depth, the control elevations are automatically adjusted upward or downward (Fouss et al. 2007).

Automated operation according to a mathematical optimization procedure and precipitation forecasts

Since the accuracy of precipitation forecasts has improved over the last decades, day-to-day operation of water table management systems becomes feasible. This has the following implications for the system depicted in Figure A.5:

- The operation mode may be switched from SI to CD several hours before precipitation is expected.
- The SI mode is avoided when precipitation is expected.

Operational objectives can be achieved better when precipitation forecasts are taken into account (Skaggs et al. 1999).

The basic components of an automated operation that uses precipitation forecasts to determine the optimal control actions are:

1. Groundwater monitoring wells, to monitor the current groundwater situation.
2. Adjustable weirs and pumping stations, to manage the surface and/or sump water level.
3. Weather stations, to measure actual precipitation and evaporation amounts.
4. A calculation method or a set of decision-making guidelines, to determine the required weir crest heights and pump discharges for obtaining the desired groundwater situation.
5. A hydrological model, to estimate the expected future groundwater situation (in the next few days) (STOWA s.d.[b]).

In the past, several analytical and numerical models have been developed to predict the groundwater situation for groundwater-dependent control. An analytical model is established by (van de Craats et al. 2021). The analytical model is implemented in an optimization procedure to determine the optimal control actions:

1. The expected groundwater levels are calculated for 21 available precipitation forecasts.
2. If the expected groundwater level exceeds the upper limit of the optimal range, many possible control actions exist. Discrete steps of when and how the drainage base can be changed are used. The time step is 6 hours and the change in drainage height is 5 cm. All relevant changes are applied at all possible times and the resulting groundwater levels are computed.
3. For each of the precipitation forecasts, the five best control options are selected. These are the control options that minimize an objective function.

4. For each control option, the time at which the drainage base should be raised again to prevent overdrainage is determined. Steps 2 to 4 are repeated if the upper limit is still exceeded.
5. The median of the best management options for each of the 21 precipitation forecasts is claimed to be the optimal strategy.

van de Craats et al. (2021) end with a number of discussion points:

- The uncertainty in precipitation forecasts should be taken into account.
- The feasibility of groundwater-dependent surface water control depends on local circumstances and groundwater response times.
- The additional water storage that can be realized depends on drain elevation.
- Attention should be given to which precipitation forecasts and forecasts lengths should be used.

Automated operation according to management-algorithm CAD
An online management-algorithm has been developed within TKI-Watertechnologie (2013-2015) (Watertechnolgie s.d.) to determine the optimal sump water level. This is referred to as Climate Adaptive Drainage (CAD). The algorithm combines field observations, precipitation forecasts and model simulations to optimize soil moisture conditions in the root zone. This is rather unusual, as controlled drainage is traditionally aimed at optimizing groundwater levels. The groundwater table indirectly affects soil moisture conditions in the root zone (through capillary rise), but other factors, like precipitation, evaporation, temperature and plant characterized, are required to quantify plant stress. The management-algorithm consists of three steps:

1. Calibration - Observations (meteorological conditions, groundwater table and soil moisture content) are used for calibration and data-assimilation of the 1-D Soil-Water-Atmosphere-Plant model (SWAP). In this step, optimal model parameters and initial conditions are generated.
2. Prediction - The groundwater table, soil moisture content, drainage flux and plant stress are simulated using the calibrated model. Precipitation predictions are used to look n days ahead. Uncertainties in precipitation predictions are also accounted for, resulting in a range of values for each simulated variable. The actual CAD-level is used as starting point.
3. Optimization of CAD-level - The optimal CAD-level is determined based on the simulated plant stress and drainage flux. The CAD-level is lowered to increase drainage if the plant stress exceeds some value. If the drainage flux exceeds its limit, the CAD-level is raised to restrict drainage. The actual CAD-level remains unchanged in case the limits are not exceeded. An iterative procedure is applied to determine the optimal CAD-level. The CAD-level is adjusted until the resulting improvements of plant stress or drainage flux are negligible (Bartholomeus et al. 2015).

B

Background information 2: motivation for Model Predictive Control (MPC)

Below, the usefulness of MPC is demonstrated by comparing the control method to feedback and feedforward control. Firstly, a brief explanation of feedback control and feedforward control is provided. Subsequently, a comparison is made.

Feedback control
The block diagram of feedback control is depicted in Figure B.1. The setpoint and measured process output form the controller input. In practice, these are the target water level and measured water level respectively (van Overloop 2006). The controller output (u), e.g. the change in actuator settings, is computed as a function of the difference between the target water level and the measured water level. This difference is typically referred to as the control error (e). The change in structure settings is often computed using a Proportional Integral controller (PI-controller). The continuous PI-controller is described by Equation B.1:

$$u(t) = K_p e(t) + K_i \int_{\tau=0}^{t} e(\tau) d\tau \tag{B.1}$$

The required change in structure setting at time t ($u(t)$) is computed using a proportional gain factor (K_p) multiplied by the control error and an integral gain factor (K_i) multiplied by the integral of the past errors (Åström et al. 2008).

Since the settings of hydraulic structures are usually not continuously adjusted, the discrete PI-controller is given by the equation below:

$$u(k) = c_P e(k) + c_I \sum_{j=0}^{k-1} e(j) \tag{B.2}$$

where k is the time step index (van Overloop 2006).

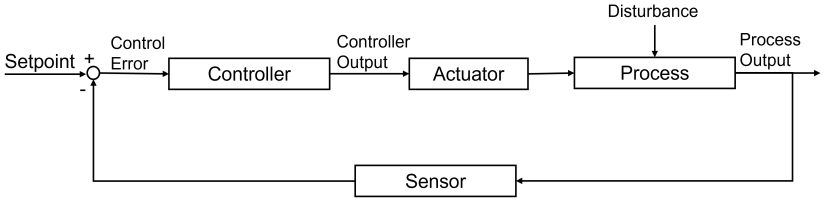

Figure B.1: Block diagram feedback control.

Feedforward control
The block diagram of feedforward control is presented in Figure B.2. It can be observed that the setpoint and measured, uncontrolled input (disturbance) are forwarded to the controller. The controller determines the structure settings that are required to cancel out the effect of the disturbance such that, ideally, zero deviation from setpoint is achieved. Feedforward control is generally referred to as open loop control, since the process output is not taken into account by the controller. Since the internal model does not perfectly represent the physical system and measurements are often inaccurate, the actual deviation will never be zero. By combining feedback and feedforward control, this imperfection can be compensated for by a feedback control action (van Overloop 2006).

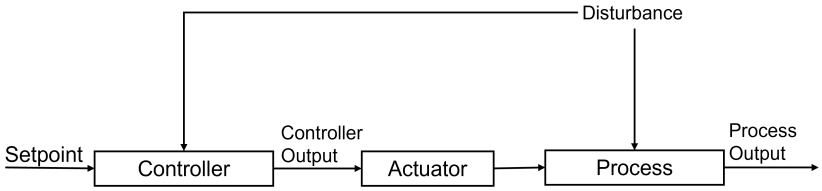

Figure B.2: Block diagram feedforward control.

Comparison
The above control methods can adequately control a water system in many cases. However, there are often constraints that complicate this. For instance, the pump capacity or the number of allowable weir crest adjustments per time interval may be limited (van Overloop 2006).

Figure B.3 clearly shows the difference between three different control methods: 1) feedback control (brown lines), 2) feedback control in combination with feedforward control (green lines), and 3) MPC (grey lines). The disturbances and maximum control flow are the same for each controller. The upper graph shows the control flow in time. The red dashed line indicates the maximum control flow. The lower graph displays the controlled water level in time. The light green line represents setpoint, while the red dashed lines indicate the allowable range of water levels. The lower graph shows that feedback control results in a significant overshoot of setpoint. To minimize the water level deviation from setpoint over the entire prediction horizon, the MPC controller increases the control flow to the limit even before the disturbance inflow takes place, which is observed in the upper graph. MPC anticipates by bringing the water level down in advance to prevent excessive rise of water levels later. Figure B.3 shows that the deviation from setpoint is much smaller for the MPC controller than for the feedback controller (van Overloop 2006).

Based on Figure B.3, it can be concluded that MPC uses the existing discharge facilities in a very efficient manner. With MPC, the system requirements can be fulfilled without expanding discharge capacity (Tian 2015). On the other hand, MPC may also be risky. Inaccurate precipitation forecasts may result in unnecessary emptying of the water system. Since MPC requires an internal model, it is a more advanced and computationally expensive control method. MPC is an appropriate method when the quality standards are stringent (van Overloop 2006).

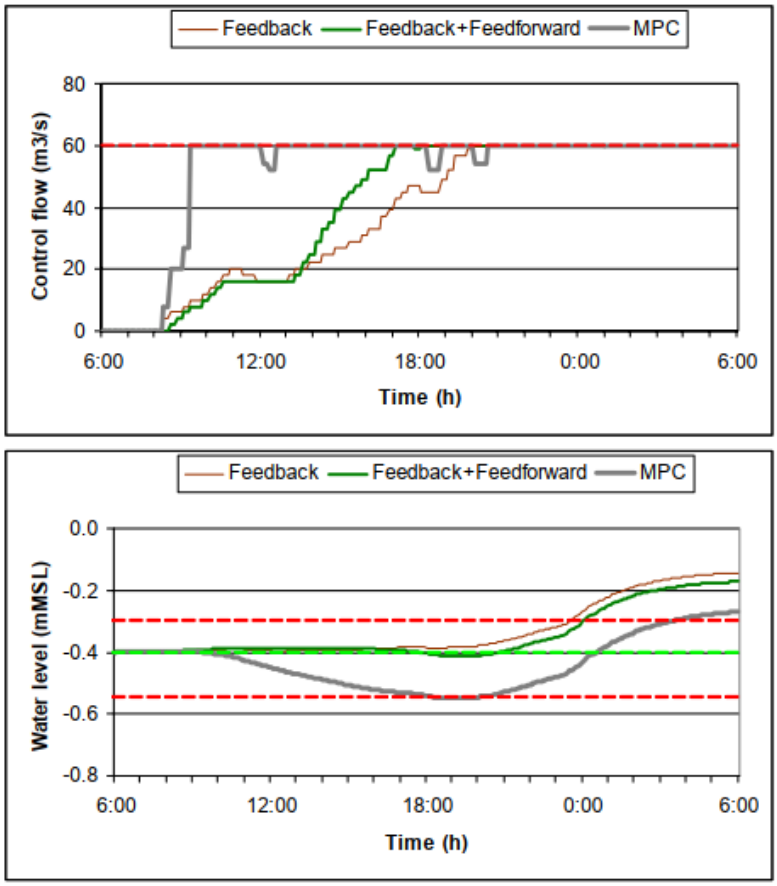

Figure B.3: Comparing the performance of feedback control, feedback control in combination with feedforward control and MPC. MPC anticipates disturbances by bringing the water level down in advance to prevent excessive rise of water levels later (van Overloop 2006).

C

Overview FloPy packages

This appendix contains an overview of the applied FloPy packages for construction of the base model, which is described in Section 5.1.1. The table lists the packages, their abbreviations and their use. If necessary, some additional information is provided in the final column (”Notes”).

Table C.1: Overview of FloPy packages.

Package	Abbreviation	Use	Notes
Simulation object	-	-	Standard
Temporal Discretization	TDIS	Defines temporal discretization	Any temporal discretization may be defined
Groundwater Flow	GWF	-	Standard
Iterative Model Solver	IMS	Defines solver complexity and convergence criteria	Convergence criteria should be strict, due to small cells
Discretization	DIS	Defines spatial discretization	Plot of any size can be constructed
Initial Condition	IC	Defines initial condition	Uniform initial groundwater head equal to summer target water level ($h_{SW,target}$ [m NAP]) is assumed
Node Property Flow	NPF	Defines hydraulic conductivity	Unconfined flow is assumed
General Head Boundary	GHB	Defines boundary condition bottom model	-
River	RIV	Defines boundary condition model sides (ditch) Defines drains	-
Recharge	RCH	Defines recharge	Any recharge may be defined
Storage	STO	Defines specific yield, specific storage and calculation mode (steady-state or transient)	-
Output Control	OC	-	Standard

D

Explanation case study area-specific parameters | Polder Het Langeveld

D.1. Plot size: plot length (L_{plot}) and plot width (W_{plot})

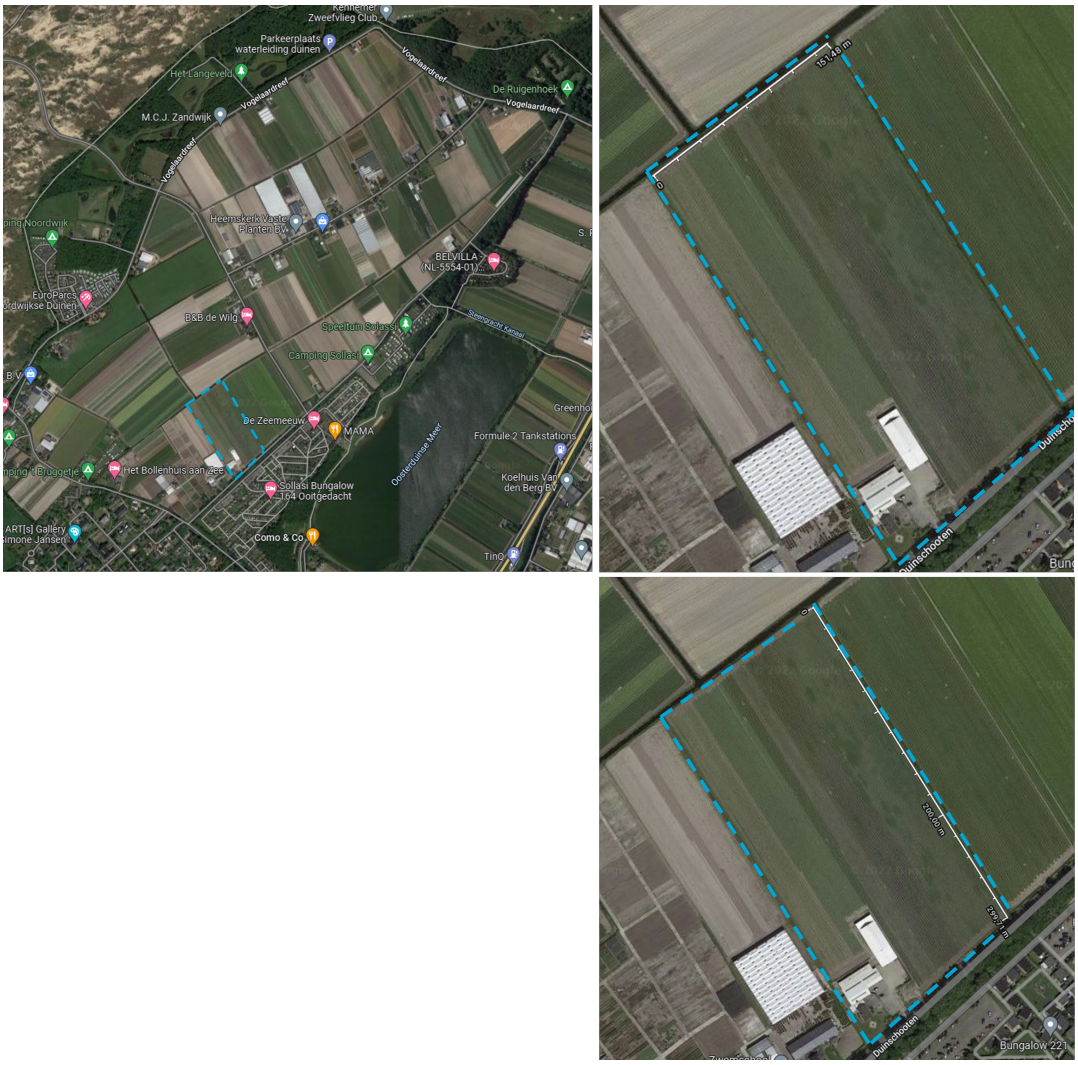

Figure D.1: Location and plot size of representative agricultural plot Polder Het Langeveld.

The average plot size in Polder Het Langeveld is determined using Google Maps. The ”average” plot is selected based on the top left image in Figure D.1. L_{plot} and W_{plot} are measured using the ”Measure distance” tool, which is illustrated by the images on the right. L_{plot} and W_{plot} are rounded off to 296 m and 152 m respectively.

D.2. Surface level (h_{SL})

h_{SL} is determined based on Figure 4.9 and Figure D.2. Figure 4.9 shows that there are significant elevation differences within Polder Het Langeveld. h_{SL} is therefore equated to the surface level at the representative plot, which is approximately 1 m NAP. Figure D.2 depicts the elevation profile in the area. The profile is retrieved from ”Actueel Hoogtebestand Nederland” 3 (AHN3), a file with detailed and precise altitude data of the Netherlands (Actueel Hoogtebestand Nederland s.d.).

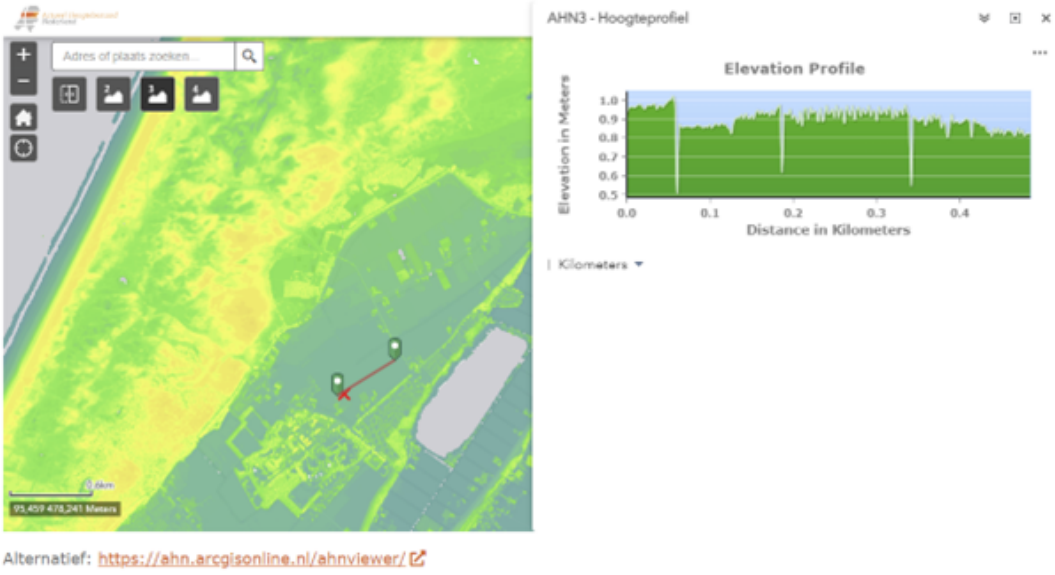

Figure D.2: Elevation profile at representative plot Polder Het Langeveld (Actueel Hoogtebestand Nederland s.d.).

D.3. Soil profile and soil-related properties: top layer thickness (d), horizontal and vertical hydraulic conductivity (k and k_{33}), specific yield (S_y), specific storage (S_s) and resistance confining layer (c)

Figures D.3 to D.8 contain subsurface cross-sections. The figures are retrieved from DINOloket, which is the provider of data and information on the Dutch subsurface (TNO s.d.[a]).

Figure D.3: Most probable lithological class cross-section 1 Polder Het Langeveld (GeoTOP) (TNO s.d.[a]).

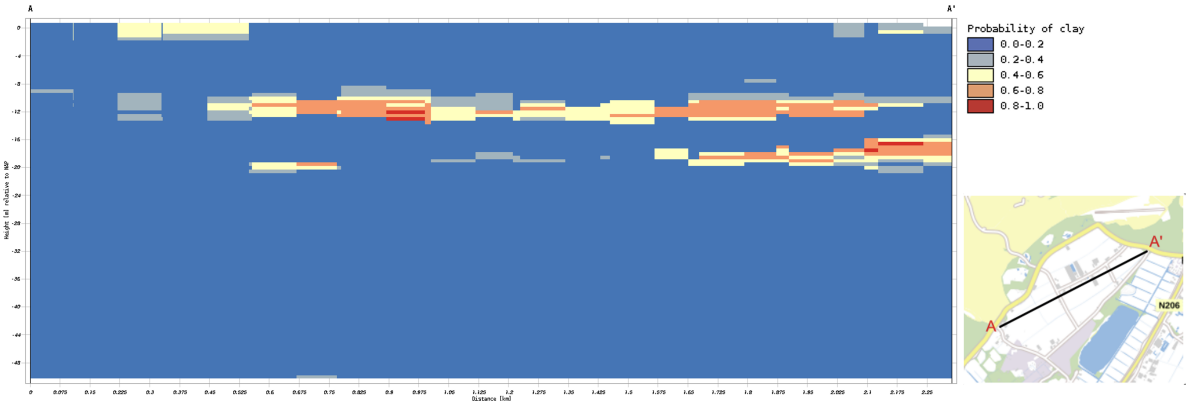

Figure D.4: Chance of clay cross-section 1 Polder Het Langeveld (GeoTOP) (TNO s.d.[a]).

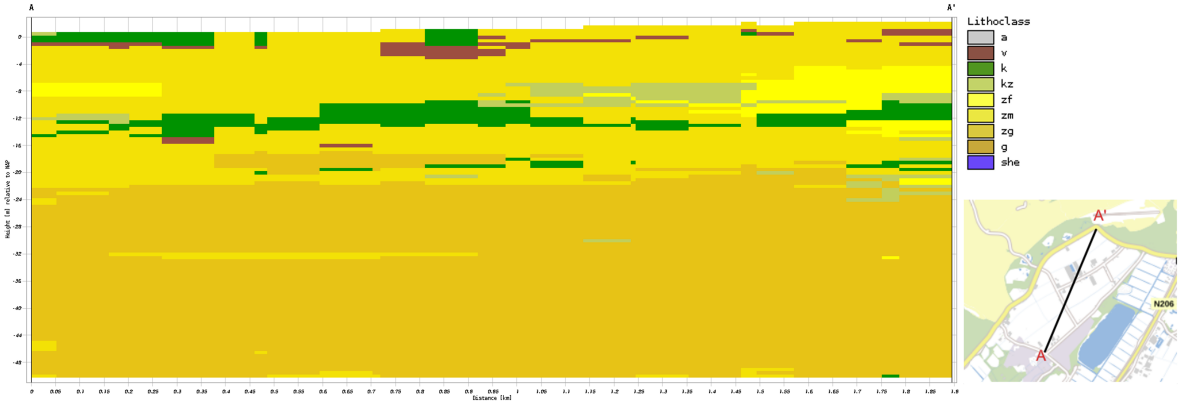

Figure D.5: Most probable lithological class cross-section 2 Polder Het Langeveld (GeoTOP) (TNO s.d.[a]).

Table D.1: Explanation of abbreviations lithological classes DINOloket (Stafleu et al. 2019).

Abbreviation	Corresponding lithological class
a	Anthropogenic
v	peat
k	clay
kz	clayey sand, sandy clay and loam
zf	fine sand
zm	medium sand
zg	coarse sand
g	gravel
she	shells

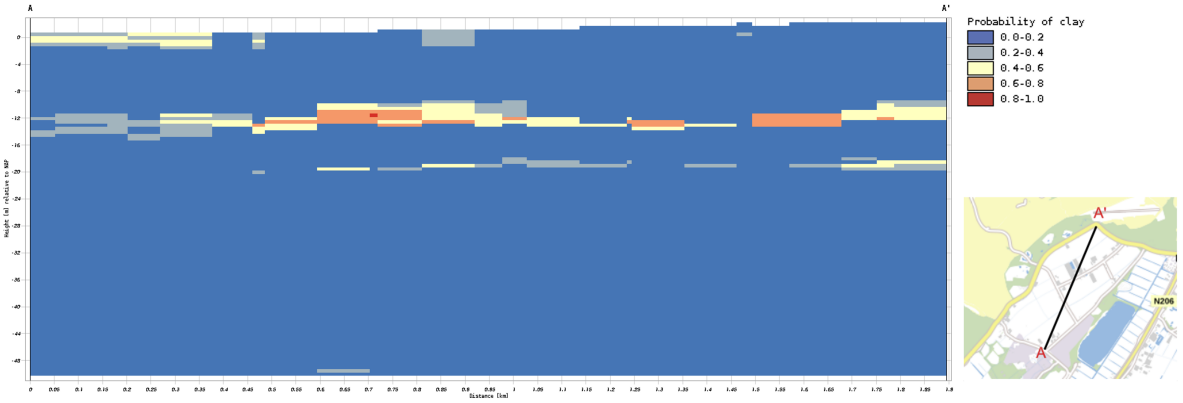

Figure D.6: Chance of clay cross-section 2 Polder Het Langeveld (GeoTOP) (TNO s.d.[a]).

Figures D.3 to D.6 are based on the subsurface model GeoTOP, which is a three dimensional geological model of soil profile and soil type for the Netherlands. The maximum model depth is 50 m below NAP. The subsurface is divided into a regular three dimensional grid of volume cells. Subsurface data from borehole logs are interpolated to create region-wide subsurface maps. A stochastic interpolation technique is applied, which means that the model is run multiple times and multiple different, but statistically equally likely, outcomes are obtained. Subsequently, the probability of occurrence is calculated for each soil type (lithoclass) (Stafleu et al. 2019). The figures consider two different cross-sections, like indicated. Table D.1 contains an explanation of the abbreviations in the legends.

It can be observed that medium sand dominates the soil profile until a depth of approximately -8 to -10 m NAP. Thin layers of clay and peat are also present. Below the sand layer, a clay layer of variable thickness is found. On average, the clay layer is 2 m thick and it is located between -8 and -13 m NAP. The presence of an impermeable layer is crucial for the performance of a water table control system, as it prevents excessive vertical seepage. Therefore, the probability of clay is visualized in Figure D.4 and D.6. The clay layer exists with a certainty of at least 50% in most locations along the cross-sections, which is reasonable. A sandy aquifer that extends to a depth of at least 50 m is found below the clay layer.

Since the above figures are based on a model rather than on direct observations, two borehole logs are depicted in Figure D.7 and Figure D.8 to double-check the soil profile. The borehole logs indicate a similar soil profile as the GeoTOP cross-sections.

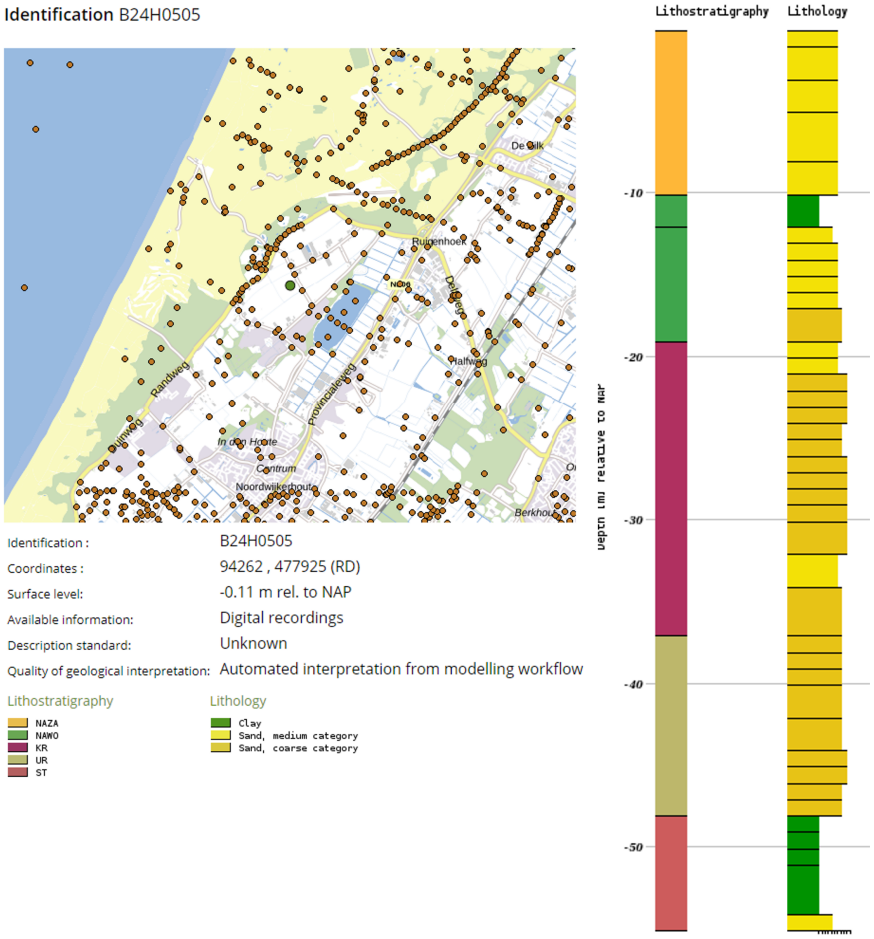

Figure D.7: Borehole log 1 Polder Het Langeveld (TNO s.d.[a]).

The following properties are assigned to the sandy top layer:

- k = 7 m/d, which corresponds to dune sand according to Bot (2016). Since Polder Het Langeveld is located next to a dune area, this is assumed to be a reasonable estimate.
- k_{33} = 1.4 m/d, which is derived from k by considering an anisotropy factor of 0.2. 0.2 is a common anisotropy factor for sand (Bot 2016).
- S_y = 0.2, which is a typical value for sand according to (Grondwaterformules.nl s.d.[a]).
- S_s = 4*10^{-5} m^{-1} (Bot 2016).

The resistance of the clay layer (c) is set equal to 1000 d, which corresponds to a hydraulic conductivity of 0.002 m/d. This is a reasonable hydraulic conductivity for clay (Bot 2016).

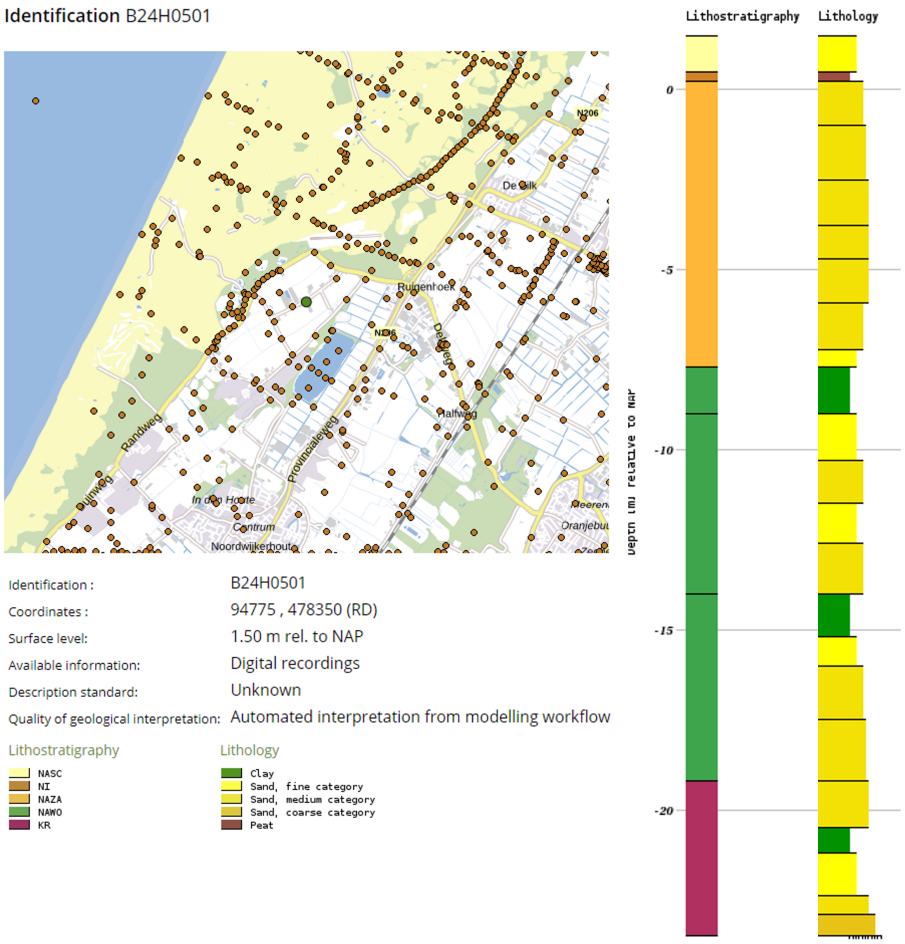

Figure D.8: Borehole log 2 Polder Het Langeveld (TNO s.d.[a]).

D.4. Piezometric heads: initial groundwater head ($h_{GW,initial}$) and head in lower aquifer (h_{aq})

The initial groundwater head is equated to the summer target level. Figure 4.10 illustrates that there are large differences in summer target level throughout the polder, which is caused by surface level elevation differences. To ensure that the summer target level corresponds to h_{SL}, the prevailing summer target level at the representative plot is selected for $h_{GW,initial}$, which is 0.40 m NAP.

h_{aq} is determined based on Figure D.9, which contains an isohypses map of the bottom aquifer. In Polder Het Langeveld, h_{aq} varies between -0.2 and 0.5 m NAP. This is also confirmed by Figure D.10 and D.11, which contain time series of groundwater head in the bottom aquifer measured at two locations. Figure D.10 shows that 0.60 m NAP is the average piezometric head at a location near the dunes. The piezometric head equals -0.10 m NAP at the other side of the polder, which is illustrated by Figure D.11. This gradual decrease in eastward direction is caused by water infiltration in the dune area. The variation in time is limited at both locations, meaning that the assumption of constant h_{aq} is legitimate. Based on the figures, 0.10 m NAP seems a reasonable value for h_{aq}. Figure D.9 illustrates that this corresponds to the head at the location of the representative plot.

Since the target water level is greater than h_{aq}, Polder Het Langeveld is characterized by downward seepage.

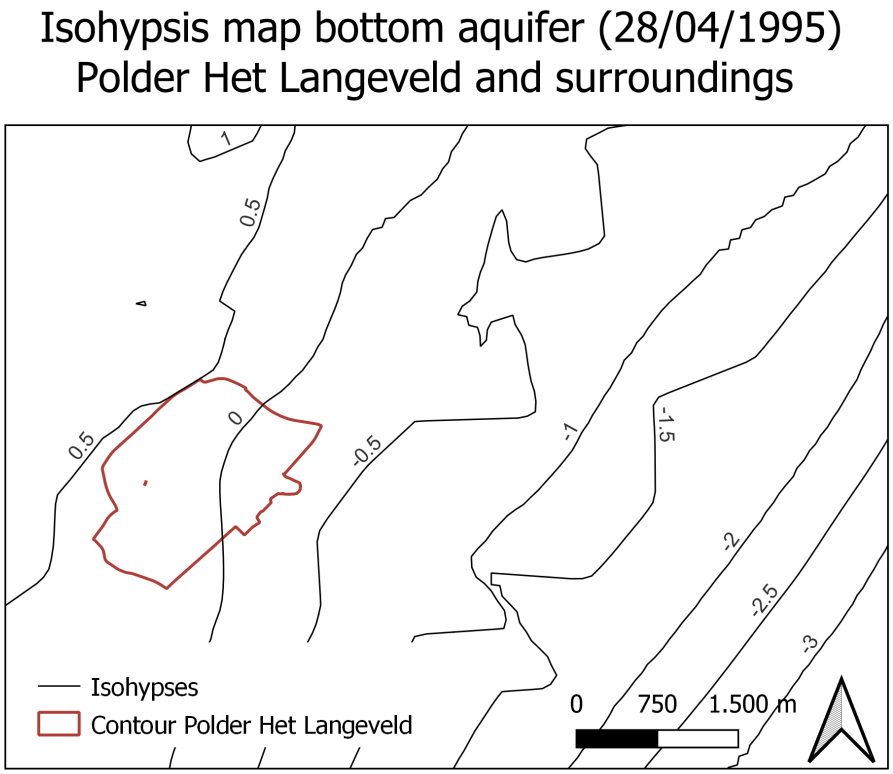

Credits: Noortje Romeijn (21/10/2022)
Projection: Amersfoort / RD New (EPSG:28992)
Data: isohypses aquifer 1, 28/04/1995, retrieved from https://www.grondwatertools.nl/gwsinbeeld/
Unit: m rel. NAP

Figure D.9: Isohypses map bottom aquifer Polder Het Langeveld and surroundings (TNO s.d.[b]).

Identification B24H0100

Monitoring pipe identification:	B24H0100-002
Coordinates:	93954, 478752 (RD)
Surface level:	6.7 m rel. to NAP
Top of filter relative to NAP:	-39.8 m
Filter base relative to NAP:	-40.8 m
Filter top relative to surface level:	46.5 m
Base of filter relative to surface level:	47.5 m
Diver present:	no
Startdate:	06-03-1974
Enddate:	05-01-2011
Number of measurements:	173

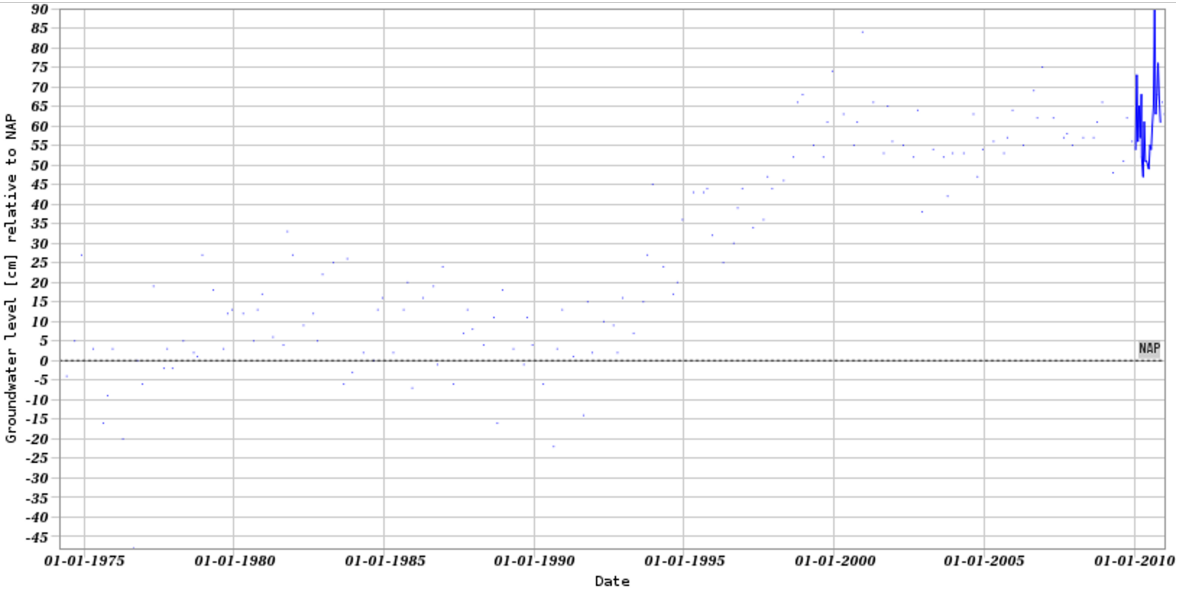

Figure D.10: Time series of groundwater head in bottom aquifer Polder Het Langeveld (B24H0100) (TNO s.d.[a]).

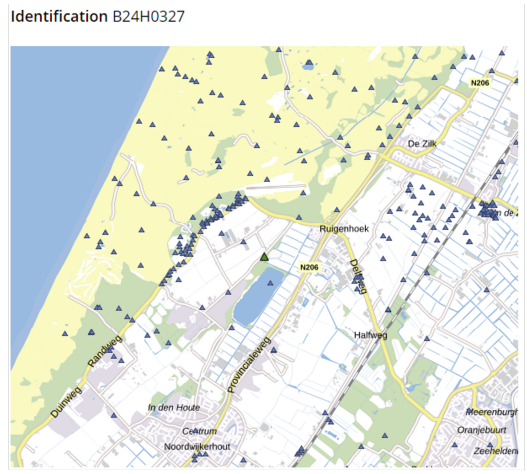

Monitoring pipe identification:	B24H0327-002
Coordinates:	95107, 478109 (RD)
Surface level:	0.8 m rel. to NAP
Top of filter relative to NAP:	-26.7 m
Filter base relative to NAP:	-27.7 m
Filter top relative to surface level:	27.5 m
Base of filter relative to surface level:	28.5 m
Diver present:	no
Startdate:	06-03-1974
Enddate:	31-12-2018
Number of measurements:	92356

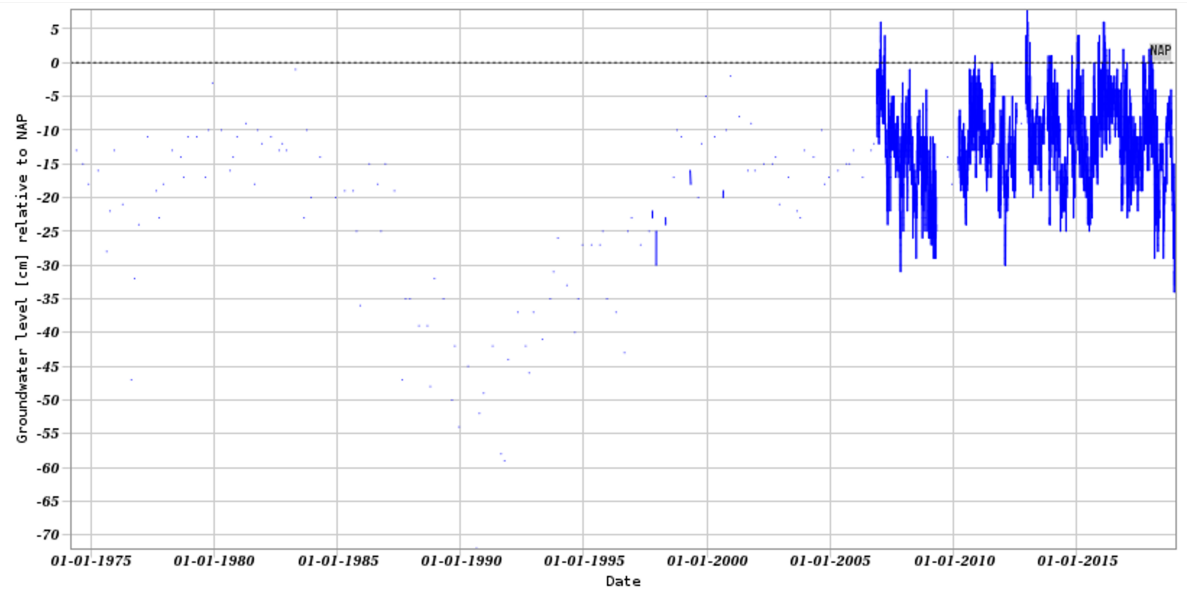

Figure D.11: Time series of groundwater head in bottom aquifer (B24H0327) (TNO s.d.[a]).

D.5. Characteristics ditch: width (W_{ditch}), bottom elevation ($h_{bot,ditch}$) and bed hydraulic resistance (c_{ditch})

W_{ditch} is determined by applying the ”Statistical Summary” tool of QGIS to ”legger” data. Table D.2 summarizes the results of the statistical analysis for Polder Het Langeveld. The median value, which is less affected by outliers than the mean value, is approximately 2 m. Since only half of the ditch is modelled, W_{ditch} is set equal to 1 m.

Table D.2: Statistical summary of ditch widths Polder Het Langeveld (derived from ”legger” data (valid on 25/07/2022)).

Statistical parameter	Value [m]
Minimum	0.00
Maximum	28.30
Mean	2.66
Median	2.04
Q1	1.45
Q3	2.95

$h_{bot,ditch}$ is obtained by subtracting the average ditch water depth from the summer target water level (0.40 m NAP). The ”Statistical Summary” tool of QGIS is again applied to ”legger” data to calculate the representative ditch water depth. Table D.3 summarizes the results of the statistical analysis. $h_{bot,ditch}$ is equated to 0.05 m NAP, which relies on the median value of the water depths.

Table D.3: Statistical summary of water depths Polder Het Langeveld (derived from ”legger” data (valid on 25/07/2022)).

Statistical parameter	Value [m]
Minimum	0.00
Maximum	1.00
Mean	0.33
Median	0.35
First quartile	0.25
Third quartile	0.40
Majority (most frequently occurring value)	0.25

c_{ditch} is equal to 2 d, which corresponds to the value provided by Bot (2016) for a ditch with regular current in sand. A significant current was observed during the field visit.

D.6. Characteristics drains: diameter (D_{drain}), drain resistance (c_{drain}) and bottom elevation ($h_{bot,drain}$)

According to Bot (2016), typical values for drain diameter (D_{drain}) are 50 mm to 100 mm, depending on the surface area to be drained and design discharge. D_{drain} is therefore equated to 0.10 m.

Modelling of individual drains is rather uncommon, meaning that the values for drain resistance found in literature are not suitable for defining the drain resistance of individual drains. Namely, these specify the resistance of a larger area under the influence of multiple drains. In this study, c_{drain} is required to capture two-dimensional effects in a one-dimensional model. In reality, streamlines are curved due to the presence of drains, while flow between cells is horizontal in a 1D-model.

Two simple MODFLOW models are constructed to determine c_{drain}. The model area is restricted to the area between two drains. Figure D.12 depicts the 2D-model. Its cells are 0.10 m by 0.10 m, which corresponds to the size of an individual drain (D_{drain} = 0.10 m). All boundary cells are impermeable, except for the blue coloured cells. These are constant head cells to which a constant head of 0 m is assigned. The soil properties (k, k_{33}, S_y and S_s) are similar to those of Polder Het Langeveld. Figure

D.13 depicts the 1D-model, whose cells are 2 m by 2 m. The z-direction is not spatially discretized. In this case, the RIV package is assigned to the blue coloured cells. A constant head of 0 m is assigned.

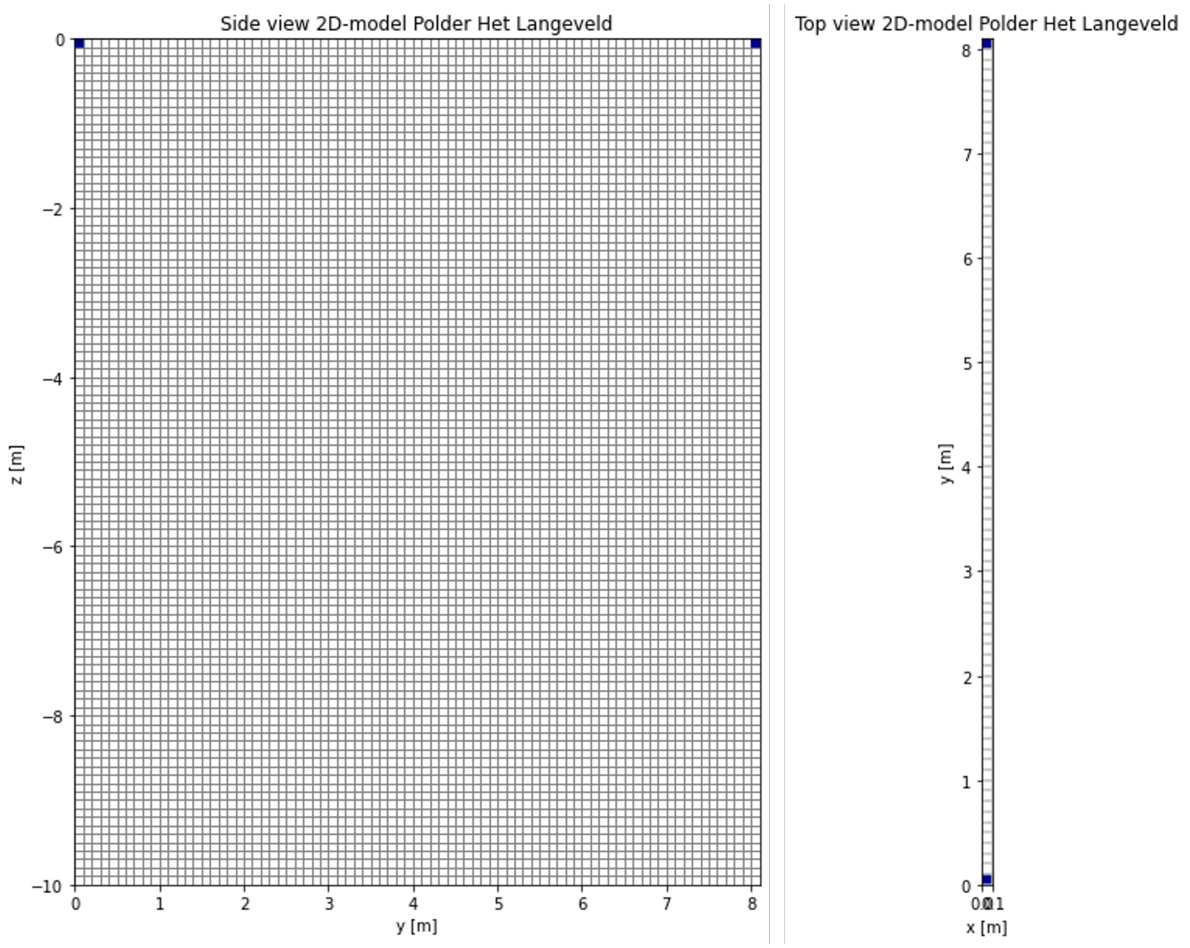

Figure D.12: 2D-model for determination of c_{drain}. The model area is restricted to the area between two drains. The blue coloured cells are constant head cells.

A steady-state simulation is performed with both models. The recharge flux equals 1 mm/d. c_{drain}, which is part of the RIV package (1D-model), is adjusted such that the same piezometric head is obtained exactly in-between two drains. This is illustrated by Figure D.14 and D.15. Figure D.15 shows that c_{drain} = 0.14 d is obtained.

Like explained in Section 5.1.1, $h_{bot,drain}$ is equal to $h_{bot,ditch}$, such that the drains are always submerged.

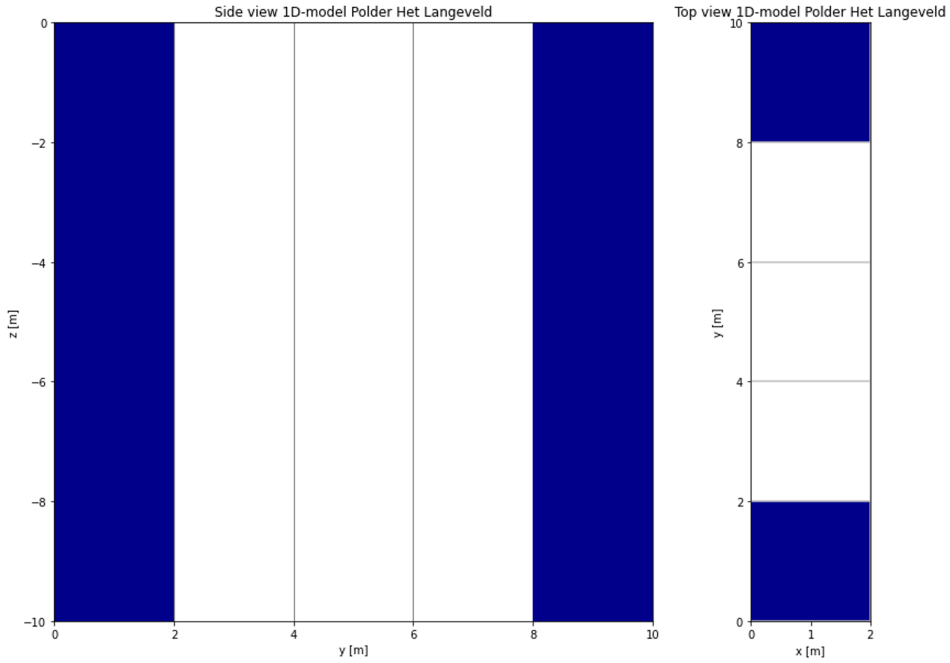

Figure D.13: 1D-model for determination of c_{drain}. The model area is restricted to the area between two drains. The RIV package is assigned to the blue coloured cells.

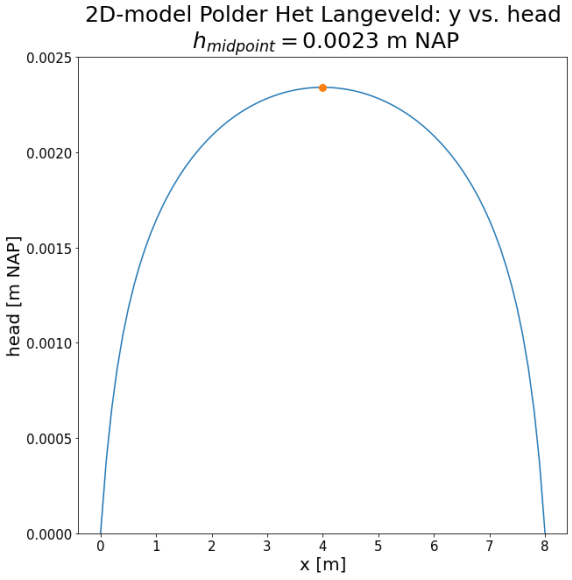

Figure D.14: Result of a steady-state simulation with the 2D-model. The groundwater head is plotted against y.

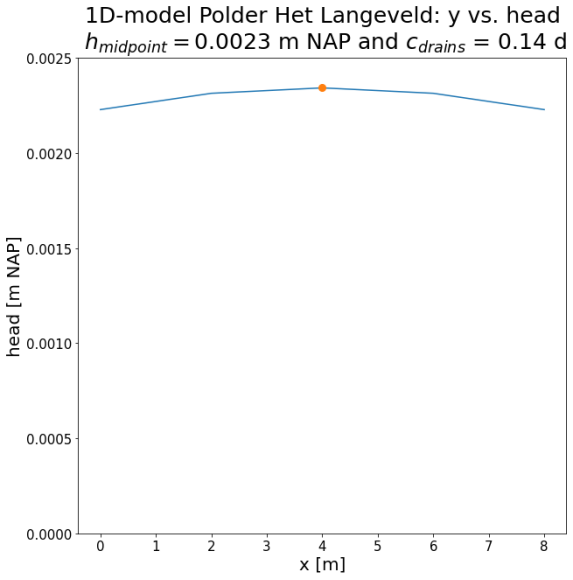

Figure D.15: Result of a steady-state simulation with the 1D-model. The groundwater head is plotted against y.

E

Explanation case study area-specific parameters | Polder Vierambacht

E.1. Plot size: plot length (L_{plot}) and plot width (W_{plot})

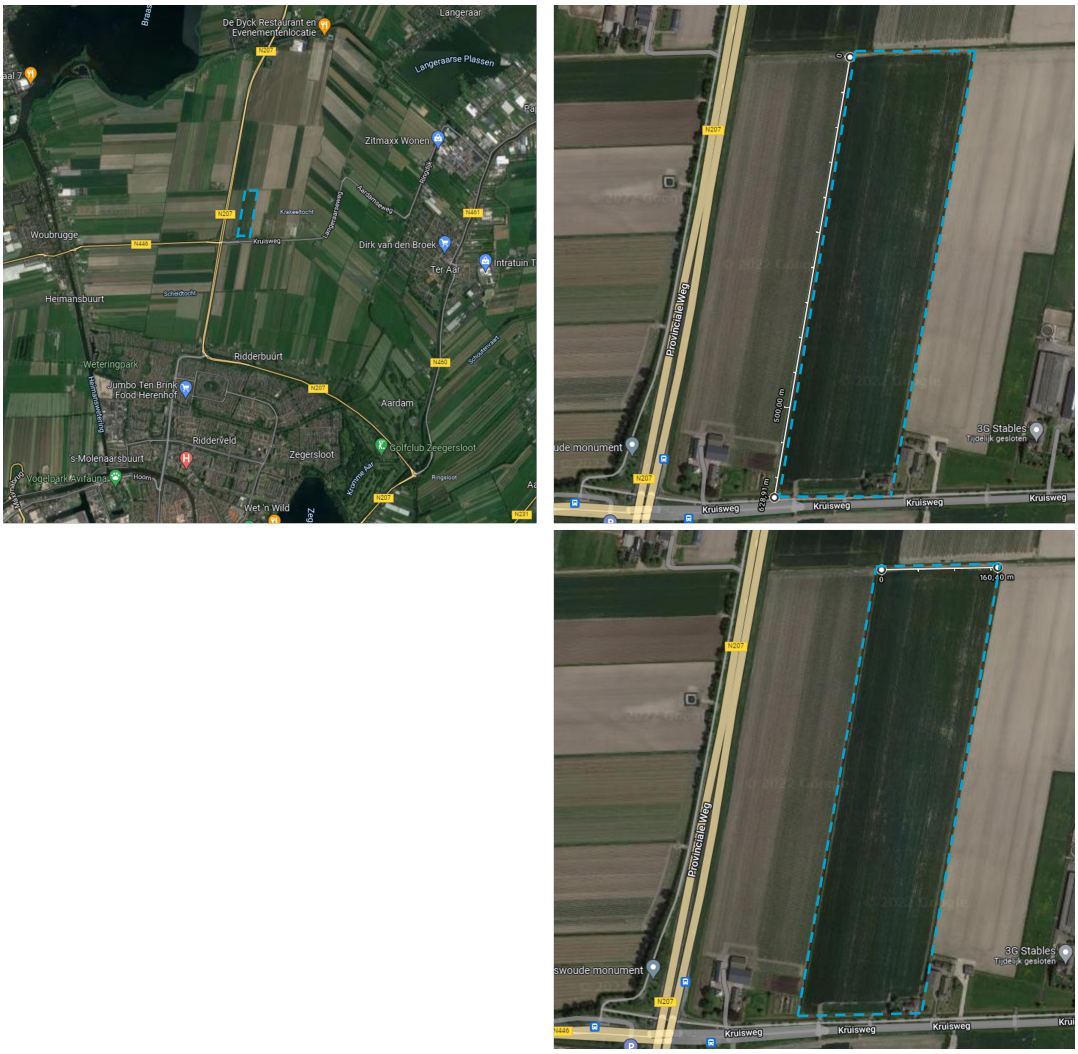

Figure E.1: Location and plot size of representative agricultural plot Polder Vierambacht.

The average plot size in Polder Vierambacht is also determined based on satellite images. The location of the ”average” plot is illustrated by the top left image in Figure E.1. L_{plot} and W_{plot} are measured using the ”Measure distance” tool and rounded off to 628 m and 160 m respectively.

E.2. Surface level (h_{SL})

h_{SL} is determined based on Figure 4.13. The variation in surface level throughout Polder Vierambacht is limited. A surface level of -5 m NAP is assumed to be representative.

E.3. Soil profile and soil-related properties: top layer thickness (d), horizontal and vertical hydraulic conductivity (k and k_{33}), specific yield (S_y), specific storage (S_s) and resistance confining layer (c)

Figures E.2 to E.8 contain subsurface cross-sections. Again, these figures are retrieved from DINOloket.

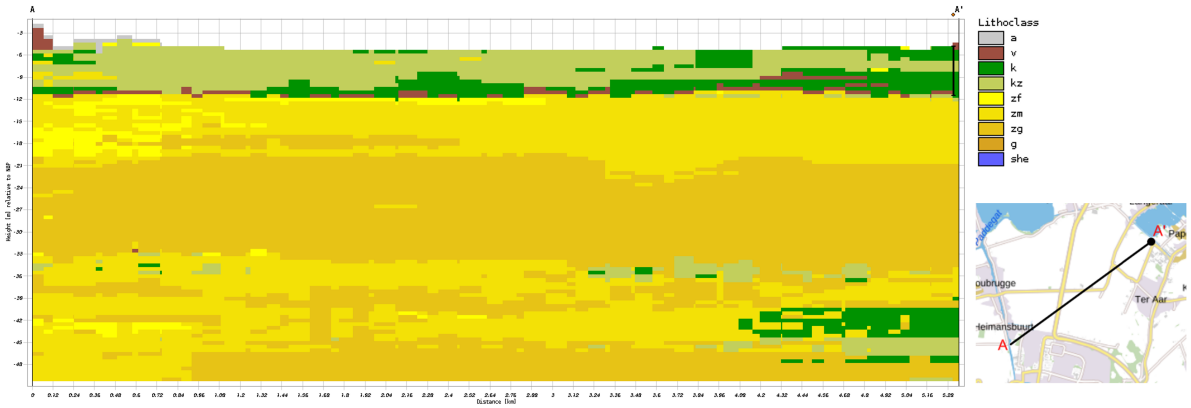

Figure E.2: Most probable lithological class cross-section 1 Polder Vierambacht (GeoTOP) (TNO s.d.[a]).

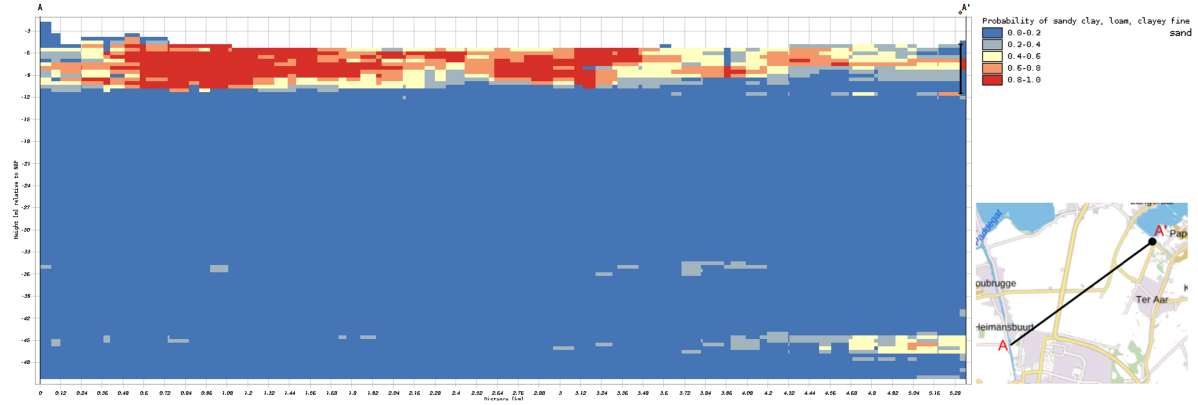

Figure E.3: Chance of sandy clay, loam, clayey fine sand cross-section 1 Polder Vierambacht (GeoTOP) (TNO s.d.[a]).

Figures E.2 to E.5 are based on the subsurface model GeoTOP. Like in Appendix D, two different cross-sections are considered. A 6 m thick top layer can be distinguished. It consists of clayey sand, sandy clay and loam. Figure E.4 shows that the top layer consists of a considerable amount of sand in some areas. The probability of sandy clay, loam and clayey fine sand is therefore examined too. Below the clayey top layer, a thin peat layer is found. The peat layer has an average thickness of 0.5 m. The

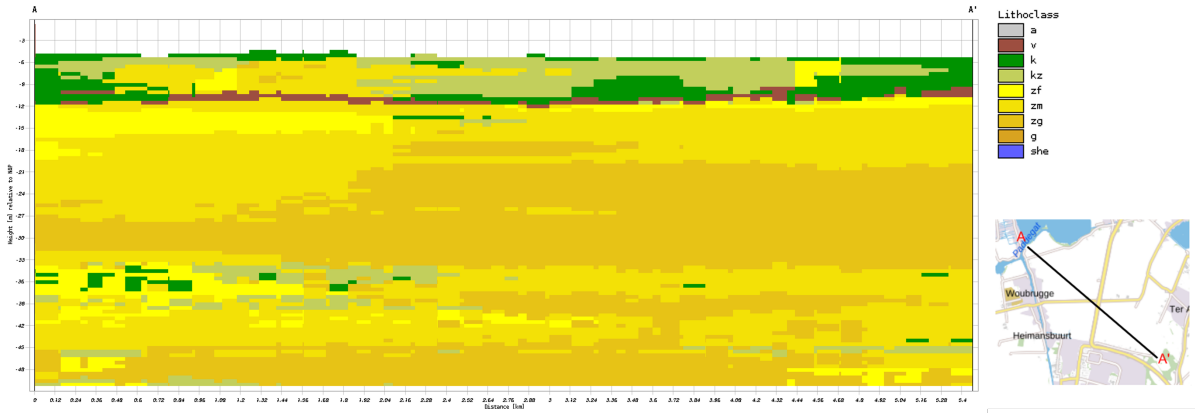

Figure E.4: Most probable lithological class cross-section 2 Polder Vierambacht (GeoTOP) (TNO s.d.[a]).

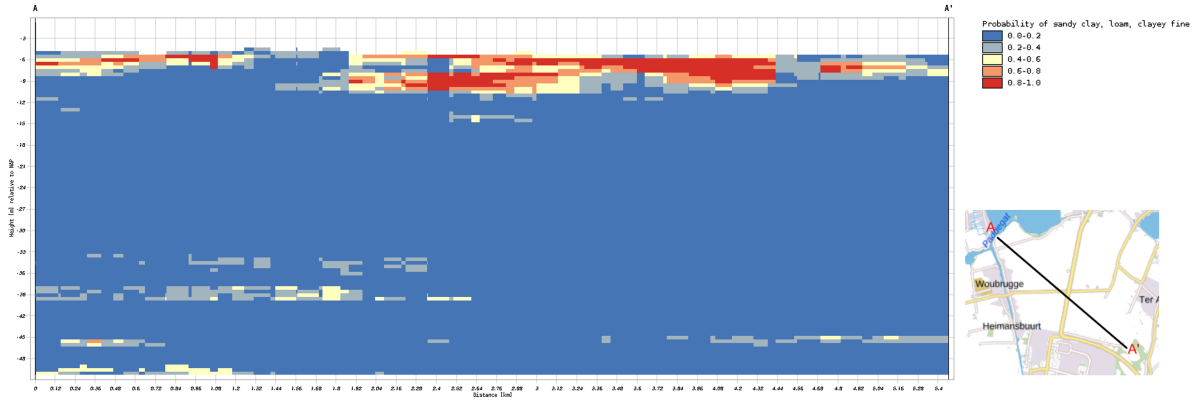

Figure E.5: Chance of sandy clay, loam, clayey fine sand cross-section 2 Polder Vierambacht (GeoTOP) (TNO s.d.[a]).

peat layer separates the top layer from a sandy aquifer that extends to a depth of at least 50 m.

Three borehole logs are consulted to confirm the above observations. They are depicted in Figures E.6, E.7 and E.8. The borehole logs are comparable to the GeoTOP cross-sections.

The thin peat layer is part of the geological unit ”Formatie van Nieuwkoop, Basisveen Laag”, which is a compacted layer that is characterized by a high hydraulic resistance. The hydraulic gradient across this layer is therefore significant (Appendix E.4). The resistance of the peat layer (c) is set equal to 500 d, which corresponds to a hydraulic conductivity of 0.001 m/d. This value is determined by rough calibration to groundwater level measurements (Chapter 7).

The following properties are assigned to the top layer:

- k = 0.1 m/d, which a representative value for sandy clay and loam according to Bot (2016).
- k_{33} = 0.02 m/d, which is derived from k by considering an anisotropy factor of 0.2 (Bot 2016).
- S_y = 0.08 (Bot 2016). Other sources that support this choice are Heath (1983) and Morris et al. (1967).
- S_s = 4*10^{-5} m^{-1} (Bot 2016).

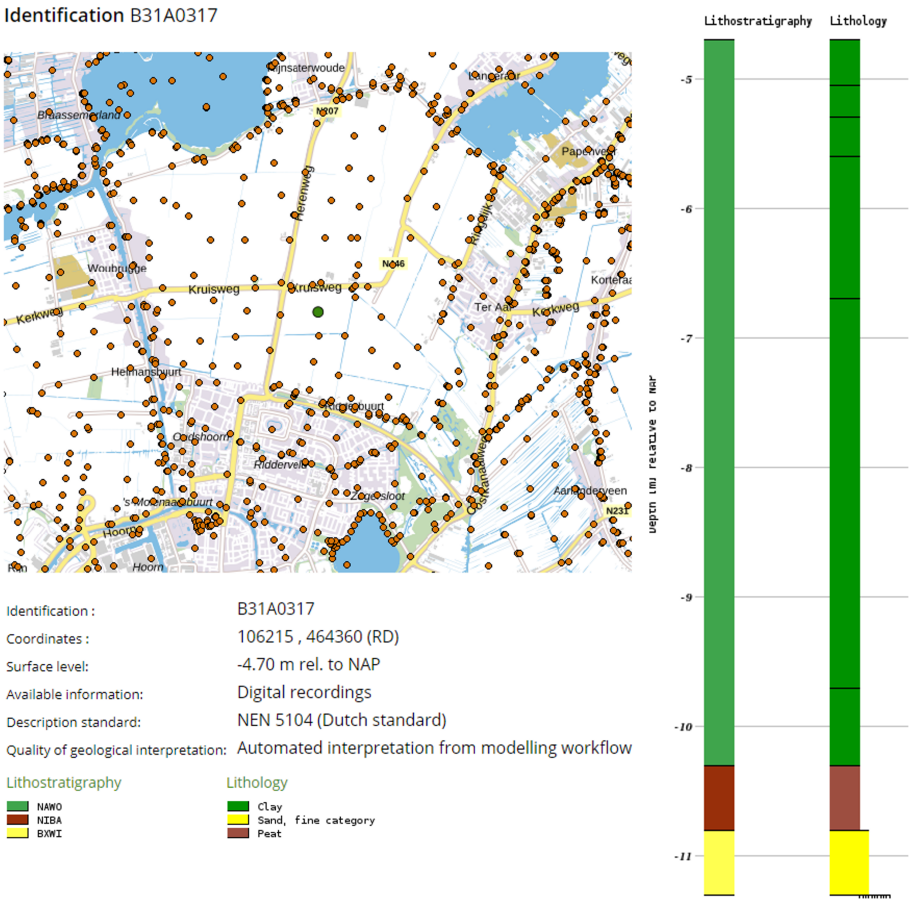

Figure E.6: Borehole log 1 Polder Vierambacht (TNO s.d.[a]).

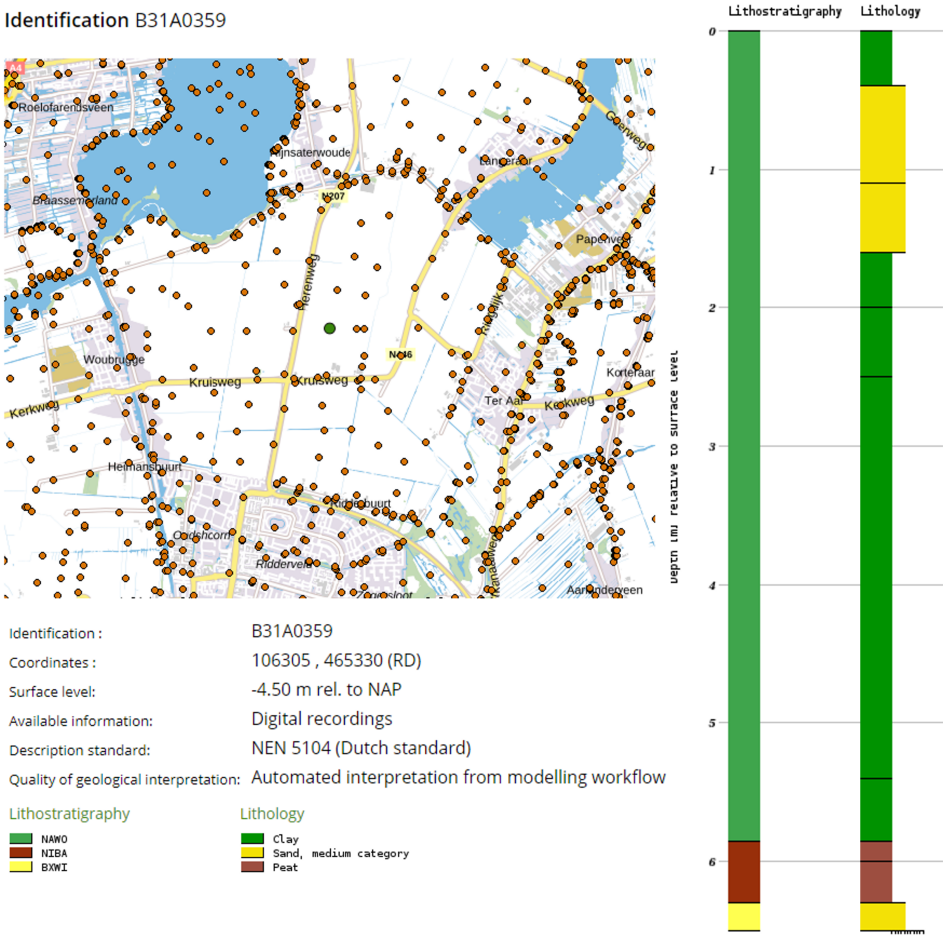

Figure E.7: Borehole log 2 Polder Vierambacht (TNO s.d.[a]).

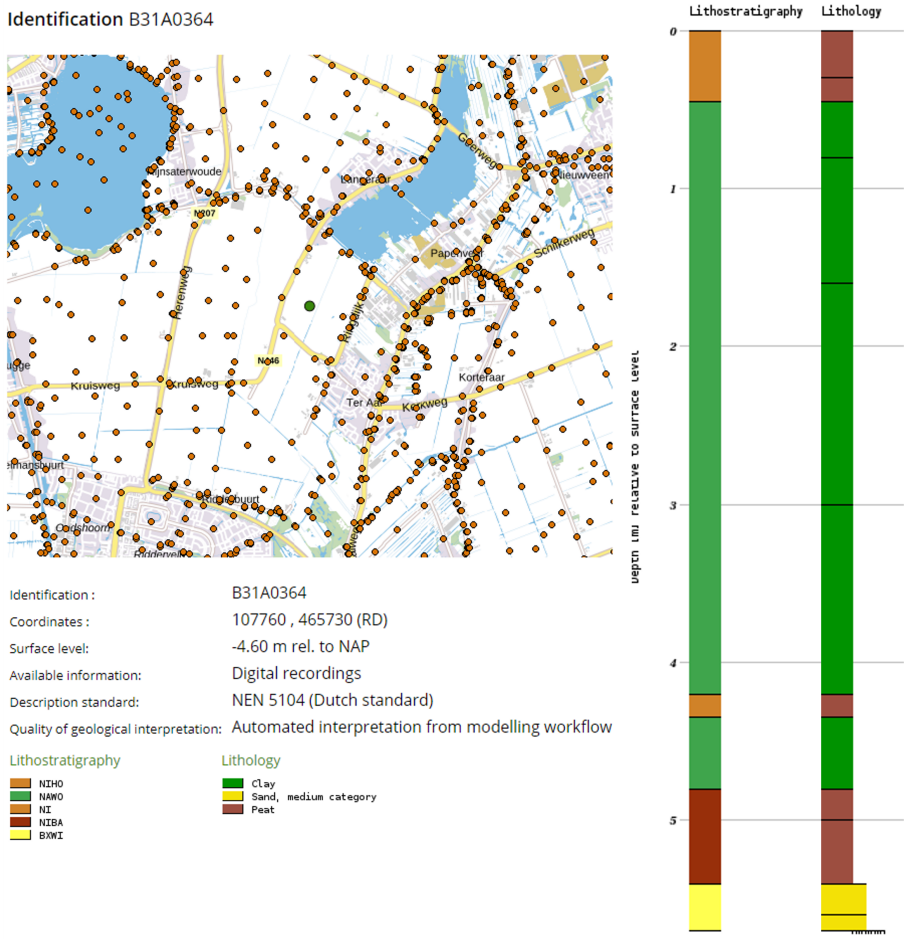

Figure E.8: Borehole log 3 Polder Vierambacht (TNO s.d.[a]).

E.4. Piezometric heads: initial groundwater head ($h_{GW,initial}$) and head in lower aquifer (h_{aq})

$h_{GW,initial}$ is again equated to the summer target level at the representative plot, which is -5.83 m NAP (Figure 4.14).

h_{aq} is determined based on Figure E.9. The contour line of -4.5 m NAP runs straight through the polder, which suggests that -4.5 m NAP is an appropriate estimate for h_{aq}. This is also confirmed by Figure E.10 and E.11, which contain time series of groundwater head in the bottom aquifer measured at two locations. The average piezometric head in the bottom aquifers equals -4.6 m NAP at location 1 (Figure E.10), while the average piezometric head equals -4.2 m NAP at location 2 (Figure E.11). Again, the fluctuations in groundwater head are limited, which justifies the assumption of constant h_{aq}.

Since the target water level is much smaller than h_{aq}, Polder Vierambacht experiences a significant amount of upward seepage.

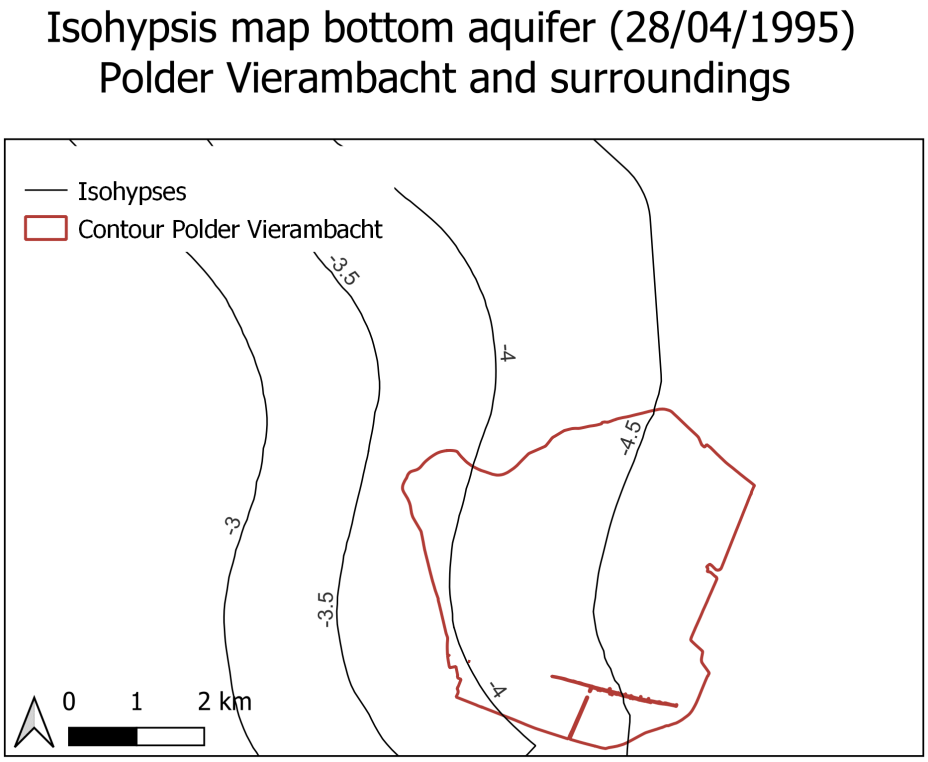

Credits: Noortje Romeijn (22/01/2022)
Projection: Amersfoort / RD New (EPSG:28992)
Data: isohypses aquifer 1, 28/04/1995, retrieved from https://www.grondwatertools.nl/gwsinbeeld/
Unit: m rel. NAP

Figure E.9: Isohypses map bottom aquifer Polder Vierambacht and surroundings (TNO s.d.[b]).

Identification B31A0128

Monitoring pipe identification:	B31A0128-001
Coordinates:	107810, 464140 (RD)
Surface level:	-1.07 m rel. to NAP
Top of filter relative to NAP:	-19.66 m
Filter base relative to NAP:	-20.16 m
Filter top relative to surface level:	18.59 m
Base of filter relative to surface level:	19.09 m
Diver present:	no
Startdate:	15-02-1971
Enddate:	14-12-1995
Number of measurements:	584

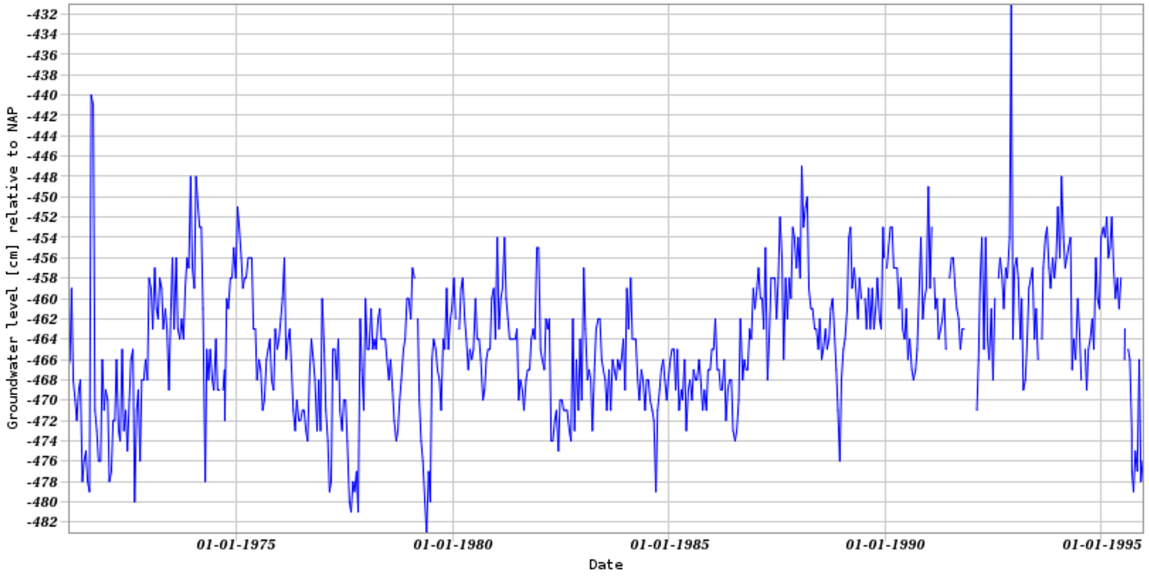

Figure E.10: Time series of groundwater head in bottom aquifer Polder Vierambacht (B31A0128) (TNO s.d.[a]).

Identification B31A0129

Monitoring pipe identification:	B31A0129-001
Coordinates:	105500, 463370 (RD)
Surface level:	-4.03 m rel. to NAP
Top of filter relative to NAP:	-22.73 m
Filter base relative to NAP:	-23.23 m
Filter top relative to surface level:	18.7 m
Base of filter relative to surface level:	19.2 m
Diver present:	no
Startdate:	15-02-1971
Enddate:	14-11-1991
Number of measurements:	498

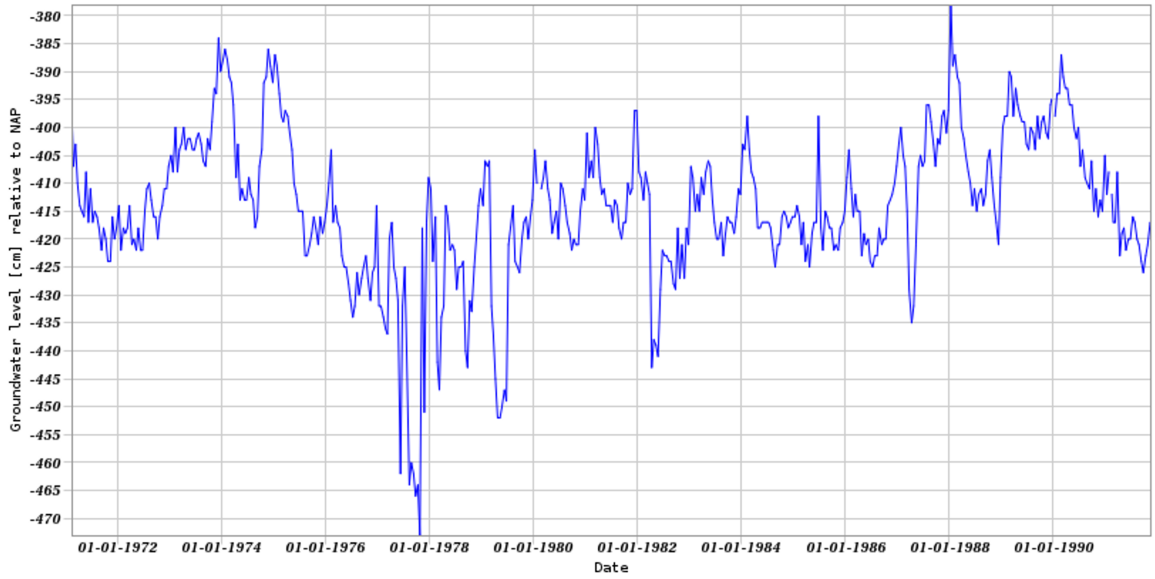

Figure E.11: Time series of groundwater head in bottom aquifer Polder Vierambacht (B31A0129) (TNO s.d.[a]).

E.5. Characteristics ditch: width (W_{ditch}), bottom elevation ($h_{bot,ditch}$) and bed hydraulic resistance (c_{ditch})

W_{ditch} is again determined by applying the ”Statistical Summary” tool of QGIS to ”legger” data. Table E.1 summarizes the results of the statistical analysis for Polder Vierambacht. The median value, which is less affected by outliers than the mean value, is approximately 2 m. Since only half of the ditch is modelled, W_{ditch} is set equal to 1 m.

Table E.1: Statistical summary of ditch widths Polder Vierambacht (derived from ”legger” data (valid on 25/07/2022)).

Statistical parameter	Value [m]
Minimum	0.00
Maximum	44.30
Mean	2.69
Median	2.15
Q1	1.48
Q3	3.04

$h_{bot,ditch}$ is obtained by subtracting the average ditch water depth from the summer target water level (-5.83 m NAP). The ”Statistical Summary” tool of QGIS is applied to ”legger” data to calculate the representative ditch water depth. Table E.2 summarizes the results of the statistical analysis. $h_{bot,ditch}$ is equated to -6.18 m NAP, which relies on the median value of the water depths.

Table E.2: Statistical summary of water depths Polder Vierambacht (derived from ”legger” data (valid on 25/07/2022)).

Statistical parameter	Value [m]
Minimum	0.00
Maximum	1.60
Mean	0.32
Median	0.35
First quartile	0.25
Third quartile	0.35
Majority (most frequently occurring value)	0.35

c_{ditch} equals 5.0 d, which is in correspondence with the value provided by Bot (2016) for a ditch with regular current in clay or loam.

E.6. Characteristics drains: diameter (D_{drain}), drain resistance (c_{drain}) and bottom elevation ($h_{bot,drain}$)

D_{drain} equals 0.10 m, such that the drains in both case study areas have a similar size.

The procedure to determine c_{drain} is already explained in Appendix D.6. Figure E.12 depicts the 2D-model, whereas Figure E.13 depicts the 1D-model. Again, a steady-state simulation is performed with both models. The recharge flux equals 1 mm/d. c_{drain}, which is part of the RIV package (1D-model), is adjusted such that the same piezometric head is obtained exactly in-between two drains. This is illustrated by Figure E.14 and E.15. Figure E.15 shows that c_{drain} = 7.00 d is obtained.

Like explained in Section 5.1.1, $h_{bot,drain}$ is equal to $h_{bot,ditch}$, such that the drains are always submerged.

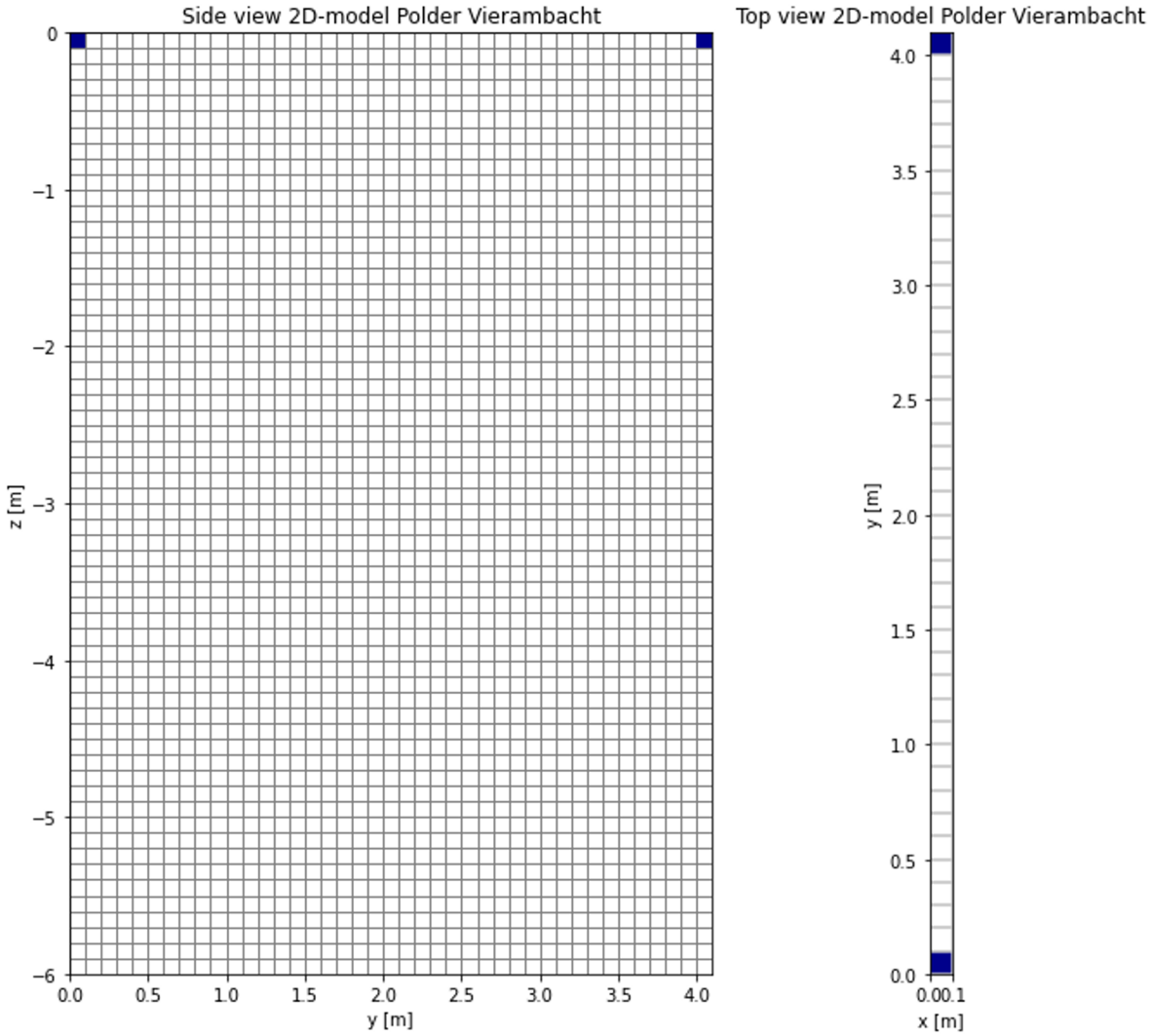

Figure E.12: 2D-model for determination of c_{drain}. The model area is restricted to the area between two drains. The blue coloured cells are constant head cells.

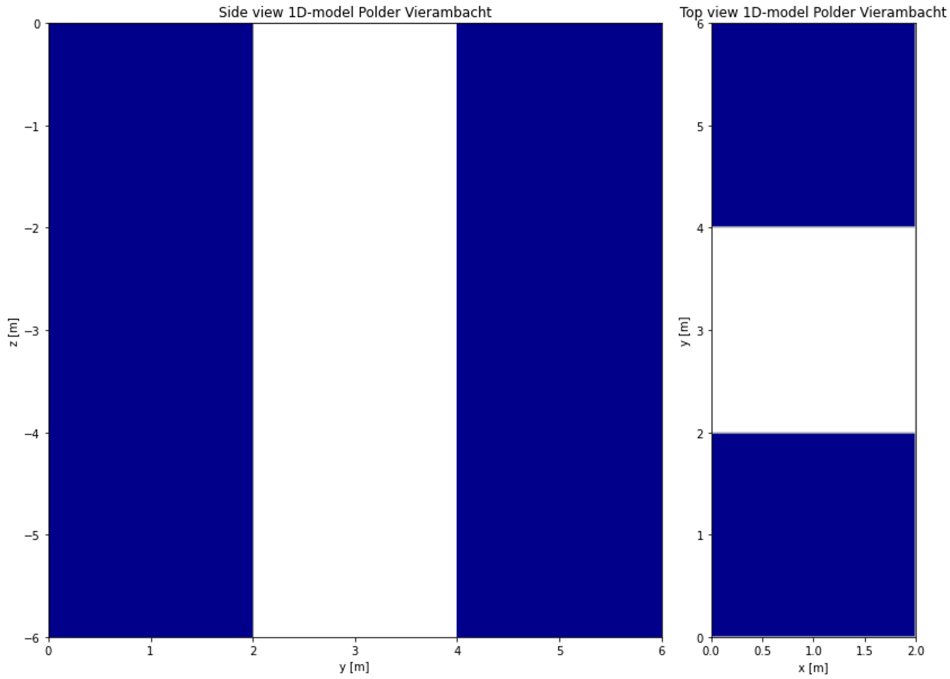

Figure E.13: 1D-model for determination of c_{drain}. The model area is restricted to the area between two drains. The RIV package is assigned to the blue coloured cells.

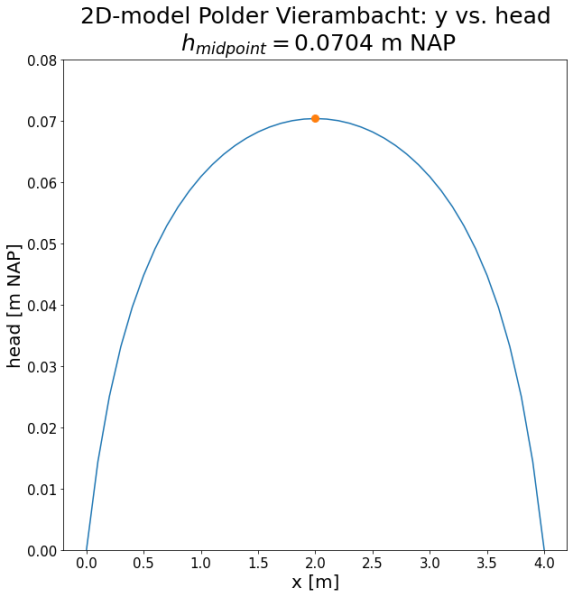

Figure E.14: Result of a steady-state simulation with the 2D-model. The groundwater head is plotted against y.

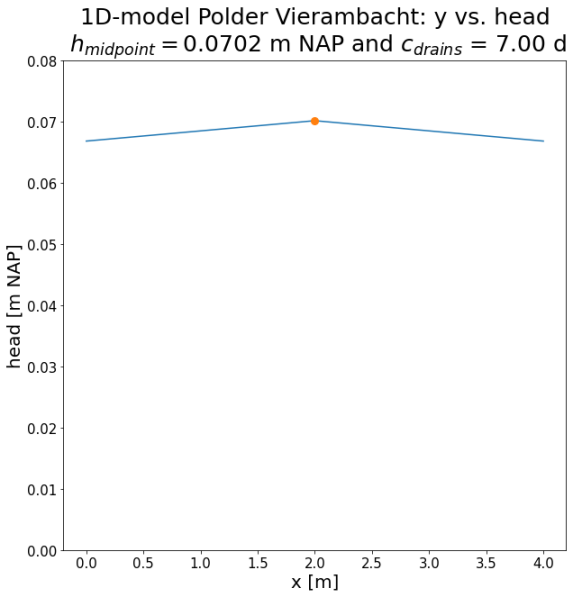

Figure E.15: Result of a steady-state simulation with the 1D-model. The groundwater head is plotted against y.

F

Overview MODFLOW simulations

This appendix contains an overview of the performed MODFLOW simulations with the basic MODFLOW model (excluding feedback) and the extended MODFLOW model (including feedback).

F.1. Excluding feedback

Table F.1: Overview MODFLOW simulations excluding feedback, corresponding to Figure 7.2 and Figure 7.3.

	No.	R [mm/d]	Δh_{SW} [m]	Δh_{drain} [m]	Short-term control action
Polder Het Langeveld, variant 1	1	0.7, 2.5 & 5	-0.10	-	Anticipating water excess
	2	0.7, 2.5 & 5	-0.05	-	Anticipating water excess
	3	0.7, 2.5 & 5	-0.01	-	Anticipating water excess
	4	0.7, 2.5 & 5	0.00	-	-
	5	0.7, 2.5 & 5	0.01	-	Anticipating water shortage
	6	0.7, 2.5 & 5	0.05	-	Anticipating water shortage
	7	0.7, 2.5 & 5	0.10	-	Anticipating water shortage
Polder Het Langeveld, variant 2 & Polder Vierambacht, variant 2	8	0.7, 2.5 & 5	-0.10	-0.10	Anticipating water excess
	9	0.7, 2.5 & 5	-0.05	-0.05	Anticipating water excess
	10	0.7, 2.5 & 5	-0.01	-0.01	Anticipating water excess
	11	0.7, 2.5 & 5	0.00	0.00	-
	12	0.7, 2.5 & 5	0.01	0.01	Anticipating water shortage
	13	0.7, 2.5 & 5	0.05	0.05	Anticipating water shortage
	14	0.7, 2.5 & 5	0.10	0.10	Anticipating water shortage
Polder Het Langeveld, variant 3 & Polder Vierambacht, variant 3	15	0.7, 2.5 & 5	0.00	-0.10	Anticipating water excess
	16	0.7, 2.5 & 5	0.00	-0.05	Anticipating water excess
	17	0.7, 2.5 & 5	0.00	-0.01	Anticipating water excess
	18	0.7, 2.5 & 5	0.00	0.00	-
	19	0.7, 2.5 & 5	0.00	0.01	Anticipating water shortage
	20	0.7, 2.5 & 5	0.00	0.05	Anticipating water shortage
	21	0.7, 2.5 & 5	0.00	0.10	Anticipating water shortage

Table F.2: Temporal discretization simulations excluding feedback.

Polder	Variant	Δt [d]	Simulation length [d]
Polder Het Langeveld	variant 1	1	40
	variant 2	1/3	5
	variant 3	1/3	5
Polder Vierambacht	variant 2	1/2	20
	variant 3	1/2	20

F.2. Including feedback

Table F.3: Overview MODFLOW simulations including feedback, corresponding to Figure 7.4 and 7.5.

	No.	R [mm/d]	Δh_{weir} [m]	Short-term control action
Polder Het Langeveld, variant 1	1	0.7, 2.5 & 5	0.01	Anticipating water shortage
& Polder Het Langeveld, variant 2	2	0.7, 2.5 & 5	0.05	Anticipating water shortage
& Polder Vierambacht, variant 2	3	0.7, 2.5 & 5	0.10	Anticipating water shortage
Polder Het Langeveld, variant 3	4	2.5	0.05	Anticipating water shortage
Polder Vierambacht, variant 3	5	2.5, 3.0*	0.05	Anticipating water shortage

* Note that an alternative steady-state calculation has been run. Initially, R = -5.0 mm/d instead of R = 0.7 mm/d to enforce a low groundwater table (starting position).

Table F.4: Temporal discretization simulations including feedback.

Polder	Variant	Δt [d]	Simulation length [d]
Polder Het Langeveld	variant 1	1/24	15
	variant 2	1/24	15
	variant 3	1/24	5
Polder Vierambacht	variant 2	1/24	15
	variant 3	1/24	5

G

MODFLOW model verification

This appendix contains figures that verify the MODFLOW model setup. Section G.1 and G.2 cover the results of convergence analyses that were performed to determine the required spatial and temporal discretization. The model schematization is verified in Section G.3. MODFLOW model results are compared to actual groundwater level measurements in Section G.4.

G.1. Spatial discretization

The required spatial discretization is determined by means of a convergence analysis. A steady-state calculation is performed. R equals 2.5 mm/d. h_{SW} and/or h_{drain} equal(s) $h_{SW,target}$. The calculation is repeated for multiple spatial discretizations:

Polder Het Langeveld: Δx = 0.25 m, 0.5 m, 1 m, 2 m and 4 m.
Polder Vierambacht: Δx = 0.25 m, 0.5 m, 1 m and 2 m.

The results are depicted in Figure G.1, G.2 and G.3. Variant 1 is not considered for Polder Vierambacht, since it is not feasible (Figure 7.6). The piezometric heads along a cross-section through the plot's centre point are plotted for various Δx. It can be observed that the lines converge as Δx decreases.

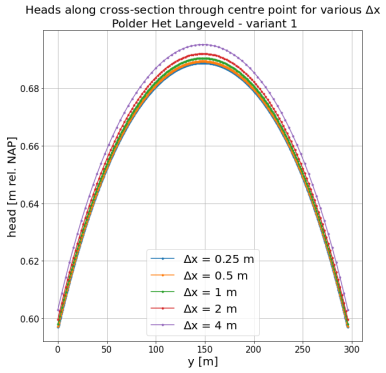

Figure G.1: Spatial discretization - variant 1, Polder Het Langeveld

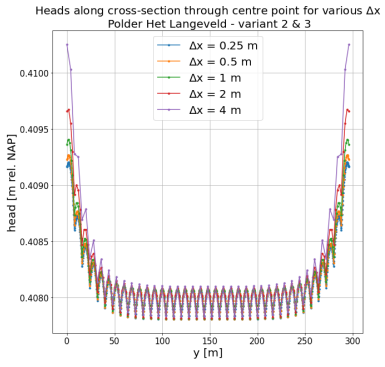

Figure G.2: Spatial discretization - variant 2 & 3, Polder Het Langeveld

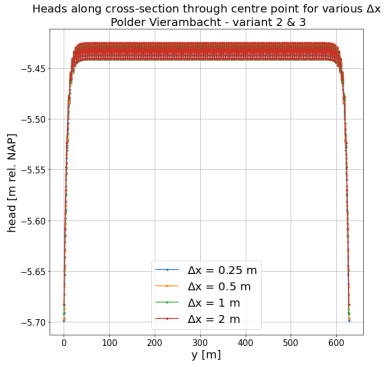

Figure G.3: Spatial discretization - variant 2 & 3, Polder Vierambacht

The accuracy of the simulation results is determined relative to the simulation results corresponding to Δx = 0.25 m, which is assumed to represent the actual solution. The Root Mean Square Error (RMSE) is used as accuracy measure. The results are depicted in Figure G.4, G.5 and G.6. RMSE is plotted against Δx. The required spatial discretization is selected based on the criterion RMSE < 5 mm. This criterion is fulfilled by $\Delta x \leq$ 2 m in case of variant 1, Polder Het Langeveld. Δx = 2 m also leads to

a sufficiently accurate solution in case of variant 2 and 3, Polder Het Langeveld and Polder Vierambacht.

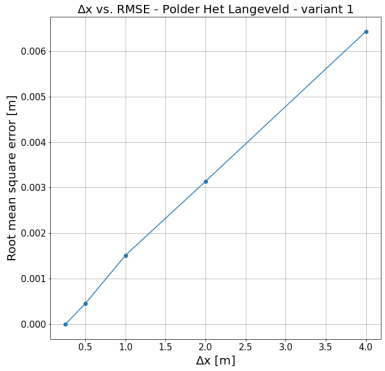

Figure G.4: Spatial discretization - variant 1, Polder Het Langeveld

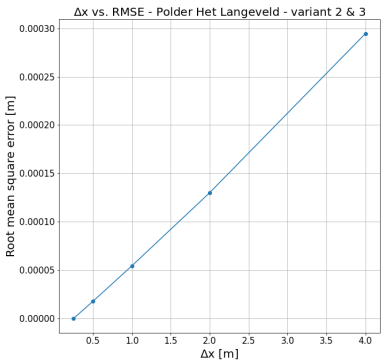

Figure G.5: Spatial discretization - variant 2 & 3, Polder Het Langeveld

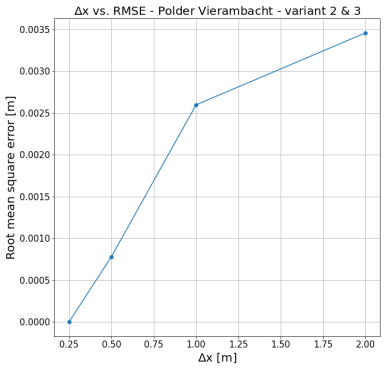

Figure G.6: Spatial discretization - variant 2 & 3, Polder Vierambacht

G.2. Temporal discretization

The required temporal discretization is determined for the simulations excluding and including feedback.

Excluding feedback

The required temporal discretization is also determined by means of a convergence analysis. A transient calculation is performed. The initial groundwater situation corresponds to the steady-state solution for R = 0.7 mm/d and h_{SW} and/or h_{drain} = $h_{SW,target}$. At t = 0, the surface water level is instantaneously raised by 10 cm. The simulation is repeated for multiple temporal discretizations:

Polder Het Langeveld: Δt = 1/48 d, Δt = 1/24 d, Δt = 1/12 d, Δt = 1/6 d, Δt = 1/3 d, Δt = 1/2 d and Δt = 1 d.
Polder Vierambacht: Δt = 1/48 d, Δt = 1/24 d, Δt = 1/12 d, Δt = 1/6 d, Δt = 1/3 d, Δt = 1/2 d and Δt = 1 d.

The results are depicted in Figure G.7, G.8 and G.9. The groundwater response at 12 m from the ditch is plotted against time for various Δt in case of Polder Het Langeveld. In case of Polder Vierambacht, the groundwater response at 6 m from the ditch is plotted. It can be observed that the lines converge as Δt decreases.

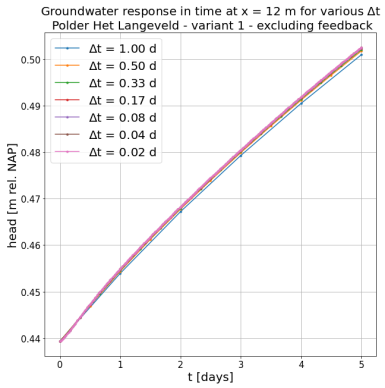

Figure G.7: Temporal discretization (excluding feedback) - variant 1, Polder Het Langeveld

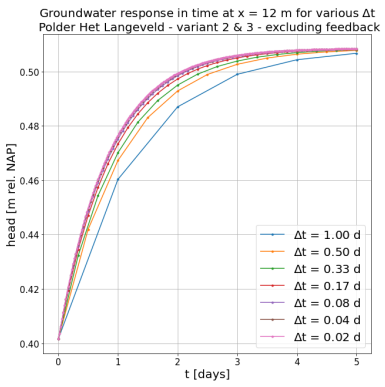

Figure G.8: Temporal discretization (excluding feedback) - variant 2 & 3, Polder Het Langeveld

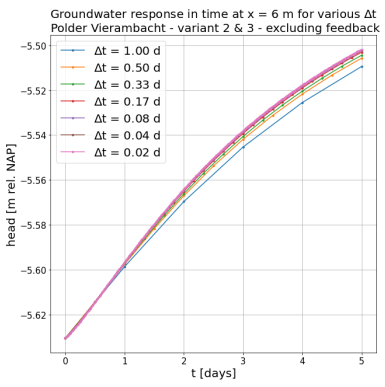

Figure G.9: Temporal discretization (excluding feedback) - variant 2 & 3, Polder Vierambacht

The accuracy of the simulation results is determined relative to the simulation results corresponding

to Δt = 1/48 d, which is assumed to represent the actual solution. Again, RMSE is used as accuracy measure. The results are depicted in Figure G.10, G.11 and G.12. RMSE is plotted against Δt. The required temporal discretization is selected based on the criterion RMSE < 5 mm. This criterion is already fulfilled by Δt = 1 d in case of variant 1, Polder Het Langeveld. The required temporal discretization is Δt = 1/3 d in case of variant 2 and 3, Polder Het Langeveld. Δt = 1/2 d is sufficient in case of variant 2 and 3, Polder Vierambacht.

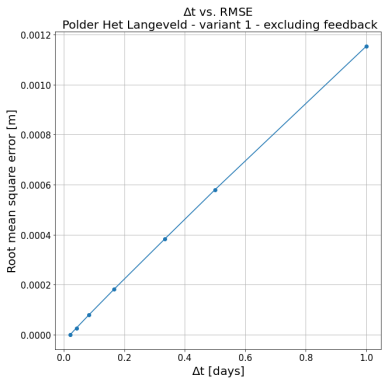

Figure G.10: Temporal discretization (excluding feedback) - variant 1, Polder Het Langeveld

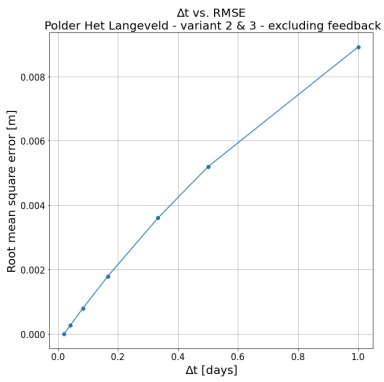

Figure G.11: Temporal discretization (excluding feedback) - variant 2 & 3, Polder Het Langeveld

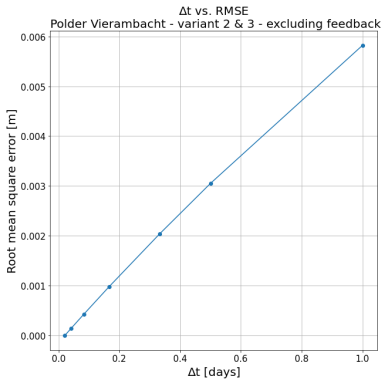

Figure G.12: Temporal discretization (excluding feedback) - variant 2 & 3, Polder Vierambacht

Including feedback

The required temporal discretization is also determined for the simulations including groundwater-surface water feedback. These results are depicted below. The initial groundwater situation corresponds to the steady-state solution for R = 0.7 mm/d and h_{SW} and/or h_{drain} = $h_{SW,target}$. At t = 0, the weir crest is instantaneously by 10 cm. The calculation is repeated for multiple temporal discretizations:

Polder Het Langeveld: Δt = 1/48 d, Δt = 1/24 d, Δt = 1/12 d and Δt = 1/6 d.
Polder Vierambacht: Δt = 1/48 d, Δt = 1/24 d, Δt = 1/12 d and Δt = 1/6 d.

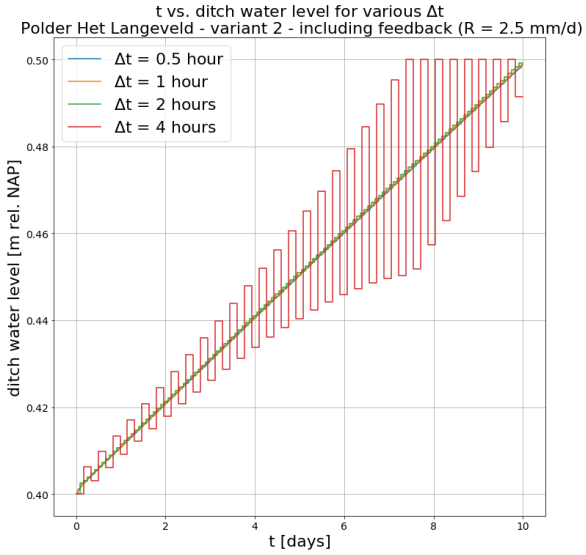

Figure G.13: Temporal discretization (including feedback) - variant 2, Polder Het Langeveld

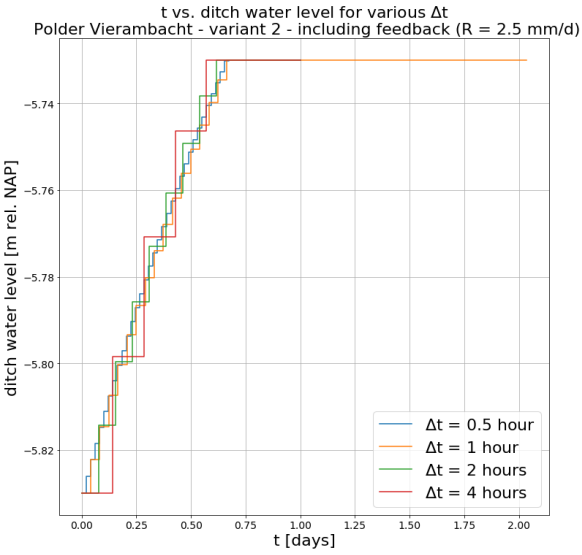

Figure G.14: Temporal discretization (including feedback) - variant 2, Polder Vierambacht

Again, it can be observed that the lines converge as Δt decreases. Figure G.13 shows that the ditch water level oscillates for Δt = 1/6 d (variant 2, Polder Het Langeveld). Proper solutions are obtained

for $\Delta t \leq$ 1/12 d. Δt = 1/24 d is selected to be conservative. Figure G.14 shows that rather large time steps result in proper solutions for variant 2, Polder Vierambacht. However, Δt = 1/24 d is selected to be conservative.

G.3. Model schematization

The model schematization is verified by comparing the results of the constructed MODFLOW model (1-layer model) to the results of a 3-layer MODFLOW model. Instead of applying the GHB package to simulate the confining layer, the confining layer and the first few metres of the bottom aquifer are actually included in the 3-layer model. For all variants and both case study areas, the steady-state groundwater situation for R = 0.7 mm/d and h_{SW} = $h_{SW,target}$ and/or h_{drain} = $h_{SW,target}$ is simulated using both MODFLOW models. Figure G.15 contains the result for variant 1, Polder Het Langeveld. The simulated groundwater heads along a cross-section that is perpendicular to the drains and includes the centre point of the plot are plotted. The blue line corresponds to the 1-layer MODFLOW model, whereas the orange line corresponds to the 3-layer MODFLOW model. The lines coincide, which means that the 1-layer model correctly schematizes groundwater flow. Figure G.16 contains a similar graph for variant 2 and 3, Polder Het Langeveld. Due to the choice of boundary conditions, the steady-state groundwater situation in case of variant 2 corresponds to the steady-state groundwater situation in case of variant 3. Therefore, both variants are represented by the same figure. Again, the simulation result of the 1-layer MODFLOW model coincides with the simulation result of the 3-layer MODFLOW model. The simulation results for variant 2 and 3, Polder Vierambacht, are shown in Figure G.17. Once more, the steady-state groundwater situation in case of variant 2 corresponds to the steady-state groundwater situation in case of variant 3 due to the choice of boundary conditions. The blue and orange lines coincide. The figures demonstrate that the 1-layer model correctly schematizes groundwater flow.

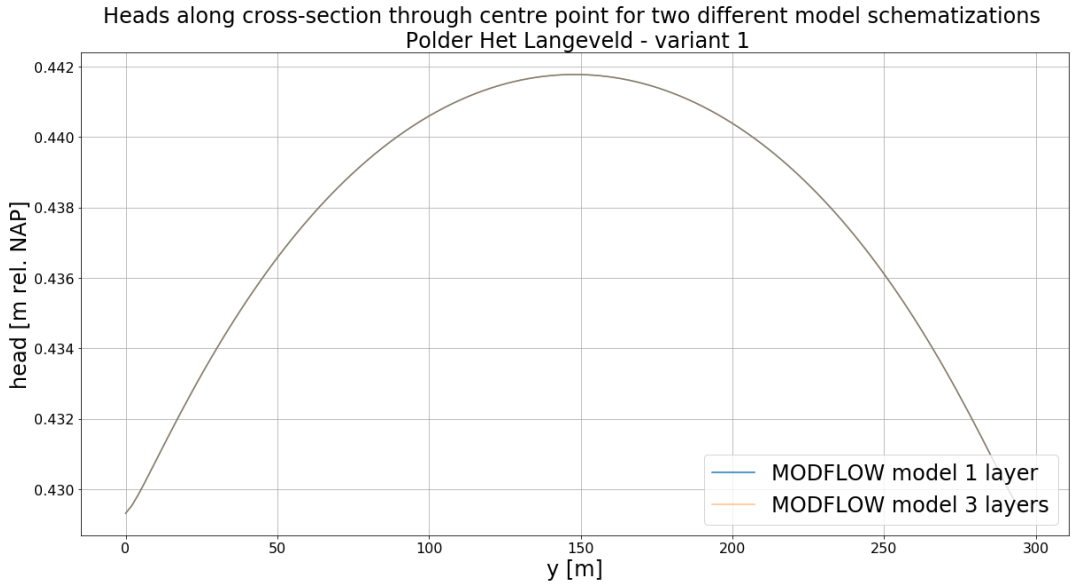

Figure G.15: Verification model schematization variant 1 Polder Het Langeveld.

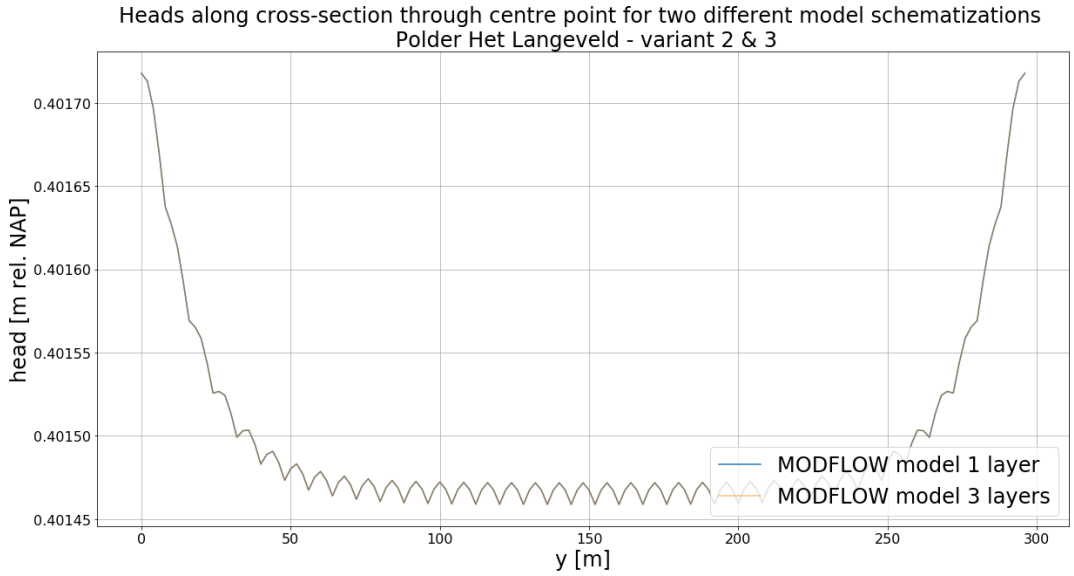

Figure G.16: Verification model schematization variant 2 and 3 Polder Het Langeveld.

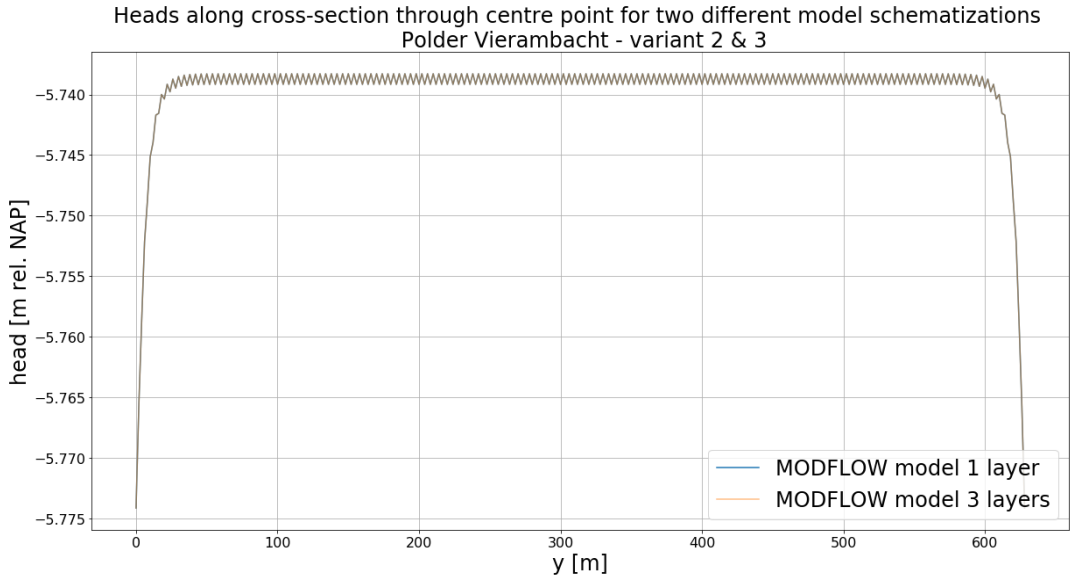

Figure G.17: Verification model schematization variant 2 and 3 Polder Vierambacht.

G.4. Representation of the physical system

Figure G.18 and G.19 contain actual groundwater level time series for Polder Het Langeveld and Polder Vierambacht respectively. They are retrieved from DINOloket. These figures are compared to Figure 7.6 to check whether the constructed MODFLOW model correctly represents the physical system.

Figure 7.6 shows that the steady-state groundwater level (R = 0.7 mm/d and h_{SW} = $h_{SW,target}$ and/or h_{drain} = $h_{SW,target}$) equals approximately 0.45 m NAP for variant 1 Polder Het Langeveld, and 0.40 m NAP for variant 2 and 3 Polder Het Langeveld. In Polder Het Langeveld, the average groundwater level during the period 1954 to 1966 was approximately 0.50 m NAP, which is derived from Figure G.18. This means that the groundwater levels calculated by MODFLOW correspond quite well to the groundwater level observations.

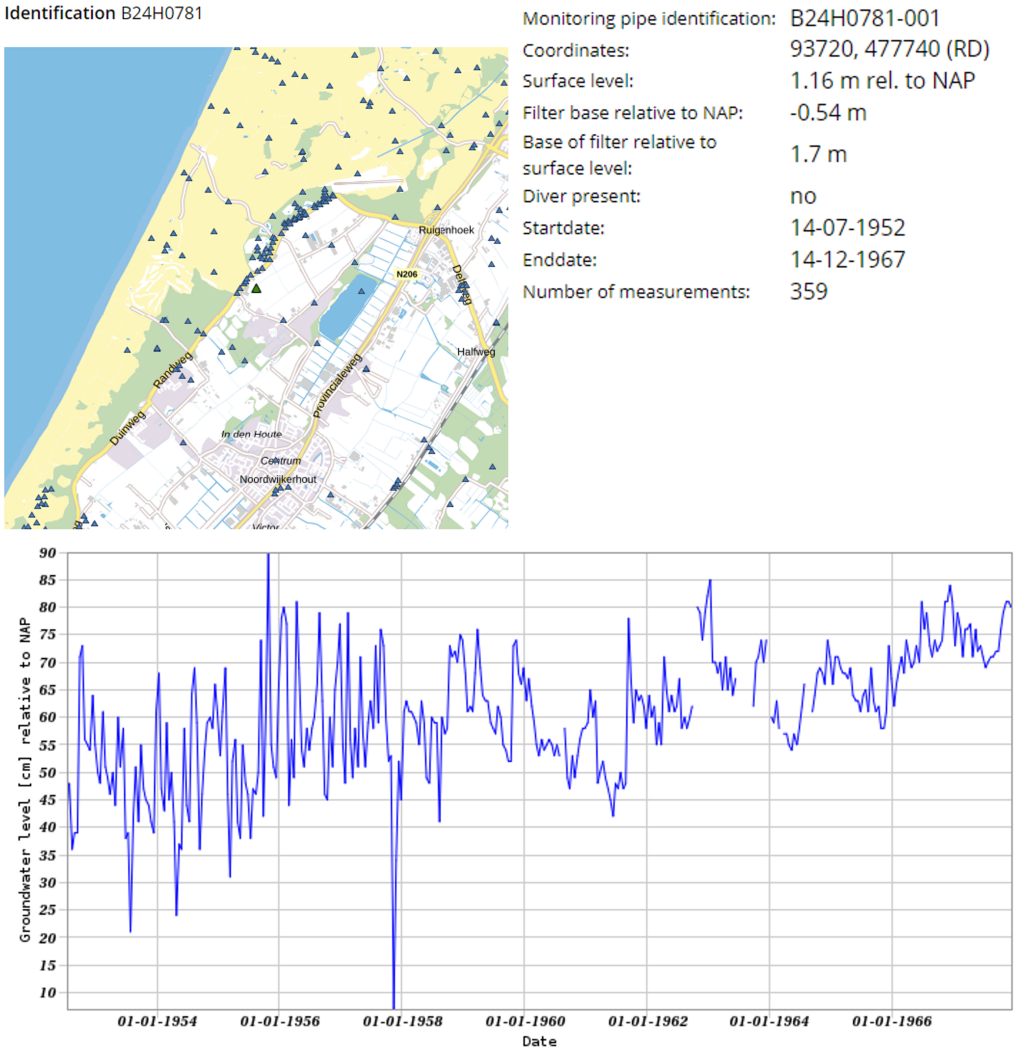

Figure G.18: Groundwater observations Polder Het Langeveld (TNO s.d.[a]).

Figure 7.6 shows that the steady-state groundwater level (R = 0.7 mm/d and h_{SW} = $h_{SW,target}$ and/or h_{drain} = $h_{SW,target}$) equals approximately -5.55 m NAP for variant 2 and 3 Polder Vierambacht (variant 1 is omitted). The average groundwater level during the period 1990 to 2015 was slightly higher; approximately -5.40 m NAP (Figure G.19). However, -5.55 m NAP corresponds well to the groundwater levels in the final years (2010 to 2015). Furthermore, a downward trend is observed. Therefore, it is concluded that the groundwater levels calculated by MODFLOW correspond quite well to the groundwater level observations.

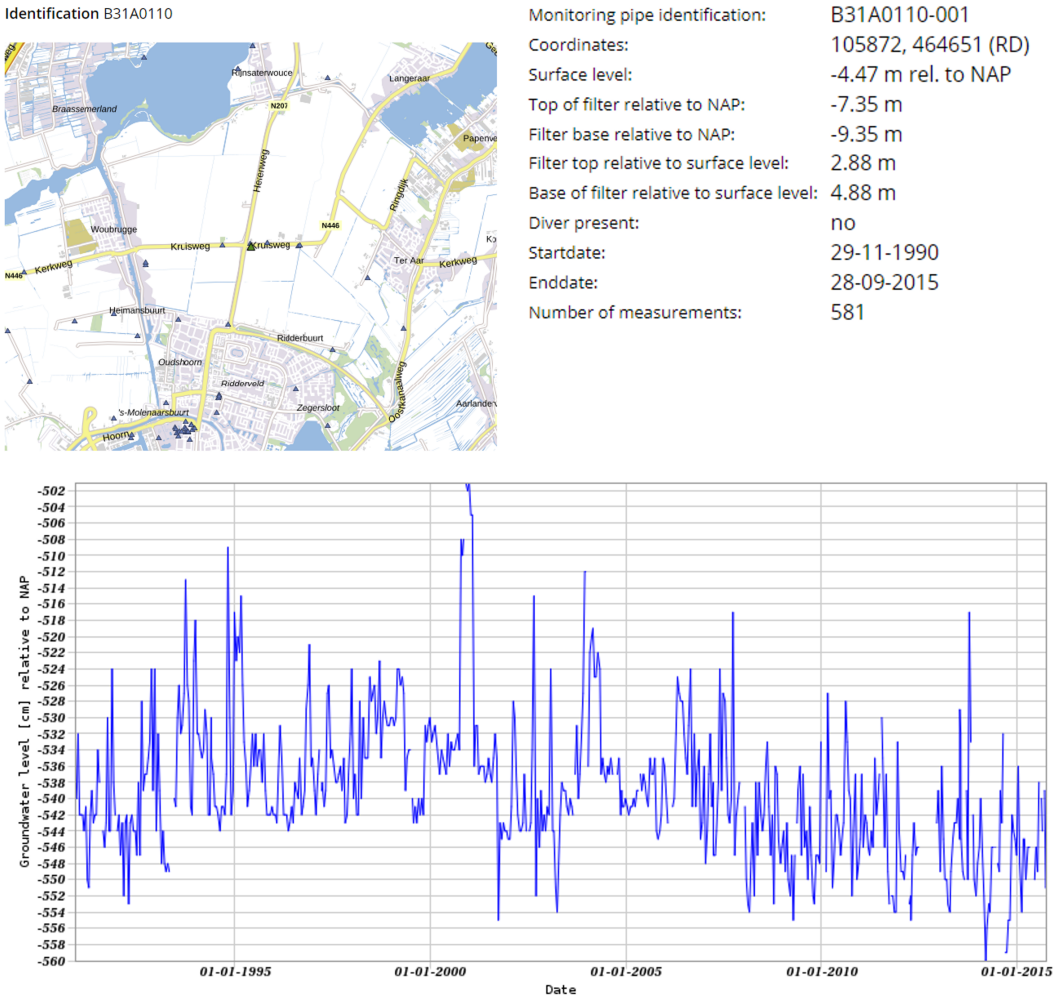

Figure G.19: Groundwater observations Polder Vierambacht (TNO s.d.[a]).